frontiers | Research Topics

Micro/nanorobots in nanobiotechnology

Edited by
Fengtong Ji, Yue Dong, Tianlong Li and Katherine Villa

Published in
Frontiers in Bioengineering and Biotechnology

ISSN 1664-8714
ISBN 978-2-8325-5192-9
DOI 10.3389/978-2-8325-5192-9

About Frontiers

Frontiers is more than just an open access publisher of scholarly articles: it is a pioneering approach to the world of academia, radically improving the way scholarly research is managed. The grand vision of Frontiers is a world where all people have an equal opportunity to seek, share and generate knowledge. Frontiers provides immediate and permanent online open access to all its publications, but this alone is not enough to realize our grand goals.

Frontiers journal series

The Frontiers journal series is a multi-tier and interdisciplinary set of open-access, online journals, promising a paradigm shift from the current review, selection and dissemination processes in academic publishing. All Frontiers journals are driven by researchers for researchers; therefore, they constitute a service to the scholarly community. At the same time, the *Frontiers journal series* operates on a revolutionary invention, the tiered publishing system, initially addressing specific communities of scholars, and gradually climbing up to broader public understanding, thus serving the interests of the lay society, too.

Dedication to quality

Each Frontiers article is a landmark of the highest quality, thanks to genuinely collaborative interactions between authors and review editors, who include some of the world's best academicians. Research must be certified by peers before entering a stream of knowledge that may eventually reach the public - and shape society; therefore, Frontiers only applies the most rigorous and unbiased reviews. Frontiers revolutionizes research publishing by freely delivering the most outstanding research, evaluated with no bias from both the academic and social point of view. By applying the most advanced information technologies, Frontiers is catapulting scholarly publishing into a new generation.

What are Frontiers Research Topics?

Frontiers Research Topics are very popular trademarks of the *Frontiers journals series*: they are collections of at least ten articles, all centered on a particular subject. With their unique mix of varied contributions from Original Research to Review Articles, Frontiers Research Topics unify the most influential researchers, the latest key findings and historical advances in a hot research area.

Find out more on how to host your own Frontiers Research Topic or contribute to one as an author by contacting the Frontiers editorial office: frontiersin.org/about/contact

Micro/nanorobots in nanobiotechnology

Topic editors

Fengtong Ji — University of Cambridge, United Kingdom
Yue Dong — Harbin Institute of Technology, Shenzhen, China
Tianlong Li — Harbin Institute of Technology, China
Katherine Villa — Institut Català d'Investigació Química, Spain

Citation

Ji, F., Dong, Y., Li, T., Villa, K., eds. (2024). *Micro/nanorobots in nanobiotechnology*. Lausanne: Frontiers Media SA. doi: 10.3389/978-2-8325-5192-9

Table of contents

frontiers | Frontiers in Bioengineering and Biotechnology

TYPE Editorial
PUBLISHED 10 July 2024
DOI 10.3389/fbioe.2024.1453307

OPEN ACCESS

EDITED AND REVIEWED BY
Gianni Ciofani,
Italian Institute of Technology (IIT), Italy

*CORRESPONDENCE
Fengtong Ji,
fj284@cam.ac.uk

RECEIVED 22 June 2024
ACCEPTED 24 June 2024
PUBLISHED 10 July 2024

CITATION
Ji F, Li T, Villa K and Dong Y (2024), Editorial: Micro/nanorobots in nanobiotechnology. *Front. Bioeng. Biotechnol.* 12:1453307. doi: 10.3389/fbioe.2024.1453307

Editorial: Micro/nanorobots in nanobiotechnology

Fengtong Ji[1,2]*, Tianlong Li[3], Katherine Villa[4] and Yue Dong[5]

[1]Wellcome Trust/Cancer Research UK Gurdon Institute, University of Cambridge, Cambridge, United Kingdom, [2]Department of Physiology, Development and Neuroscience, University of Cambridge, Cambridge, United Kingdom, [3]State Key Laboratory of Robotics and System, Harbin Institute of Technology, Harbin, China, [4]Institute of Chemical Research of Catalonia (ICIQ), The Barcelona Institute of Science and Technology (BIST), Tarragona, Spain, [5]Guangdong Provincial Key Laboratory of Intelligent Morphing Mechanisms and Adaptive Robotics, School of Mechanical Engineering and Automation, Harbin Institute of Technology, Shenzhen, China

KEYWORDS

nanotechnology, micro/nanorobots, biomedicine, cancer therapy, clinical treatment, medical diagnosis

Editorial on the Research Topic
Micro/nanorobots in nanobiotechnology

Six decades have passed since Richard Feynman spearheaded one research direction towards small-scale machinery, heralding the dawn of nanotechnology. Advances in microscopy have significantly enhanced our understanding of fundamental principles at the microscopic level and have provided us with versatile methods for control in microenvironments. Among these advancements, micro/nanorobots emerge as unique devices that facilitate direct interaction with microscopic entities, such as cells and molecules. These tiny machines, powered by field energy conversion, enable precise control and serve as customisable building blocks to perform tasks in various environments, particularly within complex biological systems. This Research Topic aims to elucidate nanorobot-cell interactions and inspire the development of novel functions for micro/nanorobots in biological contexts, ultimately advancing innovative treatments in clinical applications.

Considering the potential of micro/nanorobots in the biomedical field, the review articles in this Research Topic offer insights into the capabilities of such self-propelled systems in medicine. Active control of micro/nanorobots can enhance local drug delivery and improve therapeutic effectiveness whilst minimising side effects on healthy tissues. Passive nanomedicines or non-motile particles have proven effective in cancerous environments, including tumours in the liver, breast, glioma, pancreas, lung, oesophagus, and cervical regions, as well as in treating endocrine diseases such as diabetic complications and circulatory system diseases, such as ischemic stroke and thrombosis. Integrating nanorobotics into these systems has the potential to synergistically improve targeted drug delivery, biological barrier penetration (such as the blood-brain barrier and deep tissues), and overall treatment efficiency.

Nanorobots can facilitate tissue growth and organoid formation when we examine their interactions with tissues. At the cellular level, they enhance intracellular delivery of substances such as oxygen (Zhang et al., 2019), siRNA (Esteban-Fernández De Ávila et al., 2016), and other complexes, thereby achieving gene silencing (Yin et al., 2013) and knockout (Hansen-Bruhn et al., 2018). Both the cytoplasm and nucleus are accessible targets (He et al., 2022). The hydrogel magnetic microrobots discussed in this Research Topic have been employed to deliver drugs that inhibit cancer cell proliferation and mobility and induce apoptosis.

In the realm of biomedical diagnosis, functionalised micro/nanorobots can bind to target genes, activate fluorescence signals, and enable rapid and sensitive diagnoses for conditions such as head and neck cancer (Qualliotine et al., 2019), HeLa cells (Esteban-Fernández De Ávila et al., 2015), and Alzheimer's disease (Sun et al., 2021). They can also detect the SARS-CoV-2 virus by recognising its spike protein (Mayorga-Martinez et al., 2022). Additionally, nanorobots can enhance the efficiency of the enzyme-linked immunosorbent assay (ELISA) (Wang et al., 2022) and improve imaging diagnoses of deep tissues, such as intestinal diseases, which are traditionally examined using an endoscope.

A typical treatment cycle of a nanorobotic system comprises four sections: drug loading, targeted drug delivery, drug release (if the drugs are coated internally or require specific contact with tissues for efficacy), and nanorobot degradation or exclusion from the body. Regarding actuation, three external driving fields are discussed in this Research Topic: acoustic, magnetic, and electrical fields, due to their biocompatibility and non-contact control manners. Additionally, light, thermal and chemical (Simó et al., 2024) energies may enhance some objectives, endowing nanorobots with multiple functions to navigate complex and dynamic environments. Biosafety is a priority when applying micro/nanorobots in biological environments and during imaging procedures such as positron emission tomography (PET), computed tomography (CT), photoacoustic computed tomography (PACT), optical coherence tomography (OCT), magnetic resonance imaging (MRI), and X-ray. A potential solution is to integrate living cells (e.g., microorganisms, macrophages, platelets, stem cells, and chimeric antigen receptor T cells) or cell membranes (e.g., platelet, tumour cell, macrophage, and red blood cell membranes) to fabricate biohybrid micro/nanorobots. These have proven effective in modulating the immune system (Zhou et al., 2020).

Numerous reviews have emerged during COVID-19 and its aftermath due to the lockdown, but now most research activities, including experiments, have returned to normal thanks to the sacrifices made by all humanity. Clinical trials and medical translation of nanobiotechnology are complex processes that take time to manage. Biological experiments demand significant time commitment and patience to obtain valid data proving efficacy. Long-term dedication is essential for researchers to solidify the fundamentals, and cross-disciplinary integration is necessary to bridge the gap between laboratory research and clinical applications. Biomimetic inspiration can be drawn from nature for materials and designs, meanwhile, emerging technologies including artificial intelligence (Yang et al., 2024) may drastically advance nanorobotic biotechnology in healthcare. Nowadays, open-access articles are becoming a new trend removing barriers to knowledge, and the impact of refereed articles relies on researchers' integrity and scientific discoveries. Time will reveal what research is pivotal and constructive to the community and society, guiding younger generations to shape the future together. We look forward to witnessing the breakthroughs of nanorobots that address the health challenges everyone faces.

Author contributions

FJ: Writing–original draft, Writing–review and editing. TL: Writing–review and editing. KV: Writing–review and editing. YD: Writing–review and editing.

Conflict of interest

The authors declare that the research was conducted in the absence of any commercial or financial relationships that could be construed as a potential conflict of interest.

Publisher's note

References

Esteban-Fernández De Ávila, B., Angell, C., Soto, F., Lopez-Ramirez, M. A., Báez, D. F., Xie, S., et al. (2016). Acoustically propelled nanomotors for intracellular siRNA delivery. *ACS Nano* 10 (5), 4997–5005. doi:10.1021/acsnano.6b01415

Esteban-Fernández De Ávila, B., Martín, A., Soto, F., Lopez-Ramirez, M. A., Campuzano, S., Vásquez-Machado, G. M., et al. (2015). Single cell real-time miRNAs sensing based on nanomotors. *ACS Nano* 9 (7), 6756–6764. doi:10.1021/acsnano.5b02807

Hansen-Bruhn, M., de Ávila, B. E. F., Beltrán-Gastélum, M., Zhao, J., Ramírez-Herrera, D. E., Angsantikul, P., et al. (2018). Active intracellular delivery of a Cas9/sgRNA complex using ultrasound-propelled nanomotors. *Angew. Chem. - Int. Ed.* 57 (10), 2657–2661. doi:10.1002/anie.201713082

He, S., Pang, W., Wu, X., Yang, Y., Li, W., Qi, H., et al. (2022). Bidirectional regulation of cell mechanical motion *via* a gold nanorods-acoustic streaming system. *ACS Nano* 16 (5), 8427–8439. doi:10.1021/acsnano.2c02980

Mayorga-Martinez, C. C., Vyskočil, J., Novotný, F., Bednar, P., Ruzek, D., Alduhaishe, O., et al. (2022). Collective behavior of magnetic microrobots through immuno-sandwich assay: On-the-fly COVID-19 sensing. *Appl. Mat. Today* 26, 101337. doi:10.1016/j.apmt.2021.101337

Qualliotine, J. R., Bolat, G., Beltrán-Gastélum, M., de Ávila, B. E. F., Wang, J., and Califano, J. A. (2019). Acoustic nanomotors for detection of human papillomavirus–associated head and neck cancer. *Otolaryngol. - Head. Neck Surg. (United States)* 161 (5), 814–822. doi:10.1177/0194599819866407

Simó, C., Serra-Casablancas, M., Hortelao, A. C., Di Carlo, V., Guallar-Garrido, S., Plaza-García, S., et al. (2024). Urease-powered nanobots for radionuclide bladder cancer therapy. *Nat. Nanotechnol.* 19 (4), 554–564. doi:10.1038/s41565-023-01577-y

Sun, Y., Luo, Y., Xu, T., Cheng, G., Cai, H., and Zhang, X. (2021). Acoustic aggregation-induced separation for enhanced fluorescence detection of Alzheimer's biomarker. *Talanta* 233, 122517. doi:10.1016/j.talanta.2021.122517

Wang, Y., Liu, X., Chen, C., Chen, Y., Li, Y., Ye, H., et al. (2022). Magnetic nanorobots as maneuverable immunoassay probes for automated and efficient enzyme linked immunosorbent assay. *ACS Nano* 16 (1), 180–191. doi:10.1021/acsnano.1c05267

Yang, L., Jiang, J., Ji, F., Li, Y., Yung, K. L., Ferreira, A., et al. (2024). Machine learning for micro- and nanorobots. *Nat. Mach. Intell.* 6, 605–618. doi:10.1038/s42256-024-00859-x

Yin, T., Wang, P., Li, J., Zheng, R., Zheng, B., Cheng, D., et al. (2013). Ultrasound-sensitive siRNA-loaded nanobubbles formed by hetero-assembly of polymeric micelles and liposomes and their therapeutic effect in gliomas. *Biomaterials* 34 (18), 4532–4543. doi:10.1016/j.biomaterials.2013.02.067

Zhang, F., Zhuang, J., Esteban Fernández De Ávila, B., Tang, S., Zhang, Q., Fang, R. H., et al. (2019). A nanomotor-based active delivery system for intracellular oxygen transport. *ACS Nano* 13 (10), 11996–12005. doi:10.1021/acsnano.9b06127

Zhou, J., Kroll, A. V., Holay, M., Fang, R. H., and Zhang, L. (2020). Biomimetic nanotechnology toward personalized vaccines. *Adv. Mat.* 32 (13), 1901255. doi:10.1002/adma.201901255

frontiers | Frontiers in Bioengineering and Biotechnology

TYPE Review
PUBLISHED 27 June 2023
DOI 10.3389/fbioe.2023.1219054

OPEN ACCESS

EDITED BY
Tianlong Li,
Harbin Institute of Technology, China

REVIEWED BY
Renfeng Dong,
South China Normal University, China
Shimin Yu,
Ocean University of China, China
Xiaolong Lu,
Nanjing University of Aeronautics and Astronautics, China

*CORRESPONDENCE
Lijun Yan,
ylj@hrbcu.edu.cn
Wenlan Li,
lwldzd@163.com

RECEIVED 08 May 2023
ACCEPTED 05 June 2023
PUBLISHED 27 June 2023

CITATION
Zhao Q, Cheng N, Sun X, Yan L and Li W (2023), The application of nanomedicine in clinical settings.
Front. Bioeng. Biotechnol. 11:1219054.
doi: 10.3389/fbioe.2023.1219054

The application of nanomedicine in clinical settings

Qingsong Zhao[1], Nuo Cheng[2], Xuyan Sun[2], Lijun Yan[1]* and Wenlan Li[1]*

[1]Postdoctoral Programme of Meteria Medica Institute of Harbin University of Commerce, Harbin, China, [2]Department of Endocrinology, The Fourth Hospital of Harbin Medical University, Harbin, China

As nanotechnology develops in the fields of mechanical engineering, electrical engineering, information and communication, and medical care, it has shown great promises. In recent years, medical nanorobots have made significant progress in terms of the selection of materials, fabrication methods, driving force sources, and clinical applications, such as nanomedicine. It involves bypassing biological tissues and delivering drugs directly to lesions and target cells using nanorobots, thus increasing concentration. It has also proved useful for monitoring disease progression, complementary diagnosis, and minimally invasive surgery. Also, we examine the development of nanomedicine and its applications in medicine, focusing on the use of nanomedicine in the treatment of various major diseases, including how they are generalized and how they are modified. The purpose of this review is to provide a summary and discussion of current research for the future development in nanomedicine.

KEYWORDS

cross-disciplinary, micro-/nanorobots, nanotechnology, nanomedicine, drug delivery

1 Introduction

Modern medicine is studied to pursue a new interdisciplinary discipline named nanomedicine which combines nanotechnology and medicine (Zingg and Fischer, 2019; Germain et al., 2020). An application of nanotechnology in medicine is called nanomedicine, while a pharmaceutical product containing nanotechnology is known as nanomedicines. For example, a pharmaceutical containing a nanotechnology component, usually the actual drug or a vehicle that delivers it. Nanomedicine is an umbrella term for nanotechnology with medical applications, whereas "nanomedicines" are pharmaceuticals containing nanotechnology components (Hall et al., 2012).

A lecture given by Richard Feynman in 1959 at Caltech envisaged machines and devices made of individual atoms, now known as "bottom-up" nanotechnology (Olsman and Goentoro, 2018). Gerd Binnig and Harold Rohrer won the Nobel Prize in Physics in 1986 for their scanning tunneling microscopy technique, which enables the picking up of individual atoms and assembling them into the desired arrangement, thus greatly enabling the development of a new technology. Carbon 60 was discovered by Richard Smalley, Robert Curl, and Harold Kroto in 1995, winning the Nobel Prize in Chemistry. As a result of their research on graphene, a two-dimensional carbon molecule made up of nanoscale atoms, Andre Geim and Konstantin Novoselov were awarded the Nobel Prize in Physics in 2010.

United States and European regulatory agencies approved the first generation of nanomedicines in the mid-1990s (Ferrari, 2010). A typical application of nanomedicine is liposomes, which are nanoparticles (NPs) derived from lipid molecules, similar to the basic structure of cell membranes. With nanomedicines, cytotoxic drugs are selectively delivered

to focal areas using nanotechnology, increasing drug concentrations in targeted areas, reducing damage to non-targeted areas, minimizing side effects, and achieving more therapeutic outcomes at a lower cost than conventional therapeutic modalities (Martin et al., 2020).Nanotechnology can establish new routes of drug delivery and, through controlled release systems, improve the absorption and utilization of drugs and increase the targeting rate of drugs to a greater extent than in conventional medicine.

Through the use of drug-loaded micro/nanorobots, the some drugs can be effectively tracted and penetrated into the relevant tissues. Nanotechnology has opened up new possibilities for drug delivery (Maheswari et al., 2018). In recent years, a large number of drug delivery systems have been developed, including liposomes composed of phospholipid bilayers (Liu Y. et al., 2021). Hydrophilic cores and lipophilic lipids bind hydrophilic and hydrophobic drugs in liposomes, which are phospholipid vesicles. Targeting on cancer therapies, liposomes are commonly used as carriers for targeted delivery. Inorganic nanoparticles are known to carry drugs via surface coupling (Wang X. et al., 2021), dendritic polymers with shell-core properties (Kheraldine et al., 2021), as well as polymeric nanoparticles. Among the propulsion sources for drug-delivery nanorobots are magnetically driven (Hu et al., 2020; Sindhu et al., 2021; Zhao et al., 2022; Li et al., 2023), which uses a magnetic field to propel the device, optically driven (Dong et al., 2016), which utilizes semiconductor-based photoinduced catalysis to provide propulsion, acoustically driven (Ahmed et al., 2015), chemically driven (Mou et al., 2016), and biologically driven (Park et al., 2017; Halder and Sun, 2019). An external field drive for micro-nanorobots can be provided by magnetic, optical, and acoustic waves. It has the advantages of easy adjustment and high controllability, but it relies more heavily on off-field devices for power. Among these types of drives, magnetic drives are the most commonly used, and compared with other micro-/nanorobot drive methods, magnetic drives influenced by magnetic field gradients and magnetic field torques possess the characteristics of being easy to acquire, easy to adjust magnetic fields, and capable of penetrating into biological tissues without significant damage. It can be used in a variety of liquid environments, which is the relatively most mature driving method. Micro-/nanorobots fabricated with magnetic drive as the power module can be broadly classified into spiral-propelled micro-/nanorobots (Walker et al., 2015), oscillating magnetic field-driven flexible micro-/nanorobots (Li et al., 2017; Xin et al., 2019; Liu J. et al., 2021; Ji et al., 2021) and other types of magnetic field-driven micro-/nanorobots, such as gradient magnetic field-driven micro-/nanorobots (Li et al., 2016; Wang et al., 2022). Researchers are also attempting to create micro-/nanorobots using a combination of magnetic drive and other drive methods at the same time due to the features such as easy adjustment of magnetic fields and non-destructive penetration into biological tissues. This can be accomplished by giving certain magnetic properties to micro-/nanorobots while applying other driving methods. In recent years, more types of magnetic nanorobots have been designed, Yu et al. have fabricated trimeric nanorobots using three magnetic Janus colloids of different diameters (Yu et al., 2022). Inspired by the biological claws of tardigrades, Li et al. have designed a magnetically driven swimming microrobots with claw geometry and a red blood cell (RBC) membrane camouflage on its surface. It achieves controlled motion and targeted dwellings in a high velocity blood flow environment, providing a new idea for the precise treatment of malignant tumors (Li et al., 2023). Micro-/nanorobots powered by light are mainly actuated by photoinduced catalysis in semiconductors, and the action of light-driven micro-/nanorobots in biological tissues can be controlled by adjusting light intensity, light frequency, light area, light duration or by enhancing photocatalytic efficiency (Wang Q. et al., 2020; Yang et al., 2021).Additionally, research on micro-/nanorobots propelled by acoustics is essential, particularly the use of ultrasonic waves that can penetrate biological tissues with greater reliability (Díez et al., 2017; Mu et al., 2021). Wang et al. described a novel intracellular antigen delivery strategy using ultrasound (US)-propelled gold nanowires (AuNWs) nanomotors modfied with a model antigen (ovalbumin, OVA). Due to the excellent biocompatibility of AuNWs nanomotors, it can improve antigen cross-presentation and cellular immunity and thus promote immune efficiency of vaccines (Wang J. et al., 2021). In terms of chemical drives, bubble propulsion mechanisms have received the most attention to date. By adjusting the intensity and pulse of UV irradiation, Mou et al. can remotely control whether or not bubbles are generated, while utilizing the photocatalytic water redox reaction on TiO_2/Pt under UV irradiation16. It is important to note; however, that bubble recoil propulsion does have limitations, and the floating bubbles are unstable in most physiological environments outside of the gastrointestinal tract of human (Jang et al., 2019). As a result of their inherent limitations, nanorobots remain challenging in design and preparation today, including complex fabrication techniques, difficulties in surface modification, difficulties in flowing biofluids, and poor biocompatibility or poor biodegradability, depending on the materials (Zhang et al., 2020).

There are many applications of nanomaterials, including drug delivery, medical imaging, and other fields, that benefit from their unique physicochemical properties and photothermal effects, namely, its small size, light weight, easy adjustment, strong penetrationand non-destructive penetration into biological tissues. In recent years, nanomedicine has shown great potential for applications. For instance, nanomedicines have been widely applied. Since the first nanomedicine doxorubicin (DOX) was introduced in 1995 (Barenholz, 2012), researchers have developed a wide range of nanomedicines to date, including paclitaxel albumin nanoparticles (Chen et al., 2021) and elitecan liposomes (Wang T. et al., 2021), which are used to treat a variety of serious diseases. The use of nanomedicine for disease monitoring and minimally invasive surgery is among the many clinical applications of nanomedicine. Consequently, the development of nanomedicine in disease monitoring and minimally invasive surgery is not to be underestimated, as nanorobots have many advantages over conventional robots, including the ability to monitor and treat lesions more efficiently (Mir et al., 2017).

1.1 Clinical applications of nanomedicine

Research for nanotechnology application in the medical field has focused on the diagnosis of diseases, targeted delivery, and minimally invasive surgical procedures. As a result of their small size, light weight, flexibility, and nondestructive penetration into

biological tissues, micro-/nanorobots achieve results that are difficult or even impossible to achieve by conventional mean (Fadeel and Alexiou, 2020). In terms of chemical reactivity, fluorescence, magnetic permeability, and electrical conductivity, nanomaterials demonstrate significant differences, and these properties could lead to significant advancements in the development of new drugs (Jacob et al., 2020). Imaging techniques in the biomedical field are used to monitor the pharmacokinetics and pharmacodynamics of nanomedicine, as well as to improve nanomedicine-based therapeutic regimens in preclinical research (Tuguntaev et al., 2022).

1.1.1 The use of nanomedicine in the treatment of major diseases

With the unique advantages of nanotechnology, targeted drug delivery has become a reality. By delivering therapeutic drugs through nanocarriers and targeting their delivery to the focal area, it is possible to increase the concentration of therapeutic drugs in the focal area while minimizing side effects and damage to non-targeted areas. Many nanomedicines have been developed by researchers in the last few decades for different diseases, especially for some major diseases, which have greatly reduced pain and economic pressure for patients.

1.1.1.1 Oncology therapy related applications

The It is widely recognized that medical nanotechnology is a promising approach to solve cancer challenges. Worldwide, cancer is the leading cause of death, accounting for nearly 10 million (or nearly one in six) deaths, according to a report published by the World Health Organization (WHO). Among the conventional cancer treatments, surgical resection, radiotherapy, and chemotherapy are the most common. The current conventional treatment for cancer kills cells indiscriminately in the focal area of the body, causing severe pain to the patient during the treatment procedure (Li et al., 2020). Drug delivery via nanomedicine carriers is a viable alternative to conventional chemotherapy which suffers from poor water solubility, poor tissue targeting, and severe systemic toxic effects (Kumstel et al., 2020). Nanomedicine carriers increase drug concentration within the target area and thus improve drug utilization and efficacy by increasing the drug concentration in the target area. As well, the nano drug carriers can be administered within the tumor vasculature, thereby reducing the drug dose and the toxic side effects on other tissues and organs.

In the world, liver cancer is the sixth most common type of cancer. Hepatocellular carcinoma (HCC) has an 18% 5-year survival rate, making it the second most lethal cancer following pancreatic cancer. Its insidious onset and insensitivity to chemotherapy make its treatment unsatisfactory (Zhang X. et al., 2016). As nanodrugs are able to increase drug bioavailability and hepatic targeting while reducing side effects on normal tissues, they offer greater possibilities for treating hepatocellular carcinoma when conventional therapies are ineffective (Bakrania et al., 2021; Elnaggar et al., 2021). In the field of targeted therapies, sorafenib (SOR) was the first systemic drug to demonstrate efficacy in patients with advanced HCC and has been used as a first-line treatment for more than 10 years. SOR alone is unlikely to achieve therapeutic expectations because of its inherent toxic side effects and the development of tumor resistance. This could be caused by the development of resistant tumor variants. In addition to traditional anticancer drugs, nanomedicines can be combined together to enhance delivery, retention, and release of these drugs into target cells and tumor tissues, thereby increasing the therapeutic effectiveness of cancer treatment. The combination of SOR and adriamycin has been proven to provide better therapeutic effects in patients with advanced hepatocellular carcinoma in clinical trials. Using a hybrid lipid-polymer nanoparticle containing a tumor-targeting peptide (iRGD), Zhang J. et al. (2016) developed a (DOX) and SOR delivery system containing iRGD (see Figure 1A). In contrast to single drug delivery, the hybrid delivery system resulted in greater bioavailability of the drug, improving the effectiveness of the anti-tumor treatment. The results of this study demonstrate that nanoparticles combined with clinical anticancer drugs are capable of enhancing anti-HCC efficacy, which is a direction of future research. In addition to the combination of nanoparticles and anticancer drugs, the combination of therapeutic nucleic acids and nanoparticles has also shown promise for application. In the research of Oh et al. (2016), DOX bound by electrostatic interaction was delivered through liposomes coated with siRNA, and the combination of DOX and siRNA inhibited tumor growth (see Figure 1B). Therefore, synergistic antitumor therapy has the potential to effectively target tumor cells and improve the antitumor effect, demonstrating its great potential. A nanodrug (HA @ PDC-DOX_2) was also developed and synthesized by Wang J. et al. (2020), consisting of peptide-adriamycin as the core and hyaluronic acid as the shell, to enhance the stability and targeting capability of PDC-DOX_2 (see Figure 1C). A new gold nanoparticle (Do-AuNP) was successfully synthesized from the extract of Dendrobium (DO), a traditional Chinese medicine. Experimental results show Do-AuNP has better anti-tumor efficiency as compared to gold nanoparticles in either vitro or *in vivo*, providing a new approach (Zhao et al., 2021). One of the key directions in nanomedicine research for the future will be to combine nanoparticles with molecules, therapeutic drugs or inter-nanoparticles in order to enhance the stability, therapeutic effects, and reduce the toxic effects of nanomedicines.

In addition to being the most common malignant tumor in women, breast cancer is also the leading cause of cancer deaths in women. Researchers have developed a variety of nanomedicines using a variety of materials to solve the problem of serious side effects caused by therapeutic drugs. These nanomedicines target cancer cells specifically and do not affect normal cells. It has been reported that Cheng et al. (2021) have developed a novel nanomedicine (CuQDA/IO@HA) containing copper ions and quercetin to specifically target cancer cells via CD44 and induce specific cytotoxicity in breast cancer (BRCA)-mutated cancer cells. More importantly, CuQDA/IO@HA demonstrated no significant adverse effects on normal tissues or organs, demonstrating the ability to treat cancer cells by integrating metal ions with nanomedicines. It is possible to reapply nanodrugs by integrating metal ions. A number of nanomedicines based on nucleic acids, including DNA and RNA, have been found to be particularly effective when combined with chemotherapy. To enhance the therapeutic efficacy and targeting on breast cancer, Zhan et al. (2019) developed a novel tumor-targeting nanomedicine (AS1411-T-5-FU) that was combined with 5-fluorouracil (5-FU) using DNA-based delivery systems (see Figure 2A). As a result, this

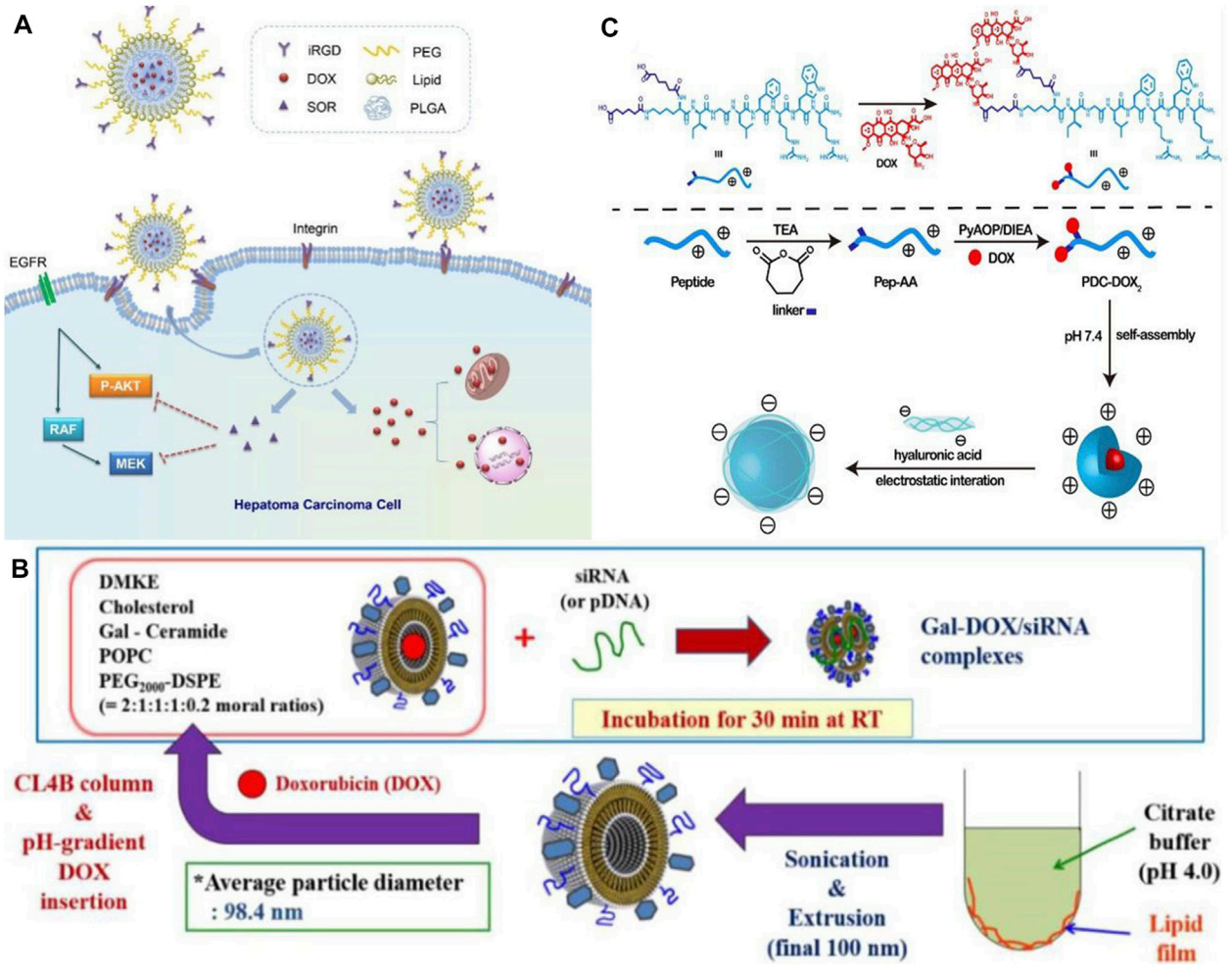

FIGURE 1
(A) Co-delivery of DOX and SOR by iRGD-modified lipid-polymer hybrid nanoparticles (Zhang J. et al., 2016). Reproduced with permission. Copyright 2016, Nanomedicine: Nanotechnology, Biology and Medicine; **(B)** Schematic of preparation of Gal-DOX/siRNA-L (Oh et al., 2016). Reproduced with permission. Copyright 2016, Nanomaterials; **(C)** Schematic illustration of formation of HA @ PDC-DOX_2 (Wang J. et al., 2020). Reproduced with permission. Copyright 2020, Materials Science and Engineering: **(C)**

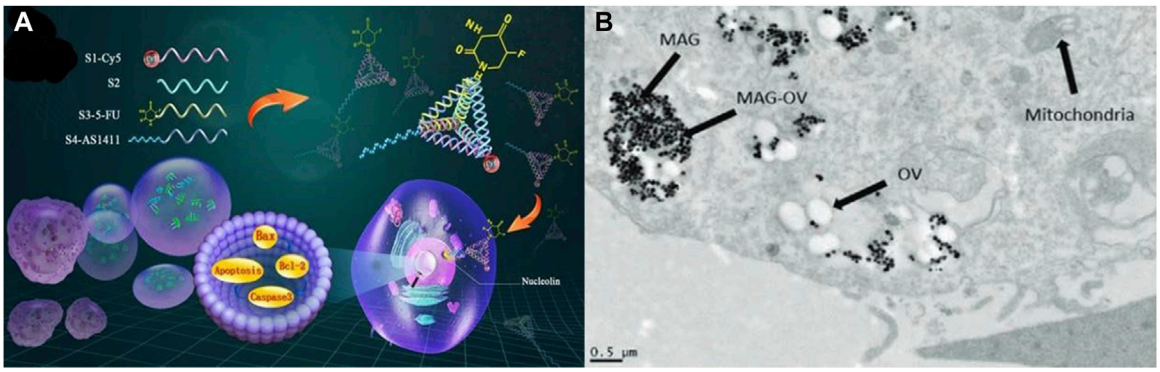

FIGURE 2
(A) Schematic diagram of the structure of the nanomedicine (AS1411-T-5-FU) (Zhan et al., 2019). Reproduced with permission. Copyright 2019, ACS Applied Materials & Interfaces; **(B)** Estimated atomic % of detected surface elements (Howard et al., 2022). Reproduced with permission. Copyright 2022, Small.

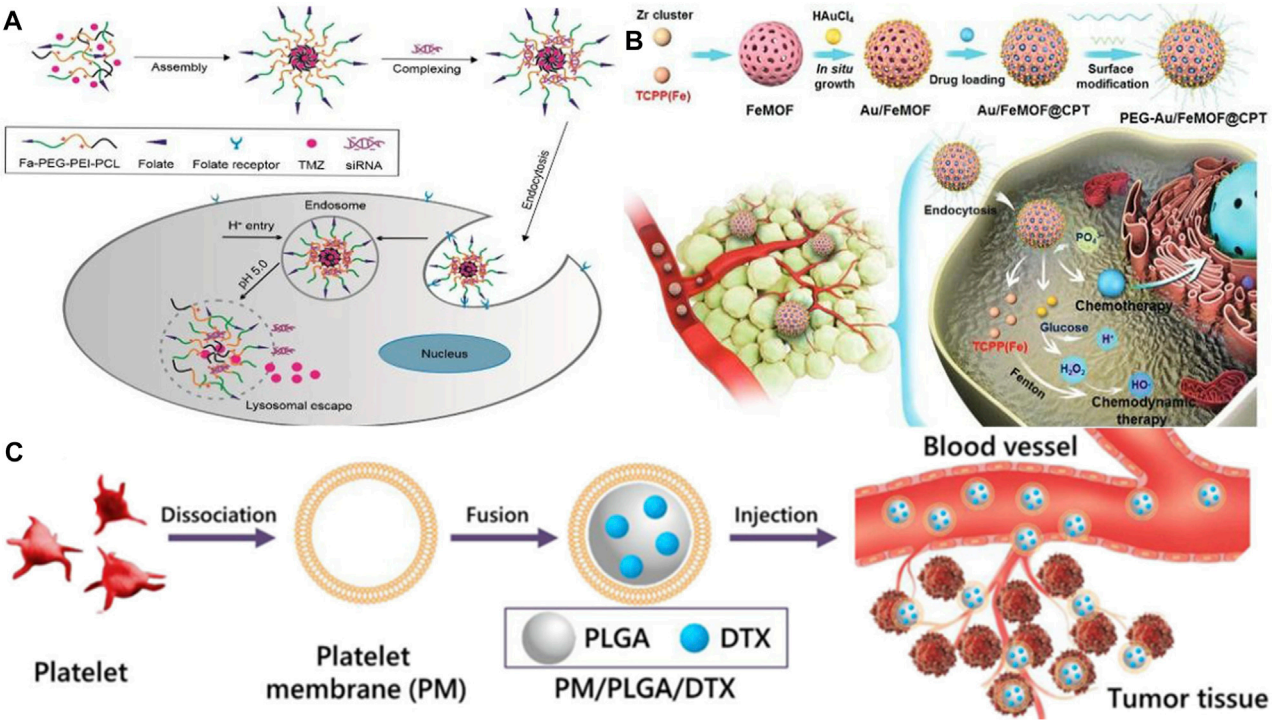

FIGURE 3
(A) Schematic illustration of the preparation for TMZ-FaPec@siRNa micelle and the release of TMZ and siRNa inside cancer cells (Peng et al., 2018). Reproduced with permission. Copyright 2018, International Journal of Nanomedicine; **(B)** Preparation process of the nanomedicine (Au/FeMOF@CPT NPs) (Ding et al., 2020). Reproduced with permission. Copyright 2020, Advanced Science **(C)** Schematic diagram of the preparation of platelet membrane-coated docetaxel (DTX)-loaded poly (lactic co-glycolic acid) (PLGA) nanoparticles (PM/PLGA/DTX) (Chi et al., 2019). Reproduced with permission. Copyright 2019, Journal of Nanoparticle Research.

nanomedicine is capable of targeting and killing breast cancer cells more effectively than 5-fluorouracil alone, showing DNA's potential as a nanomedicine material. Nucleic acid nanodrugs, however, face considerable difficulties in clinical applications due to their poor biocompatibility and low drug loading efficiency. Alternatively, Howard et al. (2022) assembles herpes simplex virus (HSV1716) with magnetic nanoparticles in order to precisely target cancer cells through magnetic actuation (see Figure 2B), preventing antibodies from attacking the virus *in vivo* before it can act, allowing the virus to proliferate in cancer cells while accumulating immune cells in the tumor, It can improve the treatment effect of disseminated tumors by 50% by promoting antitumor immunity, inducing tumor shrinkage, and increasing survival in a homozygous mouse model of breast cancer. Each material has its own advantages and disadvantages, and it appears to be a promising direction for future research utilizing the advantages of the materials themselves to their fullest extent and utilizing chemical coupling as a means of circumventing their shortcomings.

It is extremely difficult to treat glioma using conventional therapy as the blood-brain barrier severely hinders the anticancer effects of chemotherapy on glioma. However, various specific transporters on the blood-brain barrier can be utilized as targets to deliver tumor drugs using targeted nanoparticle delivery systems (Deng et al., 2020).Hortelao et al. designed an experimental nanorobot which was modified by urease and constructed with SiO_2 as a shell. It can load therapeutic drugs into tumor cells for release. As a result of loading nanobots with therapeutic drugs and releasing them in the tumor area, the drug concentration in the focal area increased and the drug utilization rate improved, and the drug was also reduced as it was released into other tissues and side effects were reduced (Llopis-Lorente et al., 2019). Therefore, it is apparent that nanodrugs are more effective at breaking through the blood-brain barrier than traditional chemotherapy treatments, which offers more treatment options for those suffering from brain diseases. The benefit of this approach is that it provides a greater variety of treatment options for brain diseases and achieves a more rapid therapeutic effect. Nevertheless, drug resistance is also a problem when treating glioma with a single drug. The combination of drugs, however, has good performance in treating glioma. The synergistic effect of the combination of therapeutic drugs and siRNA can significantly improve the anticancer effect in various cancers. In an experiment conducted by Peng et al. (2018), a targeted nanocarrier carrying temozolomide (TMZ) and anti-BCL-2 siRNA was used to assess the physicochemical properties and release profile of this drug, both *in vitro* and *in vivo* (see Figure 3A). Moreover, the drug promoted targeted drug delivery and inhibited tumor growth by activating pro-apoptotic genes in cancer cells, resulting in a significant apoptotic response and prolonging patients' survival periods. It is necessary to develop drugs for the treatment of brain diseases that are capable of crossing the blood-brain barrier, as well as to evaluate the clinical effectiveness of the drugs and to target drug resistance.

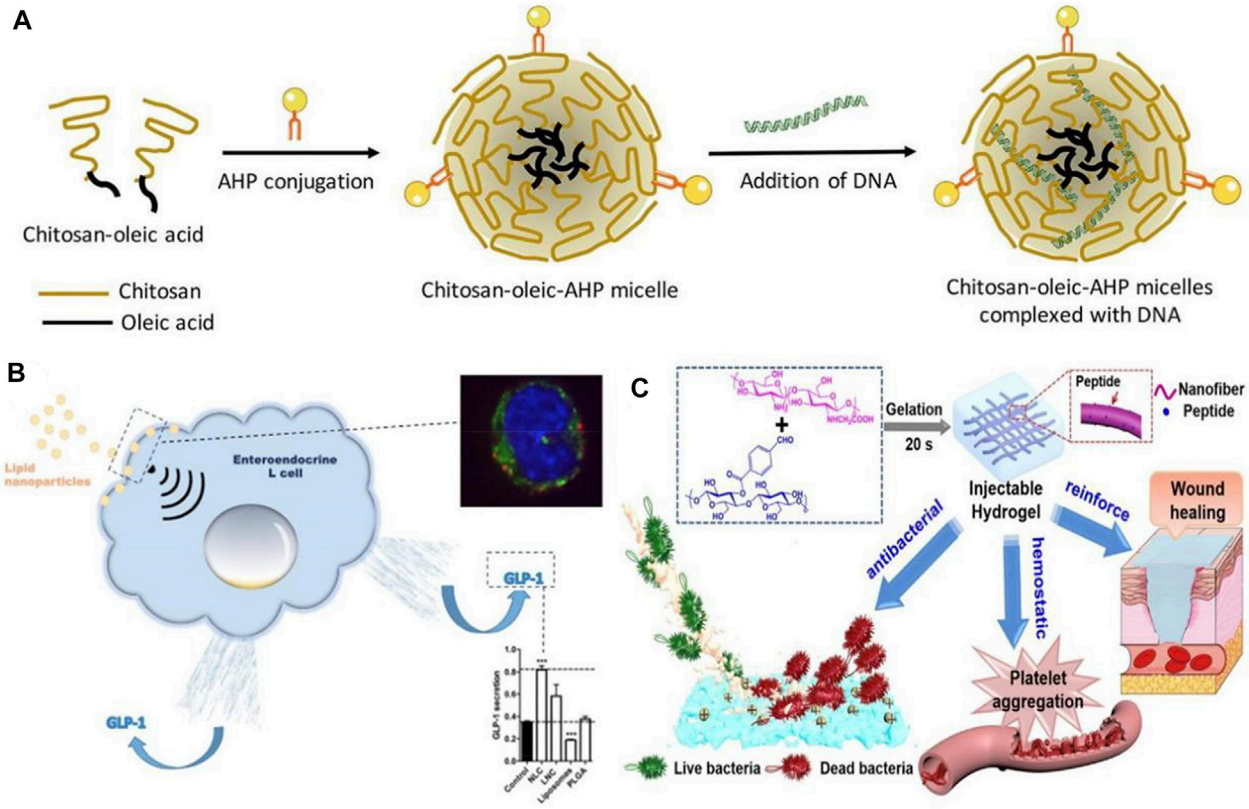

FIGURE 4
(A) Schematic illustration of formation of chitosan-oleic-adipose homing peptide (AHP) micelles complexed with DNA (Banerjee et al., 2020). Reproduced with permission. Copyright 2020, International Journal of Pharmaceutics; **(B)** Activation of intestinal L-cell GLP-1 secretion by lipid nanoparticles (Beloqui et al., 2016). Reproduced with permission. Copyright 2016, Molecular Pharmacology; **(C)** Diagram of the functional role of nanofiber-reinforced hydrogel (NFRH) (Qiu et al., 2021). Reproduced with permission. Copyright 2021, Journal of Colloid and Interface Science.

Less than 5% of pancreatic cancer patients survive 5 years after being diagnosed, making it the world's deadliest cancer. To enhance the quality of life and prolong the survival time of patients with pancreatic cancer, Gao et al. (2020) proposed delivery of drugs by ultrasound-targeted microbubble destruction (UTMD), which has significantly improved the therapeutic effect on patients with advanced pancreatic cancer. Due to its high biological toxicity, however, it has some limitations when applied to patients who are in good physical condition because it places high demands on their physical function. As reported by Ding et al. (2020), a hybrid nanodrug was fabricated (Au/FeMOF@CPT NPs) with metal organic backbone nanoparticles (MOF) and gold nanoparticles (Au NPs) (see Figure 3B), which improved the stability of the nanodrug in the organism. It was effective because cancer cells contain high concentrations of phosphate, resulting in the drug's complete release. Even though gold nanoparticles are one of the least toxic metal nanoparticles, high concentrations may be genotoxic, and drug safety needs to be considered as well (Desai et al., 2021a). Nanomedicines are also being investigated for their potential therapeutic applications in the treatment of tumors in other organs, including the lung (see Figure 3C) (Chi et al., 2019; Wang S. et al., 2020), the esophagus (Chen et al., 2020; Salapa et al., 2020), and the cervical region (Sadoughi et al., 2021; Venkatas and Singh, 2021). Considering nanomedicines' excellent targeting capability, future research should focus on improving the bioavailability of drugs, increasing their concentration in tumor sites, addressing possible drug resistance, and increasing their therapeutic potential.

1.1.1.2 Endocrine disease treatment applications

Our standard of living has been improving in recent years, and the lifestyle and diet structure have also been changing. As a result, the incidence of diabetes mellitus (DM) and other diseases has been increasing, while traditional hypoglycemic drugs have proved difficult to treat diabetes, causing great inconvenience to patients (Vessby et al., 2000). Additionally, diabetic patients are more likely to require a prolonged hospital stay and have a higher cost of hospitalization, particularly if they have chronic complications (Karahalios et al., 2018). For the purpose of alleviating the side effects associated with long-term insulin injections and the administration of first-line diabetes treatments, including biguanides, sulfonylureas, and glycosidase inhibitors, a variety of nanoparticle-based delivery systems have been developed to replace conventional medications (Chatzipirpiridis et al., 2015; Wang et al., 2018). According toBanerjee et al. (2020), plasmid lipocalin (pADN)-based nanodrugs were developed for treating insulin resistance in type 2 diabetes in experiments with diabetic rats (see Figure 4A). They avoided enzymatic degradation of the gene

product and significantly improved insulin sensitivity for up to 6 weeks, which is an effective therapeutic method. Due to the pleiotropic nature of the secreted glucagon-like peptide (GLP), L cells have attracted the attention of researchers, as Beloqui et al. (2016) A nanostructured lipid carrier was added to L cells, and the experimental results showed that nanostructured lipid carriers can increase GLP-1 secretion in murine and human L cells, which results in increased GLP-1 secretion for diabetes treatment purposes. In order to treat diabetes, exosomes can be used as nanomaterials (see Figure 4B). It has been found that these agents are capable of influencing both glucose and lipid levels, primarily through promoting glucose metabolism, enhancing lipid metabolism, and reducing lipid deposition (Ashrafizadeh et al., 2022). Therefore, they can serve as a new strategy for the treatment of diabetes.

A major focus of current research is the use of nanomedicines to treat diabetic complications, in addition to diabetes itself. Patients with diabetes are at risk for a variety of complications, including diabetic foot, diabetic neuropathy, diabetic nephropathy, diabetic retinopathy, etc. (Desai et al., 2021b; Balogh et al., 2022) One of the most common, serious, and expensive complications of diabetes is diabetic foot. As a result of hyperglycemia and abnormal glucose metabolism, diabetic patients develop lesions, neuropathy, and infection, making diabetic foot wounds difficult to heal and leading to long-term inflammation (Tatulashvili et al., 2020). In the case of diabetic feet, conventional treatment methods, such as blood glucose control and wound debridement, fail to heal the wound in a timely manner, and once infection occurs untreated, amputation is the only option (Mariadoss et al., 2022). Therefore, a drug capable of improving poor wound healing is urgently needed for diabetic. There has been some discussion regarding the potential value of nanomaterials in wound healing and infection control in this regard (Pormohammad et al., 2021; Simos et al., 2021). The development of polymeric, metallic, and ceramic nanomaterials for the treatment of acute and chronic wounds has been found to accelerate the regeneration of damaged dermal and epidermal tissues (Parani et al., 2016). Nanoparticles of silver (AgNPs) synthesized by Varaprasad et al. (2010) are suitable for use as antimicrobial dressings and wound dressings, which represents an important advancement in the field of antimicrobial dual-ion technology. By disrupting bacterial biofilms and causing aggregation of blood cells and platelets, the peptide-modified NFRH developed by Qiu et al. (2021) may accelerate wound healing by disrupting bacterial biofilms (see Figure 4C). A growing number of diabetic patients are living in China, which has led to an increased need for treatment of diabetes and its complications, especially the severe complications of diabetes.

1.1.1.3 Circulatory system therapeutic applications

The pathogenesis of many diseases, including deep vein thrombosis, pulmonary embolism, and ischemic stroke, involves thrombosis (Priya et al., 2021). In clinical practice, antiplatelet agents, anticoagulants, and fibrinolytic drugs are commonly used in the treatment of thrombosis, including arterial and venous thrombosis (Loyau et al., 2018; Khoukaz et al., 2020). In contrast, traditional thrombolytic drugs have a short half-life, low bioavailability, poor targeting, and low output efficiency, and the treatment must be repeated multiple times. An efficient drug is urgently needed to combat the encroachment of thrombotic disease in patients. Researchers have thus turned their attention to the treatment of thrombosis after nanomedicines were first introduced for the treatment of oncological diseases. Worldwide, ischemic stroke is one of the leading causes of severe disability and death, posing a serious public health problem as well as an economic burden on families of patients. Blood supply to the brain from blood vessels is impeded by thrombosis, resulting in a sudden reduction in cerebral blood flow caused by a series of pathological changes. These changes ultimately lead to cerebral ischemia, which can result in severe disability and even death (Ma et al., 2021). Consequently, a variety of nanomedicines have been developed with the goal of improving the effectiveness and precision of thrombosis treatments (Su et al., 2020). Timely and effective thrombolytic therapy is of great clinical significance, and nanomedicines such as liposomes, polymer nanoparticles, and magnetic nanoparticles offer great potential (Liu et al., 2018). Furthermore, Xu et al. (2019) developed a dextran-derived polymeric nanoparticle-based nanocarrier (tP-NP-rtPA/ZL006e) for simultaneous delivery of tissue fibrinogen and dextran-derived polymeric nanoparticles (see Figure 5A). Compared to conventional free drugs, this nanodrug reduced the ischemic area more effectively in *in vitro* and *in vivo* experiments. By contrast, the small extracellular vesicle (sEV)-based drug delivery system developed by Loch-Neckel et al. (2022) is endogenous nanovesicles that have excellent targeting capabilities and are naturally biocompatible (see Figure 5B). These devices are more advantageous in treating CNS diseases, providing greater benefits for the treatment of Alzheimer's disease, brain tumors and other diseases, as they can cross the blood-brain barrier and target specific nerve cells. Nanomaterials have also shown great potential when combined with traditional Chinese medicine. Salvianolic acid B(SAB), a water-soluble phenolic acid derived from Salvia miltiorrhiza, a traditional Chinese medicine. According to Zhang S. et al. (2022), the RR@SABNPs are a brain-targeted bionanopharmaceutical made of bovine serum albumin nanoparticles that contain salvianolic acid and functionalized red blood cell membranes that contain salvianolic acid. In addition to stability, it is biocompatible as well. Influenced by single-cell organisms, Zhang et al.propose a strategy to use programmed alternating magnetic fields to enable amoeboid microrobots to more effectively deliver thrombolytic drugs and unblock embolic vessels (Zhang et al., 2023).

Furthermore, in a mouse model of infarction, the drug significantly scavenged excess reactive oxygen species and reduced infarct size. It is anticipated that the number of patients who suffer from severe disability or even death as a result of thrombosis will be greatly reduced.

1.1.2 Other disease treatment related applications

Nanomedicine has also demonstrated promising results in the research of diseases other than tumors and blood clots mentioned above. As the sixth leading cause of death in humans, pneumonia is caused by a variety of pathogens such as bacteria, viruses, and fungi that cause damage to lung tissue or interstitial lung. Despite their effectiveness in treating common pneumonia, conventional drugs are less effective in treating some critically ill patients, such as those with acute lung injury. In light of this, the development of new drugs for the specific treatment of critically ill patients is one of the most

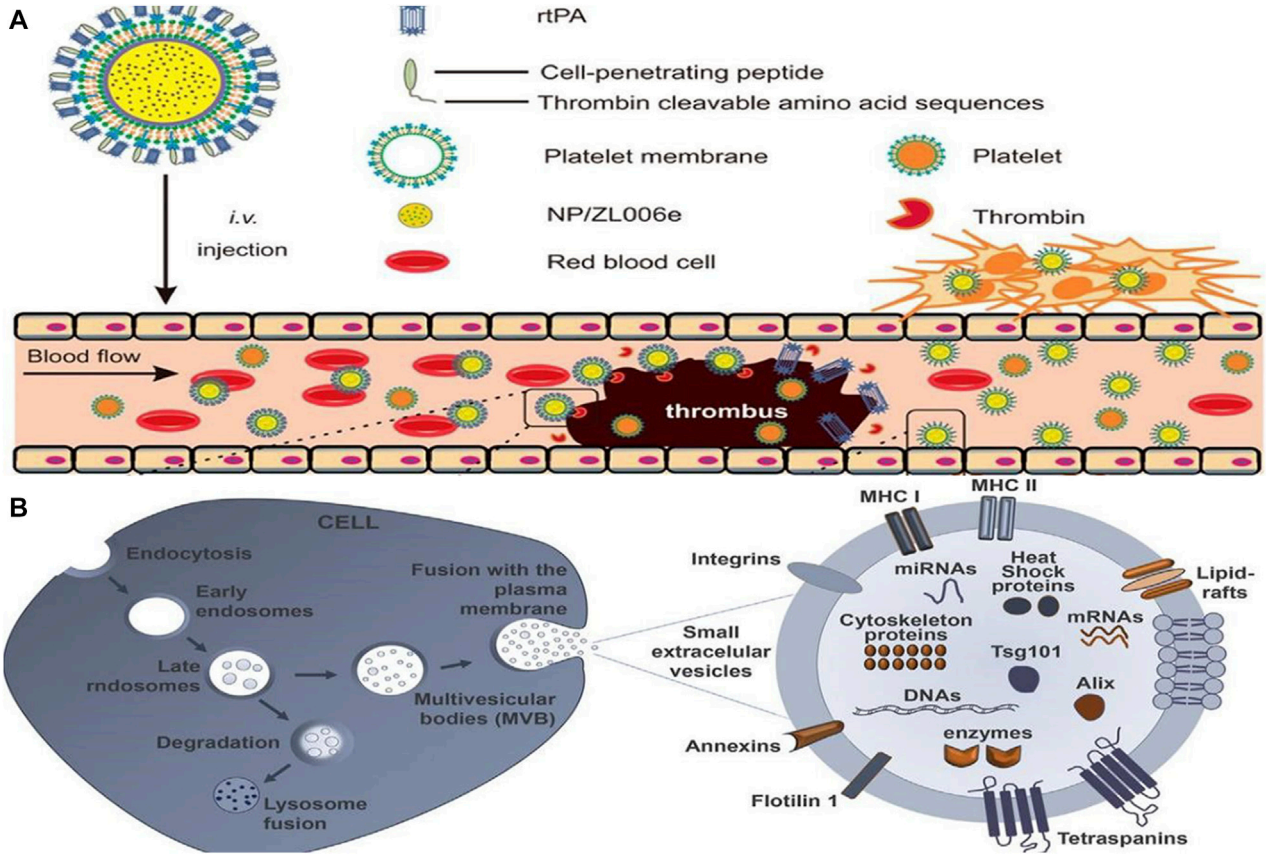

FIGURE 5
(A) Main components of the tP-NP-rtPA/ZL006e (Xu et al., 2019). Reproduced with permission. Copyright 2019, ACS Nano; **(B)** Schematic illustration of formation of sEV biogenesis (Loch-Neckel et al., 2022). Reproduced with permission. Copyright 2022, Front. Pharmacol.

hotly debated topics in current research (Muhammad et al., 2022). According to Mukhaerjee et al., silver Prussian blue (PB) analog nanoparticles (SPBANPs), a new nanopharmaceutical formulation developed by combining PB with silver salts (silver nitrate). The SPBANPs demonstrated excellent antibacterial activity in Gram-negative bacteria (*Escherichia coli*, *Klebsiella pneumoniae*, and *Pseudomonas aeruginosa*) and Gram-positive bacteria (*Bacillus subtilis*) (Mukherjee et al., 2020). A worldwide pandemic of COVID-19 has caused the development of vaccines, and nanotechnology has been an integral part of the development of efficient, safe, and relatively affordable vaccines based on nanomedicine principles in order to control the pandemic (Al-Hatamleh et al., 2021; Shapiro, 2021). It has been determined that vaccines based on nanomedicine principles will be effective, safe, and cost-effective in the fight against the COVID-19 pandemic across the globe. Nanotechnology has played an integral part in developing such vaccines (Tang et al., 2017; Niu et al., 2021). William M. Pardridge develops a drug that both encapsulates plasmid DNA encoding a therapeutic gene and crosses the blood-brain barrier (BBB). The drug uses Trojan horse liposomes (THL), also known as polyethylene glycolated immunoliposomes, formed by encapsulation of plasmid DNA inside polyethylene glycolated liposomes with a net anionic charge, and THL is developed as a receptor-targeted nanomedicine for the treatment of human central nervous system disorders. (Pardridge, 2020).

1.2 Diagnostic applications of nanomedicine

Through the advancement of nanotechnology, nanomaterials of various types, shapes, and sizes are being applied to biosensors in order to enhance their sensitivity and accuracy in detecting diseases (Spychalska et al., 2020). Salahandish et al. (2018), for instance, used graphene, a material which is highly thermally stable and has good gas barrier properties. For the detection of miRNA-21, which is a breast cancer marker, a graphene-based (NFG) nanosensor with silver nanoparticles (AgNPs) is developed with high sensitivity, which could be useful for the early diagnosis of breast cancer (see Figure 6A). Zhang et al. proposed the use of magnetic properties of iron oxide nanoparticles as MRI contrast enhancer. Such particles can form magnetic fields and are easily deformed and manipulated. This method makes MRI of lesion sites easier to visualize and also effectively reduces the amount of contrast agent used (Zhang Z. et al., 2022).

During the treatment of diabetes, it is imperative to develop new methods of monitoring blood glucose levels, since the

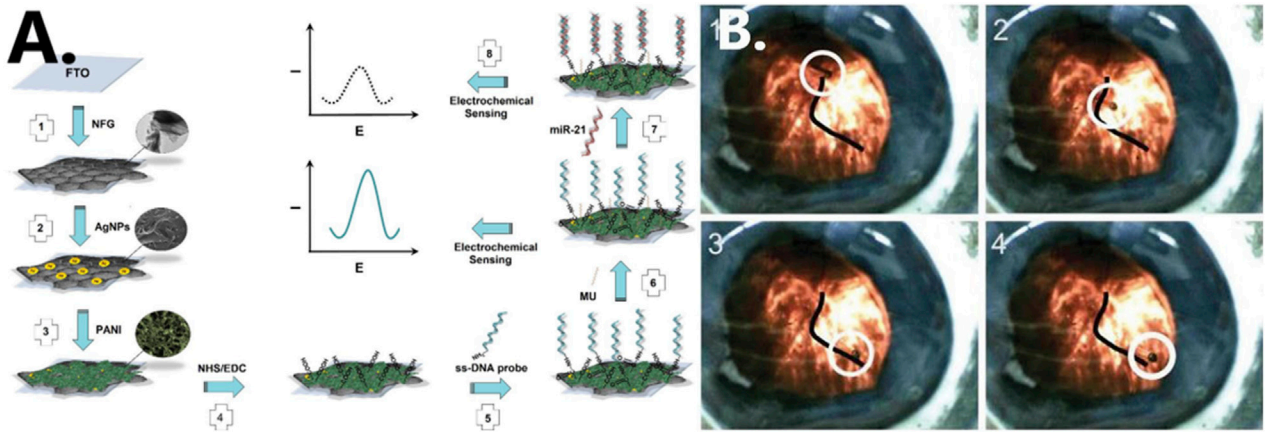

FIGURE 6
(A) Schematic illustration of formation of nanocomposite fabrication (Salahandish et al., 2018). Reproduced with permission. Copyright 2018, Biosensors and Bioelectronics; **(B)** cobalt-nickel (CoNi) microtube steered along a vein in a porcine eye (Chatzipirpiridis et al., 2015). Reproduced with permission. Copyright 2015, Advanced Healthcare Materials.

current methods are relatively cumbersome to diagnose and monitor. Biosensors based on nanoparticles offer increased glucose monitoring sensitivity, allowing clinicians and researchers to quantify diabetes levels and make further diagnoses with greater accuracy (Kovatchev, 2018; Wang Y. et al., 2021).

1.3 Surgical procedures utilizing nanomedicine

It is also possible to use nanomedicine technology in minimally invasive surgical procedures. Since micro-/nanorobots are small and lightweight, they offer increased flexibility in narrow biological tissue environments. Macro-/nanorobots can perform a number of precise micro-operations and reduce tissue damage during surgery, as well as perform functions that macro-/nanorobots cannot.

In a live rabbit eye, Chatzipirpiridis et al. successfully operated a micro-/nanorobot wirelessly by rotating around its axis and injecting a 23-gauge needle into the central vitreous fluid (see Figure 6B) (Chatzipirpiridis et al., 2015). Researchers insert nanorobots into rat brains through the nose to perform different types of movements by regulating the magnetic field. They are currently investigating the insertion of magnetic microrobots into neural tissue to induce behavioral changes in small mammals (Soto et al., 2020). In the future, it may be possible to develop micro-/nanorobots that can treat diseases in other narrow areas of the human body. In this study, it has been shown that micro-/nanorobots can significantly reduce tissue damage during surgery owing to their own properties, and their use in minimally invasive surgery holds great promise. It has demonstrated excellent potential in experimental studies, even though it has not yet been able to be scaled up to the clinical setting.

2 Nanomedicine faces numerous challenges

In Micro-/nanorobots are much smaller than macro-robots and they can pass through biological tissues to reach the lesion, allowing precise micro-operations and accurate drug delivery in complex biological environments. There is a great deal of potential in nanotechnology for the future. Medical nanotechnology still faces many problems in practical clinical applications despite the numerous breakthroughs and innovations in nanotechnology and materials science in recent decades.

1) Micro-/nanorobots are used to deliver nanomedicines due to their small size, allowing them to penetrate deep into biological tissues with less damage and to cross the blood-brain barrier to reach sites which conventional drugs are unable to reach. However, their drug-carrying capacity is slightly insufficient, and they can also have difficulty transporting large molecules. Therefore, further research is needed to promote nanorobots to break through *in vivo* biological barriers and achieve multi-drug carriage more effectively.
2) A crucial aspect of the development process is the selection of nanomaterials. In particular, the preparation of micro-/nanorobots that utilize naturally occurring microorganisms in nature must address the problem of life support for microorganisms as well as the provision of nutrients necessary for their growth. It is important to consider the toxicity, degradability and applicability of the materials used in the preparation of micro-/nanorobots using artificial technologies (such as 3D printing) and whether they can be widely used.
3) Depending on the degree of lesions, the appropriate amount of nanomedicine should be released, as well as how to provide timely and accurate feedback regarding whether the expected effect has been achieved. When the drug has been delivered and released into the body, it should be completely and safely discharged outside the body.

4) Currently, cross-disciplinary cooperation and exchange are insufficient; basic research needs to be improved, and some important theoretical issues involving nanomedicines still require further study.

3 Overview and outlook

With continuous innovations and breakthroughs in nanomedicine technology, diagnosis and treatment at the microscopic level are increasingly becoming a reality, and nanomedicine technology is widely used in clinical treatment, disease diagnosis and other medical fields. However, nanomedicine does not yet have a perfect solution to many major diseases, and safety issues and other problems remain challenging. However, the system is not yet perfect and some problems still exist. In the field of nanomedicine technology, solving the material, functional and safety-related problems of nanocarriers is still a hot spot for research with wider potential applications, which deserves more in-depth exploration and research.

Author contributions

ZQ and CN conceived the idea of the study. SX and CN analyzed the data. YL and LW interpreted the results and wrote the paper. ZQ and CN discussed the results and revised the manuscript. All authors read and approved the final manuscript. All authors contributed to the article and approved the submitted version.

Funding

This work is supported by The President's Fund of the Fourth Affiliated Hospital of Harbin Medical University (HYDSYYZ201502); Natural Science Foundation of Heilongjiang Province (LH 2020H063); Outstanding Youth Fund of the Fourth Hospital of Harbin Medical University (HYDSYYXQN202008); Heilongjiang Provincial Academy of Science and Technology Cooperation Project (YS18C06); Heilongjiang Province Postdoctoral Fund (LBH-Z21170); Sichuan Provincial Western Psychiatric Association's CSPC Leading Scientific Research Project.

Conflict of interest

The authors declare that the research was conducted in the absence of any commercial or financial relationships that could be construed as a potential conflict of interest.

Publisher's note

All claims expressed in this article are solely those of the authors and do not necessarily represent those of their affiliated organizations, or those of the publisher, the editors and the reviewers. Any product that may be evaluated in this article, or claim that may be made by its manufacturer, is not guaranteed or endorsed by the publisher.

References

Ahmed, D., Lu, M., Nourhani, A., Lammert, P. E., Stratton, Z., Muddana, H. S., et al. (2015). Selectively manipulable acoustic-powered microswimmers. *Sci. Rep.* 5, 9744. doi:10.1038/srep09744

Al-Hatamleh, M. A. I., Hatmal, M. M., Alshaer, W., Rahman, E. N. S. E. A., Mohd-Zahid, M. H., Alhaj-Qasem, D. M., et al. (2021). COVID-19 infection and nanomedicine applications for development of vaccines and therapeutics: An overview and future perspectives based on polymersomes. *Eur. J. Pharmacol.* 896, 173930. doi:10.1016/j.ejphar.2021.173930

Ashrafizadeh, M., Kumar, A., Aref, A., Zarrabi, A., and Mostafavi, E. (2022). Exosomes as promising nanostructures in diabetes mellitus: From insulin sensitivity to ameliorating diabetic complications. *Int. J. Nanomedicine* 17, 1229–1253. doi:10.2147/IJN.S350250

Bakrania, A., Zheng, G., and Bhat, M. (2021). Nanomedicine in hepatocellular carcinoma: A new frontier in targeted cancer treatment. *Pharmaceutics* 14, 41. doi:10.3390/pharmaceutics14010041

Balogh, M., Janjic, J. M., and Shepherd, A. J. (2022). Targeting neuroimmune interactions in diabetic neuropathy with nanomedicine. *Antioxidants Redox Signal.* 36, 122–143. doi:10.1089/ars.2021.0123

Banerjee, A., Sharma, D., Trivedi, R., and Singh, J. (2020). Treatment of insulin resistance in obesity-associated type 2 diabetes mellitus through adiponectin gene therapy. *Int. J. Pharm.* 583, 119357. doi:10.1016/j.ijpharm.2020.119357

Barenholz, Y. (2012). Doxil® — the first FDA-approved nano-drug: Lessons learned. *J. Control. Release* 160, 117–134. doi:10.1016/j.jconrel.2012.03.020

Beloqui, A., Alhouayek, M., Carradori, D., Vanvarenberg, K., Muccioli, G. G., Cani, P. D., et al. (2016). A mechanistic study on nanoparticle-mediated glucagon-like peptide-1 (GLP-1) secretion from enteroendocrine L cells. *Mol. Pharm.* 13, 4222–4230. doi:10.1021/acs.molpharmaceut.6b00871

Chatzipirpiridis, G., Ergeneman, O., Pokki, J., Ullrich, F., Fusco, S., Ortega, J. A., et al. (2015). Electroforming of implantable tubular magnetic microrobots for wireless ophthalmologic applications. *Adv. Healthc. Mat.* 4, 209–214. doi:10.1002/adhm.201400256

Chen, H., Huang, S., Wang, H., Chen, X., Zhang, H., Xu, Y., et al. (2021). Preparation and characterization of paclitaxel palmitate albumin nanoparticles with high loading efficacy: An *in vitro* and *in vivo* anti-tumor study in mouse models. *Drug Deliv.* 28, 1067–1079. doi:10.1080/10717544.2021.1921078

Chen, J., Zhou, L., Wang, C., Sun, Y., Lu, Y., Li, R., et al. (2020). A multifunctional SN38-conjugated nanosystem for defeating myelosuppression and diarrhea induced by irinotecan in esophageal cancer. *Nanoscale* 12, 21234–21247. doi:10.1039/D0NR06266A

Cheng, H.-W., Chiang, C.-S., Ho, H.-Y., Chou, S.-H., Lai, Y.-H., Shyu, W.-C., et al. (2021). Dextran-modified quercetin-Cu(II)/Hyaluronic acid nanomedicine with natural poly(ADP-ribose) polymerase inhibitor and dual targeting for programmed synthetic lethal therapy in triple-negative breast cancer. *J. Control. Release* 329, 136–147. doi:10.1016/j.jconrel.2020.11.061

Chi, C., Li, F., Liu, H., Feng, S., Zhang, Y., Zhou, D., et al. (2019). Docetaxel-loaded biomimetic nanoparticles for targeted lung cancer therapy *in vivo*. *J. Nanopart Res.* 21, 144. doi:10.1007/s11051-019-4580-8

Deng, G., Peng, X., Sun, Z., Zheng, W., Yu, J., Du, L., et al. (2020). Natural-killer-cell-inspired nanorobots with aggregation-induced emission characteristics for near-infrared-II fluorescence-guided glioma theranostics. *ACS Nano* 14, 11452–11462. doi:10.1021/acsnano.0c03824

Desai, N., Koppisetti, H., Pande, S., Shukla, H., Sirsat, B., Ditani, A. S., et al. (2021b). Nanomedicine in the treatment of diabetic nephropathy. *Future Med. Chem.* 13, 663–686. doi:10.4155/fmc-2020-0335

Desai, N., Momin, M., Khan, T., Gharat, S., Ningthoujam, R. S., and Omri, A. (2021a). Metallic nanoparticles as drug delivery system for the treatment of cancer. *Expert Opin. Drug Deliv.* 18, 1261–1290. doi:10.1080/17425247.2021.1912008

Díez, P., Esteban-Fernández de Ávila, B., Ramírez-Herrera, D. E., Villalonga, R., and Wang, J. (2017). Biomedical nanomotors: Efficient glucose-mediated insulin release. *Nanoscale* 9, 14307–14311. doi:10.1039/C7NR05535H

Ding, Y., Xu, H., Xu, C., Tong, Z., Zhang, S., Bai, Y., et al. (2020). A nanomedicine fabricated from gold nanoparticles-decorated metal–organic framework for cascade chemo/chemodynamic cancer therapy. *Adv. Sci.* 7, 2001060. doi:10.1002/advs.202001060

Dong, R., Zhang, Q., Gao, W., Pei, A., and Ren, B. (2016). Highly efficient light-driven TiO_2–Au Janus micromotors. *ACS Nano* 10, 839–844. doi:10.1021/acsnano.5b05940

Elnaggar, M. H., Abushouk, A. I., Hassan, A. H. E., Lamloum, H. M., Benmelouka, A., Moatamed, S. A., et al. (2021). Nanomedicine as a putative approach for active targeting of hepatocellular carcinoma. *Seminars Cancer Biol.* 69, 91–99. doi:10.1016/j.semcancer.2019.08.016

Fadeel, B., and Alexiou, C. (2020). Brave new world revisited: Focus on nanomedicine. *Biochem. Biophysical Res. Commun.* 533, 36–49. doi:10.1016/j.bbrc.2020.08.046

Ferrari, M. (2010). Frontiers in cancer nanomedicine: Directing mass transport through biological barriers. *Trends Biotechnol.* 28, 181–188. doi:10.1016/j.tibtech.2009.12.007

Gao, J., Nesbitt, H., Logan, K., Burnett, K., White, B., Jack, I. G., et al. (2020). An ultrasound responsive microbubble-liposome conjugate for targeted irinotecan-oxaliplatin treatment of pancreatic cancer. *Eur. J. Pharm. Biopharm.* 157, 233–240. doi:10.1016/j.ejpb.2020.10.012

Germain, M., Caputo, F., Metcalfe, S., Tosi, G., Spring, K., Åslund, A. K. O., et al. (2020). Delivering the power of nanomedicine to patients today. *J. Control. Release* 326, 164–171. doi:10.1016/j.jconrel.2020.07.007

Halder, A., and Sun, Y. (2019). Biocompatible propulsion for biomedical micro/nano robotics. *Biosens. Bioelectron.* 139, 111334. doi:10.1016/j.bios.2019.111334

Hall, R. M., Sun, T., and Ferrari, M. (2012). A portrait of nanomedicine and its bioethical implications. *J. Law. Med. Ethics* 40, 763–779. doi:10.1111/j.1748-720X.2012.00705.x

Howard, F. H. N., Al-Janabi, H., Patel, P., Cox, K., Smith, E., Vadakekolathu, J., et al. (2022). Nanobugs as drugs: Bacterial derived nanomagnets enhance tumor targeting and oncolytic activity of HSV-1 virus. *Small* 18, 2104763. doi:10.1002/smll.202104763

Hu, M., Ge, X., Chen, X., Mao, W., Qian, X., and Yuan, W.-E. (2020). Micro/nanorobot: A promising targeted drug delivery system. *Pharmaceutics* 12, 665. doi:10.3390/pharmaceutics12070665

Jacob, S., Nair, A. B., and Shah, J. (2020). Emerging role of nanosuspensions in drug delivery systems. *Biomater. Res.* 24, 3. doi:10.1186/s40824-020-0184-8

Jang, D., Jeong, J., Song, H., and Chung, S. K. (2019). Targeted drug delivery technology using untethered microrobots: A review. *J. Micromech. Microeng.* 29, 053002. doi:10.1088/1361-6439/ab087d

Ji, F., Li, T., Yu, S., Wu, Z., and Zhang, L. (2021). Propulsion gait analysis and fluidic trapping of swinging flexible nanomotors. *ACS Nano* 15, 5118–5128. doi:10.1021/acsnano.0c10269

Karahalios, A., Somarajah, G., Hamblin, P. S., Karunajeewa, H., and Janus, E. D. (2018). Quantifying the hidden Healthcare cost of diabetes mellitus in Australian hospital patients: Cost of diabetes in Australian hospitals. *Intern Med. J.* 48, 286–292. doi:10.1111/imj.13685

Kheraldine, H., Rachid, O., Habib, A. M., Al Moustafa, A.-E., Benter, I. F., and Akhtar, S. (2021). Emerging innate biological properties of nano-drug delivery systems: A focus on pamam dendrimers and their clinical potential. *Adv. Drug Deliv. Rev.* 178, 113908. doi:10.1016/j.addr.2021.113908

Khoukaz, H. B., Ji, Y., Braet, D. J., Vadali, M., Abdelhamid, A. A., Emal, C. D., et al. (2020). Drug targeting of plasminogen activator inhibitor-1 inhibits metabolic dysfunction and atherosclerosis in a murine model of metabolic syndrome. *ATVB* 40, 1479–1490. doi:10.1161/ATVBAHA.119.313775

Kovatchev, B. (2018). The year of transition from research to clinical practice. *Nat. Rev. Endocrinol.* 14, 74–76. doi:10.1038/nrendo.2017.170

Kumstel, S., Vasudevan, P., Palme, R., Zhang, X., Wendt, E. H. U., David, R., et al. (2020). Benefits of non-invasive methods compared to telemetry for distress analysis in a murine model of pancreatic cancer. *J. Adv. Res.* 21, 35–47. doi:10.1016/j.jare.2019.09.002

Li, T., Li, J., Morozov, K. I., Wu, Z., Xu, T., Rozen, I., et al. (2017). Highly efficient freestyle magnetic nanoswimmer. *Nano Lett.* 17, 5092–5098. doi:10.1021/acs.nanolett.7b02383

Li, T., Li, J., Zhang, H., Chang, X., Song, W., Hu, Y., et al. (2016). Magnetically propelled fish-like nanoswimmers. *Small* 12, 6098–6105. doi:10.1002/smll.201601846

Li, T., Yang, C., Wei, Z., Pei, D., and Jiang, G. (2020). <p>Recent advances of magnetic nanomaterials in the field of oncology</p>. *OTT* 13, 4825–4832. doi:10.2147/OTT.S243256

Li, T., Yu, S., Sun, B., Li, Y., Wang, X., Pan, Y., et al. (2023). Bioinspired claw-engaged and biolubricated swimming microrobots creating active retention in blood vessels. *Sci. Adv.* 9, eadg4501. doi:10.1126/sciadv.adg4501

Liu, J., Yu, S., Xu, B., Tian, Z., Zhang, H., Liu, K., et al. (2021). Magnetically propelled soft microrobot navigating through constricted microchannels. *Appl. Mater. Today* 25, 101237. doi:10.1016/j.apmt.2021.101237

Liu, S., Feng, X., Jin, R., and Li, G. (2018). Tissue plasminogen activator-based nanothrombolysis for ischemic stroke. *Expert Opin. Drug Deliv.* 15, 173–184. doi:10.1080/17425247.2018.1384464

Liu, Y., Castro Bravo, K. M., and Liu, J. (2021). Targeted liposomal drug delivery: A nanoscience and biophysical perspective. *Nanoscale Horiz.* 6, 78–94. doi:10.1039/D0NH00605J

Llopis-Lorente, A., García-Fernández, A., Murillo-Cremaes, N., Hortelão, A. C., Patiño, T., Villalonga, R., et al. (2019). Enzyme-powered gated mesoporous silica nanomotors for on-command intracellular payload delivery. *ACS Nano* 13, 12171–12183. doi:10.1021/acsnano.9b06706

Loch-Neckel, G., Matos, A. T., Vaz, A. R., and Brites, D. (2022). Challenges in the development of drug delivery systems based on small extracellular vesicles for therapy of brain diseases. *Front. Pharmacol.* 13, 839790. doi:10.3389/fphar.2022.839790

Loyau, S., Ho-Tin-Noé, B., Bourrienne, M.-C., Boulaftali, Y., and Jandrot-Perrus, M. (2018). Microfluidic modeling of thrombolysis: Effect of antiplatelet and anticoagulant agents on TPA (Tissue-Type plasminogen activator)-induced fibrinolysis. *ATVB* 38, 2626–2637. doi:10.1161/ATVBAHA.118.311178

Ma, H., Jiang, Z., Xu, J., Liu, J., and Guo, Z.-N. (2021). Targeted nano-delivery strategies for facilitating thrombolysis treatment in ischemic stroke. *Drug Deliv.* 28, 357–371. doi:10.1080/10717544.2021.1879315

Maheswari, R., Rani Gnanamalar, S. S., Gomathy, V., and Sharmila, P. (2018). Cancer detecting nanobot using positron emission tomography. *SSRN J.* 2018, 3227782. doi:10.2139/ssrn.3227782

Mariadoss, A. V. A., Sivakumar, A. S., Lee, C.-H., and Kim, S. J. (2022). Diabetes mellitus and diabetic foot ulcer: Etiology, biochemical and molecular based treatment strategies via gene and nanotherapy. *Biomed. Pharmacother.* 151, 113134. doi:10.1016/j.biopha.2022.113134

Martin, J. D., Cabral, H., Stylianopoulos, T., and Jain, R. K. (2020). Improving cancer immunotherapy using nanomedicines: Progress, opportunities and challenges. *Nat. Rev. Clin. Oncol.* 17, 251–266. doi:10.1038/s41571-019-0308-z

Mir, M., Ishtiaq, S., Rabia, S., Khatoon, M., Zeb, A., Khan, G. M., et al. (2017). Nanotechnology: From *in vivo* imaging system to controlled drug delivery. *Nanoscale Res. Lett.* 12, 500. doi:10.1186/s11671-017-2249-8

Mou, F., Kong, L., Chen, C., Chen, Z., Xu, L., and Guan, J. (2016). Light-controlled propulsion, aggregation and separation of water-fuelled TiO_2/Pt Janus submicromotors and their "on-the-fly" photocatalytic activities. *Nanoscale* 8, 4976–4983. doi:10.1039/C5NR06774J

Mu, G., Zhao, J., Dong, H., Wu, J., Grattan, K. T. V., and Sun, T. (2021). Structural parameter study of dual transducers-type ultrasonic levitation-based transportation system. *Smart Mater. Struct.* 30 (4), 045009. doi:10.1088/1361-665x/abe4e4

Muhammad, W., Zhai, Z., Wang, S., and Gao, C. (2022). Inflammation-modulating nanoparticles for pneumonia therapy. *WIREs Nanomed Nanobiotechnol* 14, e1763. doi:10.1002/wnan.1763

Mukherjee, S., Kotcherlakota, R., Haque, S., Das, S., Nuthi, S., Bhattacharya, D., et al. (2020). Silver prussian blue analogue nanoparticles: Rationally designed advanced nanomedicine for multifunctional biomedical applications. *ACS Biomater. Sci. Eng.* 6, 690–704. doi:10.1021/acsbiomaterials.9b01693

Niu, L., Fang, Y., Yao, X., Zhang, Y., Wu, J., Chen, D. F., et al. (2021). TNFα activates MAPK and Jak-Stat pathways to promote mouse Müller cell proliferation. *Exp. Eye Res.* 202, 108353. doi:10.1016/j.exer.2020.108353

Oh, H., Jo, H.-Y., Park, J., Kim, D.-E., Cho, J.-Y., Kim, P.-H., et al. (2016). Galactosylated liposomes for targeted Co-delivery of doxorubicin/vimentin SiRNA to hepatocellular carcinoma. *Nanomaterials* 6, 141. doi:10.3390/nano6080141

Olsman, N., and Goentoro, L. (2018). There's (still) plenty of room at the bottom. *Curr. Opin. Biotechnol.* 54, 72–79. doi:10.1016/j.copbio.2018.01.029

Parani, M., Lokhande, G., Singh, A., and Gaharwar, A. K. (2016). Engineered nanomaterials for infection control and healing acute and chronic wounds. *ACS Appl. Mat. Interfaces* 8, 10049–10069. doi:10.1021/acsami.6b00291

Pardridge, W. M. (2020). Brain delivery of nanomedicines: Trojan horse liposomes for plasmid DNA gene therapy of the brain. *Front. Med. Technol.* 2, 602236. doi:10.3389/fmedt.2020.602236

Park, B.-W., Zhuang, J., Yasa, O., and Sitti, M. (2017). Multifunctional bacteria-driven microswimmers for targeted active drug delivery. *ACS Nano* 11, 8910–8923. doi:10.1021/acsnano.7b03207

Peng, Y., Huang, J., Xiao, H., Wu, T., and Shuai, X. (2018). Codelivery of temozolomide and SiRNA with polymeric nanocarrier for effective glioma treatment. *IJN* 13, 3467–3480. doi:10.2147/IJN.S164611

Pormohammad, A., Monych, N. K., Ghosh, S., Turner, D. L., and Turner, R. J. (2021). Nanomaterials in wound healing and infection control. *Antibiotics* 10, 473. doi:10.3390/antibiotics10050473

Priya, V., Viswanadh, M. K., Mehata, A. K., Jain, D., Singh, S. K., and Muthu, M. S. (2021). Targeted nanotherapeutics in the prophylaxis and treatment of thrombosis. *Nanomedicine* 16, 1153–1176. doi:10.2217/nnm-2021-0058

Qiu, W., Han, H., Li, M., Li, N., Wang, Q., Qin, X., et al. (2021). Nanofibers reinforced injectable hydrogel with self-healing, antibacterial, and hemostatic properties for chronic wound healing. *J. Colloid Interface Sci.* 596, 312–323. doi:10.1016/j.jcis.2021.02.107

Sadoughi, F., Hallajzadeh, J., Asemi, Z., Mansournia, M. A., and Yousefi, B. (2021). Nanocellulose-based delivery systems and cervical cancer: Review of the literature. *CPD* 27, 4707–4715. doi:10.2174/1381612827666210927110937

Salahandish, R., Ghaffarinejad, A., Omidinia, E., Zargartalebi, H., Majidzadeh-A, K., Naghib, S. M., et al. (2018). Label-free ultrasensitive detection of breast cancer MiRNA-21 biomarker employing electrochemical nano-genosensor based on sandwiched AgNPs in PANI and N-doped graphene. *Biosens. Bioelectron.* 120, 129–136. doi:10.1016/j.bios.2018.08.025

Salapa, J., Bushman, A., Lowe, K., and Irudayaraj, J. (2020). Nano drug delivery systems in upper gastrointestinal cancer therapy. *Nano Converg.* 7, 38. doi:10.1186/s40580-020-00247-2

Shapiro, R. S. (2021). COVID-19 vaccines and nanomedicine. *Int. J. Dermatol* 60, 1047–1052. doi:10.1111/ijd.15673

Simos, Y. V., Spyrou, K., Patila, M., Karouta, N., Stamatis, H., Gournis, D., et al. (2021). Trends of nanotechnology in type 2 diabetes mellitus treatment. *Asian J. Pharm. Sci.* 16, 62–76. doi:10.1016/j.ajps.2020.05.001

Sindhu, R. K., Kaur, H., Kumar, M., Sofat, M., Yapar, E. A., Esenturk, I., et al. (2021). The ameliorating approach of nanorobotics in the novel drug delivery systems: A mechanistic review. *J. Drug Target.* 29, 822–833. doi:10.1080/1061186X.2021.1892122

Soto, F., Wang, J., Ahmed, R., and Demirci, U. (2020). Medical robotics: Medical micro/nanorobots in precision medicine. *Adv. Sci.* 7 (21), 2070117. doi:10.1002/advs.202070117

Spychalska, K., Zając, D., Baluta, S., Halicka, K., and Cabaj, J. (2020). Functional polymers structures for (Bio)Sensing application—a review. *Polymers* 12, 1154. doi:10.3390/polym12051154

Su, M., Dai, Q., Chen, C., Zeng, Y., Chu, C., and Liu, G. (2020). Nano-medicine for thrombosis: A precise diagnosis and treatment strategy. *Nano-Micro Lett.* 12, 96. doi:10.1007/s40820-020-00434-0

Tang, H., Xiang, D., Wang, F., Mao, J., Tan, X., and Wang, Y. (2017). 5-ASA-Loaded SiO_2 nanoparticles-a novel drug delivery system targeting therapy on ulcerative colitis in mice. *Mol. Med. Rep.* 15, 1117–1122. doi:10.3892/mmr.2017.6153

Tatulashvili, S., Fagherazzi, G., Dow, C., Cohen, R., Fosse, S., and Bihan, H. (2020). Socioeconomic inequalities and type 2 diabetes complications: A systematic review. *Diabetes and Metabolism* 46, 89–99. doi:10.1016/j.diabet.2019.11.001

Tuguntaev, R. G., Hussain, A., Fu, C., Chen, H., Tao, Y., Huang, Y., et al. (2022). Bioimaging guided pharmaceutical evaluations of nanomedicines for clinical translations. *J. Nanobiotechnol* 20, 236. doi:10.1186/s12951-022-01451-4

Varaprasad, K., Mohan, Y. M., Ravindra, S., Reddy, N. N., Vimala, K., Monika, K., et al. (2010). Hydrogel-silver nanoparticle composites: A new generation of antimicrobials. *J. Appl. Polym. Sci.* 115, 1199–1207. doi:10.1002/app.31249

Venkatas, J., and Singh, M. (2021). Nanomedicine-mediated optimization of immunotherapeutic approaches in cervical cancer. *Nanomedicine* 16, 1311–1328. doi:10.2217/nnm-2021-0044

Vessby, B., Karlström, B., Öhrvall, M., Järvi, A., Andersson, A., and Basu, S. (2000). Diet, nutrition and diabetes mellitus. *Upsala J. Med. Sci.* 105, 151–160. doi:10.1517/03009734000000061

Walker, D., Kübler, M., Morozov, K. I., Fischer, P., and Leshansky, A. M. (2015). Optimal length of low Reynolds number nanopropellers. *Nano Lett.* 15, 4412–4416. doi:10.1021/acs.nanolett.5b01925

Wang, H., Yu, S., Liao, J., Qing, X., Sun, D., Ji, F., et al. (2022). A robot platform for highly efficient pollutant purification. *Front. Bioeng. Biotechnol.* 10, 903219. doi:10.3389/fbioe.2022.903219

Wang, J., Liu, X., Qi, Y., Liu, Z., Cai, Y., and Dong, R. (2021). Ultrasound-propelled nanomotors for improving antigens cross-presentation and cellular immunity. *Chem. Eng. J.* 416 (4), 129091. doi:10.1016/j.cej.2021.129091

Wang, J., Qian, Y., Xu, L., Shao, Y., Zhang, H., Shi, F., et al. (2020). Hyaluronic acid-shelled, peptide drug conjugate-cored nanomedicine for the treatment of hepatocellular carcinoma. *Mater. Sci. Eng. C* 117, 111261. doi:10.1016/j.msec.2020.111261

Wang, Q., Dong, Q., Yang, Q., Wang, J., Xu, S., and Cai, Y. (2020). Highly efficient visible-light-driven oxygen-vacancy-based $Cu_{2+1}O$ micromotors with biocompatible fuels. *Nanoscale Horizons* 5 (2), 325–330. doi:10.1039/c9nh00592g

Wang, S., Yan, C., Zhang, X., Shi, D., Chi, L., Luo, G., et al. (2018). Antimicrobial peptide modification enhances the gene delivery and bactericidal efficiency of gold nanoparticles for accelerating diabetic wound healing. *Biomater. Sci.* 6, 2757–2772. doi:10.1039/C8BM00807H

Wang, S., Zhang, F., Yu, G., Wang, Z., Jacobson, O., Ma, Y., et al. (2020). Zwitterionic-to-Cationic charge conversion polyprodrug nanomedicine for enhanced drug delivery. *Theranostics* 10, 6629–6637. doi:10.7150/thno.47849

Wang, T., He, W., Du, Y., Wang, J., and Li, X. (2021). Redox-sensitive irinotecan liposomes with active ultra-high loading and enhanced intracellular drug release. *Colloids Surfaces B Biointerfaces* 206, 111967. doi:10.1016/j.colsurfb.2021.111967

Wang, X., Zhong, X., Li, J., Liu, Z., and Cheng, L. (2021). Inorganic nanomaterials with rapid clearance for biomedical applications. *Chem. Soc. Rev.* 50, 8669–8742. doi:10.1039/D0CS00461H

Wang, Y., Wang, C., Li, K., Song, X., Yan, X., Yu, L., et al. (2021). Recent advances of nanomedicine-based strategies in diabetes and complications management: Diagnostics, monitoring, and therapeutics. *J. Control. Release* 330, 618–640. doi:10.1016/j.jconrel.2021.01.002

Xin, C., Yang, L., Li, J., Hu, Y., Qian, D., Fan, S., et al. (2019). Conical hollow microhelices with superior swimming capabilities for targeted cargo delivery. *Adv. Mat.* 31, 1808226. doi:10.1002/adma.201808226

Xu, J., Wang, X., Yin, H., Cao, X., Hu, Q., Lv, W., et al. (2019). Sequentially site-specific delivery of thrombolytics and neuroprotectant for enhanced treatment of ischemic stroke. *ACS Nano* 13, 8577–8588. doi:10.1021/acsnano.9b01798

Yang, Q., Xu, H., Wen, H., Zhao, H., Liu, X., Cai, Y., et al. (2021). Graphene oxide induced enhancement of light-driven micromotor with biocompatible fuels. *Appl. Mater. Today* 22, 100943. doi:10.1016/j.apmt.2021.100943

Yu, S., Li, T., Ji, F., Zhao, S., Liu, K., Zhang, Z., et al. (2022). Trimer-like microrobots with multimodal locomotion and reconfigurable capabilities. *Mater. Today Adv.* 14, 100231. doi:10.1016/j.mtadv.2022.100231

Zhan, Y., Ma, W., Zhang, Y., Mao, C., Shao, X., Xie, X., et al. (2019). DNA-based nanomedicine with targeting and enhancement of therapeutic efficacy of breast cancer cells. *ACS Appl. Mat. Interfaces* 11, 15354–15365. doi:10.1021/acsami.9b03449

Zhang, J., Hu, J., Chan, H. F., Skibba, M., Liang, G., and Chen, M. (2016). IRGD decorated lipid-polymer hybrid nanoparticles for targeted Co-delivery of doxorubicin and sorafenib to enhance anti-hepatocellular carcinoma efficacy. *Nanomedicine Nanotechnol. Biol. Med.* 12, 1303–1311. doi:10.1016/j.nano.2016.01.017

Zhang, S., Li, R., Zheng, Y., Zhou, Y., and Fan, X. (2022). Erythrocyte membrane-enveloped salvianolic acid B nanoparticles attenuate cerebral ischemia-reperfusion injury. *IJN* 17, 3561–3577. doi:10.2147/IJN.S375908

Zhang, W., Deng, Y., Zhao, J., Zhang, T., Zhang, X., Song, W., et al. (2023). Amoeba-inspired magnetic venom microrobots. *Small* 2023, 2207360. doi:10.1002/smll.202207360

Zhang, X., Li, N., Zhang, S., Sun, B., Chen, Q., He, Z., et al. (2020). Emerging carrier-free nanosystems based on molecular self-assembly of pure drugs for cancer therapy. *Med. Res. Rev.* 40, 1754–1775. doi:10.1002/med.21669

Zhang, X., Ng, H. L. H., Lu, A., Lin, C., Zhou, L., Lin, G., et al. (2016). Drug delivery system targeting advanced hepatocellular carcinoma: Current and future. *Nanomedicine Nanotechnol. Biol. Med.* 12, 853–869. doi:10.1016/j.nano.2015.12.381

Zhang, Z., Wang, H., Yang, H., Song, W., Dai, L., Yu, S., et al. (2022). Magnetic microswarm for MRI contrast enhancer. *Chem. Asian J.* 17, e202200561. doi:10.1002/asia.202200561

Zhao, S., Sun, D., Zhang, J., Lu, H., Wang, Y., Xiong, R., et al. (2022). Actuation and biomedical development of micro-/nanorobots – a review. *Mater. Today Nano* 18, 100223. doi:10.1016/j.mtnano.2022.100223

Zhao, W., Li, J., Zhong, C., Zhang, X., and Bao, Y. (2021). Green synthesis of gold nanoparticles from *Dendrobium officinale* and its anticancer effect on liver cancer. *Drug Deliv.* 28, 985–994. doi:10.1080/10717544.2021.1921079

Zingg, R., and Fischer, M. (2019). The consolidation of nanomedicine. *WIREs Nanomed Nanobiotechnol* 11, e1569. doi:10.1002/wnan.1569

frontiers | Frontiers in Bioengineering and Biotechnology

TYPE Review
PUBLISHED 12 September 2023
DOI 10.3389/fbioe.2023.1277964

OPEN ACCESS

EDITED BY
Tianlong Li,
Harbin Institute of Technology, China

REVIEWED BY
Haoran Mu,
Shanghai Jiao Tong University, China
Dongfang Li,
Yale University, United States
Fuzhou Niu,
Suzhou University of Science and Technology, China

*CORRESPONDENCE
Wenlong Liang,
liangwenlong@hrbmu.edu.cn
Yufu Wang,
wangyufu@hrbmu.edu.cn

†These authors have contributed equally to this work

RECEIVED 15 August 2023
ACCEPTED 31 August 2023
PUBLISHED 12 September 2023

CITATION
Niu J, Liu C, Yang X, Liang W and Wang Y (2023), Construction of micro-nano robots: living cells and functionalized biological cell membranes.
Front. Bioeng. Biotechnol. 11:1277964.
doi: 10.3389/fbioe.2023.1277964

Construction of micro-nano robots: living cells and functionalized biological cell membranes

Jiawen Niu[1†], Chenlu Liu[1†], Xiaopeng Yang[1], Wenlong Liang[2*] and Yufu Wang[1*]

[1]Department of Orthopedic Surgery, The Second Affiliated Hospital of Harbin Medical University, Harbin, China, [2]Department of Breast Surgery, The Second Affiliated Hospital of Harbin Medical University, Harbin, China

Micro-nano robots have emerged as a promising research field with vast potential applications in biomedicine. The motor is the key component of micro-nano robot research, and the design of the motor is crucial. Among the most commonly used motors are those derived from living cells such as bacteria with flagella, sperm, and algal cells. Additionally, scientists have developed numerous self-adaptive biomimetic motors with biological functions, primarily cell membrane functionalized micromotors. This novel type of motor exhibits remarkable performance in complex media. This paper provides a comprehensive review of the structure and performance of micro-nano robots that utilize living cells and functionalized biological cell membranes. We also discuss potential practical applications of these mirco-nano robots as well as potential challenges that may arise in future development.

KEYWORDS

micro-nano robots, micromotors, living cells and cell membranes, drug delivery, immunotherapy, phototherapy

1 Introduction

The field of robotics has experienced a rapid development, resulting in their widespread use in various industries. These robots come in different sizes, ranging from microscopic to macroscopic, with the latter being commonly used in industrial production, service industries, and military warfare. However, the size of macroscopic robots limits their application in certain situations, such as *in vivo* interventional diagnosis and treatment (Soto et al., 2022). This limitation has led to the emergence of micro-nano robots (Wang and Pumera, 2015; Esteban-Fernández et al., 2018; Venugopalan et al., 2020; Wang and Zhang, 2021; Wang X et al., 2022), which are capable of operating on the micro-nano scale and exhibit remarkable flexibility and adaptability. Furthermore, it is capable of working collaboratively within a cluster (Law et al., 2022). In recent decades, micro-nano robots have emerged as a promising field of research with applications in biomedicine, particularly in targeted drug delivery and disease diagnosis and treatment (Zhang et al., 2022a; Wang et al., 2023; Zhang L et al., 2023).

Over the past decade, significant advancements have been made in the design and production of micromotors that utilize various driving methods (Hines et al., 2017; Wang C et al., 2018; Venugopalan et al., 2020). These artificial micro-nano robots can be powered by different propulsion mechanisms including magnetic actuation (Huang et al., 2022; T et al.,

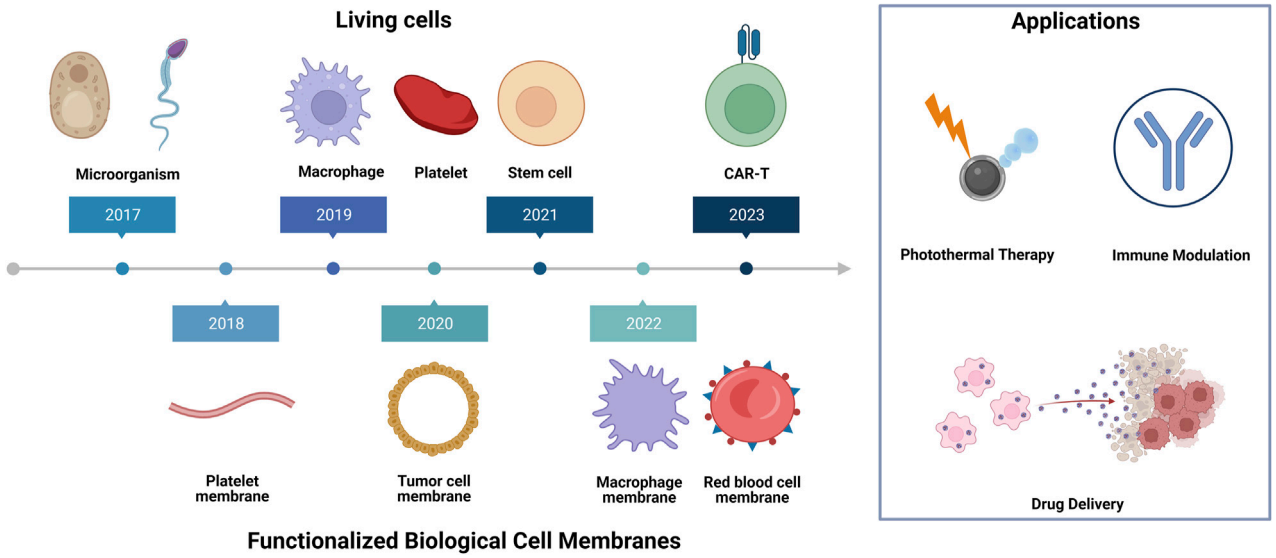

FIGURE 1
Living cells and functionalized biological cell membranes micro-nano robots for biomedical applications. Illustration presents a schematic representation of various synthetic micro-nano robotic micromotors, which are functionalized by different cells and cell membranes for a variety of biomedical applications, including photothermal therapy, immune modulation and drug delivery.

2018; Yu et al., 2022), light-actuated (Kadiri et al., 2021), chemical propulsion that relies on surrouding chemical fuels (Xu et al., 2020), ultrasound propulsion (Wu et al., 2014) as well as biohybrid propulsion (Carlsen and Sitti, 2014; Ceylan et al., 2017; Buss et al., 2020; Zhang et al., 2022b; Zhang B et al., 2023). These methods allow micro-nano robots to operate in complex fluid environments and perform biomedically relevant tasks such as targeted drug delivery (Singh et al., 2019; Ji et al., 2021) and precision surgery (Nguyen et al., 2018). This progress has positioned artificial micromotors as a leading area of biomedical research. While there have been successful reports of animal experiments (Gao et al., 2015; Oral and Pumera, 2023) there are still several critical issues that must be addressed before micro-nano robots can be safely and effectively applied to living systems and translated into practical applications. The reliability and biosafety of micromotors depend on synthetic materials, which can trigger immune reactions and contamination in complex living systems. Thus, for *in vivo* application of micromotors, it is crucial to design them biomimetically and ensure their biocompatibility to ensure their efficient operation in physiological environments without any adverse effects.

The combination of micromotor capabilities with the biological properties of native cells have led to the development of living cell-based micromotors (Li et al., 2017; Venugopalan et al., 2020). This innovative approach offers new possibilities to overcome current obstacles faced by micromotors in biomedical operations. By drawing inspiration from nature, the basic biological functions of natural cells, including immune immunity, antigen presentation, cell or tissue-specific targeting, and selective binding of bacteria or pathogens can be harnessed and synthesized into motile micro-nanorobots. But living cells sometimes can fully meet the needs of micromotor's construction. Cell membrane coating technology is an advanced and powerful technology that utilizes complex proteins, channels, and biological functions of target cell membranes (Li T. et al., 2018; Fang et al., 2018). The coupling of cell membrane and micromotor produces new biocompatible devices that offer a wide range of possibilities for various applications in the field of biomedicine, generating great attention and interest among researchers (Gao et al., 2016; Le et al., 2021).

This review delves into the latest research on the synthesis of micromotors using living cells and functionalized biological cell-membrane. The article also introduces the construction of mircomotors, including the fabrication methods of materials and their integration with biological tissues (Sun et al., 2020). The control method and movement mode of the micromotors are discussed, and examples of typical micromotors are given, with a focus on their application in the field of biomedicine (Figure 1). The review concludes by proposing some challenges and future prospects for developing a new generation of mirco/nano robtic motors.

2 Micro-nano robotic motors based on living cells

Biohybrid robots, which integrate biological entities and synthetic materials, have emerged as a revolutionary development in the field of robotics (Webster-Wood et al., 2022). The power system of organisms in nature has evolved over tens of thousands of years, making it an ideal model for efficient locomotion and adaptation to environmental changes. As a result, the combination of biological tissues and synthetic materials has enabled the creation of motors with these capabilities. The

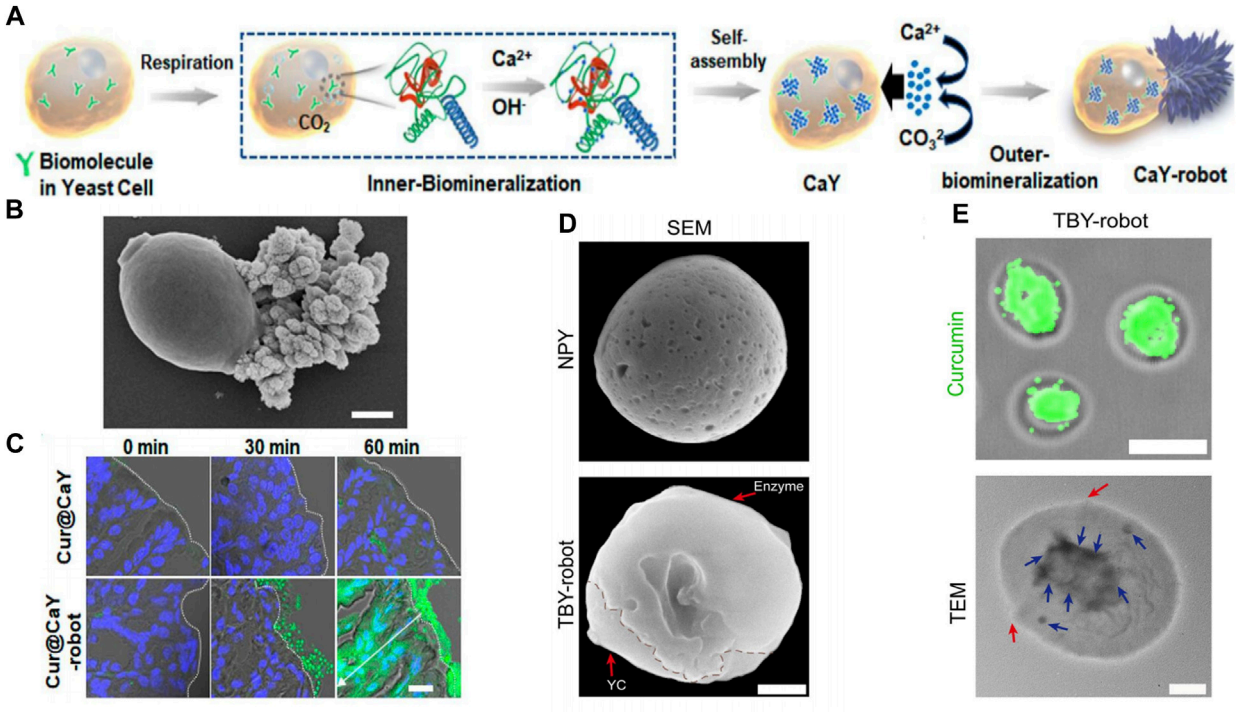

FIGURE 2
(A) Mechanism of yeast-cell-based Cur@CaY-robot. **(B)** SEM images of CaY-robots. **(C)** Histological section of the stomach at different times after the oral intervention. Reproduced with permission. Copyright 2023, ACS nano. **(D)** SEM images of CaY-robots. **(E)** Fluorescence image (top) of TBY-robot loaded with Cur. TEM image (bottom) of a TBY-robot. Red arrows indicate the boundary of conjugated enzymes. Blue arrows indicate the packaged NPs. Reproduced with permission. Copyright 2023, Science Advances.

emergence of biohybrid robots has sparked a wave of scientific research, with many scientists achieving remarkable results in their studies (Lv et al., 2023). In the following section, we will discuss the latest advancements in biological components and synthetic materials for micro-nano robotic motors based on living cells.

2.1 Microorganism

Micro-nano robotic motors can be categorized into two types based on their driving method. The first type requires external drive which can be limiting due to the need for complex equipment and additional costs (Wang Y et al., 2018; Gao et al., 2021). The second type is known as chemical/catalytic motors, which are powered by intrinsic components such as biological enzymes and redox reactions, generating gas to propel the robot (Tang et al., 2020). As they do not require external equipment, self-propelled micromotors are more convenient for practical applications.

Asymmetric materials have emerged as promising candidates for self-propelled micro-nano robots in recent years. Hahn's team has developed an asymmetric micro-nano robot powered by urea, which used urea in the stomach as a bioavailable power source to penetrate the gastric mucosal layer (Choi et al., 2021a). However, these materials were often plagued by low biocompatibility and potential biotoxicity of foreign substances. Therefore, the development of biocompatible micro-nano robots is crucial for their widespread use, particularly in overcoming physiological barriers and facilitating efficient drug delivery.

Yeast cells are single-celled microorganisms that are highly compatible and degradable by living organisms. They are capable of regulating and inducing the biosynthesis of various inorganic nanostructures in cells through a simple and safe synthesis process. Zhang et al. designed a self-propelled yeast cell (CaY) micromotor (Zhang L et al., 2023), (Cur@CaY-robot) (Figure 2A), through dual-biomineralized and acid catalysis of calcium carbonate ($CaCO_3$). Under mild conditions, the cellular respiration of nano-$CaCO_3$ in yeast cells was biomineralized, providing a nano-scaffold for high-encapsulation curcumin (Cur,a popular anti-inflammatory drug). Simultaneously, the $CaCO_3$ crystals outside the yeast cells provided an asymmetric power source for self-propulsion through uniaxial growth.

In the case of micromotor, yeast cells were responsible for loading Cur, while the asymmetric outer layer of $CaCO_3$ crystals produced a significant amount of carbon dioxide (Figure 2B). This allowed Cur@CaY-robot to move efficiently in gastric acid and penetrate deeply into the thick gastric mucus, thus improving drug accumulation in the stomach wall tissue and effectively treating gastritis. Additionally, the calcium ions released by the robot synergistically restored gastric motility in mice with gastritis. The yeast micro-nano robot has excellent biocompatibility and biodegradability, as well as good drug-loading ability (Figure 2C).

In addition, micromotors based on microalgae (Choi et al., 2023) and sperm (Xu et al., 2018) have also been widely designed and

adopted. Microalgae with multiple flagella have been utilized as a micromotor platform due to their excellent biocompatibility, fast movement without the need for toxic fuel, long lifespan, and versatility in various aqueous environments. As well, some sperm utilize their flexible flagella to generate traveling deformation waves, allowing them to swim in the opposite direction. The sperm cell also possesses a remarkable capability to encapsulate hydrophilic drugs. This unique feature allows the sperm membrane to safeguard drugs from dilution in body fluids, immune reactions, and enzymatic degradation. These abilities and features endow them with multiple functions such as drug delivery, antitumor therapy, and promotion of wound healing.

2.2 Macrophage

Living cells have developed unique abilities, such as an endogenous biological motor. Macrophages, for instance, are a cell type with migratory and chemotactic properties that can follow chemokine concentration gradients to target lesion sites and penetrate biological barriers, eliminating the need for hazardous fuels or complex actuation devices (Shi and Pamer, 2011).

Enzymes have been increasingly used as catalytic bioengines due to their capability of converting biocompatible substrate biofuels into driving forces (Hortelao et al., 2021; Arqué et al., 2022; Wang H et al., 2022). These enzyme-driven robots have been successfully created by immobilizing enzymes asymmetrically on the surface of inorganic substances or by asymmetrically polymerizing enzymes into aggregates that display attraction at specific barriers. Additionally, these robots can respond to enzyme-substrate gradients, mimicking the collective driving force exhibited by humans. However, the limitation of single-enzyme bioengine drive restricts self-propelled micro-nano robots to local physiological environments. Adapting to changes in the microenvironment becomes challenging when attempting to reach distant or deep lesions that are separated by multiple biological barriers, such as in gastrointestinal (GI) inflammation including chronic gastritis and inflammatory bowel disease.

Zhang et al. developed a self-propelled and self-adaptive twin-bioengine yeast micro-nano robot (TBY-robot) that could navigate autonomously to sites of gastrointestinal inflammation through enzyme-macrophage switching (EMS) (Zhang W et al., 2023) (Figure 2D). Glucose peroxidase (GOx) and catalase (Cat) were commonly used as feed additives to relieve oxidative stress, maintained microbial system homeostasis, and enhanced intestinal function. The researchers synthesized a TBY-robot by immobilizing GOx and Cat asymmetrically on the surface of anti-inflammatory NP-packed YCs (NPY). The Janus-distributed enzymes could break down glucose to create localized glucose concentrations that could be used to power the TBY-robot. When there was a gradient of glucose concentration in the intestine, the micro-nano robots could pass through the intestinal mucosal barrier and transport across the intestinal epithelial barrier by microfolded cells. Once they arrived at the designated site, the TBY-robot would switch to the macrophage biological engine and autonomously migrate to the inflammatory site of the gastrointestinal tract through a chemokine-mediated macrophage relay.

Notably, the EMS was a crucial component for the TBY-robot to carry out active and targeted anti-inflammatory drug delivery. The small intestine was the only area where a glucose concentration gradient exists due to glucose digestion and absorption, while the colon and stomach lacked a glucose power source. As a result, these robots could not directly access inflammatory sites in the colon and stomach through single-enzyme bioengines. But the TBY-robot with enzyme actuation and macrophage relay can cross multiple biological barriers and autonomously navigate to long-distance and deep lesions. Additionally, the TBY-robot's enteric coating prevented the inactivation of the enzyme biological engine, stoped the drug from penetrating into the gastric juice which evaluated by Cur loading effciency (Figure 2E), and could not simultaneously release the drug directly in the alkaline colonic environment.

The study found that the micro-nano robots' lymphatic-blood transport pathway was confirmed through the blockade of microfolded cell transport and splenectomy. In animal models of colitis and gastritis in mice, the TBY-robot showed promising results in reducing inflammation and improving disease pathology. The TBY-robot had features of enzyme activation and macrophage chemotaxis, specifically EMS ability, which allowed it to adapt to changes in the environment, penetrated multiple biological barriers, reached deep inflammatory sites, and provided precise treatment for gastric and intestinal inflammation. This TBY-robot was a safe and versatile delivery tool for the treatment of gastrointestinal inflammation and other inflammatory diseases.

2.3 Stem cell

Mesenchymal stem cells (MSCs) have the potential to differentiate into multiple cell types and are often used for cartilage regeneration (Filardo et al., 2016). They can also reduce inflammation and treat damaged cartilage through chondrogenic differentiation and peripheral tolerance induction. This therapy can delay or avoid the need for cartilage replacement surgery. As the number of cells in the lesion is one of the critical parameters, researchers found that the low targeting efficiency of MSCs requires invasive procedures and the use of large numbers of cells combined with intra-articular injection or stent implantation (Goldberg et al., 2017).

To improve the targeting of MSC therapy, researchers were using magnetically driven micro-nano robots. These robots helped target MSC delivery, support MSC through porous structures, and used electromagnetic actuation (EMA) system composed of multiple electromagnetic coils to make the targeting of MSCs precise. These micromotors had shown biocompatibility ability to carry cells, and cell transplantation *in vitro* or in simple *in vivo* environments (Li et al., 2018b).

In their study, Go G et al. developed a micro-nano robot system for knee articular cartilage regeneration using human fat-derived MSCs (Go et al., 2020). The effectiveness of the system was verified through *in vivo* experiments, with consideration given to its feasibility for clinical trials. The micro-nano robotic system allowed for targeted delivery of MSCs via needle-based injection and magnetic targeting. The system included a magnetically driven micro-nanorobot for cell loading, an EMA system for targeted MSC

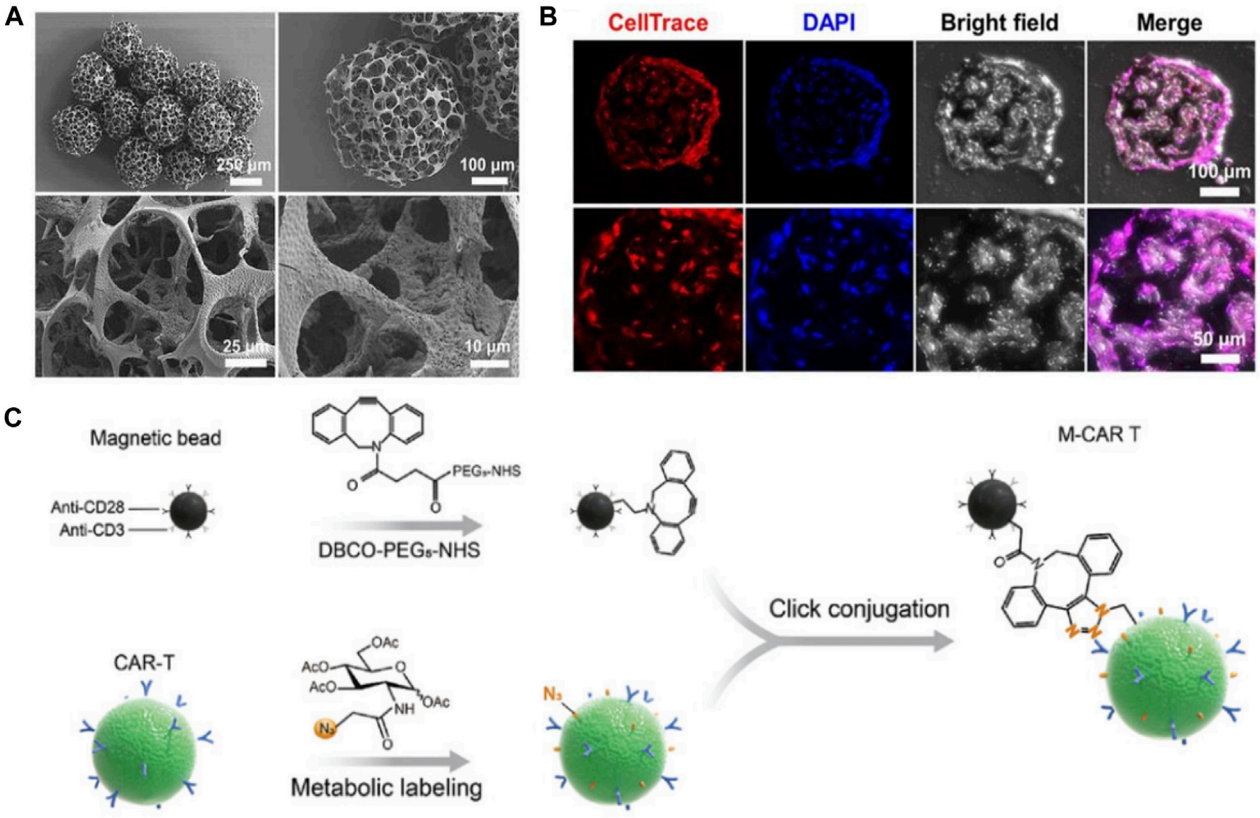

FIGURE 3
(A) SEM images of magnetic microrobots. **(B)** Confocal images of MSCs that were incubated in microrobots for 24 h. Reproduced with permission. Copyright 2020, Science Robotics. **(C)** Schematic illustration of M-CAR Ts'structure. Reproduced with permission. Copyright 2023, Advanved Materials.

delivery in accordance with clinical treatment procedures. The micro-nano robots were created by adsorbing magnetic micro-clusters on the surface of PLGA micro-stents (Figure 3A). The microrobot's porous microstructure could support MSCs (Figure 3B)and inject them into the joint cavity. It also had magnetic driving capabilities provided by ferrous ferulate and positively charged chitosan adsorbed on its surface, forming magnetic micro-clusters. Ferumoxytol, an FDA-approved superparamagnetic oxidized nano-iron drug, was coated with polydextrose sorbitol carboxymethylether and magnetic nanoparticles (MNPs). And the chitosan, a natural multifunctional polysaccharide and representative cationic polymer, was biocompatible and degradable. The magnetic microclusters had adsorbed micro-nanorobots with stronger magnetic properties compared to previous studies. These micro-nanorobots ensured activity, degradability, proliferation, and chondrogenic differentiation of MSCs. In order to improve the effectiveness of stem cell-based cell transplantation, a microrobot-mediated MSC delivery system was developed and tested in an *in vivo* model using small mammalian knee articular cartilage. The system included a targeting mechanism and a magnet designed to immobilize the microrobot at the site of the cartilage defect after positioning. The size and position of the magnet were optimized based on the location of the defect, and the magnetic strength was tailored to the microrobot. Results showed that the combination of microrobots and targeting devices led to higher targeting efficiency of stem cells and improved therapeutic capability.

2.4 Other cells

Chimeric antigen receptor T (CAR-T) cell therapy has demonstrated promising results in treating hematological malignancies. However, its efficacy in treating solid tumors has been limited by the immunosuppressive microenvironment and physical barriers. CAR-T cells must navigate a complex vascular system in high-speed blood flow to reach the tumor tissue, which significantly reduces their delivery efficiency (Turley et al., 2015; Ma et al., 2019; Larson and Maus, 2021). Therefore, an ideal CAR-T therapy requires a new type of cell that can successfully navigate the circulatory system, penetrate the tumor tissue, and survive in the harsh tumor environment to exert sufficient antitumor effects.

Recent studies have shown that magnetic particles modified with T cell activators anti-CD3 and anti-CD28 can effectively induce antigen-specific expansion of T cells in tumor tissue through magnetic guidance and actuation (Kalamasz et al., 2004). These modified magnetic particles also provided the bioactive micro-nanorobot with an asymmetric structure and greater acoustic impedance mismatch with medium, making it suitable for ultrasound-driven controllable motion (Wu et al., 2014). This

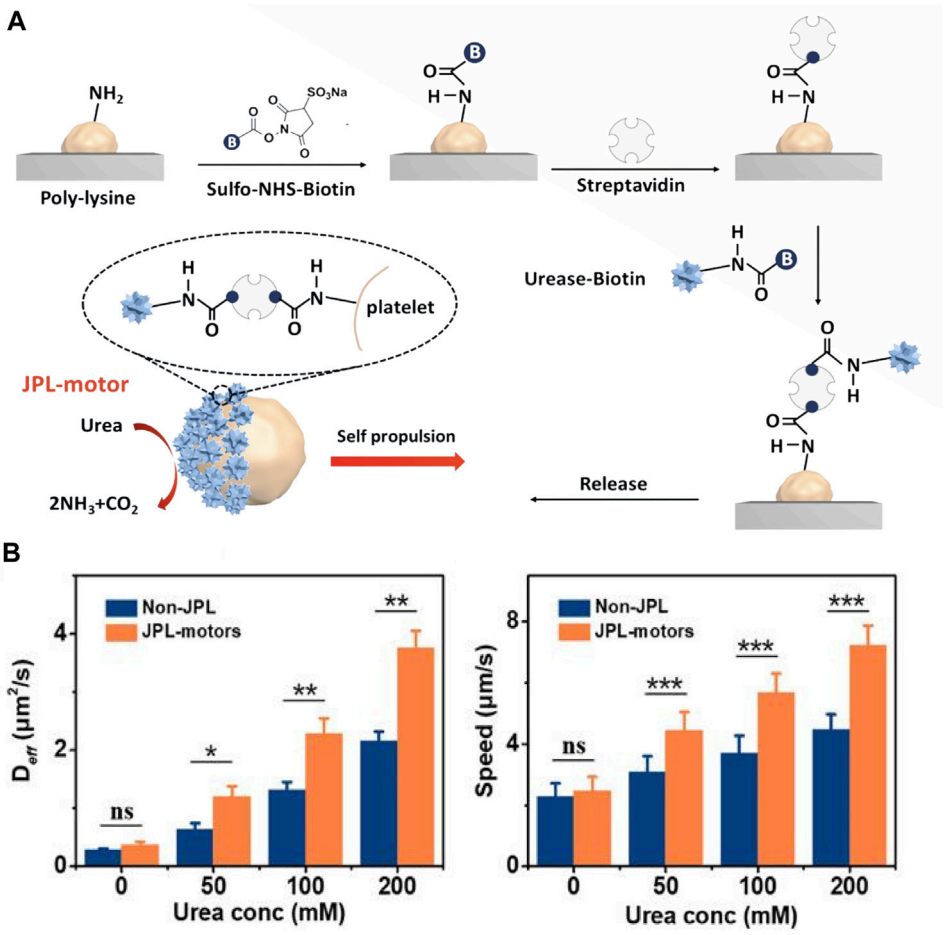

FIGURE 4
(A) Schematic of the fabrication of JPL-motors. Platelets were attached first to a PLL surface and then modified with urease via a biotin-streptavidin-biotin binding complex. **(B)** D_{eff} and speed of JPL-motors and non-JPLs in the presence of different urea concentrations. Reproduced with permission. Copyright 2020, Science robotics.

magnetic-acoustic power can be used to manipulate CAR-T cells and facilitate spatial targeting and penetration of solid tumors. In order to enhance the efficacy of CAR-T cell immunotherapy in solid tumors, researchers have developed a microrobot that utilizes immunomagnetic beads coated with anti-CD3 and CD28 antibodies to promote the proliferation and activation of CAR-T cells in the tumor microenvironment.

Tang et al. developed immunomagnetic bead-engineered CAR-T microrobots (M-CAR Ts) that guided by magnetic-acoustic sequential actuation which exhibited precise anti-flow motion and obstacle avoidance capacity, allowing it to maintain its planned route for targeted delivery (Tang et al., 2023) (Figure 3C). M-CAR Ts therapy had unique acoustic manipulation properties and could penetrate artificial tumor tissue through magneto-acoustic sequences. *In vivo*, M-CAR Ts could be targeted and concentrated in the peritumoral area through programmed magnetic guidance. This allowed for precise propulsion of M-CAR Ts into deep tumor tissue, overcoming the limitation of a single driving method. Overall, M-CAR Ts were versatile platform for precise tumor targeting and tissue penetration, which could enhance cell-based solid tumor therapies.

Besides, Tang et al. developed urease-powered Janus platelet micromotors (JPL-motors) (Tang et al., 2020) (Figure 4A). These eliminated the need for external motor, making the robot autonomous and long-lasting. The integration of endogenous enzymes with platelet cells resulted in a biocompatible cell robotic system with unique synergistic capabilities for various biomedical applications. The availability of urea as a common biological substrate in humans, particularly in the urinary system, made this type of microenvironment an attractive option for initial clinical studies. The method proposed in this study offered a straightforward and reliable approach to asymmetrically modify cell surfaces using urease. The Janus structure, which allowed for asymmetric driving forces and active locomotion, was more desirable than full enzymes covering the entire cell membrane.

The current technique for Janus cell modification involved attaching platelets to a poly (L-lysine) (PLL) - modified substrate to block the attached platelet surface and then used biotin-streptavidin-biotin conjugation to modify the exposed cell membrane with urease. This study showed that the use of urea fuel in biocatalytic reactions of surface-bound urease could generate efficient propulsion through chemielectrophoresis. As a result, JPL-

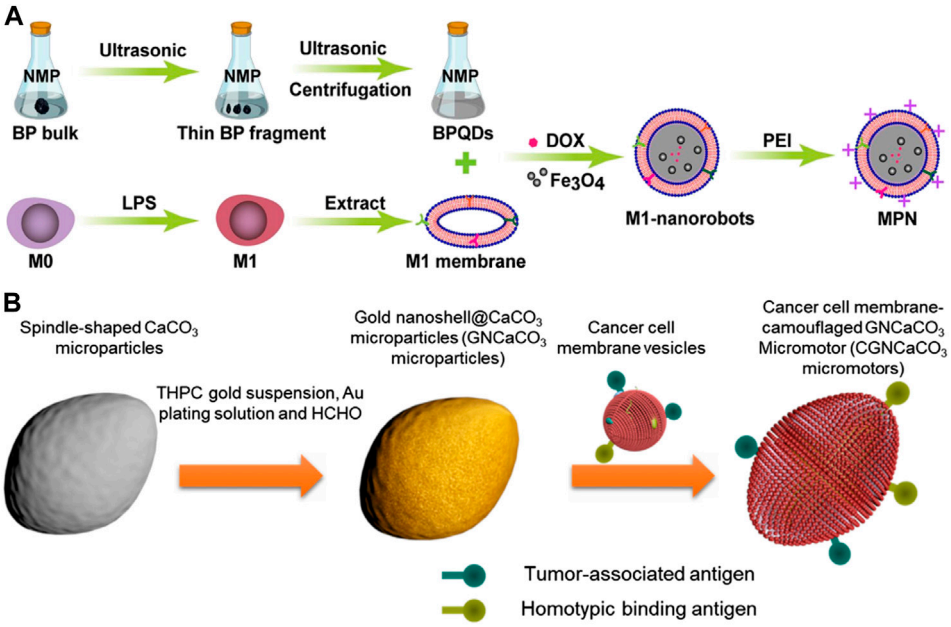

FIGURE 5
(A) Schematic of biomimetic M1 macrophage membrane-camouflaged magnetic nanorobots for cancer therapy. Reproduced with permission. Copyright 2022, ACS Applied Materials&Interfaces. **(B)** Schematic fabrication of acoustic-propelled micromotor based on cancer cell membrane-coated gold nanoshell@$CaCO_3$ microparticle. Reproduced with permission. Copyright 2020, Advanced Therapeutics.

motors exhibited efficient locomotion in various biological fluids with the presence of urea, and significantly enhanced propulsion compared to urease-fully modified (non-JPL) platelets due to their asymmetric structure (Figure 4B). The research also indicated that the modification of urease had minimal effects on the functional proteins present on the surface of platelets, which allowed for the design of targeting platforms based on the intrinsic and specific binding of platelets to biological targets. The study demonstrated that JPL-motors fueled with urea could effectively bind to cancer cells and bacteria, leading to an enhanced therapeutic effect when loaded with anticancer and antibiotic drugs respectively.

By combining platelets with a urease biocatalytic engine, a biocompatible and biodegradable cellular robot with self-propelling ability was created. The surface engineering technique of Janus urease coatings was found to be a simple and robust approach to functionalize native cell surfaces asymmetrically, which had a great potential for the development of advanced cellular motors.

3 Micro-nano robotic motors based on functionalized biological cell membranes

Since the development of cell membrane coating technology, several methods have been employed to functionalize cell membranes in a non-destructive manner. These methods include lipid insertion, membrane hybridization, metabolic engineering and gene modification, which aim to incorporate diverse functions into natural cell membranes. The modification of membranes is anticipated to augment the multifunctional and multitasking capabilities of cell membrane-coated micromotors, enabling them to better adapt to complex biological environments. The process of preparing functionalized micromotors with cell membrane coating typically involves three main steps: first, the synthesis of active micromotors; second, the preparation of cell membrane vesicles; third, the fusion of the cell nanovesicles and micromotors. This section will address the various designs of cell membrane coatings based on different micromotor designs.

3.1 Macrophage membrane

The role of immune cells in controlling tumor progression is gaining recognition, particularly macrophages due to their long half-life and tumor targeting abilities. Depending on the microenvironment, macrophages can differentiate into M1 and M2 phenotypes with distinct functions. M1 macrophages inhibit cancer cell growth while M2 macrophages promote it (Xia et al., 2020; Yang et al., 2022).

Song et al. drew inspiration from M1 macrophages and designed an anticancer micromotor that encapsulated black phosphorus quantum dots (BPQDS) to obtain photothermal and photoacoustic properties, as well as magnetically oxidized nanoparticles for magnetic control (Song et al., 2022) (Figure 5A). The study demonstrated the potential of modified magnetic nanoparticles (MPNs) for effective tumor therapy. The MPNs were modified with positively charged polyethyleneimine (PEI) to facilitate cell phagocytosis. These nanoparticles had good biocompatibility, precise motion control, and excellent photoacoustic (PA) imaging capabilities. Additionally, they could utilize the intrinsic properties of macrophages and the immune

properties of M1 macrophages. Under near-infrared radiation (NIR), MPNs could generate high levels of reactive oxygen species (ROS) to exert anti-tumor effects. In a mouse mammary tumor model, antitumor drug doxorubicin (DOX)-loaded MPNs demonstrated a good tumor growth inhibitory effect under external magnetic field and near-infrared irradiation. Overall, the study suggested that MPNs were promising nanotherapeutic platforms for micro-nanorobot tumor therapy.

3.2 Cancer cell membrane

Cancer cell membranes coating technology has advantages in cancer drug targeting and imaging due to the homogeneous targeting capabilities provided by membrane antigens (Fang et al., 2018). These membrane antigens also aid in regulating anticancer immunity (Kroll et al., 2017). Additionally, cancer cells are easily cultured and their cell membranes can be easily extracted, further enhancing the benefits of this technology (Fang et al., 2014).

Polymeric nanoparticles have been functionalized with cancer cell membranes to replicate the antigenic composition of the original cancer cells. This design has opened up possibilities for two types of anticancer therapies. Firstly, cancer cell membrane-coated nanoparticles (CCNPs) have been demonstrated to successfully bind tumor-associated antigens to immune adjuvants of antigen-presenting cells (Oroojalian et al., 2021), thereby stimulating anti-cancer immune responses. Secondly, CCNPs contain cell adhesion molecules sourced from cancer cells, enabling them to participate in homotypic binding, a phenomenon observed in cancer cells that causes them to stick together and resulting in tumor growth. The homotypic binding property of CCNPs allows it to be involved in the cell-specific targeting of cancer cells, which is a crucial aspect of localized and directed cancer therapy (Zeng et al., 2022).

H et al. developed micromotors called $CGNCaCO_3$, which were made of G422 murine cancer cell membrane-camouflaged gold nanoshell-covered $CaCO_3$ (H et al., 2019) (Figure 5B). The fabrication process involved synthesizing $CaCO_3$ particles, functionalizing gold nanoshells, and fusing cancer cell membrane vesicles with the $GNCaCO_3$ particles. The $CGNCaCO_3$ micromotor was able to autonomously move under the exposure of an external acoustic field and accumulate on cancer cells due to its homotypic binding to cancer cell membranes. When injected subcutaneously, the micromotor enhanced the immune activity by camouflaging cancer cells. The $CGNCaCO_3$ micromotor possessed biological characteristics similar to those of natural cancer cells, enabling it to promote a diverse range of antigens and biological processes that were not achievable with common synthetic motors.

3.3 Red blood cell membrane

Red blood cell (RBC) membranes have been extensively studied as a coating material in various applications such as drug delivery (Aryal et al., 2013), imaging (Rao et al., 2017), photothermal therapy (Piao et al., 2014), and immune modulation (Hu et al., 2013). The RBC membrane coating mimics host RBC and provides superior immune concealment (Chen et al., 2019).

Swimming micro-nano robots in the circulatory system hold great promise in precision medicine. However, they currently face challenges such as limited adhesion to blood vessels, strong blood flow, and clearance by the immune system. These factors reduce the effectiveness of targeted interactions. Li et al. discussed the design of a swimming micro-nano robot inspired by the claw structure of tardigrades (Li et al., 2023) (Figure 6A). The robot featured a claw-engaged geometry, a surface camouflaged with RBC membrane, and magnetically actuated retention with a rotating magnetic field (RMF) for better navigation. These minimized the effects from blood flow. The researchers used intravascular optical coherence tomography (IVOCT) to monitor the activity and dynamics of the microrobots in the jugular vein of rabbits. The results showed that magnetic propulsion was highly efficient even at flow rates of approximately 2.1 cm/s, which was compared with the blood flow characteristics in rabbits. The microrobots remained in the blood vessels for more than 36 h (Figure 6B).

The effect of RBC membrane coating on vascular movement of swimming microrobots was also investigated. In static plasma, the swimming microrobots without RBC membrane coating showed a gentle wobble behavior and remained immobile under the RMF in the *xz* plane (maximum magnetic field of 30 mT). This reflected that the adhesion of the claw-engaged structures in blood vessels was too high to overcome the magnetic movement of the swimming microrobots. In contrast, some swimming microrobots coated with RBC membranes exhibited linear motion in blood vessels, suggesting that the RBC membrane coating effectively regulated the adhesion of swimming microrobots in blood vessels. In conclusion, the controllable motion and magnetic drive retention in blood vessels significantly improved the efficiency of targeted drug delivery.

In addition, RBC membranes have been modified onto various substrates, including magnesium microparticles (Wei et al., 2019), magnetic hemoglobin (Gao et al., 2019), perfluorocarbon nanoemulsions (Zhang et al., 2019) and chitosan-heparin layer-by-layer assembled capsules (Shao et al., 2018). These modifications have resulted in a diverse range of applications, including rapid detoxification, photodynamic therapy, oxygen delivery, and thrombus ablation with multiple functions.

3.4 Other cell membrane

Platelets (PL) are known to display unique surface moieties that help them adhere to various disease-associated substrates, which can be linked to vascular injury, immune evasion, and pathogen interactions (Wang et al., 2020). Additionally, platelets play an important role in regulating immune responses, maintaining hemostasis, and participating in wound healing, making them critical players in interacting with many types of cells (Chen and López, 2005; Olsson et al., 2005). Due to their wide range of biological interface capabilities, platelet membrane micromotors have been developed using their membranes. Early studies of PL membrane-encapsulated nanoparticles have shown that they have several essential functions, including reduced cellular uptake by immune cells (Kunde and Wairkar, 2021), subendothelial adhesion (Hu CM et al., 2015), improved tumor targeting (Hu Q et al., 2015), and enhanced affinity for pathogens (Zhuang et al., 2020).

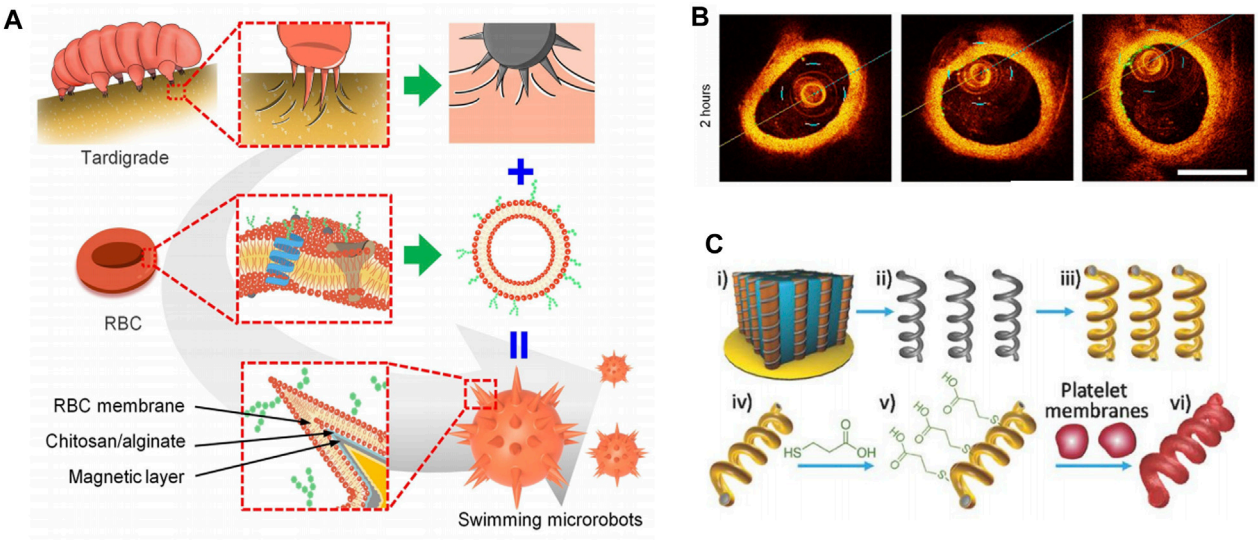

FIGURE 6
(A) Biomimetic design of swimming microrobot. Reproduced with permission. **(B)** Time-lapse IVOCT images of microrobots. Copyright 2023, Science Advances. **(C)** Schematic preparation of magnetic-driven micromotor consisting of platelet membrane-functionalized helical Ni/Au/Pd nanostructure. Reproduced with permission. Copyright 2018, Advanved Materials.

TABLE 1 Biofunction and application of mirco-nano robots.

Construction	Biofunciton	Application	References
Sperm	Swim into the tumors	Drug delivery	Xu et al. (2018)
Microalgae	Alleviate the hypoxic condition and modulate the immune responses	Wound healing	Choi et al. (2023)
Macrophage	Phagocytic ability	Cargo delivery	Dai et al. (2022)
Stem cell membranes	Secretion of paracrine factors	Therapeutic cardiac regenertation	Tang et al. (2017)
T cell membranes	Ability to recruit and localize at tumor sites	Enhance drug targeting	Zhang et al. (2017)
Cancer cell membranes	Promote anticancer immune responses	Drug delivery	Fang et al. (2014)
Lung epithelial cell	Surface receptors that pathogens depend on for cellular entry	Neutralize the virus	Zhang et al. (2020)
Leukemia cell	Targeting sites of inflammation	Drug delivery	Park et al. (2021)

In a recent study, Li et al. fused platelet membrane-derived vesicles (PL-vesicles) onto the surface of helical nanomotors to create PL-nanomotors (Li et al., 2018c). The helical structures were created through Pd/Cu co-electrodeposition in 400 nm pores of polycarbonate films, followed by dissolving the copper, releasing Pd nanostructures, and depositing Ni/Au bilayers to give them magnetic properties (Figure 6C). The synthesized magnetic helical nanostructures were then modified with 3-mercaptopropionic acid (MPA) to provide a negative charge to the Au surface, allowing for effective coating of the helical motor after incubation under ultrasound.

Therefore, its magnetic propulsion was not affected by the presence of biofilms. The study evaluated the propulsion and anti-biofouling abilities of PL nanospheres in whole blood. The results showed that the PL-nanomotor had higher propulsion efficiency compared to the bare nanomotor. The bare nanomotor was hampered by severe biofouling, while the light-emitting nanomotor exhibited efficient magnetic actuation. These findings further supported the protective effect of platelet membrane coating against biofouling in complex biological matrices and suggested potential *in vivo* studies.

4 Applications of living cells and functionalized biological cell membranes micro-nano robots

(Table 1) lists applications for various micromotors. When the efficient locomotor capabilities of synthetic micro-nano robots are combined with the biological functions of native living cells or cell membranes, these micromotors gain unique capabilities that greatly

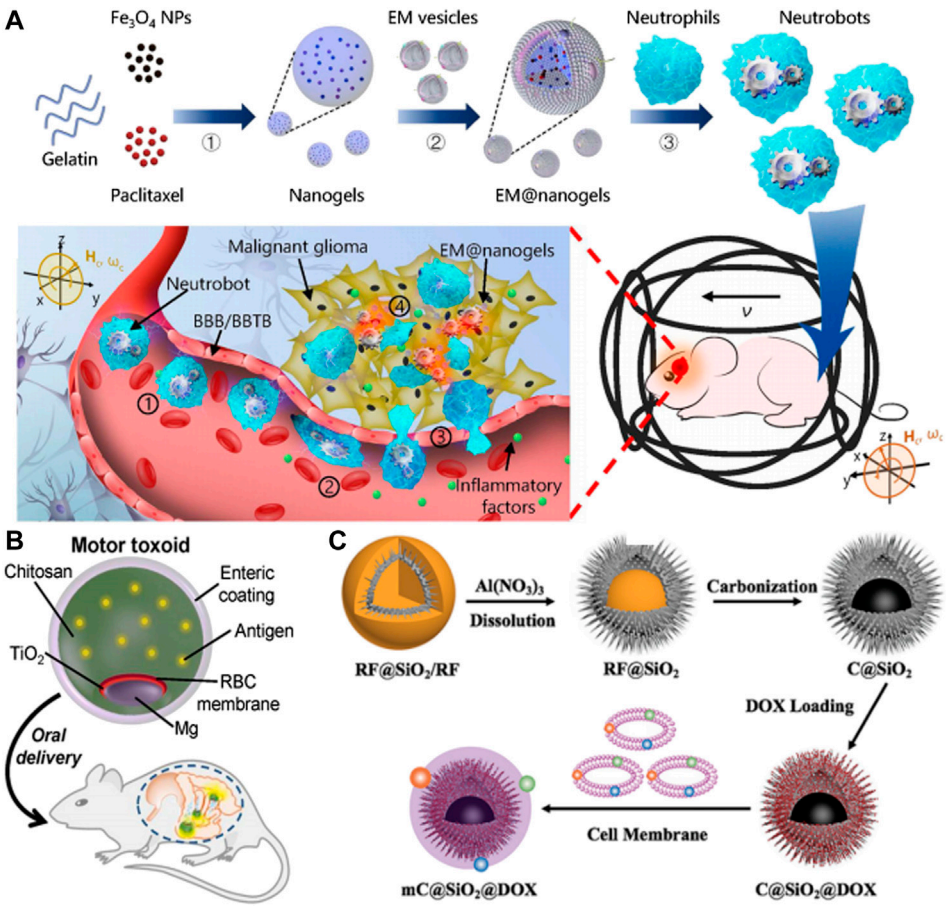

FIGURE 7
(A) Schematic of active therapeutics of dual-responsive neutrobots *in vivo*. Reproduced with permission. Copyright 2021, Science Robotics. **(B)** Toxin binding RBC membrane-coated Mg micromotor (micromotor toxoid) for oral vaccination. Reproduced with permission. Copyright 2019, Nano Letters. **(C)** Schematic illustration of the self-thermophoretic propulsion nanomotors actively seeking and effectively endocytosing into tumor cells under NIR light irradiation, thereby enhancing photothermal and chemotherapy. Reproduced with permission. Copyright 2020, Small.

enhance their performance in improving various biomedical applications. These applications include drug delivery, immunomodulation, and phototherapy. The following sections will discuss these functions in more detail.

4.1 Drug delivery

Neutrophils (NE) are crucial in the immune response as they remove infections through various means like phagocytosis, degranulation, reactive oxygen species, and NE extracellular traps (NETs) (Jorch and Kubes, 2017; Papayannopoulos et al., 2018). During inflammation, NE can cross the blood-brain barrier/blood-brain tumor barrier (BBB/BBTB) by following the gradient of inflammatory factors (Deoliveira et al., 2016; Oliveira et al., 2018). NEs have been utilized as drug carriers to target inflammatory tumors due to their chemotactic properties. Although some reduction in tumor size has been observed, complete cure of cancer in mice has not been achieved due to limitations in drug-loading capacity, migration speed, and accumulation efficiency of existing NE carriers (Xue et al., 2017; Chu et al., 2018; Tang et al., 2019). Therefore, NE-based swimming microrobots with significantly enhanced drug loading, locomotor, and navigation capabilities hold promise for active delivery *in vivo*.

Zhang et al. developed dual-responsive (DR) hybrid NE microrobots, also were knowed as neutrobots, that could be used for the treatment of active malignant glioma *in vivo* (Zhang et al., 2021) (Figure 7A). These robots had the ability to move intravascularly using magnetic propulsion and exhibit chemotactic behavior along gradients of inflammatory factors. To achieve this, the robots were coated with paclitaxel (PTX) magnetic nanogel, which was coated on the outer membrane of *E. coli (E.coli)* and then phagocytized by NE. The camouflage provided by the *Escherichia coli* membrane prevented the drug from leaking into the NE, resulting in a bioactivity similar to NEs. The neutrobots could be individually propelled and exhibited swarm locomotion in a rotating magnetic field (RMF), and had demonstrated efficient operation in blood *in vitro*. *In vitro* model of the BBB, magnetic actuation was found to significantly increase the accumulation of neutrophils at the site of lesion. Additionally, chemotactic motility allowed for BBB penetration. The efficacy of

active targeted delivery was further confirmed *in vivo* through the use of double-reactive neutrophils for the treatment of postoperative glioma. The biohybrid neutrobots developed in this study demonstrated the ability to harness NE's natural characterisitic, which were otherwise difficult to replicate. Such dual-response neutrobots might improve the efficiency of active targeted delivery and noninvasive precision therapy.

Despited significant progress in intracellular and active targeted drug delivery of micromotors, *in vivo* applications still posed challenges. While RMF had been proven effective for intracellular and targeted delivery of external stimuli, precise directional and temporal control of ultrasound and photostimulation remained difficulties. Additionally, active targeting of chemoattractant micro-nano robots *in vivo* is hindered by the complex coexistence of the circulatory system and various chemical gradients, which makes the chemotactic motility of micro-nano robots unfavorable. To improve practical application, the sensitivity of micro-nano robots *in vivo* must be enhanced for precise motion control with an extended tactical operating range (Choi et al., 2021b).

4.2 Immune modulation

The task of creating effective micro-nano robots delivery systems for transporting and enclosing antigenic agents and immunostimulants is a significant challenge in the field of nanomedicine (Fang and Zhang, 2016; Zhou J. et al., 2020). The use of micromotors with enhanced drug loading, sustained release, targeted delivery, and oral inoculation has become increasingly popular.

One effective strategy to immobilize and neutralize toxins to the carrier surface is through cell membrane coating technology. Combining this technology with a micromotor platform has the potential to improve cargo delivery and enhance tissue penetration. A recent development in this field was the unique biomimetic micromotor toxoid strategy for oral vaccines. This method involved preparing micromotor toxoids in a sequential process that confered antigenicity by coating the micromotors with a toxin-inserted erythrocyte membrane.

In Wei et al.s' study, motor toxoid was administered orally to a mouse and targeted to the gut (Wei et al., 2019) (Figure 7B). Once in the gut, the micromotors were activated and propelled through the surrounding fluid to enhance retention and penetration of the antigen payload. To protect the motor toxoids from activation and degradation in the low pH environment of the stomach, a pH-responsive enteric coating was used. The study evaluated the ability of motor toxoids to induce an immune response to staphylococcal α-toxin by administering it along with static microparticle toxoid as a passive control group. Based on the absorbance data of the ELISA assay, it could be inferred that the motor toxoid exhibited a higher production of α-toxin antibodies in comparison to the static microparticle toxoid. The IgA titers data indicated that the motor toxoid platform increased IgA production by approximately ten times.

The combination of the cell membrane-based toxin retention platform and micromotor technology showed promise for the development of safe, effective, and easily administered immunotherapeutic agents. This system could extend to safely deliver various toxic antigen cargoes and provides efficient active delivery capability.

4.3 Photothermal therapy

In the field of external propulsion, NIR light propulsion has significant potential for biomedical applications. This is due to its ability to penetrate deep into tissues, its biocompatibility, remote control capabilities, ease of operation, and fast response. For instance, Li et al. developed a tubular mesoporous silicon-based micromotor that can be driven by NIR light (Li et al., 2021). These micromotors, when injected into the bloodstream and activated at the site of a lesion using infrared light, gain the ability to move and facilitate their penetration into damaged blood vessels. By utilizing the heat generated from near-infrared light, the micromotor can function as a photothermal ablation agent for inflammatory macrophages.

In addition to optimizing self-propelling and drug loading abilities, micromotors need to possess good antibioadhesion and specific targeting capabilities to serve as effective drug delivery systems. In recent years, cell membrane coating technology has emerged as a promising approach to fulfill these requirements. Zhou et al. had demonstrated a NIR light-driven biomimetic micromotor which was composed of carbon@silica (C@SiO_2) with semi-yolk@spiky-shell structure loaded with anticancer drug DOX and MCF-7 breast cancer cell membrane (mC@SiO_2@DOX) for cancer therapy (Zhou M. et al., 2020) (Figure 7C). This mC@SiO_2@DOX motor was evaluated for photothermal and chemotherapy of breast cancer. Owing to the asymmetric spatial distribution, the biomimetic mC@SiO_2@DOX nanomotor demonstrated efficient self-generated thermal propulsion capability. Additionally, the coating of MCF-7 cancer cell membrane significantly reduced the bioadhesion of nanomotors in biological media and exhibited highly specific self-recognition to the source cell line. The combination of efficient propulsion and cognate targeting greatly enhanced cell adhesion and increases cellular uptake efficiency from 26.2% to 67.5%. As a result, the biomimetic mC@SiO_2@DOX nanomotor showed a promising photothermal and chemotherapy synergistic effect, with a growth inhibition rate of MCF-7 cells exceeding 91%. The intelligent design of this fuel-free, NIR light-driven biomimetic nanomotors might open doors for the application of self-propelled nanomotors in biomedicine.

In summary, the homotypic targeting effect of cancer cell membrane-coated micromotors is ideal for localized chemotherapy and phototherapy at tumor sites. Additionally, this targeting capability can also be utilized with other cell membranes, including platelets and leukocytes, for similar therapeutic purposes. The fast motion capability of the micromotor, combined with the specific targeting capabilities of cell membranes, makes it a promising tool for future cancer treatments.

5 Future prospects

This article provides a comprehensive overview of the recent advancements in micro-nano robotic motors, covering its fundamental components, control techniques, and initial applications. The field of micro-nano robots is currently undergoing a significant transformation, thanks to the diligent efforts of researchers, which could have far-reaching implications in various domains such as biology, medicine, and engineering.

Despite the significant strides made in this field, there are still obstacles that impede laboratory research from translating into real-world applications. For instance, after micro-nano robots complete *in vivo* tasks, their residual presence in the body can be cytotoxic, potentially leading to unintended harmful outcomes. In this case, micro-nano robots made of biodegradable materials have become the trend in healthcare and biomedical applications (Sitti et al., 2015). Therefore, the development of micro-nano robots must consider and tackle several crucial issues to ensure technological progress.

The first problem the limited cell sources available for the biological components of micro-nano robots. Stem cell technology could be a solution, but the high cost of this technology limits its ability to meet market demands. Furthermore, the short lifespan of robots, which cannot exceed several months, affects their practical application value. Developing micro-nano robots that can maintain their locomotion ability for longer periods can address this issue (Halder and Sun, 2019). Therefore, there is a need to draw inspiration from nature to find ways to generate long-term cell cultures and even achieve cell immortalization.

Second, the challenge of maintaining locomotor performance in micro-nano robots is closely tied to the optimization of materials. These materials must meet several requirements, including biocompatibility, stability, durability, and flexibility (Sun et al., 2020). Despite the widespread use of various materials in constructing micromotors, they still struggle to create an environment that effectively induces cell orientation or differentiation, similar to that provided by organisms. In response, material science and fabrication techniques should be integrated more closely to develop more advanced materials with bioinspired form and function.

The third issue in micro-nano robots concerns the limitation of practical applications due to the culture and testing of robots in liquid environments. While attempts have been made to manipulate the atmospheric conditions by encapsulating biological entities in closed media, the resulting biohybrid systems are only viable for a few days (Li et al., 2023). To overcome this limitation, researchers are exploring the development of a human-like built-in circulatory system or biomimetic vascular network. This would enable effective detachment from the culture medium environment. Meanwhile, current micromotors are mainly designed for a single function, whereas the potential of robotics lies in building complex systems that can perform multiple functions to adapt to various environments.

Micro-nano robots have demonstrated impressive performance and hold practical potential across various fields. Future research should aim to enhance their performance and explore their applications in biological and medical domains. This review aims to inspire multidisciplinary researchers to address these issues and foster the development of micro-nano robots. We are confident that micro-nano robots will continue to achieve exciting advancements in the future.

Author contributions

JN: Writing–original draft, Writing–review and editing. CL: Writing–original draft, Writing–review and editing. XY: Writing–original draft. WL: Writing–review and editing. YW: Writing–review and editing.

Funding

The author(s) declare financial support was received for the research, authorship, and/or publication of this article. This work was supported by the National Natural Science Foundation of China (Grant no. 81972054), the Natural Science Foundation of Heilongjiang Province (Grant No. YQ 2021H010), the Postdoctoral Scientific Research Development Fund of Heilongjiang Province (Grant No. LBHQ19044).

Conflict of interest

The authors declare that the research was conducted in the absence of any commercial or financial relationships that could be construed as a potential conflict of interest.

Publisher's note

References

Arqué, X., Patiño, T., and Sánchez, S. (2022). Enzyme-powered micro- and nano-motors: key parameters for an application-oriented design. *Chem. Sci.* 13 (32), 9128–9146. doi:10.1039/d2sc01806c

Aryal, S., Hu, C. M., Fang, R. H., Dehaini, D., Carpenter, C., Zhang, D. E., et al. (2013). Erythrocyte membrane-cloaked polymeric nanoparticles for controlled drug loading and release. *Nanomedicine (Lond).* 8 (8), 1271–1280. doi:10.2217/nnm.12.153

Buss, N., Yasa, O., Alapan, Y., Akolpoglu, M. B., and Sitti, M. (2020). Nanoerythrosome-functionalized biohybrid microswimmers. *Apl. Bioeng.* 4 (2), 026103. doi:10.1063/1.5130670

Carlsen, R. W., and Sitti, M. (2014). Bio-hybrid cell-based actuators for microsystems. *Small* 10 (19), 3831–3851. doi:10.1002/smll.201400384

Ceylan, H., Giltinan, J., Kozielski, K., and Sitti, M. (2017). Mobile microrobots for bioengineering applications. *Lab. Chip* 17 (10), 1705–1724. doi:10.1039/c7lc00064b

Chen, J., and López, J. A. (2005). Interactions of platelets with subendothelium and endothelium. *Microcirculation* 12 (3), 235–246. doi:10.1080/10739680590925484

Chen, Y., Zhang, Y., Zhuang, J., Lee, J. H., Wang, L., Fang, R. H., et al. (2019). Cell-membrane-Cloaked oil nanosponges enable dual-modal detoxification. *ACS Nano* 13 (6), 7209–7215. doi:10.1021/acsnano.9b02773

Chiang, C. S., Lin, Y. J., Lee, R., Lai, Y. H., Cheng, H. W., Hsieh, C. H., et al. (2018). Combination of fucoidan-based magnetic nanoparticles and immunomodulators enhances tumour-localized immunotherapy. *Nat. Nanotechnol.* 13 (8), 746–754. doi:10.1038/s41565-018-0146-7

Choi, H., Jeong, S. H., Kim, T. Y., Yi, J., and Hahn, S. K. (2021a). Bioinspired urease-powered micromotor as an active oral drug delivery carrier in stomach. *Bioact. Mater* 9, 54–62. doi:10.1016/j.bioactmat.2021.08.004

Choi, H., Kim, B., Jeong, S. H., Kim, T. Y., Kim, D., Oh, Y. K., et al. (2023). Microalgae-based biohybrid microrobot for accelerated diabetic wound healing. *Small* 19 (1), e2204617. doi:10.1002/smll.202204617

Choi, H., Yi, J., Cho, S. H., and Hahn, S. K. (2021b). Multifunctional micro/nanomotors as an emerging platform for smart healthcare applications. *Biomaterials* 279, 121201. doi:10.1016/j.biomaterials.2021.121201

Chu, D., Dong, X., Shi, X., Zhang, C., and Wang, Z. (2018). Neutrophil-based drug delivery systems. *Adv. Mater* 30 (22), 1706245. doi:10.1002/adma.201706245

Dai, Y., Jia, L., Wang, L., Sun, H., Ji, Y., Wang, C., et al. (2022). Magnetically actuated cellrobot system: precise control, manipulation, and multimode conversion. *Small* 18 (15), e2105414. doi:10.1002/smll.202105414

De, Oliveira, S., Rosowski, E. E., and Huttenlocher, A. (2016). Neutrophil migration in infection and wound repair: going forward in reverse. *Nat. Rev. Immunol.* 16 (6), 378–391. doi:10.1038/nri.2016.49

Esteban-Fernández, d., Ávila, B., Angsantikul, P., Ramírez-Herrera, D. E., Teymourian, H., Dehaini, D., et al. (2018). Hybrid biomembrane-functionalized nanorobots for concurrent removal of pathogenic bacteria and toxins. *Sci. Robot.* 3 (18), eaat0485. doi:10.1126/scirobotics.aat0485

Fang, R. H., Kroll, A. V., Gao, W., and Zhang, L. (2018). Cell membrane coating nanotechnology. *Adv. Mater* 30 (23), e1706759. doi:10.1002/adma.201706759

Fang, R. H., Hu, C. M., Luk, B. T., Gao, W., Copp, J. A., Tai, Y., et al. (2014). Cancer cell membrane-coated nanoparticles for anticancer vaccination and drug delivery. *Nano Lett.* 14 (4), 2181–2188. doi:10.1021/nl500618u

Fang, R. H., and Zhang, L. (2016). Nanoparticle-based modulation of the immune system. *Annu. Rev. Chem. Biomol. Eng.* 7, 305–326. doi:10.1146/annurev-chembioeng-080615-034446

Filardo, G., Perdisa, F., Roffi, A., Marcacci, M., and Kon, E. (2016). Stem cells in articular cartilage regeneration. *J. Orthop. Surg. Res.* 11, 42. doi:10.1186/s13018-016-0378-x

Gao, C., Lin, Z., Wang, D., Wu, Z., Xie, H., and He, Q. (2019). Red blood cell-mimicking micromotor for active photodynamic cancer therapy. *ACS Appl. Mater Interfaces* 11 (26), 23392–23400. doi:10.1021/acsami.9b07979

Gao, J., Chu, D., and Wang, Z. (2016). Cell membrane-formed nanovesicles for disease-targeted delivery. *J. Control Release* 224, 208–216. doi:10.1016/j.jconrel.2016.01.024

Gao, L., Akhtar, M. U., Yang, F., Ahmad, S., He, J., Lian, Q., et al. (2021). Recent progress in engineering functional biohybrid robots actuated by living cells. *Acta Biomater.* 121, 29–40. doi:10.1016/j.actbio.2020.12.002

Gao, W., Dong, R., Thamphiwatana, S., Li, J., Gao, W., Zhang, L., et al. (2015). Artificial micromotors in the mouse's stomach: a step toward *in vivo* use of synthetic motors. *ACS Nano* 9 (1), 117–123. doi:10.1021/nn507097k

Go, G., Jeong, S. G., Yoo, A., Han, J., Kang, B., Kim, S., et al. (2020). Human adipose-derived mesenchymal stem cell-based medical microrobot system for knee cartilage regeneration *in vivo*. *Sci. Robot.* 5 (38), eaay6626. doi:10.1126/scirobotics.aay6626

Goldberg, A., Mitchell, K., Soans, J., Kim, L., and Zaidi, R. (2017). The use of mesenchymal stem cells for cartilage repair and regeneration: a systematic review. *J. Orthop. Surg. Res.* 12 (1), 39. doi:10.1186/s13018-017-0534-y

Halder, A., and Sun, Y. (2019). Biocompatible propulsion for biomedical micro/nano robotics. *Biosens. Bioelectron.* 139, 111334. doi:10.1016/j.bios.2019.111334

Hines, L., Petersen, K., Lum, G. Z., and Sitti, M. (2017). Soft actuators for small-scale robotics. *Adv. Mater* 29 (13), 1603483. doi:10.1002/adma.201603483

Hortelao, A. C., Simó, C., Guix, M., Guallar-Garrido, S., Julián, E., Vilela, D., et al. (2021). Swarming behavior and *in vivo* monitoring of enzymatic nanomotors within the bladder. *Sci. Robot.* 6 (52), eabd2823. doi:10.1126/scirobotics.abd2823

Hu Cm, C. M., Fang, R. H., Wang, K. C., Luk, B. T., Thamphiwatana, S., Dehaini, D., et al. (2015). Nanoparticle biointerfacing by platelet membrane cloaking. *Nature* 526 (7571), 118–121. doi:10.1038/nature15373

Hu, C. M., Fang, R. H., Luk, B. T., and Zhang, L. (2013). Nanoparticle-detained toxins for safe and effective vaccination. *Nat. Nanotechnol.* 8 (12), 933–938. doi:10.1038/nnano.2013.254

Hu Q, Q., Sun, W., Qian, C., Wang, C., Bomba, H. N., and Gu, Z. (2015). Anticancer platelet-mimicking nanovehicles. *Adv. Mater* 27 (44), 7043–7050. doi:10.1002/adma.201503323

Huang, C., Lai, Z., Wu, X., and Xu, T. (2022). Multimodal locomotion and cargo transportation of magnetically actuated quadruped soft microrobots. *Cyborg Bionic Syst.* 2022, 0004. doi:10.34133/cbsystems.0004

Ji, F., Li, T., Yu, S., Wu, Z., and Zhang, L. (2021). Propulsion gait analysis and fluidic trapping of swinging flexible nanomotors. *ACS Nano* 15 (3), 5118–5128. doi:10.1021/acsnano.0c10269

Jorch, S. K., and Kubes, P. (2017). An emerging role for neutrophil extracellular traps in noninfectious disease. *Nat. Med.* 23 (3), 279–287. doi:10.1038/nm.4294

Kadiri, V. M., Günther, J. P., Kottapalli, S. N., Goyal, R., Peter, F., Alarcón-Correa, M., et al. (2021). Light- and magnetically actuated FePt microswimmers. *Eur. Phys. J. E, Soft matter* 44 (6), 74. doi:10.1140/epje/s10189-021-00074-1

Kalamasz, D., Long, S. A., Taniguchi, R., Buckner, J. H., Berenson, R. J., and Bonyhadi, M. (2004). Optimization of human T-cell expansion *ex vivo* using magnetic beads conjugated with anti-CD3 and Anti-CD28 antibodies. *J. Immunother.* 27 (5), 405–418. doi:10.1097/00002371-200409000-00010

Kroll, A. V., Fang, R. H., and Zhang, L. (2017). Biointerfacing and applications of cell membrane-coated nanoparticles. *Bioconjug Chem.* 28 (1), 23–32. doi:10.1021/acs.bioconjchem.6b00569

Kunde, S. S., and Wairkar, S. (2021). Platelet membrane camouflaged nanoparticles: biomimetic architecture for targeted therapy. *Int. J. Pharm.* 598, 120395. doi:10.1016/j.ijpharm.2021.120395

Larson, R. C., and Maus, M. V. (2021). Recent advances and discoveries in the mechanisms and functions of CAR T cells. *Nat. Rev. Cancer* 21 (3), 145–161. doi:10.1038/s41568-020-00323-z

Law, J., Wang, X., Luo, M., Xin, L., Du, X., Dou, W., et al. (2022). Microrobotic swarms for selective embolization. *Sci. Adv.* 8 (29), eabm5752. eabm5752. doi:10.1126/sciadv.abm5752

Le, Q. V., Lee, J., Lee, H., Shim, G., and Oh, Y. K. (2021). Cell membrane-derived vesicles for delivery of therapeutic agents. *Acta Pharm. Sin. B* 11 (8), 2096–2113. doi:10.1016/j.apsb.2021.01.020

Li, J., Angsantikul, P., Liu, W., Esteban-Fernández de Ávila, B., Chang, X., Sandraz, E., et al. (2018b). Biomimetic platelet-camouflaged nanorobots for binding and isolation of biological threats. *Adv. Mater* 30 (2), 1704800. doi:10.1002/adma.201704800

Li, J., Esteban-Fernández, d., Ávila, B., Gao, W., Zhang, L., and Wang, J. (2017). Micro/nanorobots for biomedicine: delivery, surgery, sensing, and detoxification. *Sci. Robot.* 2 (4), eaam6431. doi:10.1126/scirobotics.aam6431

Li, J., Li, X., Luo, T., Wang, R., Liu, C., Chen, S., et al. (2018c). Development of a magnetic microrobot for carrying and delivering targeted cells. *Sci. Robot.* 3 (19), eaat8829. doi:10.1126/scirobotics.aat8829

Li, J., and Yu, J. (2023). Biodegradable microrobots and their biomedical applications: a review. *Nanomater. (Basel)* 13 (10), 1590. doi:10.3390/nano13101590

Li, T., Yu, S., Sun, B., Li, Y., Wang, X., Pan, Y., et al. (2023). Bioinspired claw-engaged and biolubricated swimming microrobots creating active retention in blood vessels. *Sci. Adv.* 9 (18), eadg4501. doi:10.1126/sciadv.adg4501

Li, T., Zhang, A., Shao, G., Wei, M., Guo, B., Zhang, G., et al. (2018a). Janus microdimer surface walkers propelled by oscillating magnetic fields. *Adv. Funct. Mater* 28 (25), 1706066. doi:10.1002/adfm.201706066

Li, X., Wu, R., Chen, H., Li, T., Jiang, H., Xu, X., et al. (2021). Near-infrared light-driven multifunctional tubular micromotors for treatment of atherosclerosis. *ACS Appl. Mater Interfaces* 13 (26), 30930–30940. doi:10.1021/acsami.1c03600

Lv, Y., Pu, R., Tao, Y., Yang, X., Mu, H., Wang, H., et al. (2023). Applications and future prospects of micro/nanorobots Utilizing diverse biological carriers. *Micromachines (Basel)* 14 (5), 983. doi:10.3390/mi14050983

Ma, S., Li, X., Wang, X., Cheng, L., Li, Z., Zhang, C., et al. (2019). Current progress in CAR-T cell therapy for solid tumors. *Int. J. Biol. Sci.* 15 (12), 2548–2560. doi:10.7150/ijbs.34213

Nguyen, K. T., Go, G., Choi, E., Kang, B., Park, J. O., and Kim, C. S. (2018). A guide-wired helical microrobot for mechanical thrombectomy: A feasibility study. *Annu. Int. Conf. IEEE Eng. Med. Biol. Soc.* 2018, 1494–1497. doi:10.1109/EMBC.2018.8512455

Oliveira, T. H. C., Marques, P. E., Proost, P., and Teixeira, M. M. M. (2018). Neutrophils: a cornerstone of liver ischemia and reperfusion injury. *Lab. Invest.* 98 (1), 51–62. doi:10.1038/labinvest.2017.90

Olsson, M., Bruhns, P., Frazier, W. A., Ravetch, J. V., and Oldenborg, P. A. (2005). Platelet homeostasis is regulated by platelet expression of CD47 under normal conditions and in passive immune thrombocytopenia. *Blood* 105 (9), 3577–3582. doi:10.1182/blood-2004-08-2980

Oral, C. M., and Pumera, M. (2023). *In vivo* applications of micro/nanorobots. *Nanoscale* 15 (19), 8491–8507. doi:10.1039/d3nr00502j

Oroojalian, F., Beygi, M., Baradaran, B., Mokhtarzadeh, A., and Shahbazi, M. A. (2021). Immune cell membrane-coated biomimetic nanoparticles for targeted cancer therapy. *Small* 17 (12), e2006484. doi:10.1002/smll.202006484

Papayannopoulos, V. (2018). Neutrophil extracellular traps in immunity and disease. *Nat. Rev. Immunol.* 18 (2), 134–147. doi:10.1038/nri.2017.105

Park, J. H., Jiang, Y., Zhou, J., Gong, H., Mohapatra, A., Heo, J., et al. (2021). Genetically engineered cell membrane-coated nanoparticles for targeted delivery of dexamethasone to inflamed lungs. *Sci. Adv.* 7 (25), eabf7820. doi:10.1126/sciadv.abf7820

Piao, J. G., Wang, L., Gao, F., You, Y. Z., Xiong, Y., and Yang, L. (2014). Erythrocyte membrane is an alternative coating to polyethylene glycol for prolonging the circulation lifetime of gold nanocages for photothermal therapy. *ACS Nano* 8 (10), 10414–10425. doi:10.1021/nn503779d

Rao, L., Meng, Q. F., Bu, L. L., Cai, B., Huang, Q., Sun, Z. J., et al. (2017). Erythrocyte membrane-coated upconversion nanoparticles with minimal protein adsorption for enhanced tumor imaging. *ACS Appl. Mater Interfaces* 9 (3), 2159–2168. doi:10.1021/acsami.6b14450

Ricotti, L., Trimmer, B., Feinberg, A. W., Raman, R., Parker, K. K., Bashir, R., et al. (2017). Biohybrid actuators for robotics: A review of devices actuated by living cells. *Sci. Robot.* 2 (12), eaaq0495. doi:10.1126/scirobotics.aaq0495

Shao, J., Abdelghani, M., Shen, G., Cao, S., Williams, D. S., and Hest, J. C. M. (2018). Erythrocyte membrane modified Janus polymeric motors for thrombus therapy. *ACS Nano* 12 (5), 4877–4885. doi:10.1021/acsnano.8b01772

Shi, C., and Pamer, E. G. (2011). Monocyte recruitment during infection and inflammation. *Nat. Rev. Immunol.* 11 (11), 762–774. doi:10.1038/nri3070

Singh, A. V., Ansari, M. H. D., Laux, P., and Luch, A. (2019). Micro-nanorobots: important considerations when developing novel drug delivery platforms. *Expert Opin. Drug Deliv.* 16 (11), 1259–1275. doi:10.1080/17425247.2019.1676228

Sitti, M., Ceylan, H., Hu, W., Giltinan, J., Turan, M., Yim, S., et al. (2015). Biomedical applications of untethered mobile milli/microrobots. *Proc. IEEE Inst. Electr. Electron Eng.* 103 (2), 205–224. doi:10.1109/JPROC.2014.2385105

Song, X., Qian, R., Li, T., Fu, W., Fang, L., Cai, Y., et al. (2022). Imaging-guided biomimetic M1 macrophage membrane-camouflaged magnetic nanorobots for photothermal immunotargeting cancer therapy. *ACS Appl. Mater Interfaces* 14 (51), 56548–56559. doi:10.1021/acsami.2c16457

Soto, F., Karshalev, E., Zhang, F., Esteban Fernandez de Avila, B., Nourhani, A., and Wang, J. (2022). Smart materials for microrobots. *Chem. Rev.* 122 (5), 5365–5403. doi:10.1021/acs.chemrev.0c00999

Sun, L., Yu, Y., Chen, Z., Bian, F., Ye, F., Sun, L., et al. (2020). Biohybrid robotics with living cell actuation. *Chem. Soc. Rev.* 49 (12), 4043–4069. doi:10.1039/d0cs00120a

Tang, C., Wang, C., Zhang, Y., Xue, L., Li, Y., Ju, C., et al. (2019). Recognition, intervention, and monitoring of neutrophils in acute ischemic stroke. *Nano Lett.* 19 (7), 4470–4477. doi:10.1021/acs.nanolett.9b01282

Tang, J., Shen, D., Caranasos, T. G., Wang, Z., Vandergriff, A. C., Allen, T. A., et al. (2017). Therapeutic microparticles functionalized with biomimetic cardiac stem cell membranes and secretome. *Nat. Commun.* 8, 13724. doi:10.1038/ncomms13724

Tang, S., Zhang, F., Gong, H., Wei, F., Zhuang, J., Karshalev, E., et al. (2020). Enzyme-powered Janus platelet cell robots for active and targeted drug delivery. *Sci. Robot.* 5 (43), eaba6137. doi:10.1126/scirobotics.aba6137

Tang, X., Yang, Y., Zheng, M., Yin, T., Huang, G., Lai, Z., et al. (2023). Magnetic-acoustic sequentially actuated CAR T cell microrobots for precision navigation and *in situ* antitumor immunoactivation. *Adv. Mater* 35 (18), e2211509. doi:10.1002/adma.202211509

Turley, S. J., Cremasco, V., and Astarita, J. L. (2015). Immunological hallmarks of stromal cells in the tumour microenvironment. *Nat. Rev. Immunol.* 15 (11), 669–682. doi:10.1038/nri3902

Venugopalan, P. L., Esteban-Fernández, d., Ávila, B., Pal, M., Ghosh, A., and Wang, J. (2020). Fantastic voyage of nanomotors into the cell. *ACS Nano* 14 (8), 9423–9439. doi:10.1021/acsnano.0c05217

Wang, C., Sim, K., Chen, J., Kim, H., Rao, Z., Li, Y., et al. (2018). Soft ultrathin electronics innervated adaptive fully soft robots. *Adv. Mater* 30 (13), e1706695. doi:10.1002/adma.201706695

Wang, H., and Pumera, M. (2015). Fabrication of micro/nanoscale motors. *Chem. Rev.* 115 (16), 8704–8735. doi:10.1021/acs.chemrev.5b00047

Wang, H., Yu, S., Liao, J., Qing, X., Sun, D., Ji, F., et al. (2022). A robot platform for highly efficient pollutant purification. *Front. Bioeng. Biotechnol.* 10, 903219. doi:10.3389/fbioe.2022.903219

Wang, Q., and Zhang, L. (2021). External power-driven microrobotic swarm: from fundamental understanding to imaging-guided delivery. *ACS Nano* 15 (1), 149–174. doi:10.1021/acsnano.0c07753

Wang, S., Duan, Y., Zhang, Q., Komarla, A., Gong, H., Gao, W., et al. (2020). Drug targeting *via* platelet membrane-coated nanoparticles. *Small Struct.* 1 (1), 2000018. doi:10.1002/sstr.202000018

Wang, X., Zhang, D., Bai, Y., Zhang, J., and Wang, L. (2022). Enzyme-powered micro/nanomotors for cancer treatment. *Chem. Asian J.* 17 (16), e202200498. doi:10.1002/asia.202200498

Wang, Y., Shen, J., Handschuh-Wang, S., Qiu, M., Du, S., and Wang, B. (2023). Microrobots for targeted delivery and therapy in digestive system. *ACS Nano* 17 (1), 27–50. doi:10.1021/acsnano.2c04716

Wang, Y., Zhou, C., Wang, W., Xu, D., Zeng, F., Zhan, C., et al. (2018). Photocatalytically powered matchlike nanomotor for light-guided active SERS sensing. *Angew. Chem. Int. Ed. Engl.* 57 (40), 13110–13113. doi:10.1002/anie.201807033

Webster-Wood, V. A., Guix, M., Xu, N. W., Behkam, B., Sato, H., Sarkar, D., et al. (2022). Biohybrid robots: recent progress, challenges, and perspectives. *Bioinspir Biomim.* 18 (1), 015001. doi:10.1088/1748-3190/ac9c3b

Wei, X., Beltrán-Gastélum, M., Karshalev, E., Esteban-Fernández de Ávila, B., Zhou, J., Ran, D., et al. (2019). Biomimetic micromotor enables active delivery of antigens for oral vaccination. *Nano Lett.* 19 (3), 1914–1921. doi:10.1021/acs.nanolett.8b05051

Wu, Z., Li, T., Li, J., Gao, W., Xu, T., Christianson, C., et al. (2014). Turning erythrocytes into functional micromotors. *ACS Nano* 8 (12), 12041–12048. doi:10.1021/nn506200x

Xia, Y., Rao, L., Yao, H., Wang, Z., Ning, P., and Chen, X. (2020). Engineering macrophages for cancer immunotherapy and drug delivery. *Adv. Mater* 32 (40), e2002054. doi:10.1002/adma.202002054

Xu, D., Wang, Y., Liang, C., You, Y., Sanchez, S., and Ma, X. (2020). Self-propelled micro/nanomotors for on-demand biomedical cargo transportation. *Small* 16 (27), e1902464. doi:10.1002/smll.201902464

Xu, H., Medina-Sánchez, M., Magdanz, V., Schwarz, L., Hebenstreit, F., and Schmidt, O. G. (2018). Sperm-hybrid micromotor for targeted drug delivery. *ACS Nano* 12 (1), 327–337. doi:10.1021/acsnano.7b06398

Xue, J., Zhao, Z., Zhang, L., Xue, L., Shen, S., Wen, Y., et al. (2017). Neutrophil-mediated anticancer drug delivery for suppression of postoperative malignant glioma recurrence. *Nat. Nanotechnol.* 12 (7), 692–700. doi:10.1038/nnano.2017.54

Yang, C., Ming, Y., Zhou, K., Hao, K., Hu, D., Chu, B., et al. (2022). Macrophage membrane-camouflflaged shRNA and doxorubicin: A pH-dependent release system for melanoma chemo-immunotherapy. *Research (Washington D. C.).* 9768687. doi:10.34133/2022/9768687

Yu, S., Li, T., Ji, F., Zhao, S., Liu, K., Zhang, Z., et al. (2022). Trimer-like microrobots with multimodal locomotion and reconfigurable capabilities. *Mat. Today Adv.* 14, 100231. doi:10.1016/j.mtadv.2022.100231

Zeng, Y., Li, S., Zhang, S., Wang, L., Yuan, H., and Hu, F. (2022). Cell membrane coated-nanoparticles for cancer immunotherapy. *Acta Pharm. Sin. B* 12 (8), 3233–3254. doi:10.1016/j.apsb.2022.02.023

Zhang B, B., Pan, H., Chen, Z., Yin, T., Zheng, M., and Cai, L. (2023). Twin-bioengine self-adaptive micro/nanorobots using enzyme actuation and macrophage relay for gastrointestinal inflammation therapy. *Sci. Adv.* 9 (8), eadc8978. doi:10.1126/sciadv.adc8978

Zhang, F., Mundaca-Uribe, R., Askarinam, N., Gao, W., Zhang, L., Wang, J., et al. (2022a). Biomembrane-functionalized micromotors: biocompatible active devices for diverse biomedical applications. *Adv. Mater* 34 (5), e2107177. doi:10.1002/adma.202107177

Zhang, F., Zhuang, J., Esteban, Fernández., de, Ávila, B., Zhang, Q., Fang, R. H., et al. (2019). A nanomotor-based active delivery system for intracellular oxygen transport. *ACS Nano* 13 (10), 11996–12005. doi:10.1021/acsnano.9b06127

Zhang, F., Zhuang, J., Li, Z., Gong, H., de Ávila, B. E., Duan, Y., et al. (2022b). Nanoparticle-modified microrobots for *in vivo* antibiotic delivery to treat acute bacterial pneumonia. *Nat. Mater.* 21 (11), 1324–1332. doi:10.1038/s41563-022-01360-9

Zhang, H., Li, Z., Wu, Z., and He, Q. (2022c). Cancer cell membrane-camouflaged micromotor. *Adv. Ther.* 2, 1900096. doi:10.1002/adtp.201900096

Zhang, H., Li, Z., Gao, C., Fan, X., Pang, Y., Li, T., et al. (2021). Dual-responsive biohybrid neutrobots for active target delivery. *Sci. Robot.* 6 (52), eaaz9519. doi:10.1126/scirobotics.aaz9519

Zhang L, L., Zhang, B., Liang, R., Ran, H., Zhu, D., Ren, J., et al. (2023). A dual-biomineralized yeast micro-/nanorobot with self-driving penetration for gastritis therapy and motility recovery. *ACS Nano* 17 (7), 6410–6422. doi:10.1021/acsnano.2c11258

Zhang, L., Li, R., Chen, H., Wei, J., Qian, H., Su, S., et al. (2017). Human cytotoxic T-lymphocyte membrane-camouflaged nanoparticles combined with low-dose irradiation: a new approach to enhance drug targeting in gastric cancer. *Int. J. Nanomedicine* 12, 2129–2142. doi:10.2147/IJN.S126016

Zhang, Q., Honko, A., Zhou, J., Gong, H., Downs, S. N., Vasquez, J. H., et al. (2020). Cellular nanosponges inhibit SARS-CoV-2 infectivity. *Nano Lett.* 20 (7), 5570–5574. doi:10.1021/acs.nanolett.0c02278

Zhang W, W., Deng, Y., Zhao, J., Zhang, T., Zhang, X., Song, W., et al. (2023). Amoeba-inspired magnetic venom microrobots. *Small* 19 (23), e2207360. doi:10.1002/smll.202207360

Zhou, J., Kroll, A. V., Holay, M., Fang, R. H., and Zhang, L. (2020a). Biomimetic nanotechnology toward personalized vaccines. *Adv. Mater* 32 (13), 1901255. doi:10.1002/adma.201901255

Zhou, M., Xing, Y., Li, X., Du, X., Xu, T., and Zhang, X. (2020b). Cancer cell membrane camouflaged semi-Yolk@Spiky-shell nanomotor for enhanced cell adhesion and synergistic therapy. *Small* 16 (39), 2003834. doi:10.1002/smll.202003834

Zhuang, J., Gong, H., Zhou, J., Zhang, Q., Gao, W., Fang, R. H., et al. (2020). Targeted gene silencing *in vivo* by platelet membrane-coated metal-organic framework nanoparticles. *Sci. Adv.* 6 (13), eaaz6108. eaaz6108. doi:10.1126/sciadv.aaz6108

frontiers | Frontiers in Bioengineering and Biotechnology

TYPE Review
PUBLISHED 19 October 2023
DOI 10.3389/fbioe.2023.1276485

OPEN ACCESS

EDITED BY
Katherine Villa,
Institut Català d'Investigació Química, Spain

REVIEWED BY
Maria Guix,
University of Barcelona, Spain
Liangfei Tian,
Zhejiang University, China

*CORRESPONDENCE
Huijuan Dong,
dhj@hit.edu.cn
Jie Zhao,
jzhao@hit.edu.cn

RECEIVED 12 August 2023
ACCEPTED 09 October 2023
PUBLISHED 19 October 2023

CITATION
Mu G, Qiao Y, Sui M, Grattan KTV, Dong H and Zhao J (2023), Acoustic-propelled micro/nanomotors and nanoparticles for biomedical research, diagnosis, and therapeutic applications.
Front. Bioeng. Biotechnol. 11:1276485.
doi: 10.3389/fbioe.2023.1276485

Acoustic-propelled micro/nanomotors and nanoparticles for biomedical research, diagnosis, and therapeutic applications

Guanyu Mu[1], Yu Qiao[1], Mingyang Sui[1], Kenneth T. V. Grattan[1,2], Huijuan Dong[1]* and Jie Zhao[1]*

[1]State Key Laboratory of Robotics and System, Harbin Institute of Technology, Harbin, China, [2]School of Science and Technology, University of London, London, United Kingdom

Acoustic manipulation techniques have gained significant attention across various fields, particularly in medical diagnosis and biochemical research, due to their biocompatibility and non-contact operation. In this article, we review the broad range of biomedical applications of micro/nano-motors that use acoustic manipulation methods, with a specific focus on cell manipulation, targeted drug release for cancer treatment and genetic disease diagnosis. These applications are facilitated by acoustic-propelled micro/nano-motors and nanoparticles which are manipulated by acoustic tweezers. Acoustic systems enable high precision positioning and can be effectively combined with magnetic manipulation techniques. Furthermore, acoustic propulsion facilitates faster transportation speeds, making it suitable for tasks in blood flow, allowing for precise positioning and in-body manipulation of cells, microprobes, and drugs. By summarizing and understanding these acoustic manipulation methods, this review aims to provide a summary and discussion of the acoustic manipulation methods for biomedical research, diagnostic, and therapeutic applications.

KEYWORDS

micro/nanomotors, targeted drug delivery, biocompatibility, acoustic manipulation, biomedical engineering

1 Introduction

In the past decade, various methods have been used to manipulate micro droplets and particles, including electrodynamics (Pollack et al., 2000; Li and Kim, 2020), acoustics (Wiklund et al., 2012; Zhang et al., 2020), electromagnetics (Fan et al., 2020), and fluid mechanics (Zhu and Wang, 2017). Acoustic levitation and manipulation are achieved by adjusting the position of trapping point through active adjustment of the acoustic field, thus there are no specific requirements for the shape or attributes of the manipulated objects compared with other transportation methods (Li et al., 2018; Wang et al., 2022; Zhang et al., 2023). Therefore, acoustic methods has shown a number of important benefits in biomedical applications: such as simple configuration and low cost, high biocompatibility and low contamination of reagents (Zhang et al., 2018) as well as high-speed fluid driving and large driving force. Due to the above advantages, acoustic manipulation of bio-matter in air or water has demonstrated various applications in medicine (Guttenberg et al., 2005; Zhang et al., 2011; Peng Lee et al., 2013; Schmid et al., 2014) and biological research (Mohanty et al., 2020).

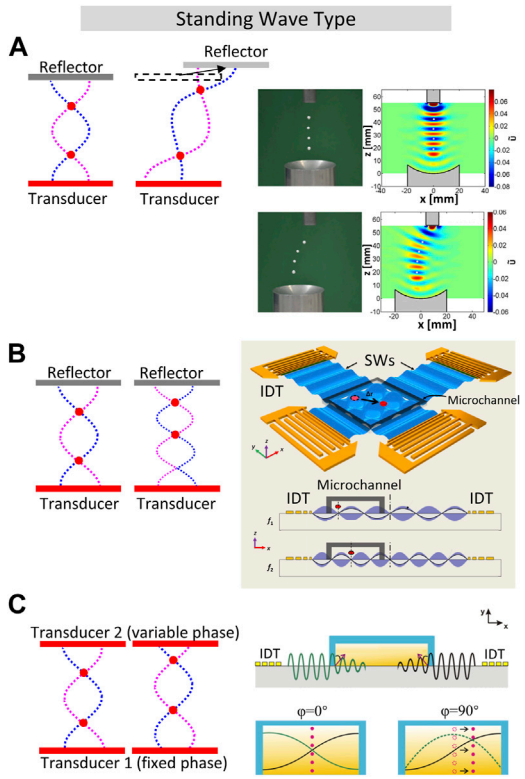

FIGURE 1
Acoustic manipulation of particles and droplets using standing waves (SW). **(A)**. SW method by moving the reflector—normally used for manipulate macro-objects. Adapted and reproduced with permission from (Andrade et al., 2015). Copyright 2015, AIP Publishing LLC. **(B)**. Standing Surface Acoustic Wave (SSAW) manipulation of biological objects, including cells and entire organisms (*C. elegans*) by adjusting the frequency of two chirped IDTs (Ding et al., 2012). **(C)**. Single human breast cancer cell manipulation using SAW by adjusting the phase shift between opposed IDTs. Reproduced with permission from (Meng et al., 2011). Copyright 2011, American Institute of Physics.

Specifically, the acoustic manipulation can be divided into Bulk Acoustic Wave (BAW) type and Surface Acoustic Wave (SAW) type according to the mode of wave propagation. BAWs are normally excited by PZT materials and they have a wide range of working frequency (from tens of kHz to tens of MHz), meaning that BAWs can manipulate objects ranging in size from millimeters to nanometers, and being particularly suitable for guiding and micro-manipulating inside biological organisms. By comparison, inter-digital transducers (IDT) are often used to generate SAW. Its operating frequency is from several hundred KHz to tens of MHz, and SAW is very ideal for acoustic manipulation of micro- and nano-objects in liquid medium, for the purpose of separation and detection. In this review, the ability of acoustic manipulation for precise delivery is vital in diverse biological research domains, such as intracellular substance delivery and controlled cell growth, targeted drug delivery and genetic marker delivery for diagnostic purpose. This review introduces the three common techniques of acoustic manipulation for micro/nano-motors: traveling waves, standing waves, and phased arrays. Additionally, we provide a summary of the medical applications of acoustic-driven micro/nano-motors.

2 Acoustic manipulation techniques commonly used in biological applications

2.1 Manipulation technique using standing waves

2.1.1 Operation principle of standing wave manipulation

Standing Wave (SW) acoustic manipulation is a technique that harnesses the power of standing waves to control and manipulate micro-objects such as particles or cells within air or a liquid medium. It operates on the principle of constructive interference between two counter-propagating sound waves. When these waves align, they create stable regions of high and low pressure, known as antinodes and nodes, respectively, within the fluid. Particles suspended in this medium experience acoustic radiation forces that drive them towards the nodes. By adjusting the phase and frequency of the sound waves, precise control over particle positioning can be achieved. SW manipulation finds applications in various fields, including biomedicine, microfluidics, and materials science, enabling tasks like cell sorting, patterning, and precise particle assembly.

SW is formed between the radiator and the reflector when their distance is an integer multiple of the half wavelength. Therefore, the SW node could be moved by adjusting the structural distance and control the wavelength by changing the frequency at the same time. In particular, (Fletcher et al., 1975), realized the movement of solid objects in the acoustic field through adjusting the position of the movable wall while concurrently modifying the frequency of the opposing speaker to keep the acoustic chamber resonant and as a result, the object was transported half the distance moved by the movable wall. This method of moving the reflector can also realize in-plane manipulation in non-resonant mode (Andrade et al., 2015), as shown in Figure 1A. In this mode, the SW is formed by the superposition of the sound wave emitted by the transducer and the first reflected wave, while higher-order reflections can be ignored because the size of the transducer is relatively small compared to the size of the reflector. Thus, the distance between the excitor and reflector does not have to be an integer multiple of the wavelength anymore. In their actual setup, the diameter of the piezoelectric transducer and the concave reflector is 10 mm and 40 mm, respectively. The polystyrene sphere is levitated at a node about a quarter wavelength away from the transducer surface and its position can be changed by moving the reflector. Due to the requirement of mechanical part to move the reflector, this SW transportation method based on moving the reflector is difficult to apply to SAW devices, which usually has a fixed distance between the transducers. Also, the wavelengths required for micrometer-sized cells/micro/nano-motors are much shorter than in air manipulation of millimeter-sized objects, making it challenging to move the reflector in such a precise way.

2.1.2 Biotweezer using frequency variation method

To manipulate micro/nanoscale objects in liquid, one-dimensional acoustic transportation can be achieved without any moving parts, by switching the frequency between different resonant modes in a resonant cavity with fixed ends.

Ding et al. (Ding et al., 2012) employed two orthogonal pairs of chirped interdigital transducer (IDT) devices to generate SAW and

micro and nanoscale biological objects, where *C. elegans* were manipulated through frequency adjustment, as depicted in Figure 1B. Their experiments also ensured that acoustic field is safe to biological samples, because the power density of acoustic tweezers was much lower compared to optical tweezers and optoelectronic tweezers. (Jooss et al., 2022). conducted *in vivo* experiments on the manipulation of microbubble particles in zebrafish embryos. Using orthogonal opposing PZT transducers, they created a high frequency (~4.0 MHz) BAW field within the zebrafish embryo and adjusted the sound pressure nodes through frequency modulation. As a result, controlled up-, down-, and cross-stream manipulation of the entire vasculature system was achieved. This enabled precise control of microbubbles *in vivo* for biomedical applications.

2.1.3 Biotweezer using phase control approach

Acoustic manipulation by adjusting the phase provides a more continuous and stable one-dimensional levitation transportation capability compared to the above two methods (Park and Ro, 2013). This is because the transducers maintain a fixed excitation frequency throughout the transportation process using the phase control method, thereby allowing the utilization of transducers with high quality factors to enhance the sound pressure of the acoustic field. Consequently, the method of generating SWs through the superposition of traveling waves emitted by a pair of transducers was developed (Matsui et al., 1995; Haake and Dual, 2002; Kozuka et al., 2007; Courtney et al., 2012; Dong et al., 2017). The position of the pressure nodes has a linear relationship with the phase difference between the two transducers. As early as 1995, (Matsui et al., 1995), conducted experiments on the relationship between the phase difference, the levitation position, and the acoustic radiation force in the air using a coaxial dual transducer device. This method is then used for precise transportation of single human breast cancer cell, the benefits of sonoporation in increasing cell permeability are also obtained simultaneously (Meng et al., 2011; Meng et al., 2014), as shown in Figure 1C.

Apart from coaxial dual transducer devices, different forms of resonant cavities could be used to expand the transportation range (Kozuka et al., 2007; Park and Ro, 2013). On a more microscopic scale, (Bernassau et al., 2013), developed an acoustic tweezer using seven PZT transducers. By selectively exciting multiple transducers at 4 MHz and adjusting the phase difference between them, they generated line or hexagonal-shaped acoustic fields for cell patterning. They successfully patterned and cultured C2C12 cell line and Schwann cells, forming columnar structures under the lattice acoustic field, suggesting potential applications in tissue engineering.

2.2 Fast transportation of micro/nano-swimmers using traveling waves

During SW transportation, the objects are captured at the SW nodes, which limits the shapes and sizes of objects and restrict the speed and distance of transportation. However, the Traveling Wave (TW) transportation method has overcome these limitations, the TW method involves the generation of acoustic waves that propagate through a medium in a single direction. Unlike SWs, where waves interact to create stationary nodes and antinodes, traveling waves maintain their directional movement. In TW manipulation, these waves create a force field that can be harnessed to control the movement and positioning of micro- and nanoparticles suspended within the medium. This method is particularly advantageous for achieving rapid and precise transport of particles continuously over long distances and travel at high speeds.

In air-based TW transportation systems, the "excitation-absorption" mode is commonly used to generate TWs, where either a transducer or absorbent materials can be utilized to absorb vibrations and thus form TWs along the vibrating plate. (Hashimoto et al., 1998; Ueha et al., 2000). achieved TW-based near field acoustic levitation and transportation using two transducers and a vibrating plate, as shown in Figure 2A, where a TW with standing wave ratio of 1.7 was formed. The terminal velocity of a large planar object weighed 8.6 g reached 0.7 m/s, which is significantly faster compared to SW transportation methods. Absorbent materials such as silicone rubber can also be utilized to generate a TW acoustic field in air to transport ethanol droplets (Ito et al., 2010; Ding et al., 2012).

The "excitation-absorption" mode can also be used to generate travelling surface acoustic waves (TSAW), so that liquid-based transportation of micro/nano robots can be achieved. TSAW could be formed either by the use of sound-absorbing gels (Renaudin et al., 2006; Li et al., 2007; Collignon et al., 2015) or by setting a spatial phase difference between the pairs of the IDTs (Sui et al., 2022; Dong et al., 2023), as shown in Figure 2B. Another method for forming TSAW is to use single curved-shape transducer that operates at high excitation frequency from 100 MHz to 1 GHz (Destgeer et al., 2017). Higher frequency TSAW is suitable for precise transportation of micro-scale objects such as selective cell sorting because of its shorter acoustic wavelength (Collins et al., 2016). Using similar principles, (Fonseca et al., 2022), generated TWs in liquid with one PZT transducer to simulate physiological flow environments in blood vessels, as illustrated in Figure 2C. Operations in blood vessels was found to be a complex and challenging procedure (Zhang et al., 2023), while the acoustic method could also successfully transport micro/nanorobots across the flow and upstream without special requirements on the material used compared to magnetic propulsion methods (Li et al., 2023), and it will not generate any additional magnetic fields. As micro/nanorobots have many potential applications in medical field, such as drug delivery (Yu et al., 2023) and noncontact biomedical operations (Ji et al., 2021), and it has been demonstrated (Yu et al., 2022) that passive micro/nanomotors are capable of being moved in complex 3D environments, which enables the possibility to realize targeted drug delivery by generating a localized acoustic field.

2.3 Transportation methods based on transducer arrays and holograms

Phased array transducers represent an acoustic manipulation technique that leverages an array of transducers, typically positioned at precise intervals, emit acoustic waves with controllable phase shifts. By carefully adjusting the timing and phase of the emission of each transducer, it is possible to manipulate the resultant acoustic field dynamically. This dynamic control allows for the creation of intricate patterns of pressure nodes and antinodes within the field. Consequently, small objects or particles within this acoustic landscape can be precisely

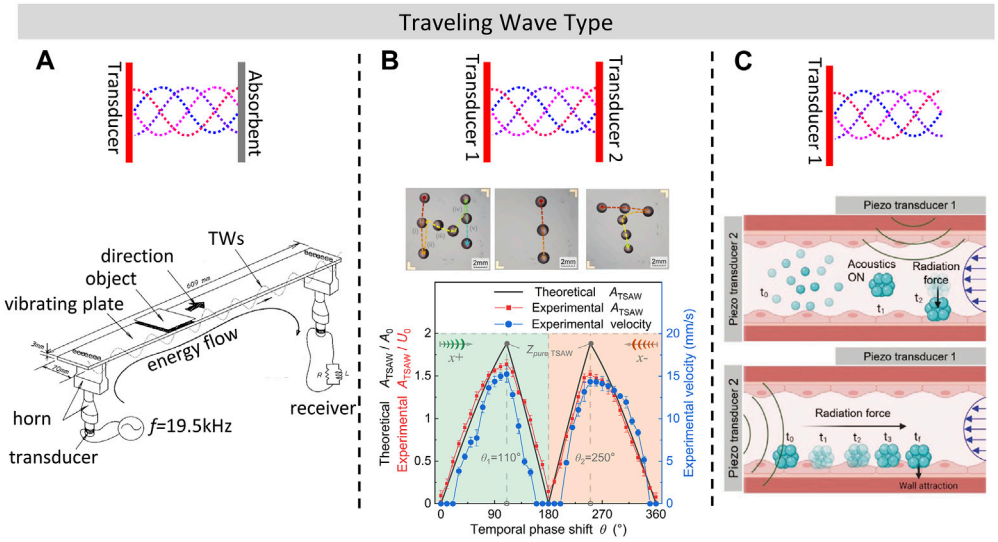

FIGURE 2
Line transportation and manipulation in plane using TW **(A)**. Acoustic transportation device using TW formed with passive electric network. Reprinted with permission from (Hashimoto et al., 1998). Copyright 1998, Acoustic Society of America. **(B)**. Droplet transportation by adjusting the temporal phase shift of SAW. Reproduced with permission from (Sui et al., 2022). Copyright 2022, The Royal Society of Chemistry. **(C)**. Traveling Surface Acoustic Wave (TSAW) manipulation of Swarmbots inside blood flow using a focused IDT (Fonseca et al., 2022). Copyright 2022 The Authors. Advanced Materials Interfaces published by Wiley-VCH GmbH. This is an open access article under the terms of the Creative Commons Attribution-Noncommercial License.

levitated and manipulated in real-time and in three dimensions. The transducer array could realize long-distance transportation of multiple objects by changing the acoustic focal points, and the transportation process is more stable compared to the above-mentioned SW method. By controlling the excitation phase difference and amplitude of the driving voltage applied to adjacent transducers, SW nodes can be generated at any position in space. In 2014, (Hoshi et al., 2014; Ochiai et al., 2014a; b), used two opposite ultrasonic phased arrays to realize three-dimensional transport of millimeter-sized polystyrene particles in air. The range of the sound field can vary widely compared to the SW method and TW method, from 25 × 25 cm^2 to 100 × 100 cm^2. The transducer arrays can also realize acoustic focus by adjusting the orientation of the transducers mechanically (Marzo et al., 2017; Youssefi and Diller, 2019; MatthewáReichert, 2020) instead of modulating the phase between the transducers, the advantage is to maximize the acoustic radiation force and reduce parasitic reflections.

Compared with opposed dual arrays, single-sided array reduces the cost and does not create additional acoustic nodes. In the single-sided array configuration type, (Koyama and Nakamura, 2010; Nakamura and Koyama, 2012; Kashima et al., 2014), built a circular piezoelectric transducer array composed of 24 piezoelectric transducers. By switching the input signal between the piezoelectric patches, manipulation of polystyrene ball with circular trajectory with an accuracy of 7.5° was realized. Daniele et al. (Foresti et al., 2013a; Foresti et al., 2013b; Vasileiou et al., 2016) developed a one-dimensional array composed of multiple 15 × 15 mm transducers. Contactless droplet mixing and cell DNA transfection were achieved. In 2015, Marzo et al. (Marzo et al., 2015) developed a single-sided acoustic levitation array and does not require the reflector structure, which provides large operating area above the transducers array. This type of device can then be used to manipulate objects noninvasively in living body, like expelling a kidney stone (Ghanem et al., 2020) as shown in Figure 3A.

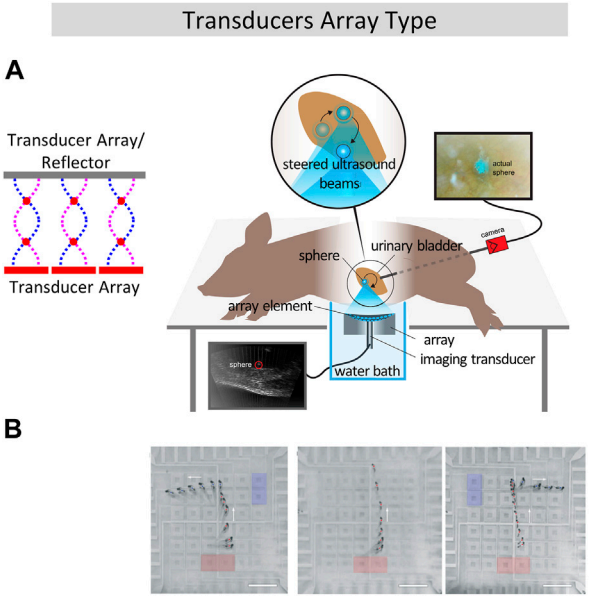

FIGURE 3
Biomedical application of line transportation using transducer arrays. **(A)** Transcutaneous acoustic manipulation of a 3-mm glass sphere inserted through the ureter into the bladder of a pig using ultrasonic phased array (Ghanem et al., 2020). **(B)** Programmable acoustofluidic manipulation of zebrafish larvae using array of hollowsquare shaped IDTs. Reproduced with permission from (Zhang et al., 2019). Copyright 2019, The Royal Society of Chemistry.

Transducer arrays can also be used to handle liquid using SAW, and have the advantage of being rewritable and programmable, compared with traditional acoustofluidic methods. In 2018, the team of Huang (Zhang et al., 2018) proposed an array of IDTs which can realize non-contact transportation of 1nL to 100 μL liquid along any planar axis via acoustic-streaming-induced traps. They also designed a hollow-square shaped IDTs and immersed it in water (Zhang et al., 2019), contactless and programmable manipulation of oil droplets and zebrafish larvae was realized on water, as shown in Figure 3B. Like PZT arrays, IDT transducer array can be arranged into other shapes than square matrix in order to accomplish complex two-dimensional patterning of single or multiple cells, such as fan-shaped (Wang et al., 2018) or ring-shaped (Tian et al., 2019) and this being very useful in the cultivation of special tissues. The phased array method for acoustic manipulation offers significant advantages in terms of real-time reconfiguration and precision. It allows for dynamic adjustments of acoustic waves, providing the flexibility to control ultrasound beams.

Acoustic holography introduces a simpler and more cost-effective approach compared to phased array transducers. It utilizes acoustic holograms to modify the output of a single ultrasonic transducer and create a designed 2D phase profile. The acoustic hologram plate could be fabricated with a costumed thickness distribution using the 3D printing technology, which is intend to form local phase retardation. This would modulate the phase shift physically (instead of electronically) to modify the phase shift in phased array. When ultrasound waves pass through the hologram, they emerge with the necessary phase distribution, diffract to form a real image at the desired location, and continue propagating. Therefore, the sound pressure distribution, designed to show high fidelity and independent of the host container geometry, is formed. Since the ultrasound is generated from one single transducer, the acoustic holography no longer requires a large number of transducers to achieve complex shaped manipulation. Melde et al. (Melde et al., 2016) were able to 3D print a hologram with 375 μm resolution and achieved 15,000 acoustic pixels in the hologram, where only one transducer operating at a frequency of 2 Mhz was used. This device can not only be used for acoustic fabrication of silicone particles soaked in a UV-crosslinker (Melde et al., 2018), but also used for building 3D cell assemblies (Ma et al., 2020a). Thus, acoustic technology has found various applications in the field of biomedical and biomaterials research. In the next section, some main biomedical applications of acoustic manipulation of micro/nano-motors and bioactive particles are reviewed.

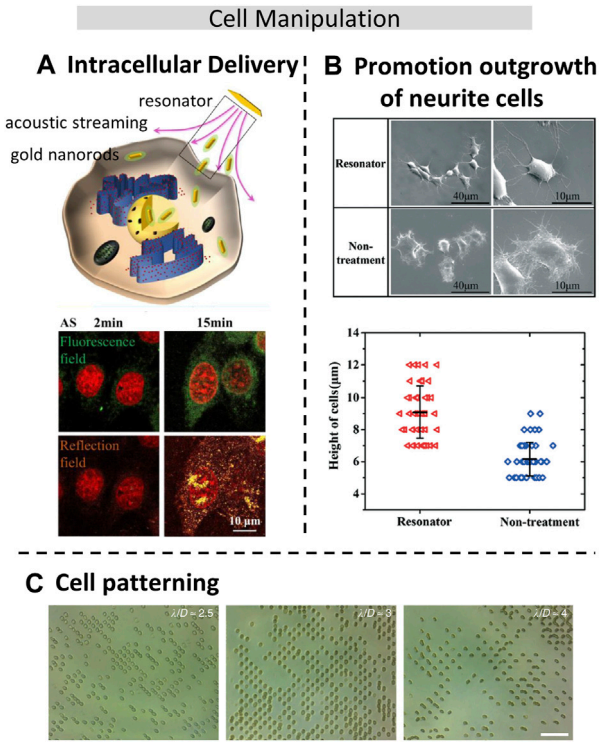

FIGURE 4
Acoustic manipulation techniques for cellular applications. **(A)**. Acoustic-induced intracellular delivery of gold nanorods (AuNRs) into the cytoplasm and even the nuclei of cancer and normal cells. Reproduced with permission from (He et al., 2022). Copyright 2022, American Chemical Society. **(B)**. The neuron-like phenotype of PC12 cells owing to shear stress caused by the acoustic streaming effect. Reproduced with permission from (He et al., 2021). Copyright 2017, The Royal Society of Chemistry. **(C)**. Red blood cell pattern in two dimensions using Standing Surface Acoustic Waves (SSAW) (Collins et al., 2015). Copyright 2015, The Authors. This work is licensed under a Creative Commons Attribution 4.0 International License.

3 Biomedical applications of acoustic driven micro/nano-motors and nanoparticles

3.1 Applications on cellular operations

Cell manipulation is a very important technology in bioengineering, micromanipulation has entered the operation level of subcellular level and has been applied to cell surgery, single-cell analysis, and cell translocation. Therefore, regulation of cell position and posture is an important part of cell micromanipulation. Among many non-contact cell manipulation techniques (Tang et al., 2022), both optical tweezers and electric methods could cause damage or induce undesired electrochemical reactions, while the acoustic methods could realize controlled rotation of biomaterials size ranging from 0.1 μm to 1000 μm. In addition to enabling cell rotation through the ultrasonic streaming flow effect, it also facilitates the transportation of complex trajectories (Ma et al., 2020b), or allows for controllable cell deformation (Guo et al., 2021) using bulk acoustic resonator. This study also shows that the cell deformation tool can be used for cell membrane permeability study, which could be used for research on cell surface modification and drug uptake efficiency. Zhao et al. (Zhao et al., 2021) developed a rapid drug screening method by changing the permeability of leukemia cells (THP-1), and increased the speed of drug screening by eight times. He et al. (He et al., 2022) have found that that acoustic treatment significantly facilitated intracellular delivery into both the cytoplasm and the nucleus, as shown in Figure 4A, with much higher efficiency compared to endocytosis. Additionally, they discovered that the acoustic treatment induced changes in the mechanical properties of both normal and cancer cells, leading to improvements in cytoskeleton integrity and cell stiffness. However, these effects were found to be

dependent on the specific cell lines used in the experiments. When acoustic streaming is applied to nerve cells, it can also stimulate the neurite growth in the desired direction, as shown in Figure 4B (He et al., 2021). Compared to other methods, acoustic-based approaches are considered safer and more efficient. Another advantage of acoustic manipulation is the ability to cell patterning through the formation of standing waves, which is particularly useful in single-cell analysis. By adjusting the wavelength of the sound waves, the size of cell patterns can be changed to accommodate cells of different sizes. Unlike other cell manipulation techniques based on magnetic and electric field, acoustic manipulation does not impact cell viability, thereby preserving the cells' biological activity and functionality. (Shi et al., 2009). achieved 1D and 2D cell patterning by placing the IDTs horizontally or vertically to form different SW acoustic fields. However, due to the larger wavelength of the acoustic waves compared to cell size, each trapping position was occupied by multiple cells. By increasing the frequency to reduce the wavelength to about one-fourth of the cell diameter, (Collins et al., 2015), realized single red blood cell pattern in two dimensions using SSAW, as shown in Figure 4C. This can also be used to the cultivation of special tissues such as engineering muscle tissue (Armstrong et al., 2018), cartilage (Armstrong et al., 2022) and guide neurite outgrowth (Gesellchen et al., 2014). Recently, (Zheng et al., 2023), assembled *in vitro* breast cancer cells (MCF-7) tumor spheroids by the use of acoustic microstreaming vortices generated with bulk acoustic waves. Biocompability is also crucial in cell manipulation (Wiklund, 2012), and it has been demonstrated that human white blood cells (Li et al., 2015), breast cancerous cells (Qian et al., 2021) can remain high viability after acoustic treatment.

3.2 Drug delivery and targeted therapy

Micro/Nano-motors offer targeted drug delivery and release capabilities driven by external fields, where acoustically-driven micro/nano-motors have no limits to the materials used and thus offering higher safety and broader applicability than magnetically driven methods. Common types of ultrasonic motors include rod/wire-shaped, tubular, and helical micro/nanorobots (Li et al., 2022), where acoustically-driven gold nanowire robots are commonly used in medical applications. However, in the application of acoustic manipulation *in vivo*, challenges arise due to the varying acoustic impedance of different tissues, making precise guidance of medical motors to the target area difficult (Lee et al., 2020). There have been several studies combining drugs with micro/nano-motors for bacteria eradication and capture. For instance, acoustic-driven nano-motors (porous gold nanowire, p-AuNW) equipped with lysozyme can eliminate bacteria within minutes (Kiristi et al., 2015), benefitting from ultrasound propulsion, which efficiently removes dead bacteria adhered to the surface of the acoustic nano-motor. This has been demonstrated on M. lysodeikticus and *E. coli* bacterial models. Moreover, Esteban et al. (Esteban-Fernández de Ávila et al., 2018) successfully used acoustic propelled nanorobots to target and neutralize methicillin-resistant *Staphylococcus aureus* (MRSA) bacteria by employing gold nanowires cloaked with the membrane of human red blood cells (RBCs) as efficient toxin decoys, as shown in Figure 5A, where the trajectory of the nanorobots were recorded with a microscope. This has demonstrated the ability of acoustic propulsion to target and rapidly neutralize harmful pathogens.

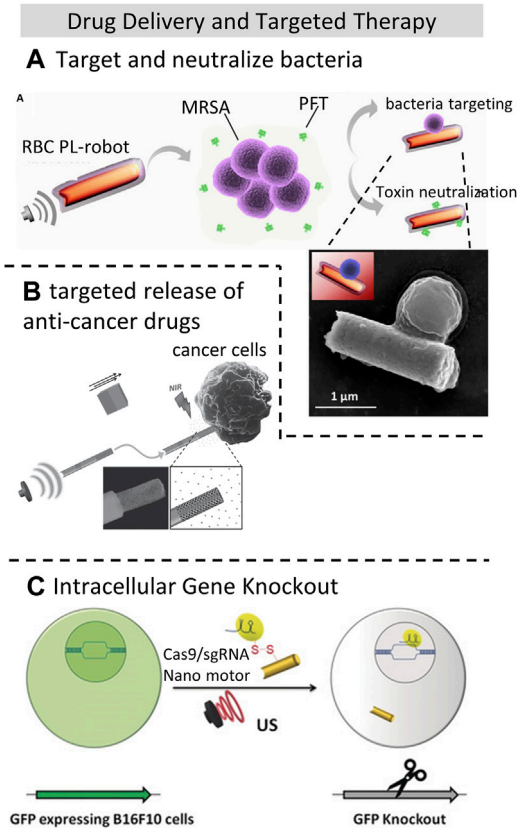

FIGURE 5
Drug delivery and targeted therapy applications using acoustic manipulation techniques **(A)**. Human red blood cells (RBCs) membrane coated nanorobots acoustically propelled to target and neutralize methicillin-resistant *Staphylococcus aureus* (MRSA) bacteria. Reproduced with permission from (Esteban-Fernández de Ávila et al., 2018). Copyright 2018, The Authors, some rights reserved; exclusive license American Association for the Advancement of Science. **(B)** Ultrasound-powered gold nanowire motors targeted release of anti-cancer drugs DOX to Hela cells. Reproduced with permission from (Garcia-Gradilla et al., 2014). Copyright 2014, WILEY-VCH Verlag GmbH and Co. KGaA, Weinheim. **(C)**. Co-delivery of paclitaxel and SsiRNA nanobubbles into lung cancer cells powered by Ultrasound. Reprinted (adapted) with permission from (Hansen-Bruhn et al., 2018). Copyright 2018 Wiley-VCH Verlag GmbH and Co. KGaA, Weinheim.

Furthermore, acoustic-driven micro/nano-motors have also shown promise in targeted release of anti-cancer drugs (Garcia-Gradilla et al., 2014; Kiristi et al., 2015), as shown in Figure 5B. Wu et al. (Wu et al., 2015) utilized RBC-based micro-motors propelled by 2.4 MHz acoustic waves to deliver the chemotherapy drug DOX, reducing its toxicity to human umbilical vein endothelial cells (HUVECs). By comparison, the cell viability has decreased 19.7% by the use of free DOX. Encapsulating chemotherapy drugs in acoustic-propelled micro-motors can effectively reduce their toxicity to healthy cells, enhancing the effectiveness and safety of cancer therapy.

Additionally, ultrasound-driven nano-motors have enabled intracellular small interfering RNA (siRNA) delivery and gene silencing, for example, using an assembly of polymeric micelles and liposomes suppress the anti-apoptosis gene sirtuin 2 (SIRT2) in nude mouse glioma model (Yin et al., 2013) and the GFP (HEK293-GFP) gene-mRNA expression in living human embryonic kidney

293 cells using gold nanowires (AuNW) wrapped with a Rolling Circle Amplification (RCA) DNA strand (Esteban-Fernández de Ávila et al., 2016). The former study only utilized ultrasound to promote cell permeability, while the latter process was achieved through ultrasound-induced concentration of nano-motors and targeted cells into standing wave pressure nodes.

Moreover, (Hansen-Bruhn et al., 2018), effectively propelled Cas9/sgRNA-loaded gold nanowires (AuNWs) across the cell membrane, achieving efficient cleavage of the target GFP genomic sequence (95% after 48 h) with no significant impact on cell viability, as shown in Figure 5C. Furthermore, this team discovered that rapid acoustic propulsion of nano-motors, combined with the high oxygen loading capacity of red blood cell membrane-cloaked perfluorocarbon nanoemulsions (RBC-PFC), enables efficient oxygen delivery to the intracellular space of J774 macrophage cells and helps maintain their viability (Zhang et al., 2019). The acoustic field can accelerate intracellular oxygen delivery to cells, and the oxygen release rate can be adjusted by tuning the ultrasound intensity.

3.3 Acoustic-driven nano-motors for diagnostics

Acoustically-driven nano-motors can also be utilized for disease diagnosis. For instance, when these coated gold nanowires (AuNWs) are loaded with ssDNA that specifically binds to target mRNA (Esteban-Fernández de Ávila et al., 2015), which allows for the rapid detection of individual complete cells, enabling real-time disease monitoring for cancer diagnosis. It holds great potential in cancer diagnosis, patient follow-up, and monitoring disease progression. Similar methods have been applied for the detection of intracellular HPV16 E6 mRNA (Qualliotine et al., 2019), which is used for the diagnosis of Human papillomavirus (HPV)–associated oropharyngeal cancer (OPC) and the Alzheimer's disease (Sun et al., 2021) using polystyrene microparticles as genetic biomarker carriers. In these methods, nano-motors are utilized to enter the cells through acoustic propulsion. They act as probes, binding to the target genes, which results in the switching of fluorescence signals. This switching of fluorescence signals enables the detection of specific genes. The use of these techniques allows for rapid and sensitive gene detection, providing powerful tools for biomedical research and diagnostics.

4 Discussion

Acoustic manipulation shows many advantages such as simplicity in fabrication, biocompatibility, non-contact operation, and compatibility compared with other microfluidic components. These features make acoustic manipulation suitable for applications in medical diagnosis and biochemical research. Despite the differences in the generation principles of BAW and SAW, the methods to control the position of sound traps during acoustic transportation and manipulation is remarkably similar. Acoustic manipulation not only enables cell rotation but also facilitates transportation along complex trajectories. Additionally, research shows that this technique can be used for studying cell membrane permeability, thereby enhancing drug uptake efficiency. Furthermore, improvements in gene silencing strategies were achieved through acoustically propelled nano particles, resulting in efficient, rapid, and accurate gene delivery and silencing response. This method holds great potential for gene therapy applications and serves as an efficient tool for targeted drug delivery. The review presents the progress of acoustic-driven micro/nanorobots in medical applications, providing novel insights for research, diagnosis, and treatment in related fields.

Applying acoustic manipulation techniques to *in vivo* operations stands as a significant challenge for the future. Within the internal environment, addressing the complexity of biological tissues, fluid dynamics effects, and precision of operations becomes crucial. Furthermore, exploring ways to enhance the manipulation capabilities of acoustically propelled micro/nanorobots, enabling more intricate cell operations and precise delivery of various types of drugs, emerges as a crucial research direction. The authors eagerly anticipate witnessing the evolution of this dynamic research field in the coming years, which is certainly worth further comprehensive exploration and dedicated investigation.

Author contributions

GM: Writing–original draft. YQ: Writing–review and editing. MS: Writing–original draft. KG: Writing–review and editing, Supervision, Validation, Resources. HD: Writing–review and editing. JZ: Writing–review and editing.

Funding

The author(s) declare financial support was received for the research, authorship, and/or publication of this article. This work is supported by the National Natural Science Foundation of China (52275014).

Acknowledgments

Grattan acknowledge support from the Royal Academy of Engineering and the Royal Society in the United Kingdom.

Conflict of interest

The authors declare that the research was conducted in the absence of any commercial or financial relationships that could be construed as a potential conflict of interest.

Publisher's note

References

Andrade, M. A. B., Pérez, N., and Adamowski, J. C. (2015). Particle manipulation by a non-resonant acoustic levitator. *Appl. Phys. Lett.* 106, 014101. doi:10.1063/1.4905130

Armstrong, J. P., Pchelintseva, E., Treumuth, S., Campanella, C., Meinert, C., Klein, T. J., et al. (2022). Tissue engineering cartilage with deep zone cytoarchitecture by high-resolution acoustic cell patterning. *Adv. Healthc. Mat.* 11, 2200481. doi:10.1002/adhm.202200481

Armstrong, J. P., Puetzer, J. L., Serio, A., Guex, A. G., Kapnisi, M., Breant, A., et al. (2018). Engineering anisotropic muscle tissue using acoustic cell patterning. *Adv. Mat.* 30, 1802649. doi:10.1002/adma.201802649

Bernassau, A., MacPherson, P., Beeley, J., Drinkwater, B., and Cumming, D. (2013). Patterning of microspheres and microbubbles in an acoustic tweezers. *Biomed. Microdevices* 15, 289–297. doi:10.1007/s10544-012-9729-5

Collignon, S., Friend, J., and Yeo, L. (2015). Planar microfluidic drop splitting and merging. *Lab. Chip* 15, 1942–1951. doi:10.1039/C4LC01453G

Collins, D. J., Morahan, B., Garcia-Bustos, J., Doerig, C., Plebanski, M., and Neild, A. (2015). Two-dimensional single-cell patterning with one cell per well driven by surface acoustic waves. *Nat. Commun.* 6, 8686. doi:10.1038/ncomms9686

Collins, D. J., Neild, A., and Ai, Y. (2016). Highly focused high-frequency travelling surface acoustic waves (SAW) for rapid single-particle sorting. *Lab. Chip* 16, 471–479. doi:10.1039/C5LC01335F

Courtney, C. R., Ong, C. K., Drinkwater, B. W., Bernassau, A., Wilcox, P., and Cumming, D. (2012). Manipulation of particles in two dimensions using phase controllable ultrasonic standing waves. *Proc. Math. Phys. Eng. Sci.* 468, 337–360. doi:10.1098/rspa.2011.0269

Destgeer, G., Jung, J. H., Park, J., Ahmed, H., Park, K., Ahmad, R., et al. (2017). Acoustic impedance-based manipulation of elastic microspheres using travelling surface acoustic waves. *RSC Adv.* 7, 22524–22530. doi:10.1039/C7RA01168G

Ding, M., Koyama, D., and Nakamura, K. (2012a). Noncontact ultrasonic transport of liquid using a flexural vibration plate. *Appl. Phys. Express* 5, 097301. doi:10.1143/APEX.5.097301

Ding, X., Lin, S. C. S., Kiraly, B., Yue, H., Li, S., Chiang, I. K., et al. (2012b). On-chip manipulation of single microparticles, cells, and organisms using surface acoustic waves. *Proc. Natl. Acad. Sci. U. S. A.* 109, 11105–11109. doi:10.1073/pnas.1209288109

Dong, H., Jia, L., Guan, Y., and Zhao, J. (2017). Experiments and simulations of the standing wave acoustic field produced by two transducers mounted in contraposition. *Proc. Mtgs. Acoust.* 32, 065002. doi:10.1121/2.0000693

Dong, H., Sui, M., Mu, G., Zhao, J., Li, T., Sun, T., et al. (2023). Velocity and direction adjustment of actuated droplets using the standing wave ratio of surface acoustic waves (SAW). *IEEE-ASME Trans. Mechatron.* 28, 2399–2404. doi:10.1109/TMECH.2023.3237664

Esteban-Fernández de Ávila, B., Angell, C., Soto, F., Lopez-Ramirez, M. A., Báez, D. F., Xie, S., et al. (2016). Acoustically propelled nanomotors for intracellular siRNA delivery. *ACS Nano* 10, 4997–5005. doi:10.1021/acsnano.6b01415

Esteban-Fernández de Ávila, B., Angsantikul, P., Ramírez-Herrera, D. E., Soto, F., Teymourian, H., Dehaini, D., et al. (2018). Hybrid biomembrane–functionalized nanorobots for concurrent removal of pathogenic bacteria and toxins. *Sci. Robot.* 3, eaat0485. doi:10.1126/scirobotics.aat0485

Esteban-Fernández de Ávila, B., Martín, A., Soto, F., Lopez-Ramirez, M. A., Campuzano, S., Vasquez-Machado, G. M., et al. (2015). Single cell real-time miRNAs sensing based on nanomotors. *ACS Nano* 9, 6756–6764. doi:10.1021/acsnano.5b02807

Fan, X., Sun, M., Sun, L., and Xie, H. (2020). Ferrofluid droplets as liquid microrobots with multiple deformabilities. *Adv. Funct. Mat.* 30, 2000138. doi:10.1002/adfm.202000138

Fletcher, J. C. A., Wang, T. G., Saffren, M. M., and Elleman, D. D. (1975). Material suspension within an acoustically excited resonant chamber. U.S. Patent No 3,882,732. Washington, DC: U.S. Patent and Trademark Office.

Fonseca, A. D. C., Kohler, T., and Ahmed, D. (2022). Ultrasound-controlled Swarmbots under physiological flow conditions. *Adv. Mat. Interfaces* 9, 2200877. doi:10.1002/admi.202200877

Foresti, D., Nabavi, M., Klingauf, M., Ferrari, A., and Poulikakos, D. (2013a). Acoustophoretic contactless transport and handling of matter in air. *Proc. Natl. Acad. Sci. U. S. A.* 110, 12549–12554. doi:10.1073/pnas.1301860110

Foresti, D., Sambatakakis, G., Bottan, S., and Poulikakos, D. (2013b). Morphing surfaces enable acoustophoretic contactless transport of ultrahigh-density matter in air. *Sci. Rep.* 3, 3176. doi:10.1038/srep03176

Garcia-Gradilla, V., Sattayasamitsathit, S., Soto, F., Kuralay, F., Yardımcı, C., Wiitala, D., et al. (2014). Ultrasound-propelled nanoporous gold wire for efficient drug loading and release. *Small* 10, 4154–4159. doi:10.1002/smll.201401013

Gesellchen, F., Bernassau, A., Dejardin, T., Cumming, D., and Riehle, M. (2014). Cell patterning with a heptagon acoustic tweezer–application in neurite guidance. *Lab. Chip* 14, 2266–2275. doi:10.1039/C4LC00436A

Ghanem, M. A., Maxwell, A. D., Wang, Y. N., Cunitz, B. W., Khokhlova, V. A., Sapozhnikov, O. A., et al. (2020). Noninvasive acoustic manipulation of objects in a living body. *Proc. Natl. Acad. Sci. U. S. A.* 117, 16848–16855. doi:10.1073/pnas.2001779117

Guo, X., Sun, M., Yang, Y., Xu, H., Liu, J., He, S., et al. (2021). Controllable cell deformation using acoustic streaming for membrane permeability modulation. *Adv. Sci.* 8, 2002489. doi:10.1002/advs.202002489

Guttenberg, Z., Müller, H., Habermüller, H., Geisbauer, A., Pipper, J., Felbel, J., et al. (2005). Planar chip device for PCR and hybridization with surface acoustic wave pump. *Lab. Chip* 5, 308–317. doi:10.1039/B412712A

Haake, A., and Dual, J. (2002). Micro-manipulation of small particles by node position control of an ultrasonic standing wave. *Ultrasonics* 40, 317–322. doi:10.1016/S0041-624X(02)00114-2

Hansen-Bruhn, M., de Ávila, B. E. F., Beltrán-Gastélum, M., Zhao, J., Ramírez-Herrera, D. E., Angsantikul, P., et al. (2018). Active intracellular delivery of a Cas9/sgRNA complex using ultrasound-propelled nanomotors. *Angew. Chem. Int. Ed.* 57, 2657–2661. doi:10.1002/anie.201713082

Hashimoto, Y., Koike, Y., and Ueha, S. (1998). Transporting objects without contact using flexural traveling waves. *J. Acoust. Soc. Am.* 103, 3230–3233. doi:10.1121/1.423039

He, S., Pang, W., Wu, X., Yang, Y., Li, W., Qi, H., et al. (2022). Bidirectional regulation of cell mechanical motion via a gold nanorods-acoustic streaming system. *ACS Nano* 16, 8427–8439. doi:10.1021/acsnano.2c02980

He, S., Wang, Z., Pang, W., Liu, C., Zhang, M., Yang, Y., et al. (2021). Ultra-rapid modulation of neurite outgrowth in a gigahertz acoustic streaming system. *Lab. Chip* 21, 1948–1955. doi:10.1039/D0LC01262A

Hoshi, T., Ochiai, Y., and Rekimoto, J. (2014). Three-dimensional noncontact manipulation by opposite ultrasonic phased arrays. *Jpn. J. Appl. Phys.* 53, 07KE07. doi:10.7567/JJAP.53.07KE07

Ito, Y., Koyama, D., and Nakamura, K. (2010). High-speed noncontact ultrasonic transport of small objects using acoustic traveling wave field. *Acoust. Sci. Technol.* 31, 420–422. doi:10.1250/ast.31.420

Ji, F., Li, T., Yu, S., Wu, Z., and Zhang, L. (2021). Propulsion gait analysis and fluidic trapping of swinging flexible nanomotors. *ACS Nano* 15, 5118–5128. doi:10.1021/acsnano.0c10269

Jooss, V. M., Bolten, J. S., Huwyler, J., and Ahmed, D. (2022). *In vivo* acoustic manipulation of microparticles in zebrafish embryos. *Sci. Adv.* 8, eabm2785. doi:10.1126/sciadv.abm2785

Kashima, R., Murakami, S., Koyama, D., Nakamura, K., and Matsukawa, M. (2014). Design of a junction for a noncontact ultrasonic transportation system. *IEEE Trans. ultrasonics, Ferroelectr. Freq. control* 61, 1024–1032. doi:10.1109/TUFFC.2014.2998

Kiristi, M., Singh, V. V., Esteban-Fernández de Ávila, B., Uygun, M., Soto, F., Aktas Uygun, D., et al. (2015). Lysozyme-based antibacterial nanomotors. *ACS Nano* 9, 9252–9259. doi:10.1021/acsnano.5b04142

Koyama, D., and Nakamura, K. (2010). Noncontact ultrasonic transportation of small objects in a circular trajectory in air by flexural vibrations of a circular disc. *IEEE Trans. Ultrason. Ferroelectr. Freq. Control* 57, 1434–1442. doi:10.1109/TUFFC.2010.1562

Kozuka, T., Yasui, K., Tuziuti, T., Towata, A., and Iida, Y. (2007). Noncontact acoustic manipulation in air. *Jpn. J. Appl. Phys.* 46, 4948–4950. doi:10.1143/JJAP.46.4948

Lee, H. S., Go, G., Choi, E., Kang, B., Park, J. O., and Kim, C. S. (2020). Medical microrobot-wireless manipulation of a drug delivery carrier through an external ultrasonic actuation: preliminary results. *Int. J. Control Autom. Syst.* 18, 175–185. doi:10.1007/s12555-019-0239-6

Li, H., Friend, J. R., and Yeo, L. Y. (2007). Surface acoustic wave concentration of particle and bioparticle suspensions. *Biomed. Microdevices* 9, 647–656. doi:10.1007/s10544-007-9058-2

Li, J., and Kim, C. J. C. (2020). Current commercialization status of electrowetting-on-dielectric (EWOD) digital microfluidics. *Lab. Chip* 20, 1705–1712. doi:10.1039/D0LC00144A

Li, J., Mayorga-Martinez, C. C., Ohl, C. D., and Pumera, M. (2022). Ultrasonically propelled micro-and nanorobots. *Adv. Funct. Mat.* 32, 2102265. doi:10.1002/adfm.202102265

Li, S., Ding, X., Mao, Z., Chen, Y., Nama, N., Guo, F., et al. (2015). Standing surface acoustic wave (SSAW)-based cell washing. *Lab. Chip* 15, 331–338. doi:10.1039/C4LC00903G

Li, T., Yu, S., Sun, B., Li, Y., Wang, X., Pan, Y., et al. (2023). Bioinspired claw-engaged and biolubricated swimming microrobots creating active retention in blood vessels. *Sci. Adv.* 9, eadg4501. doi:10.1126/sciadv.adg4501

Li, T., Zhang, A., Shao, G., Wei, M., Guo, B., Zhang, G., et al. (2018). Janus microdimer surface walkers propelled by oscillating magnetic fields. *Adv. Funct. Mat.* 28, 1706066. doi:10.1002/adfm.201706066

Ma, Z., Holle, A. W., Melde, K., Qiu, T., Poeppel, K., Kadiri, V. M., et al. (2020a). Acoustic holographic cell patterning in a biocompatible hydrogel. *Adv. Mat.* 32, 1904181. doi:10.1002/adma.201904181

Ma, Z., Zhou, Y., Cai, F., Meng, L., Zheng, H., and Ai, Y. (2020b). Ultrasonic microstreaming for complex-trajectory transport and rotation of single particles and cells. *Lab. Chip* 20, 2947–2953. doi:10.1039/D0LC00595A

Marzo, A., Barnes, A., and Drinkwater, B. W. (2017). TinyLev: a multi-emitter single-axis acoustic levitator. *Rev. Sci. Instrum.* 88, 085105. doi:10.1063/1.4989995

Marzo, A., Seah, S. A., Drinkwater, B. W., Sahoo, D. R., Long, B., and Subramanian, S. (2015). Holographic acoustic elements for manipulation of levitated objects. *Nat. Commun.* 6, 8661. doi:10.1038/ncomms9661

Matsui, T., Ohdaira, E., Masuzawa, N., and Ide, M. (1995). Translation of an object using phase-controlled sound sources in acoustic levitation. *Jpn. J. Appl. Phys.* 34, 2771. doi:10.1143/JJAP.34.2771

MatthewáReichert, W., McCardle, H., and Davis, J. H. (2020). Acoustic levitation and infrared thermography: a sound approach to studying droplet evaporation. *Chem. Commun.* 56, 4224–4227. doi:10.1039/C9CC09856A

Melde, K., Choi, E., Wu, Z., Palagi, S., Qiu, T., and Fischer, P. (2018). Acoustic fabrication via the assembly and fusion of particles. *Adv. Mat.* 30, 1704507. doi:10.1002/adma.201704507

Melde, K., Mark, A. G., Qiu, T., and Fischer, P. (2016). Holograms for acoustics. *Nature* 537, 518–522. doi:10.1038/nature19755

Meng, L., Cai, F., Jiang, P., Deng, Z., Li, F., Niu, L., et al. (2014). On-chip targeted single cell sonoporation with microbubble destruction excited by surface acoustic waves. *Appl. Phys. Lett.* 104, 073701. doi:10.1063/1.4865770

Meng, L., Cai, F., Zhang, Z., Niu, L., Jin, Q., Yan, F., et al. (2011). Transportation of single cell and microbubbles by phase-shift introduced to standing leaky surface acoustic waves. *Biomicrofluidics* 5, 044104–4410410. doi:10.1063/1.3652872

Mohanty, S., Khalil, I. S., and Misra, S. (2020). Contactless acoustic micro/nano manipulation: a paradigm for next generation applications in life sciences. *Proc. Math. Phys. Eng. Sci.* 476, 20200621. doi:10.1098/rspa.2020.0621

Nakamura, K., and Koyama, D. (2012). "Non-contact transportation system of small objects using Ultrasonic Waveguides," in *International symposium on ultrasound in the control of industrial processes (UCIP 2012)* (Madrid, Spain: IOP Conference Series: Materials Science and Engineering). 012014

Ochiai, Y., Hoshi, T., and Rekimoto, J. (2014a). Pixie dust: graphics generated by levitated and animated objects in computational acoustic-potential field. *ACM Trans. Graph.* 33, 1–13. doi:10.1145/2601097.2601118

Ochiai, Y., Hoshi, T., and Rekimoto, J. (2014b). Three-dimensional mid-air acoustic manipulation by ultrasonic phased arrays. *PLoS One* 9, e97590. doi:10.1371/journal.pone.0097590

Park, J. K., and Ro, P. I. (2013). Noncontact manipulation of light objects based on parameter modulations of acoustic pressure nodes. *J. Vib. Acoust.* 135, 031011. doi:10.1115/1.4023816

Peng Lee, C., Hsin Chen, Y., and Hang Wei, Z. (2013). Fabrication of hexagonally packed cell culture substrates using droplet formation in a T-shaped microfluidic junction. *Biomicrofluidics* 7, 014101. doi:10.1063/1.4774315

Pollack, M. G., Fair, R. B., and Shenderov, A. D. (2000). Electrowetting-based actuation of liquid droplets for microfluidic applications. *Appl. Phys. Lett.* 77, 1725–1726. doi:10.1063/1.1308534

Qian, J., Ren, J., Huang, W., Lam, R. H., and Lee, J.E. Y. (2021). Acoustically driven manipulation of microparticles and cells on a detachable surface micromachined silicon chip. *IEEE Sens. J.* 21, 11999–12008. doi:10.1109/JSEN.2021.3065694

Qualliotine, J. R., Bolat, G., Beltrán-Gastélum, M., de Ávila, B. E. F., Wang, J., and Califano, J. A. (2019). Acoustic nanomotors for detection of human papillomavirus–associated head and neck cancer. *Otolaryngol. Head. Neck Surg.* 161, 814–822. doi:10.1177/0194599819866407

Renaudin, A., Tabourier, P., Zhang, V., Camart, J., and Druon, C. (2006). SAW nanopump for handling droplets in view of biological applications. *Sens. Actuator B-Chem.* 113, 389–397. doi:10.1016/j.snb.2005.03.100

Schmid, L., Weitz, D. A., and Franke, T. (2014). Sorting drops and cells with acoustics: acoustic microfluidic fluorescence-activated cell sorter. *Lab. Chip* 14, 3710–3718. doi:10.1039/C4LC00588K

Shi, J., Ahmed, D., Mao, X., Lin, S. C. S., Lawit, A., and Huang, T. J. (2009). Acoustic tweezers: patterning cells and microparticles using standing surface acoustic waves (SSAW). *Lab. Chip* 9, 2890–2895. doi:10.1039/B910595F

Sui, M., Dong, H., Mu, G., Xia, J., Zhao, J., Yang, Z., et al. (2022). Droplet transportation by adjusting the temporal phase shift of surface acoustic waves in the exciter–exciter mode. *Lab. Chip* 22, 3402–3411. doi:10.1039/D2LC00402J

Sun, Y., Luo, Y., Xu, T., Cheng, G., Cai, H., and Zhang, X. (2021). Acoustic aggregation-induced separation for enhanced fluorescence detection of Alzheimer's biomarker. *Talanta* 233, 122517. doi:10.1016/j.talanta.2021.122517

Tang, T., Hosokawa, Y., Hayakawa, T., Tanaka, Y., Li, W., Li, M., et al. (2022). Rotation of biological cells: fundamentals and applications. *Engineering* 10, 110–126. doi:10.1016/j.eng.2020.07.031

Tian, Z., Yang, S., Huang, P. H., Wang, Z., Zhang, P., Gu, Y., et al. (2019). Wave number–spiral acoustic tweezers for dynamic and reconfigurable manipulation of particles and cells. *Sci. Adv.* 5, eaau6062. doi:10.1126/sciadv.aau6062

Ueha, S., Hashimoto, Y., and Koike, Y. (2000). Non-contact transportation using near-field acoustic levitation. *Ultrasonics* 38, 26–32. doi:10.1016/S0041-624X(99)00052-9

Vasileiou, T., Foresti, D., Bayram, A., Poulikakos, D., and Ferrari, A. (2016). Toward contactless biology: acoustophoretic DNA transfection. *Sci. Rep.* 6, 20023. doi:10.1038/srep20023

Wang, H., Yu, S., Liao, J., Qing, X., Sun, D., Ji, F., et al. (2022). A robot platform for highly efficient pollutant purification. *Front. Bioeng. Biotechnol.* 10, 903219. doi:10.3389/fbioe.2022.903219

Wang, Q., Li, Y., Ma, Q., Guo, G., Tu, J., and Zhang, D. (2018). Near-field multiple traps of paraxial acoustic vortices with strengthened gradient force generated by sector transducer array. *J. Appl. Phys.* 123, 034901. doi:10.1063/1.5004752

Wiklund, M. (2012). Acoustofluidics 12: biocompatibility and cell viability in microfluidic acoustic resonators. *Lab. Chip* 12, 2018–2028. doi:10.1039/C2LC40201G

Wiklund, M., Green, R., and Ohlin, M. (2012). Acoustofluidics 14: applications of acoustic streaming in microfluidic devices. *Lab. Chip* 12, 2438–2451. doi:10.1039/C2LC40203C

Wu, Z., De Avila, B. E. F., Martín, A., Christianson, C., Gao, W., Thamphiwatana, S. K., et al. (2015). RBC micromotors carrying multiple cargos towards potential theranostic applications. *Nanoscale* 7, 13680–13686. doi:10.1039/C5NR03730A

Yin, T., Wang, P., Li, J., Zheng, R., Zheng, B., Cheng, D., et al. (2013). Ultrasound-sensitive siRNA-loaded nanobubbles formed by hetero-assembly of polymeric micelles and liposomes and their therapeutic effect in gliomas. *Biomaterials* 34, 4532–4543. doi:10.1016/j.biomaterials.2013.02.067

Youssefi, O., and Diller, E. (2019). Contactless robotic micromanipulation in air using a magneto-acoustic system. *IEEE Robot. Autom. Lett.* 4, 1580–1586. doi:10.1109/LRA.2019.2896444

Yu, S., Li, T., Ji, F., Zhao, S., Liu, K., Zhang, Z., et al. (2022). Trimer-like microrobots with multimodal locomotion and reconfigurable capabilities. *Mat. Today Adv.* 14, 100231. doi:10.1016/j.mtadv.2022.100231

Yu, Z., Li, L., Mou, F., Yu, S., Zhang, D., Yang, M., et al. (2023). Swarming magnetic photonic-crystal microrobots with on-the-fly visual pH detection and self-regulated drug delivery. *InfoMat Early View* 2023, e12464. doi:10.1002/inf2.12464

Zhang, F., Zhuang, J., Esteban Fernández de Ávila, B., Tang, S., Zhang, Q., Fang, R. H., et al. (2019a). A nanomotor-based active delivery system for intracellular oxygen transport. *ACS Nano* 13, 11996–12005. doi:10.1021/acsnano.9b06127

Zhang, H., Wang, C., Bai, M., Yi, H., Yang, J., Zhu, Y., et al. (2023a). A micro-3-degree-of-freedom force sensor for intraocular dexterous surgical robots. *Adv. Intell. Syst.* 5, 2200413. doi:10.1002/aisy.202200413

Zhang, P., Bachman, H., Ozcelik, A., and Huang, T. J. (2020). Acoustic microfluidics. *Annu. Rev. Anal. Chem.* 13, 17–43. doi:10.1146/annurev-anchem-090919-102205

Zhang, P., Chen, C., Guo, F., Philippe, J., Gu, Y., Tian, Z., et al. (2019b). Contactless, programmable acoustofluidic manipulation of objects on water. *Lab. Chip* 19, 3397–3404. doi:10.1039/C9LC00465C

Zhang, Q., Zeng, S., Lin, B., and Qin, J. (2011). Controllable synthesis of anisotropic elongated particles using microvalve actuated microfluidic approach. *J. Mat. Chem.* 21, 2466–2469. doi:10.1039/C0JM04033A

Zhang, S. P., Lata, J., Chen, C., Mai, J., Guo, F., Tian, Z., et al. (2018). Digital acoustofluidics enables contactless and programmable liquid handling. *Nat. Commun.* 9, 2928. doi:10.1038/s41467-018-05297-z

Zhang, W., Deng, Y., Zhao, J., Zhang, T., Zhang, X., Song, W., et al. (2023b). Amoeba-inspired magnetic venom microrobots. *Amoeba-Inspired Magn. Venom. Microrobots.* Small 19, 2207360. doi:10.1002/smll.202207360

Zhao, S. K., Hu, X. J., Zhu, J. M., Luo, Z. Y., Liang, L., Yang, D. Y., et al. (2021). On-chip rapid drug screening of leukemia cells by acoustic streaming. *Lab. Chip* 21, 4005–4015. doi:10.1039/D1LC00684C

Zheng, J., Hu, X., Gao, X., Liu, Y., Zhao, S., Chen, L., et al. (2023). Convenient tumor 3D spheroid arrays manufacturing via acoustic excited bubbles for *in situ* drug screening. *Lab. Chip* 23, 1593–1602. doi:10.1039/D2LC00973K

Zhu, P., and Wang, L. (2017). Passive and active droplet generation with microfluidics: a review. *Lab. Chip* 17, 34–75. doi:10.1039/C6LC01018K

frontiers | Frontiers in Bioengineering and Biotechnology

TYPE Review
PUBLISHED 09 November 2023
DOI 10.3389/fbioe.2023.1312074

OPEN ACCESS

EDITED BY
Fengtong Ji,
University of Cambridge, United Kingdom

REVIEWED BY
Huaping Wang,
Beijing Institute of Technology, China
Qianqian Wang,
Southeast University, China

*CORRESPONDENCE
Shimin Yu,
yushimin@ouc.edu.cn
Mu Li,
limu@hrbmu.edu.cn
Lin Wang,
linwang@hit.edu.cn

RECEIVED 10 October 2023
ACCEPTED 30 October 2023
PUBLISHED 09 November 2023

CITATION
Wang H, Jing Y, Yu J, Ma B, Sui M, Zhu Y, Dai L, Yu S, Li M and Wang L (2023), Micro/nanorobots for remediation of water resources and aquatic life.
Front. Bioeng. Biotechnol. 11:1312074.
doi: 10.3389/fbioe.2023.1312074

Micro/nanorobots for remediation of water resources and aquatic life

Haocheng Wang[1], Yizhan Jing[1], Jiuzheng Yu[2], Bo Ma[3], Mingyang Sui[1], Yanhe Zhu[1], Lizhou Dai[1], Shimin Yu[4]*, Mu Li[5]* and Lin Wang[1]*

[1]State Key Laboratory of Robotics and System, Harbin Institute of Technology, Harbin, China, [2]Oil & Gas Technology Research Institute, PetroChina Changqing Oilfield Company, Xi'an, China, [3]State Engineering Laboratory of Exploration and Development of Low-Permeability Oil & Gas Field, Xi'an, China, [4]College of Engineering, Ocean University of China, Qingdao, China, [5]Department of Pharmacy, The Second Affiliated Hospital of Harbin Medical University, Harbin, China

Nowadays, global water scarcity is becoming a pressing issue, and the discharge of various pollutants leads to the biological pollution of water bodies, which further leads to the poisoning of living organisms. Consequently, traditional water treatment methods are proving inadequate in addressing the growing demands of various industries. As an effective and eco-friendly water treatment method, micro/nanorobots is making significant advancements. Based on researches conducted between 2019 and 2023 in the field of water pollution using micro/nanorobots, this paper comprehensively reviews the development of micro/nanorobots in water pollution control from multiple perspectives, including propulsion methods, decontamination mechanisms, experimental techniques, and water monitoring. Furthermore, this paper highlights current challenges and provides insights into the future development of the industry, providing guidance on biological water pollution control.

KEYWORDS

micro/nanorobot, water pollution control, water purification, actuation mechanism, decontamination mechanism, water monitoring

1 Introduction

Water is a fundamental natural resource that is indispensable for biological survival, scientific progress and industrial development. In recent years, water resources have been continuously polluted, water scarcity has become a global problem. Some studies have shown that water pollution has not improved in those days, and there has been little actual progress in pollution prevention from a global perspective, with severe water pollution causing nearly 2 million deaths per year (Fuller et al., 2022). According to the United Nations Water Development Report 2023, there has been a consistent annual increase in water consumption over the past 40 years, and 10% of the world's population is living in countries with high or severe water scarcity. Furthermore, droughts, overuse, anthropogenic pollution, political and geopolitical influences continue to cause a decrease in available water reserves (Gude, 2017), where human activities have become a major contributor to water pollution, with about 50% of anthropogenically generated wastewater being discharged directly into rivers or oceans without any treatment, resulting in serious ecosystem damages and long-term impacts (Shemer et al., 2023).

To conquer the increasing water pollution problem, various conventional purification methods have been employed, such as precipitation/encapsulation, adsorption, membrane technology, and more (Altowayti et al., 2022), these methods can achieve wastewater

recycling and reuse through graded purification and sludge treatment. The precipitation/encapsulation method can convert soluble metal ions in wastewater into insoluble precipitate in a less costly way, but the generated sludge is easily affected by various types of oils and fats in the wastewater, which increases the difficulty of treatment. The adsorption method is mainly used for the treatment of organic pollutants in wastewater, the pollutants are stripped off by the adhesion generated at the interface of different phases. Adsorption is considered a low development and maintenance cost option (Abu Bakar et al., 2021), however, in the face of wastewater with more complex components, different adsorption layers are often required, which increases the construction cost in the implementation of the project. Membrane treatment is a relatively new water treatment method, which can extract both dissolved solutes and insoluble dispersed particles in water, targeting a wide range of pollutants and being very environmentally friendly (Yusuf et al., 2020). However, membrane treatment requires pre-treatment, which can otherwise damage the membrane (Rahman et al., 2023), this raises the cost of membrane treatment for further use. Although traditional water purification methods have been developed towards low-carbon and intelligent (Altowayti et al., 2022; Li et al., 2023), their disadvantages in terms of equipment construction costs, biocompatibility and recyclability limit their further development, especially in developing countries where they will not be able to be used in large quantities (Othman et al., 2022).

In recent years, micro/nanorobots and micro/nanomotor technologies have shown great advantages such as low cost, high efficiency and environmental friendliness in environmental remediation and water purification applications, which have gained widespread attention and have great potential for development and application. Micro/nanorobots (MNRs) or micro/nanomotors (MNMs), usually refer to microscopic substances with actuation capability between 1 and 1 mm in size, which can be both organic or inorganic, even artificially edited and modified microorganisms from nature. Micro/nanorobots convert external energy into self-propulsion through a variety of different physicochemical mechanisms (Urso et al., 2023), with common approaches including bubble (Liu et al., 2019; Ren et al., 2022; Yang et al., 2023), light (Xiong et al., 2022; Palacios-Corella et al., 2023), acoustic (Lu et al., 2020; Wang et al., 2021; Wang et al., 2022), magnetic (Li et al., 2017; Li et al., 2018; Sun et al., 2020; Yu et al., 2022; Li et al., 2023), biological (Lai et al., 2022) and other methods (Fu et al., 2019; Kong et al., 2019; Xu et al., 2019). In addition to a wide range of drive options, the working conditions for micro/nanorobots are much easier to achieve, some studies show that micro/nanorobots can even work under natural light (Kochergin et al., 2020; Ying et al., 2021; Ullattil and Pumera, 2023), without any pre-processing, obviously providing more possibilities in water control such as pollutants' on-site instantaneous collection and degradation.

Furthermore, the self-propelled motion of the micro/nanorobots is often accompanied by the flow of surrounding fluids, eliminating the need for additional mechanical agitation required by traditional water pollution treatment methods and static nano decontamination techniques. This facilitates the process of pollutant capture and material transfer, leading to improved efficiency and reduced operation time in pollution treatment (Ying and Pumera, 2019). Additionally, micro/nanorobots can operate effectively in size-limited working conditions, especially within micro and nano-scale environments, which distinguishes them from traditional water pollution treatment methods. Based on these advantages, it is clear that micro/nanorobots are more in line with the principle of improving pollution treatment efficiency and expanding pollution treatment capacity and reducing pollution treatment cost (Raha et al., 2008). They also align with the direction of next-generation advanced water treatment technology, featuring real-time degradation, recycling, reuse, and higher material utilization rates.

Based on the studies conducted between 2019 and 2023, this paper provides an overview of micro/nanorobots' role in the field of water pollution control. Here the driving mechanisms and methods, specific decontamination methods, targeted pollutants, experimental technologies and platforms have been reviewed. This paper also discusses the feasibility and necessity of micro/nanorobots used for long-term water monitoring. Analysing principles and presenting cases, this paper describes the relevant problems currently faced and envisions the future development of the industry.

2 The actuation of micro/nanorobots

2.1 Actuation mechanisms

The actuation of micro/nanorobots is very different from that of macro-robots, the former cannot achieve effective motion through inertial force, and the "scallop theory" proposed by Pursell in 1976 well explained that time-symmetric motions of an object in low Reynolds number environments cannot result in displacement (Zhou et al., 2021a). Therefore, the actuation of micro/nanorobots is different from the "brute force actuation" of macroscopic objects and is based on a new kinematic mechanism that utilizes gradients for actuation. In fact, the motion of all micro/nanorobots is the motion from high gradient positions to low gradient positions, and all enhancement of the motion effect is the enhancement of the gradient, including a larger gradient difference, or a higher efficiency of the gradient utilization. The specific method of generating gradients is to generate asymmetry, which is done in the design process of micro/nanorobots through the selection of materials or the design of structures. Common methods to generate asymmetry include the use of magnetic fields, acoustic fields, electric fields, concentrations of chemicals, and the asymmetric structures of robots, *etc.* (Wang and Zhang, 2021).

2.2 Actuation methods

2.2.1 Bubble-driven propulsion

Bubble-driven propulsion is one of the most common methods for actuation. When micro/nanorobots move in the water, various biochemical reactions or physical phenomena on their surfaces lead to the generation of micro/nano-sized bubbles. These bubbles accumulate at the back of the micro/nanorobots and propel them forward by moving in the opposite direction. Depending on whether the body of the micro/nanorobot serves as a consumed substrate or

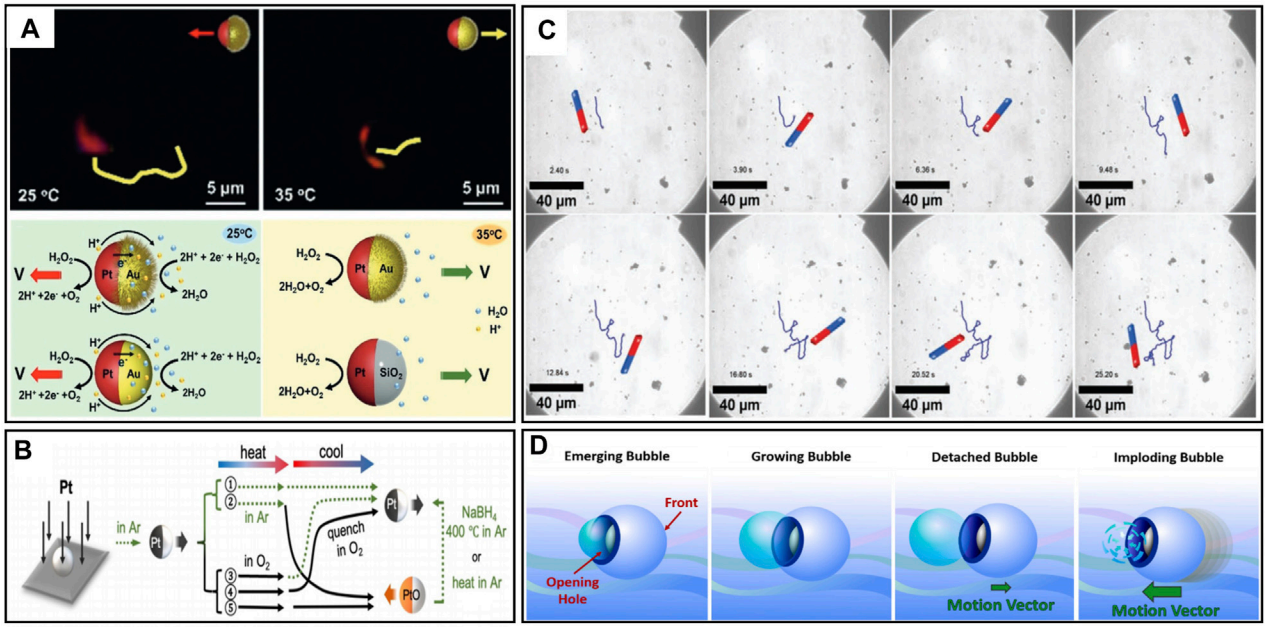

FIGURE 1
(A) Diagram of the actual movements and the surface actions of the PNIPAM@Au–Pt micromotors in the Pt direction and Au direction (Ji et al., 2019). **(B)** Varying compositions of the micromotor through five different manufacturing paths to achieve different movement effects (Lyu et al., 2022). **(C)** Motion trajectories of FeOx@MnO_2@SiO_2 micromotors at 1 wt% of H_2O_2 solution guided by a magnet (Yang et al., 2023). **(D)** Mechanism diagram for the four steps of the bubble implosion propulsion (Zhao et al., 2022).

not, bubble-driven micro/nanorobots can be categorized into two types: "catalytic fuel decomposition" and "self-decomposition".

Catalytic fuel decomposition robots contain a catalyst for fuel decomposition reactions. For example, a robot might incorporate asymmetrically distributed Pt metal, which catalyses the decomposition of gas bubbles in the presence of H_2O_2, and the robot itself does not experience any loss during the movement process. Ji et al. (2019) designed a bimetallic Janus micromotor PNIPAM@Au-Pt with bidirectional movement capability. The Pt part can be oriented to serve as either the front or back, allowing versatile movement. The driving mechanism involved Pt-catalyzed H_2O_2 decomposition, resulted in self-diffusion for movement. Temperature-induced PNIPAM chain modifications controlled the micromotor's hydrophilic and hydrophobic functions. At temperatures below 32°C, electrons and protons migrated from the Pt region to the Au region and reacted with H_2O_2 to generate oxygen, when the temperature surpassed the critical point, a phase transition occurred, changing the hemisphere of the micromotor in contact with the fuel, switched propulsion mechanism from self-electrophoretic propulsion to self-diffusive propulsion. The actual movements and the different surface reactions of the PNIPAM@Au–Pt micromotors are shown in Figure 1A. The significance of this study lies in achieving micro/nanorobots steering through thermal control, offering valuable insights for subsequent module design.

A recent study has shown that the generation of intermediate platinum oxides also affects the actuation of micro/nanorobots during Pt-catalyzed H_2O_2 decomposition. Lyu et al. (2022) observed a distinct behavior on conventional Pt-SiO_2 robots, their robots moved towards the Pt layer instead of away from it when the thickness of the Pt layer exceeded 100 nm. After excluding possible variables such as temperature, they determined that the excessive thickness of the Pt layer and the presence of platinum oxides, mainly PtO, induced a reversal in the direction of motion through an auto-electrophoretic effect. This discovery enables precise control over the motion direction of micro/nanorobots by controlling the Pt oxides. This breakthrough introduces new materials for the motion control of micro/nanorobots. Five paths for manufacturing are shown in Figure 1B.

Using expensive Pt for micro/nanorobot fabrication can lead to high production costs. Furthermore, the susceptibility to electrochemical corrosion from Sulphur-containing substances and other metal ions can degrade its catalytic performance and cause the failure of the robots, known as "Pt-poison" (Casado-Rivera et al., 2003; Orozco et al., 2013; Zhao et al., 2013). To address this, researchers have explored alternative catalytic materials like manganese oxides, such as MnO_2 (Yang et al., 2023), Mn_2O_3 (Li et al., 2021), and Mn_3O_4 (Bing et al., 2020), among which MnO_2 is most widely used. Manganese dioxide shows the advantages of abundant sources, low cost, and stable chemical properties. It can simultaneously participate in the oxidation process of pollutants and is commonly employed in the treatment of organic pollutants. Yang et al. (2023) designed a multifunctional FeO_x@MnO_2@SiO_2 microrobot capable of degrading antibiotics such as Naproxen in a peroxymonosulfate (PMS)/H_2O_2 system. In this robot, MnO_2 is responsible for decomposing H_2O_2 into oxygen bubbles, providing propulsion in the solution and generating substances for antibiotic degradation. The trajectories of a robot guided by ais shown in

Figure 1C. Through experiments of varying durations, they explored the connections between robot structure, velocity, and degradation efficiency, revealing the relationship between catalytic efficiency, motility behavior, and the mechanism of motion. A highlight of their work is that PMS can regulate the excessive formation of O_2 resulting from H_2O_2 decomposition by occupying the Mn site through interactions with the robots.

Self-decomposing micro/nanorobots directly engage in reactions as substrates. For instance, a robot containing Mg metal catalyzes H_2O_2 decomposition in an acidic environment. The endurance matches the Mg consumption time, rendering the robot immobile after the Mg depletion. Zhao et al. (2022) designed a fully biodegradable microrobot propelled by hydrogen bubbles from the Mg-hydrochloric acid reaction. The mechanism diagram is shown in Figure 1D. Investigating the impact of bubble stabilizers on propulsion patterns, they tested hydrochloric acid (six concentrations) and surfactant Triton X-100 (five concentrations). Findings demonstrated surfactant influence on the propulsion direction of the robot. Generally, bubble-driven micro/nanorobots exhibit lower motion precision than methods like magnetic driving. For self-decomposition robots, bubbles are randomly generated, producing disordered motion with limited control and switching capabilities. The very limited endurance and the potential for secondary contamination (e.g., Mg^{2+}) render self-decomposition micro/nanorobots incapable of performing tasks with high precision.

Both of these bubble-driven propulsion methods rely on fuel decomposition. However, suitable fuel chemicals are often lacking in polluted water, leading to the need for artificial addition of chemical reagents like H_2O_2. The introduction of H_2O_2 has both advantages and disadvantages. On one hand, its role as a strong oxidizing agent enhances the pollutant oxidation process, contributing significantly to pollutant degradation. Conversely, the addition of hydrogen peroxide itself is costly and the addition of additional strong oxidizing agents to an open body of water can cause unwanted secondary damage to the body of water. It is noted that bubbles themselves can function as microscopic robots. Generated bubbles, often at the micro/nano-scale, come with physical adsorption effects on their surface. The presence of microbubbles or clusters can further amplify the efficiency of water pollution treatment.

2.2.2 Light-driven propulsion

Light-driven propulsion has become a popular option for water pollution treatment due to the ready availability of natural light energy. Additionally, light-driven materials tend to generate reactive oxygen species (ROS) through the photo-Fenton reaction, enhancing the treatment efficiency of pollutants (see Section 3.1 for more details). With the deepening of the study, new light-responsive materials are applied, more specific parameters are investigated, and new light-triggered motion mechanisms are discovered.

The use of light-driven micro/nanorobots converts light energy into kinetic energy, utilizing various frequency bands of light. The more commonly used bands include visible light, near-infrared light, and ultraviolet light. However, light cannot drive all forms of matter. Photoactive materials, such as semiconductors, are necessary to create a net displacement under light.

TiO_2 is a commonly used semiconductor in the fabrication of micro/nanorobots. Not only does TiO_2 have a programmable surface charge, providing the ability to specifically identify contaminants, but it also has a Schottky barrier at its interface, which would result in higher photocatalytic activity. The common use of TiO_2 is with the combination of different metals. In fact, among the many metal-TiO_2 combinations, platinum is the most effective and provides the most stable power (Maric et al., 2020). One common surface reaction of the metal/TiO_2 robots is shown in Figure 2A.

Functional optimization based on TiO_2 robots is a major research direction in the field. Xiao et al. (2020) tripled the motion speed of a conventional TiO_2 robot by adding an Au/Ag bilayer coating. Through their experiments, they ruled out the possibility that the Ag in the bimetallic layer alone could lead to the speed increase and determined that the metallic coating works through synergy to increase the speed of the TiO_2 robot in the light. This synergistic action did not depend on any fuel, and the kinematic efficacy enhancement was achieved even in pure water.

Except for TiO_2, other materials are also applied in the manufacturing of micro/nanorobots. Villa et al. (2019) designed a micro/nanorobot using the photoactive substance $BiVO_4$ to capture microorganisms. Under visible light, this robot can actively seek out and non-destructively adhere to yeast cell walls through linear motion, allowing for controlled capture and release of yeast cells by switching the visible light on and off, which can serve as disinfection motile tools for the removal of microbial contamination in water (Figure 2B). Li et al. (2023) constructed near-infrared light-driven micro/nanorobots named JMPPs@Au by depositing Au nanoparticles (NPs) onto the half surface of MPPs. The motion propelled by NIR light is explained in Figure 2C. By controlling the light on and off, their experiments demonstrated the positive impact of light on pollution removal.

These materials absorb photon energy, generating electron-hole pairs (e^--h^+) exposed to light. When excess electrons accumulate on the surface of the material, they can react with pure water, generating bubbles and initiating a photochemical reaction under light irradiation. This process ultimately leads to bubble creation or autophoresis, showing another major advantage of certain light-driven robots, which is their independence from external fuel sources (Urso et al., 2023). Wang et al. (2020) designed a cost-effective, easily fabricated robot with good motion capabilities even under low light intensity. The robot did not rely on any fuel source operating across the entire visible light spectrum. It achieved impressive movement, covering 18 times its body length in just 1 s in pure water. Even at one-third the intensity of sunlight it showed great motion effect. This study presents the fastest pure water-driven micro/nanorobots and highlights the advantages of non-toxicity and minimal secondary pollution.

Since the robot can be activated by all light larger than the material band gap, this represents a large range of light that can open up light-driven micro/nanorobots, which provides the possibility of controllable multimodal motions. Xing et al. (2020) reported a micro/nanorobot with pH-responsive multilight propulsion. The surface reactions of the robot are shown in Figure 3A. The robot was first propelled by self-diffusion in 3.0% hydrogen peroxide. Then, the weak acidity of H_2O_2 triggered the disassembly and reorganization of gold nanoparticles on the robot, leading to a contact between gold and platinum nanoparticles, which changed the propulsion mechanism to self-electrophoresis. Asymmetric and

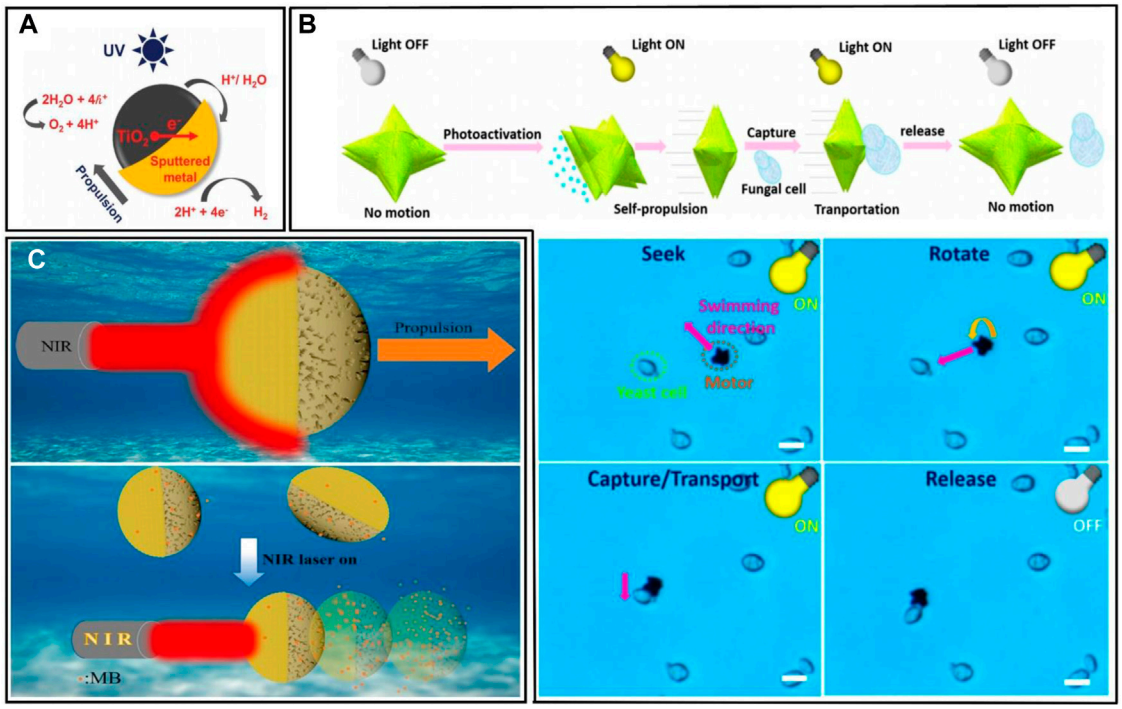

FIGURE 2
(A) Schematic illustration of the reactions of the metal/TiO_2 micromotors under UV light irradiation in study (Maric et al., 2020). **(B)** Sketch of the workflow of $BiVO_4$ micromotors for microorganisms' removal, and photos of $BiVO_4$ micromotors capturing microorganisms under UV light irradiation (Villa et al., 2019). **(C)** Scheme of NIR light-propelled motion for MB removal. This microrobot made a 10.2% increase in the removal efficiency of MB dye under NIR light irradiation (Li et al., 2023).

aggregated gold nanoparticles can also generate a thermal gradient under laser irradiation, thus generating motion by auto-electrophoresis. The robot can achieve three different mechanisms of optical propulsion. Chen et al. (2021) designed a Cu_2O@CdSe micro/nanorobot driven by visible light, which is able to move horizontally or vertically by only adjusting the direction of the asymmetric light field, and the stopping and going can be controlled by switching on and off the light (Figure 3B). This design accomplished multidirectional positioning of the robot. Feng et al. (2021) designed a robot with more complex functions, and their robot can achieve orientation control and vertical motion, horizontal motion, and rotation.

With easier-to-create driving environment, more readily available driving fuel, fast robot movement speed, wide range of target pollutants, and beneficial concomitant reactions such as the photo-Fenton reaction, light-driven micro/nanorobots have demonstrated great advantages for applications in water pollution treatment.

2.2.3 Magnetic actuation

Magnetic actuation presents another prevalent option. A micro/nanorobot with magnetic abilities exhibits motion that consumes minimal energy in an inhomogeneous magnetic field, where the asymmetry primarily arises from the magnetic field gradient. In contrast to various other drive methods, magnetic drives can provide very high accuracy, which is advantageous when performing precision operations (Ji et al., 2021; Ji et al., 2023). Meanwhile, the main drawbacks of magnetically driven micro/nanorobots are that the mechanical structure is relatively fixed and typically requires stronger actuation forces to overcome friction from the substrate or surrounding fluids (Hou et al., 2023a).

The magnetism of a micro/nanorobot is designed by adding magnetizing materials to the robot. Common materials include Ni, Fe_2O_3, Fe_3O_4, *etc.* The use of these materials provides modularity to the robot design, which can be referred to as a "magnetic drive module". A magnetically propelled sponge porous microrobot is presented by Ma and wang (2019). This robot possessed super-hydrophobicity and achieved *in situ* oil removal. They enhanced a commercially available sponge material by incorporating superhydrophobic PDA/Fe_3O_4 nanoparticles, resulting in the creation of a three-dimensional porous superhydrophobic sponge with magnetic properties, which can be used to effectively adsorb various types of oil contaminations. They also conducted experiments in path planning, enabling the robot to follow different routes for removing oil droplets from water. This demonstrated precise motion control throughout the operation. The sponge robot maintained a high absorption capacity even after five reuses, providing a reference for the potential reuse of superhydrophobic sponges for environmental remediation.

In fact, the incorporation of magnetically driven materials into robots has gained widespread acceptance, even in challenging environments where magnetic propulsion is difficult to achieve, such as open water. Additionally, in operational contexts that do not require delicate manipulation, researchers still incorporate magnetic materials where appropriate, primarily to harness the magnetic properties for recycling purposes. The study by Singh et al.

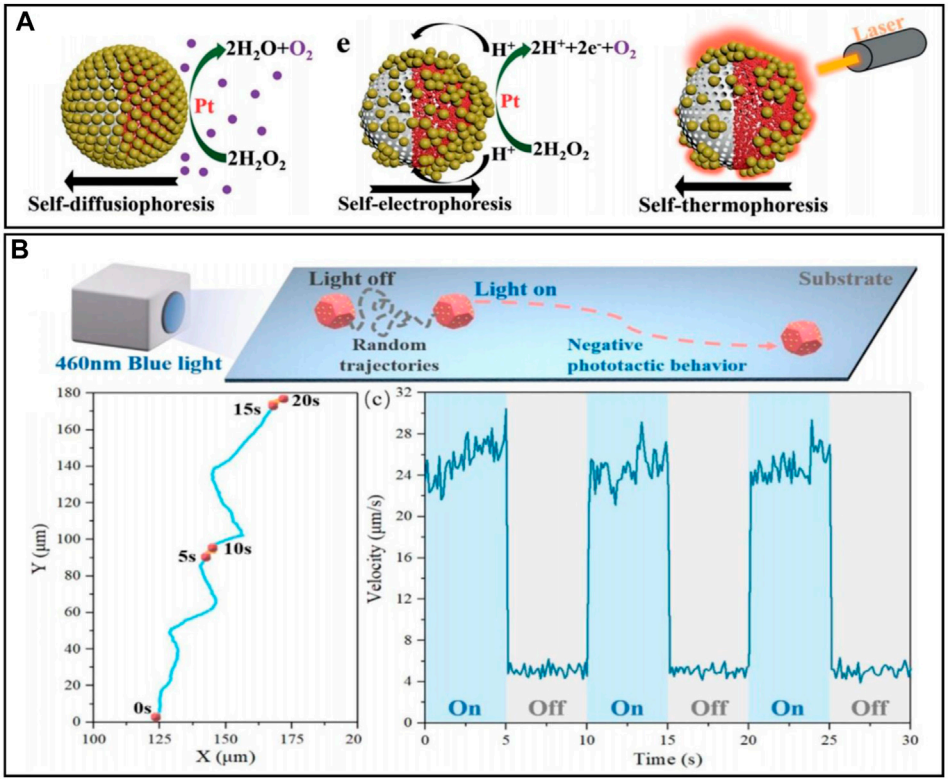

FIGURE 3
(A) Schematic illustration of the propulsion mechanism, switched self-electrophoretic propulsion, light-induced self-thermophoretic propulsion (Xing et al., 2020). **(B)** Schematic illustration of light-controlled self-propulsion behavior of Cu_2O@CdSe micromotors. Trajectories and the speed of the Cu_2O@CdSe micromotors changed as the light switched on and off. Experimental conditions: 0.005 mM tannic acid solution and 1.8 W/cm^2 blue light (Chen et al., 2021).

(2020) also highlights the magnetic recyclability of micro/nanorobots. Their micro/nanorobot was developed using carbon nanospheres with Pt for H_2O_2 decomposition (propulsion) and Ni for magnetic attraction (magnetically driven module). The robot was specifically designed for dye degradation and cannot degrade oil droplet material in real-time. Therefore, after operating in an oil-contaminated environment, the retrieval of both the contaminants and the micro/nanorobot is necessary. As shown in Figure 4A, tasks can be easily accomplished using magnets.

Furthermore, there are examples of micro/nanorobots exhibiting multimodal motions under magnetic field actuation. Sun et al. (2023) developed a magnetic hydrogel micro/nanorobot (MHM) capable of mechanically disrupting biofilms. The work of the robot can be found in Figure 4B. By incorporating Fe_3O_4 material, the robot responds to an external magnetic field and utilizes Fe_3O_4 for contaminant treatment through the Fenton reaction. The MHM operated in two modes of motion controlled by an applied magnetic field, planar rotational and oscillatory modes. The study noted that the robot can be loaded with H_2O_2, which in this case, served as a biocide rather than a motion fuel. Zhang et al. (2021) designed a match-shaped micro/nanorobot with two modes of motion, rotary motion and linear motion under a magnetic field (Figure 4C). By switching the external magnetic field, they can realize the *in situ* switching of motion modes. This study is promising for micro-motion and sensing applications. In addition, it has been shown in the literature that liquid-based reconfigurable microrobots can offer additional possibilities under magnetic control. Ferromagnetic fluids have different motion and deformation behaviours, e.g., they can split/aggregate, or transform states. In addition, the self-assembly and collective behaviour of ferromagnetic fluids show excellent motions, which may show more applications in the field of water pollution treatment in the future (Wang et al., 2023a).

Clusters of micro/nanorobots can be used to compensate for the shortcomings of individual robot motion. Various approaches such as parallel operation and coordinated operation on multiple objects have been proposed, as well as advanced drive mechanisms and operation schemes (Wang et al., 2023b). However, trying to make clusters that are in the same environment exhibit different responses is currently subject to further research. Xu et al. (2022) proposed a new decoupled control method to achieve different movements for micro/nanorobots in the same magnetic field. They designed the micro/nanorobots with different magnetization directions to perform phase-different planar crawling motions within an oscillating magnetic field. Based on this model, complex co-operation of micro/nanorobots under the same excitation will become possible.

2.2.4 Biological actuation

Biological actuation refers to the modification of natural microorganisms into robots through surface modifications and

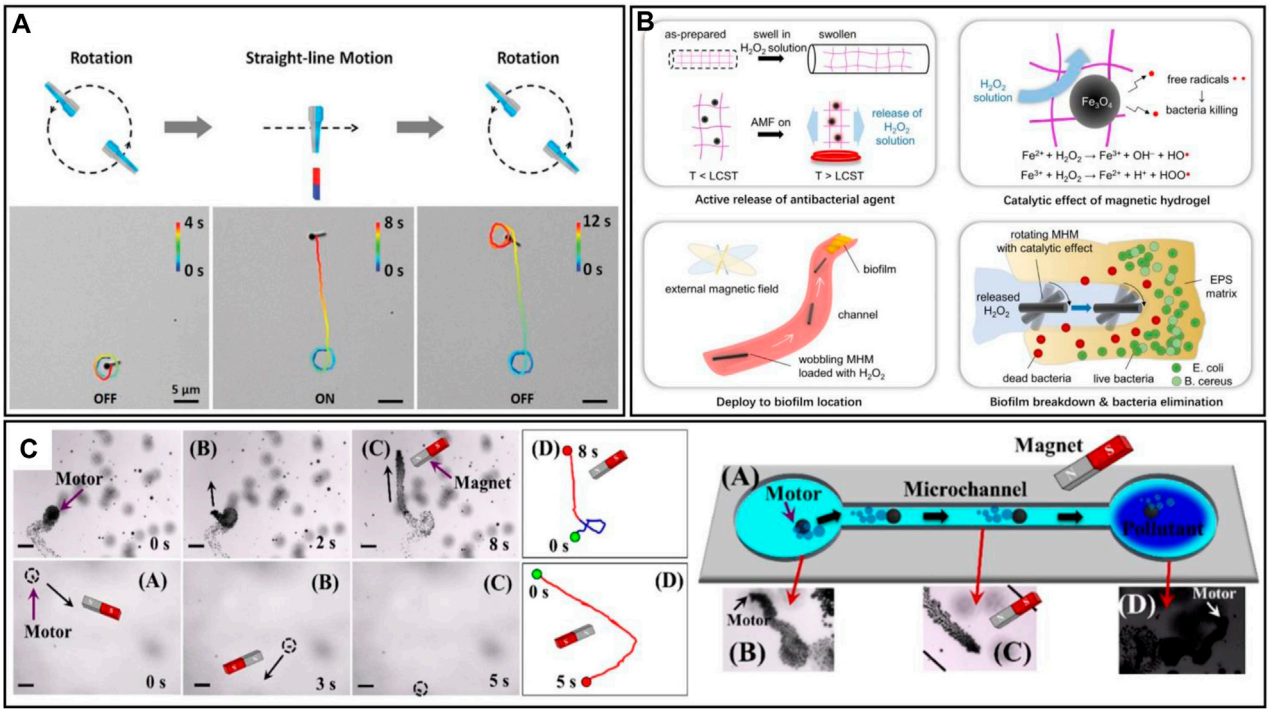

FIGURE 4
(A) The motion trajectory of a magnetically guided micromotor move in H_2O_2 fuel and pure water. The Figure also shows a micromotor traps contaminants in the microchannel, and the real-time images of the process (Singh et al., 2020). **(B)** Schematic illustration of cargo release when heated above the lower critical solution temperature (LCST) of the motors; bacteria-killing free radicals generated in the process of Fenton reaction when the motors are immersed in the H_2O_2 solution; a wobbling motion of the motor driven by the external magnetic field; disruption on the biofilm by catalyzing the released H_2O_2 solution (Sun et al., 2023). **(C)** Schematic illustration of the motion of the magnetic matchstick micromotor in the magnetic field. The Figure also shows trajectories of the magnetic matchstick micromotor moving in 2% H_2O_2 solution when the magnetic field is on or off (Zhang et al., 2021).

the addition of functional modules. Unlike the previously mentioned drives, which are externally controlled, this category represents truly self-driven micro/nanorobots. As microorganisms are natural materials, the utilization of bio-driven micro/nanorobots offers viable ways to mitigate the risk of potential secondary contamination.

Soto et al. (2019) designed a rotifer microrobot, named "rotibot", by utilizing a marine rotifer as a carrier (Figure 5A). The rotifer was electrostatically attached inside the mouth by functionalized microbeads. The movement of the cilia of the rotifer created fluid flow toward its mouth, enabling the treatment of contaminants through functionalized microspheres. The robot relied exclusively on the self-propulsion of the rotifers and did not require any external fuel. Through experiments, the robot demonstrated its effectiveness as a dynamic micro-cleaning platform for the removal of a variety of environmental contaminants, including *E. coli*, neurotoxicants, and different heavy metals. Additionally, Shimizu et al. (2021) achieved the design of a biohybrid windmill by placing captured microalgae within an orthogonal frame. By incorporating capture chambers at the edges of the frame, they constrained the motion of the captured microalgae to be isotropic to the orthogonal axes. This design aimed to prevent motion cancellation caused by the non-uniform movement of the microalgae. Experimental tests demonstrated that the bio-windmill could rotate at an angular velocity of 0.78 rad/s. Similar to this work, Xie et al. (2021) achieved the manipulation of artificial microstructures through algal cells by capturing algal cells in tiny structures. The orientation of the robot can be controlled by capitalizing on the phototropism of the algae with the integration of an external light source. The motion of the robot when entering the Y-shaped tunnel is shown in Figure 5B. This study successfully demonstrated the cargo transport and autorotation capabilities of an algal microrobot, showing its potential for precise object manipulation on a miniature scale.

In addition to the aforementioned examples, algae have also been used in the assembly of other types of robots. Zhang et al. (2021) developed algal microrobots that can be used to remove the SARS-CoV2 virus from wastewater by modifying the surface of algae with ACE2 receptors (Figure 5C). ACE2 receptors, known for their high affinity to viral spiking proteins, serve as potent cellular receptors for SARS-CoV-2, enabling targeted virus recognition. The researchers selected Chlamydomonas reinhardtii due to its ease of mass production, swift mobility in various water environments, extended lifespan, and feasibility for surface modifications. Their experimental results demonstrated an impressive 89% removal rate of SARSCoV-2 pseudo-virus, providing a design concept and template for real-time purification of coronavirus wastewater. Similarly, Moghazy et al. (2023) employed Nile algae to create porous cellulose microspheres

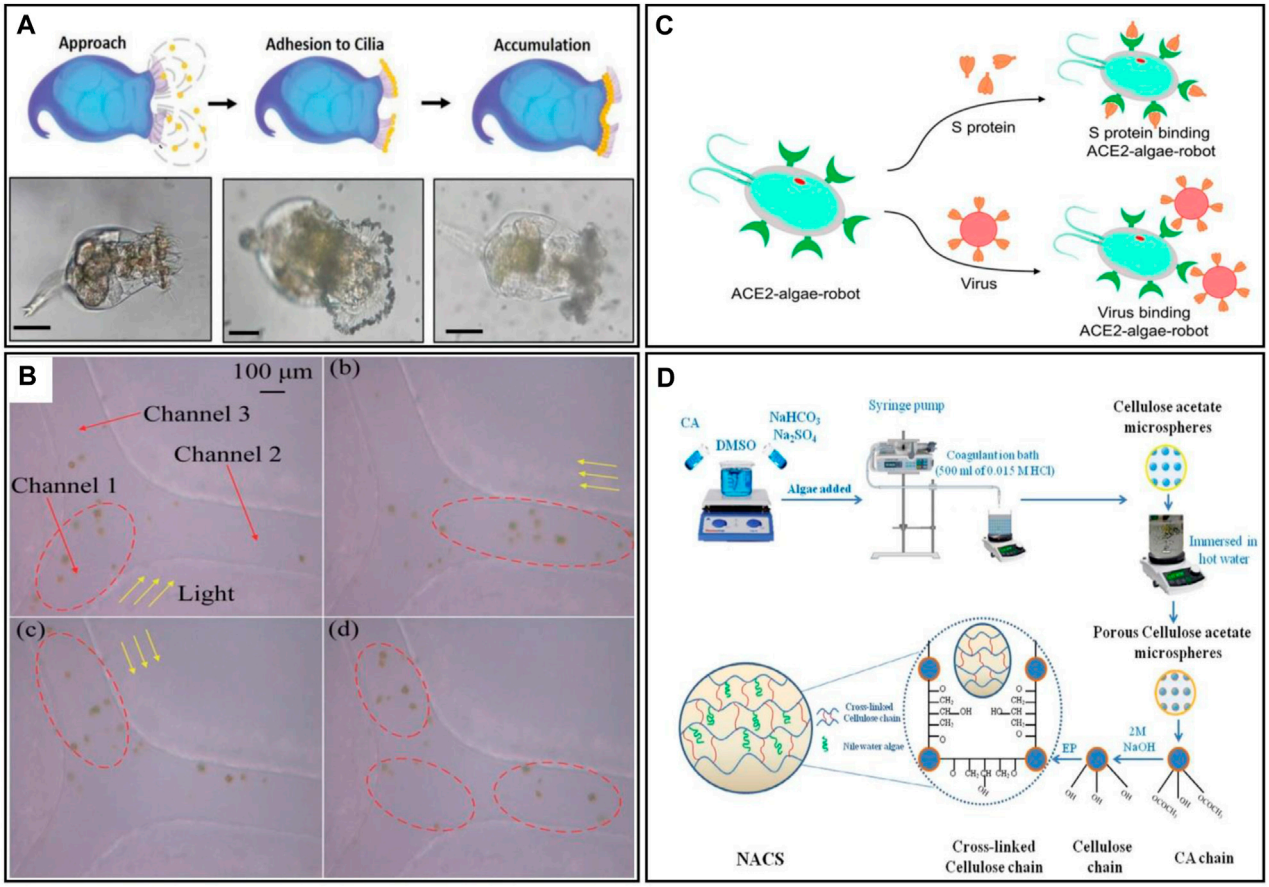

FIGURE 5
(A) Schematic illustration of the Mechanism for the formation of the rotibot, and the microscopy images of the Mechanism for the formation of the rotibot (Soto et al., 2019). **(B)** Images of mass *E. elegans* cells swimming in the Y-shaped microfluidic channel. Algal cells are in the red ellipses, yellow arrows represent light direction (Xie et al., 2021). **(C)** Schematic illustration of the ACE2-algae-robot remove the spike protein and SARS-CoV-2 virus (Zhang et al., 2021). **(D)** Schematic illustration of the fabrication of the Nile water algae cross-linked cellulose microsphere (NACS) (Moghazy et al., 2023).

designed for the removal of methylene blue dye and copper ions from aqueous media, significantly enhancing the adsorption capacity of their robots. The fabrication of their robot is illustrated in Figure 5D.

2.2.5 Other actuation methods

Besides the above methods, there are also common actuation methods such as the Marangoni effect, thermal-driven propulsion, acoustic actuation, optimal actuation and electric manipulation. More specifically, techniques like laser scanning and even photosynthesis have been utilized.

The Marangoni effect is the phenomenon of mass transfer due to the existence of a surface tension gradient at the interface of two liquids with different surface tensions. This effect can be triggered by various mechanisms. For example, Sun et al. (2019) designed a novel micro/nanorobot with controllable motion behavior based on infrared light. The propulsion of this robot relied on the Marangoni effect generated when polypyrrole nanoparticles (PPyNPs) were exposed to infrared light. PPyNPs exhibit strong absorption bands in the near-infrared region, allowing them to convert light energy into heat. This process reduced the local surface tension near the irradiated area, leading to the generation of a solution tension gradient. The cessation of the robot's motion can be achieved by adding surfactants to eliminate the thermal Marangoni effect, counteracting most of the tension gradient. Another classic example is the robot designed by Yoshida et al. (2021) for release via ethanol, which also serves as a classic design for energy storage. During operation, the loaded ethanol diffused spontaneously. The released ethanol rises to the free surface due to buoyancy and reduces the surface tension of the water, created a tension gradient that enables the robot to move.

Ultrasonic and electric fields are also significant driving methods for micro/nanorobots. Xiaolong Lu et al. designed a device based on locally enhanced acoustic flow for driving microrobots. The platform conducted precisely transport along a given path. Through numerical simulations and specific experiments, it was demonstrated that the acoustically driven microrobots have high motion accuracy (Lu et al., 2019). Reorientation of the water dipole moment due to a rotating electric field can rotate carbon nanotubes immersed in aqueous solution, which gives theoretical basis for electric manipulation of

underwater micro/nanorobots. The study of Zhongyu Fu et al. showed that the radius and length of the nanorobot affects the rotation angle, speed and cycle time, providing a reference for the use of micro/nanorobots underwater guided by electric fields (Fu et al., 2019).

A classic case of thermal drive is the thermal fluctuation-based motor designed by Lou et al. (2021) utilizing inherent thermal motion. Their self-thermal reflective nanorobot, built on Janus particles with unidirectional transmission, can reverse direction by adjusting the frequency of an external potential. The motor achieved a speed close to the superposition of the drift speed of a pure Brownian motor and the self-propulsion speed of a pure auto-thermophoretic particle. Furthermore, Kim et al. (2019) designed a laser scanning-based micro/nanorobot using shape memory alloy (SMA). Each laser scan triggered a material deformation, enabling the crawling motion of the robot. The wireless self-recovery-like motion achieved by this robot can serve as a reference for other deformable micro-scale structural driving methods.

2.2.6 Enhancement of drive effects

The enhancement of micro/nanorobot motion effects through algorithm optimization is also a mainstream direction. Algorithms and various optimized control methods can be used to compensate for design flaws in the robot body and improve motion performance. Hou et al. (2023b) designed a microdrill that enabled propulsion driven by a magnetic field. By introducing a camera system, they implemented a control strategy that can utilize vision for dynamic feedback, thereby switching the direction and frequency of rotation according to the local environment, enabling the microdrill to move flexibly and penetrate obstacles efficiently. Xu et al. (2022) developed a broad learning system (BLS) based learning servo control strategy and applied it to a micro-robotic system. They combined the traditional Lyapunov theory with a new learning-based approach to obtain constraints on the controller parameters. Their model did not require adjusting of the controller parameters and achieved an applied extension of BLS. Liu et al. (2021) proposed a path planning algorithm for three-dimensional motion of micro/nanorobots. Their design can compensate for the angle between the robot's direction and the magnetic direction when there are weight perturbations and lateral perturbations in 3D space. Experiments demonstrated that their method has sub-millimeter accuracy in three-dimensional space.

Through the design and integration of modules, it is possible to achieve the effect of "1 + 1>2". Zheng et al. (2021) designed a hand module that can grip tiny objects by changing the local ion density or pH. Through experiments, they performed grasping and transport of magnetic microspheres, demonstrating the effectiveness of the design. This programmable hand-like structure offers possibilities for the dynamics of micro-nano robots. Zheng et al. (2022) also designed a single-step aniso-electrodeposition method that can be used to fabricate modular micro/nanorobots. Such modular robots can achieve a wide range of motions such as spiralling, twisting, bending and curling, and perform multiple tasks such as propulsion, grasping and object transfer simultaneously in response to magnetic field, ionic and pH stimuli. In addition, the authors further explored the possibility of loading other functional modules (e.g., cells, drugs, and magnetic nanoparticles) onto this module to achieve multifunctionality.

In addition, hybrid actuation has been developed through module integration in the design of micro/nanorobots (Wang et al., 2020). In the field of water pollution, the main focus is on hybrid designs between optical, bubble and magnetic drives (Ying et al., 2019; Shen et al., 2020; Li et al., 2022; Mayorga-Burrezo et al., 2023). Through the hybrid-driven operation, the operation accuracy can be improved, the operation range can be increased, the operation conditions can be reduced, the material recovery can be realized, and it can also improve the efficiency of water pollutant degradation.

3 Water pollutant control using micro/nanorobots

3.1 Control principles and detection methods of water purification

3.1.1 Control principles using micro/nanorobots

Continuous discharge of wastewater has significantly degraded soil and water quality, posing severe threats to organisms and ecosystems. Despite increasing evidence of worsening water pollution, research in this area remains limited (Bayabil et al., 2022). Along with the development of industry, more and more new pollutants gradually begin to accumulate and have negative ecological effects. These pollutants include polycyclic aromatic hydrocarbons, pharmaceuticals and personal care products, pesticides, phthalates, hormones, engineered nanomaterials, and perfluorinated compounds (Eumann and Schildbach, 2012; Gkika et al., 2022). Furthermore, these new pollutants, along with traditional pollutants such as metal ions and oil, synergistically interact with ecosystems, leading to more serious ecological disasters. For example, some studies have shown that the diffusion of antibiotics and heavy metals, among other factors, can result in bacteria mutations in wastewater. This, in turn, leads to the gradual increase of drug resistance and the development of new types of pathogenic bacteria, ultimately leading to infections with biological populations (Sambaza and Naicker, 2023). The spread of pollution in wastewater poses a threat that necessitates strategies to prevent further harm. This global public health issue demands immediate human action through wastewater treatment and water purification.

There are three primary steps involved in using micro/nanorobots for wastewater treatment and water purification, (i) capture, (ii) transfer, and (iii) degradation.

(i) The capture process typically involves electrostatic adsorption or chemical binding. However, as previously mentioned, the limited strength of the electrostatic adsorption effect may not always meet the requirements for effective use.
(ii) Transferring pollutants is sometimes not essential, as the development of micro/nanorobot technology is just beginning and cannot yet fully achieve real-time degradation of pollutants. Therefore, the proposed transfer is a compromise method to collect unprocessable pollutants and utilize other degradation methods. In the case of heavy metal pollution, the transfer of harmful elements out of the water body is also necessary.

(iii) The degradation process is the core of water pollution treatment, centered around a series of biochemical reactions that generate chemically active substances to break down pollutants into environmentally friendly substances. The most frequently employed active substance is Reactive Oxygen Species (ROS), which was first utilized in 1987 (Glaze et al., 1987), to facilitate the decomposition of organic matter into water and carbon dioxide. This approach simultaneously fulfills the fundamental requirement of avoiding secondary pollution, including the contamination of intermediate substances and the introduction of new pollutants during the treatment process. Numerous common mechanisms exist for pollutant degradation, with several of the more commonly used methods outlined here.

(i) Fenton reaction, involves the production of hydroxyl radicals from ferrous or ferric ions and hydrogen peroxide.

(ii) Fenton-like reaction, which is a similar process induced by other catalysts, e.g., Pt with H_2O_2 to produce hydroxyl radicals.

(iii) Heterogeneous photocatalysis, which means photons with energy greater than or equal to the band gap of the material irradiate the photocatalytic material (semiconductor or photosensitizer), generating electron-hole pairs that migrate to the surface of the photocatalyst, where they react with water and oxygen to produce ROS. ROS production is easier if a strong oxidizing agent, such as H_2O_2, is present in the process.

This is precisely why Fe_2O_3 nanoparticles are extensively employed in large quantities in the case above. Fe_2O_3 serves not only as an active semiconductor for visible light, enabling multiphase catalytic reactions under such illumination, but also as a catalyst for the Fenton reaction, which directly participates in the generation of active substances and promotes pollutant degradation. Additionally, Fe_2O_3 possesses magnetic properties, making it suitable for use as a magnetic module in micro/nanobots. As a result, it imparts the products with the capability of precise propulsion and magnetic recycling under magnetic control. This feature enhances the versatility of the products even further (Urso et al., 2023).

3.1.2 Detection methods and integrated platforms

Detection methods play a crucial role in water purification experiments. Traditional water quality testing is mainly based on liquid or gas chromatography, combined with mass spectrometry. However, these methods demand substantial quantities of freezers and solvents for preparation (Wang et al., 2017), resulting in high operational costs. These methods are less effective in identifying trace contaminants like toxic ions and persistent organic pollutants. Different pollutants necessitate distinct observation and detection techniques. For instance, metal toxic ions are commonly detected using Atomic Absorption Spectroscopy (AAS) and Inductively Coupled Plasma Mass Spectrometry (ICP-MS), which offer high sensitivity but require bulky and expensive instruments unsuitable for on-site analysis. Dyes often rely on their distinct ultraviolet absorption peaks, while plastics are typically detected through Fourier Transform Infrared Reflection (FTIR), Raman spectrometry, and Mass Spectrometry (MS). Different sizes of pollution also require diverse equipment and methods. For micron-level pollution, initial detection is often accomplished through optical microscopy and scanning electron microscopy observations, whereas nanoscale pollution requires tools like transmission electron microscopy and nanoparticle tracking and analysis techniques (using diffraction imaging) for accurate observation. In the context of the micro/nanorobots discussed in this paper, fluorescence techniques and pulse voltammetry are the commonly employed detection methods (Rojas et al., 2016).

The advancement of experimental techniques in water refinement has spurred the exploration of integrated and functional experimental platforms. Zhao et al. (2023) developed a micro/nanorobot-based colorimetric detection platform, enabling rapid quantitative and high throughput qualitative colorimetry. The micromotors within the platform not only catalyze chemical reactions but can also transform into a rotor through magnetic drive, accelerating reactions via micro-stirring. Their platform system was made with 48 micro-orifices, which can perform up to 48 micro-droplet reactions simultaneously while rapidly catalyzing the target substances and displaying the corresponding colors for spectroscopic testing and analysis. The compact and portable integrated platform brings the traditional laboratory experience to water body testing, thereby significantly facilitating water quality assessment (Zhao et al., 2013).

Fan et al. (2023) faced the limitations of a single light source and developed a control platform based on multiple light field coupling, which realized the light-drive propulsion for both individual and collective micro/nanorobots, achieved by programming four light sources to emit in different directions. This platform served as a versatile tool for applying optical actuation to similar robots, meeting a range of purposes. Denniss et al. (2022) developed a low-cost, modular and open-source dynamic optical microenvironment, known as DOME, capable of inducing collective behaviors using light. This platform aimed to enhance the visualization of biologically-modified micro/nanorobots. The open-source modular design ensured high scalability and easy adaptation to new requirements, allowing the effective operation of different types of bio-modified micro/nanorobots by adjusting physicochemical parameters such as light source, microscope settings, ambient atmosphere, temperature, and so on. The DOME platform also offered the potential for future expansion of drive methods, the creation of a multi-drive observation setup, and even the integration of intelligent algorithms for analyzing single-unit behavior and group phenomena of the robots, along with monitoring physicochemical parameters. The images and the illustrations of the above platforms this paper mentioned above is shown in Figure 6.

3.2 Latest research on water pollution control using micro/nanorobots

3.2.1 Removal of micro/nanoplastics

Plastics are composed of long chains of polymers, with covalent bonds connecting the monomers. Due to their low cost and good performance, they are widely used in industry and daily life. However, the non-biodegradability of certain plastics has resulted

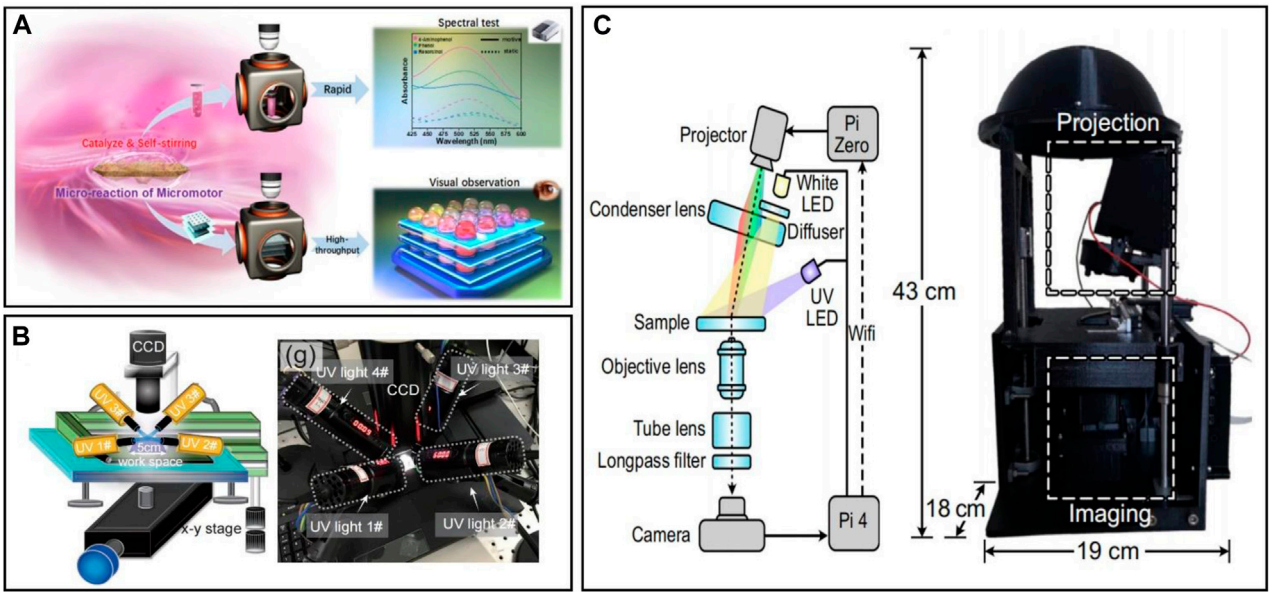

FIGURE 6
(A) Schematic illustrations of an integrated catalytic micromotor platform which enable efficient dual-mode colorimetric detection by self-stirring micro-reaction (Zhao et al., 2023). **(B)** Schematic illustration of the multi-light-fields based optical driving platform and a physical view of the multi-light-fields-based optical driving platform (Fan et al., 2023). **(C)** A picture of Dynamic Optical MicroEnvironment (DOME) with dimensions and the schematic illustration of the optical components (blue) and the wireless communication links (dashed lines) within DOME (Denniss et al., 2022).

in their accumulation within the ecosystem. Moreover, plastics not only serve as environmental pollutants themselves but also trigger a series of ecological hazards. Micro/nanoplastics encompass a range of plastic particles with dimensions smaller than 5 mm. Owing to their small size and large surface area, microplastics readily absorb pollutants and offer substrates for the growth of microorganisms like bacteria. Additionally, they attract diverse pollutants through adsorption, culminating in heightened toxicity. Generally, nanoplastics are prone to suspension and dispersion due to water turbulence. Their higher surface-volume ratio results in enhanced adsorption of microorganisms and contaminants, facilitating deeper penetration into biological tissues. Recently, micro/nanoplastics have been found in various organisms. Shrimp ingest these particles while feeding on decaying material or plankton, causing issues such as appetite loss and tissue deformation (Urso et al., 2023). Research in 2022 measured the mass concentration of plastic polymer components in human blood for the first time, showing the absorption of plastic particles into the bloodstream (Leslie et al., 2022). In addition, micro/nanoplastic particles have been found in different plant and animal species, including fish and algae (Ribeiro et al., 2023).

Micro/nanorobots use various methods for capturing and degrading micro/nano plastics. The three primary capture methods include i) electrostatic interaction, ii) electrophoretic attraction and iii) adhesion. i) Electrostatic interactions require surface charge programming, typically achieved by pH adjustment. For example, TiO_2 becomes positively charged in acidic conditions and negatively charged in alkaline surroundings. However, precise pH control can be challenging even in confined spaces. ii) Electrophoretic attraction relies on creating chemical gradients around operating micro/nanorobots, facilitating the capture of micro/nanoplastics. iii) Adhesion is achieved by mimicking DOPA proteins secreted by mussels, through a structurally similar design of another protein PDA, which can be used as coatings for microplastic adhesion. After capturing the micro/nanoplastics, the micro/nanorobot completes their oxidation through several methods. This includes breaking the chemical bonds of polymers, photocatalytic degradation, and enzymatic degradation. For example, the Fenton reaction can be employed to break the polymer bonds, while photo-active materials generate electron-hole pairs under light, initiating chemical reactions with water and other substances. This generates reactive oxygen species (ROS), achieving photocatalytic degradation. Alternatively, enzymes can be directly used for decomposition.

In recent years, a notable study on plastic treatment involves the use of two bubble-propelled micro/nanorobots conducted by Ye et al. (2021). They used two motors, Fe_3O_4-MnO_2 and Fe_2O_3-MnO_2, for microplastic decomposition, demonstrating that the Fe_2O_3-MnO_2 microrobot effectively eliminates microplastics suspended in aqueous solution through the synergistic action of catalytic degradation, surface adsorption and adsorption bubble separation mechanisms (Figure 7A). Remarkably, adsorption bubble separation led to over 10% removal of suspended microplastics from contaminated water within a span of 2 h. The study also clarified the main contributions of different remediation mechanisms in pollutant removal. Zhou et al. (2021b) prepared adherent polydopamine PDA@Fe_3O_4 magnetic microrobots called "MagRobots", by modeling the basic properties of marine mussel adhesion. Microplastic enzymatic degradation was achieved by loading lipase onto the surface of PDA@Fe_3O_4-MagRobots. Leveraging magnetic actuation, these robots exhibited good kinematic abilities, enabling them to navigate predefined path

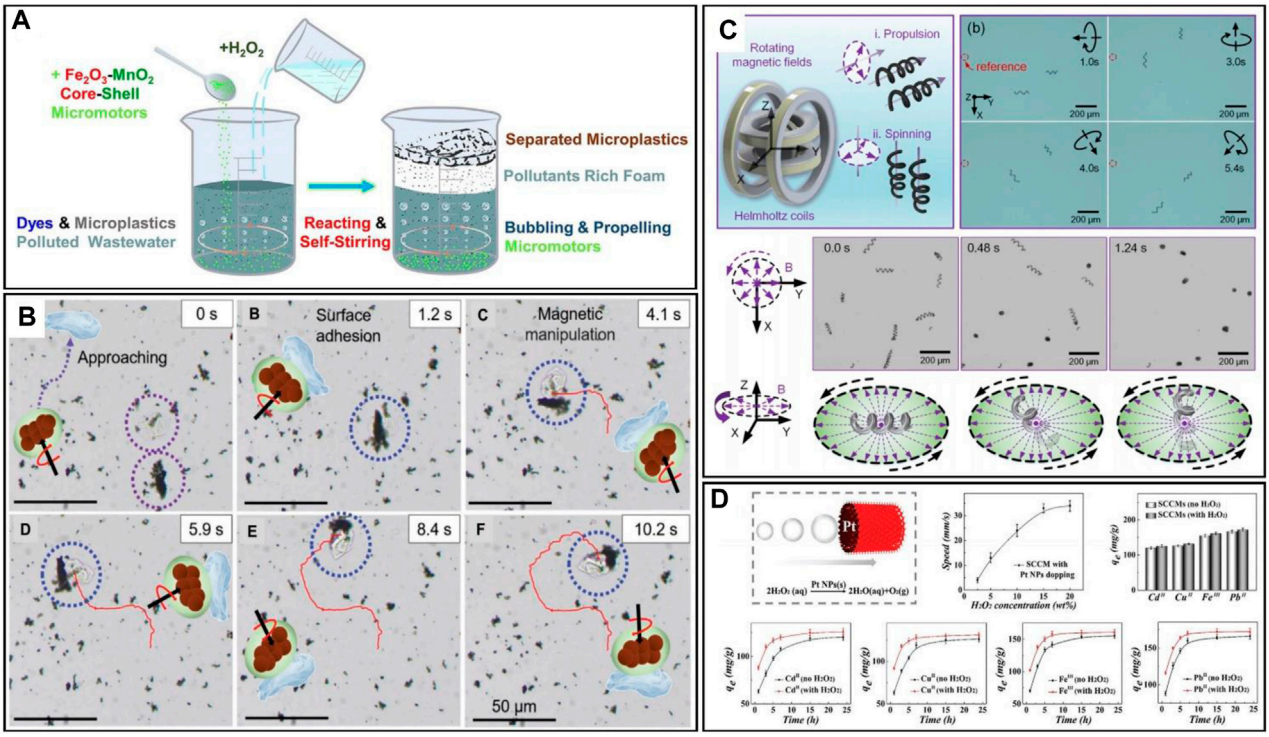

FIGURE 7
(A) Schematic illustration of adsorptive bubble separations for dissolved pollutants and microplastic removals (Ye et al., 2021). **(B)** Time-lapse of the microplastic removal process using PDA@Fe_3O_4 MagRobots. The image shows approaching, Surface adhesion and movement with the assistance of a transversal rotating magnetic field (Zhou et al., 2021b). **(C)** Schematics illustration of the BMHMs' propulsion and spinning, and time-lapse images of the BMHMs in the movement mode of directional propulsion, stand erect and spin around (Gong et al., 2021). **(D)** Schematic diagram of the self-propelled SCCM, and the plot of the movement speed of the SCCM in different concentrations of H_2O_2. The diagram also gives a comparison of the effect of the presence or absence of H_2O_2 on adsorption in a static environment, and shows adsorption of different soluble metal ions by the SCCM under different conditions (Shang et al., 2022).

and precisely target and remove microplastics at a specific point. The trajectories of the robot guided by magnetic field can be seen in Figure 7B.

3.2.2 Removal of heavy ions

Heavy metal ions, primarily consisting of elements with relative atomic masses ranging from 63 to 200, are mainly transition metals such as Ni, Hg, Pb, Cu, Zn and Cd. These metals are difficult to degrade when dissolved in water, thus they are prevalent pollutants with the capacity to accumulate in sedimentary layers within soil, plants and animals, posing a persistent threat to public health. This includes potential risks such as myocardial infarction and lung cancer. The conventional approach to removing heavy metal ions is electrocoagulation, which offers a practical solution for eliminating heavy metals and other pollutants from water. This method is particularly attractive due to the small size of sludge generated during treatment, but its widespread implementation in many facilities is limited by the high costs involved (Aguiar et al., 2023). Furthermore, hexavalent ferrate has been used to remove various metal ions, including Pb, Cd, Fe, Zn, Mn, Cu, As, Co, Ni, and Al. Research findings indicate that hexavalent ferrate can be used as a multipurpose chemical for the effective removal of toxic metal ions. However, its efficiency in removing certain harmful metals is limited, and it can even have adverse effects on water quality. Practical tests involving hexavalent ferrate have been carried out, but the outcomes have often been unsatisfactory (Dong et al., 2019). Over the past years, micro/nanorobots have emerged as a promising approach for treating metal ions, attracting attention for their fast and thorough clean-up capabilities.

(i) Lead ions. Lead ions are among the most abundant heavy metals in the Earth's crust and are widely used in industry. Unfortunately, the widespread utilization of lead has led to its prevalence as an environmental pollutant. Being a toxic heavy metal, lead is a neurotoxic metal with no metabolic benefits, easily absorbed by the body, non-biodegradable by living organisms, and extremely difficult to discharge (Wu et al., 2023). Addressing this issue, Gong et al. (2021) designed Fe_3O_4-MnO_2 biohybrid magnetic helical microrobots (BMHMs) based on Spirulina cells. Actuated by the rotating magnetic fields, these robots can accomplish spinning around three orthogonal axes (demonstrated in Figure 7C). These microrobots demonstrated a remarkable ability to remove Pb^{2+} from wastewater and achieved an adsorption efficiency exceeding 95%. It is noteworthy that the BMHMs can also be recycled after simple regeneration.

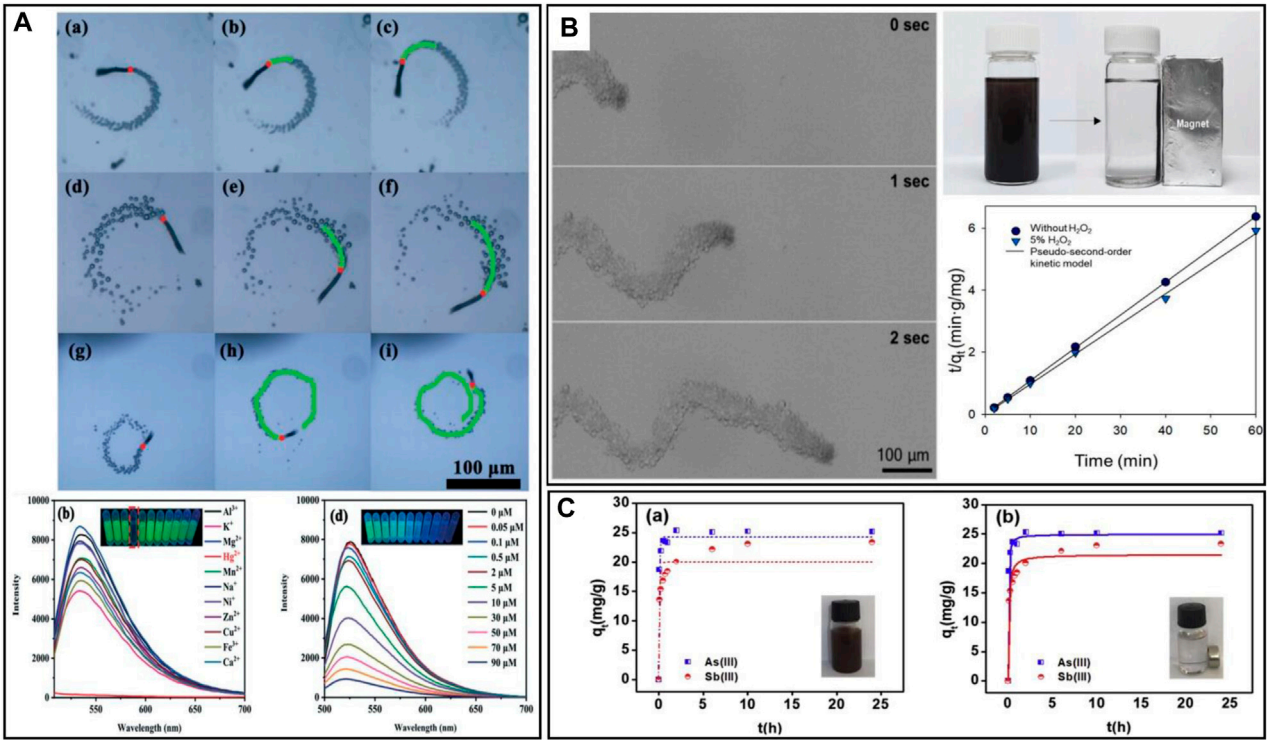

FIGURE 8
(A) One second Time-lapse images of the AO–Mn_2O_3/γ-AlO&lJlig;OH micromotor in H_2O_2 solutions with different concentrations of 1%, 2%, and 3%. The images below are the fluorescence effects of the measurement of different metal ions, and fluorescence effects of the measurement of different concentrations of Hg^{2+} (Li et al., 2021). **(B)** Time-lapse images of the MIMS/Pt motors in the environment of 10 wt% H_2O_2 with 0.5 wt% Triton-X100. The image of the robot recycling, shows that a magnet will do the trick. The last diagram shows the Cs removal process of the MIMS/Pt under varying conditions (Park et al., 2021). **(C)** Adsorption performance of As^{3+} and Sb^{3+} in the singular system on Fe_3O_4@TA@UiO-66 (Qi et al., 2019).

(ii) Copper ions. Copper is usually recognized as a highly hazardous heavy metal (Rahman et al., 2023). While it is essential for vital human functions and physical wellbeing, excessive copper intake can result in acute gastrointestinal symptoms, liver enzyme systems inactivation, and even movement disorders. Global copper pollution has been on the rise in the aquatic environment and has been recognized as a significant source of heavy metal contaminants due to health risks (Liu et al., 2023). In response to this concern, Shang et al. (2022) developed micro/nanorobots known as SCCMs using responsive hydrogels of carboxymethyl chitosan (CMC) and polyacrylamide (PAM) labelled with platinum nanoparticles (PtNPs). These robots demonstrated the ability to treat a wide range of heavy metal ions (see details in Figure 7D), including Cu^{2+}. The SCCMs robots exhibited a self-reporting feature, making the adsorption/desorption process visible to the naked eye through observable colour change.

(iii) Mercury, found in substances like mercury thermometers, is one of the most common and accessible heavy metals. However, it poses significant bio-toxicity, especially in the form of free mercury ions, which can lead to mercury poisoning upon entering the human body. In response, Li et al. (2021) developed a new fluorescent micromotor propelled by the asymmetric decomposition of hydrogen peroxide, with Mn_2O_3 serving as the catalyst. The fluorescence effect of the micromotor showed good selectivity and sensitivity in detecting Hg^{2+} (Figure 8C), enabling the detection of mercury ions even at low concentrations.

(iv) Radioactive ions, specifically dissolved radionuclides, exhibit mobility within the natural environment. If not appropriately treated, they can enter the aquatic environment, such as rivers and groundwater. This increases the risk of biological exposure to radioactive radiation. In contrast to other pollutants, radioactive contaminants have extremely long half-lives and are more insidious and potent toxins that can remain for extended periods (Ma et al., 2023). In this regard, Park et al. (2021) tackled the removal of radioactive ^{137}Cs from contaminated solutions using a clay Janus microsphere micro/nanorobot (Figure 8B). Their robots have outstanding repulsive magnetism and motion effects, by incorporating a magnetic module, the micro/nanorobot could precisely locate radioactive sources under an applied magnetic field in a liquid environment containing competing ions, and the results demonstrated that the robot could remove more than 98.6% of ^{137}Cs from an aqueous medium containing potassium, sodium, calcium, and magnesium ions.

(v) Arsenic. Although arsenic is not classified as a heavy metal, its contamination is often treated as such. Arsenic poses a high level of toxicity to all forms of life. The element has been designated as a Group I human carcinogen with the highest

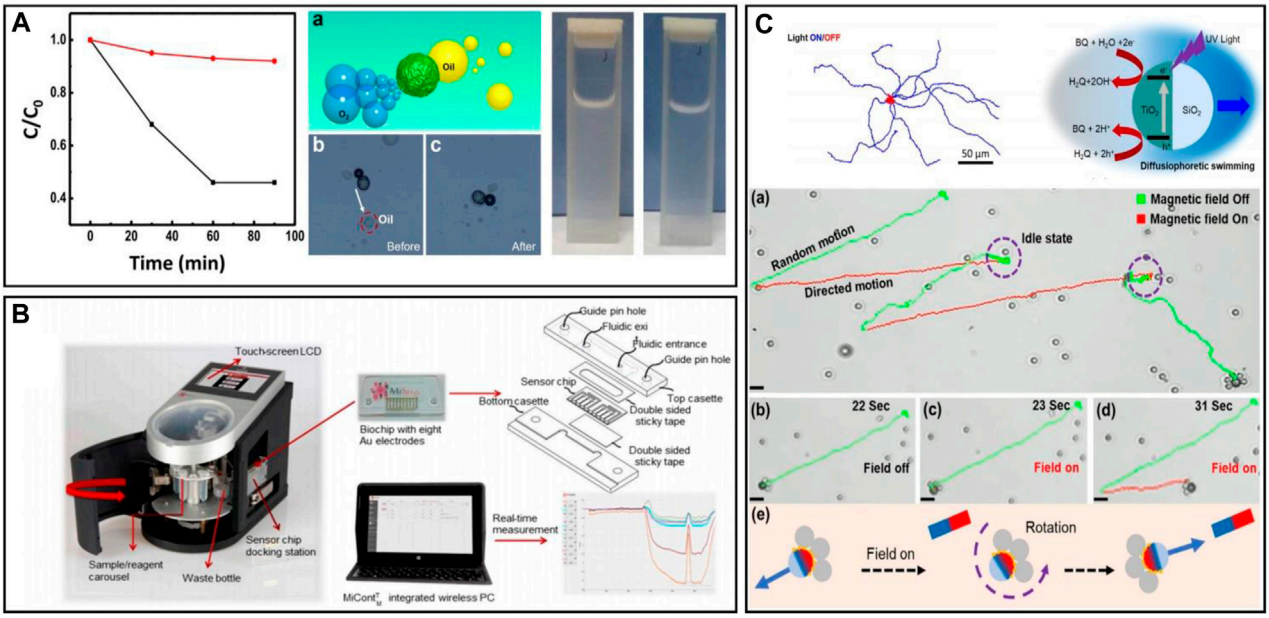

FIGURE 9
(A) Effectiveness curve and visual representation of the degreasing by the walnut-like micromotor, the red curve represents the stationary counterpart, and the images of the process of the capture of the oil by the walnut-like micromotor (Wang et al., 2019). **(B)** Schematic illustration of microfluidic-based electrochemical biosensor (Wang et al., 2022). **(C)** Trajectories of microrobots under light with light on (blue) and off (red), and the schematics illustration of the reaction. The photos below show the total and detail of the movement of PEDOT/MnO_2@Ag micromotors, and the motion mechanism guided by a magnet (Debata et al., 2022).

classification by the World Health Organization (Nicomel et al., 2016). Traditional techniques for removing arsenic include oxidation, coagulation-flocculation and membrane methods, but these approaches are currently not deemed sufficiently practical due to cost and process limitations (Dilpazeer et al., 2023). Addressing this issue, a novel magnetic core-shell microsphere named Fe_3O_4@TA@UiO-66 was developed by Qi et al. (2019). This microsphere has the capability to remove both As^{3+} and Sb^{3+} from wastewater. The adsorption experiments carried out have demonstrated the high adsorption capacity of the magnetic Fe_3O_4@TA@UiO-66 for As^{3+} and Sb^{3+} (Figure 8C). Moreover, it can be rapidly separated from the aqueous medium within 2 min after treatment and the composite exhibited effective removal performance for As^{3+} and Sb^{3+} across a wide range of solution chemical conditions.

3.2.3 Removal of oil

Environmental pollution caused by oily substances, like oil, primarily results from human activities, particularly offshore oil spills and wastewater discharges from industrial platforms. Oily substances not only induce soil toxicity but can also infiltrate the food chain via water sources, causing harm to ecosystems. The potent accumulative impact of oil pollution can easily lead to the phenomenon of bioaccumulation in organisms.

Addressing this issue, Wang et al. (2019) developed a multi-responsive walnut-shaped microrobot that achieved kinetic and magnetic responses through catalase and ferric tetroxide, generating motion via bubble formation in a fuelled environment. The hydrophobic PCL polymer component within the microrobot enabled strong adhesion upon contact with oil droplets, facilitating the collection of oil droplets from the solution (Figure 9A). The removal of oil droplets and energy reuse can be achieved through magnetic field separation. Similarly, Ma and Wang. (2019) introduced a microrobot based on a magnetically propelled superhydrophobic sponge, which effectively captured chloroform, methylene chloride, and toluene with high capacity. The sponge microrobot enabled precise motion control and selective separation simultaneously. Even after five regeneration and reuse cycles, the sponge robots maintained their high absorbency and recycling capacity. Wang et al. (2022) introduced an efficient robotic platform for pollutant adsorption (Figure 9B). The system involved a flapping-wing micro-plane for long-distance travel and a low-cost multifunctional Janus microrobot for pollutant purification. During operation, the flapping-wing aircraft flied over the targeted water body, releasing the microrobot. Comprising silicon microspheres, a nickel layer and a hydrophobic coating, the robot is designed to absorb oil and treat organic pollutants. Controlled by a rotating magnetic field, the manipulable microrobot can navigate the water environment, continuously searching for oil droplets.

3.2.4 Removal of microorganism

Waterborne diseases from pathogenic microorganisms pose a severe global health threat. Globally, approximately 1.6 million annual deaths are due to biological contaminants in water, like bacteria, viruses, protozoa and worms. These microorganisms can enter the human body to cause health risks through direct consumption of contaminated water (Kumar et al., 2019). *E. coli*, common in freshwater, is antibiotic-resistant and can cause serious

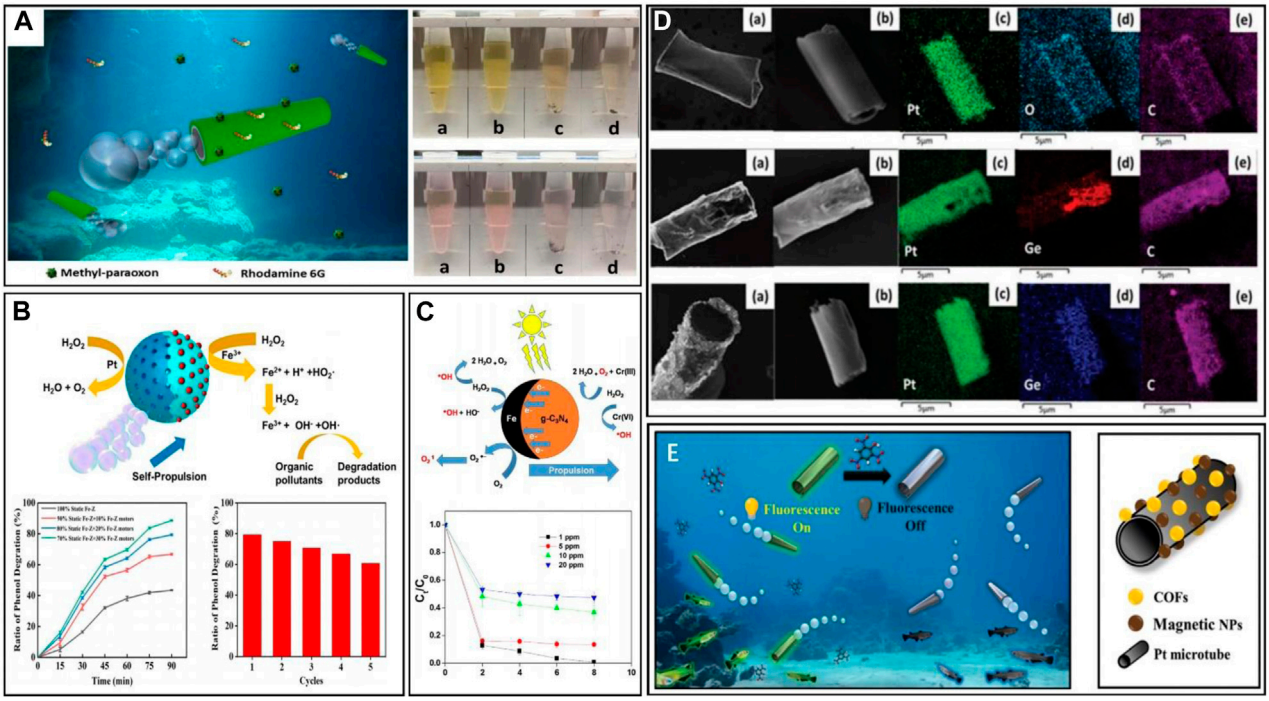

FIGURE 10
(A) Schematics illustration of the self-propulsion and pollutants purification by artificial multilayered microrocket, and diagrams of the removal of methyl-paraoxon and rhodamine 6G by artificial multilayered microrocket (Li et al., 2015). **(B)** Schematics illustration of the degradation of organic pollutants by Fe-zeolite micromotors. The diagram shows the effect of initial conditions on phenol degradation and the degradation efficiency in the reuse of the microrocket (Ma et al., 2020). **(C)** Schematics illustration of the motion of the microrobot and the generation of ROS, and the effect of initial SMX concentration on degradation (Rayaroth et al., 2021). **(D)** Energy-dispersive spectroscopy (EDS) elemental mappings of bare GO-Pt, 2D-Me-Ge modified and 2D-Ph-Ge modified microrobots respectively (Moric et al., 2020). **(E)** Fluorescent mechanism of the magnetic COF-functionalized micromotor, and the schematic diagram of the structure of the magnetic COF-functionalized micromotor (Wang et al., 2021).

illnesses like haemorrhagic colitis and haemolytic uremic syndrome through the production of verodoxin (Siri et al., 2023). Initial techniques to eliminate harmful organisms in water included antibiotics, enzymes, metal ions, *etc.*, or UV light, chlorine compounds, and ozone. However, these methods generate toxic by-products.

Debata et al. (2022) developed a structurally simple Ni-Au/TiO_2-SiO_2 Janus robot for safe capture of *E. coli*. Fuelled by hydroquinone/benzoquinone, the speed of the robot could be adjusted by changing the UV intensity (Figure 9C). The microrobot captured and transported silicon particles and *E. coli* through a Ni-Au coating, where the introduction of Ni allowed the robot to be driven by a magnetic field. *E. coli*'s safety during capture was confirmed via live/dead fluorescent dye test. Liu et al. (2020) proposed PEDOT/MnO_2@Ag microrobots for microbial killing based on the excellent bactericidal ability of silver ions. The synergistic catalytic action of MnO_2 and Ag facilitated rapid swimming in low H_2O_2 levels. Compared to a 0.2% hydrogen peroxide, *E. coli* death increased by about 14%, benefiting from the combined effect of the mass transfer due to the continuous motion of the microrobot and the dynamic release of silver ions.

3.2.5 Removal of harmful organics

In recent years, there have been reports of using micro/nanorobots for the removal of other organics present in water treatment processes, such as dyes, pesticides, psychoactive drugs, phenol and therapeutic drugs.

(i) Dyes. Textile wastewater generally contains a variety of synthetic dyes, including azo dyes, indigo dyes, triphenylmethane dyes, anthraquinone dyes and aromatic methane dyes. These dyes exhibit specific traits such as resistance to light, acid and alkali treatments, which can pose potential health risks like carcinogenicity and teratogenicity (Deng et al., 2018). In this regard, Uygun et al. (2021) designed a self-propelled microrobot powered by laccase, which effectively degraded various dyes. Their micro motors successfully removed a wide range of dyes, including acid red, reactive brown 10, alkali blue 6B, and bright blue 6, with dye concentration reduction ranging from 76% to 94%, proving the overall dye removal ability of the robot. Li et al. (2015) designed a multilayer microrocket and investigated its absorption behavior for pollutant purification. Their study proved that the H_2O_2 fuel concentration has a positive effect on the motion of the microrockets (Figure 10A), and by controlling the direction of the applied magnetic field, the motion of the microrockets in any required direction can be controlled. In addition, the motion of the multilayered microrockets enhanced the fluid dynamics and improved the removal of methyl-paraoxon and rhodamine 6G and so the water purification efficiency.

(ii) Pesticides. The use of pesticides has tripled in the last 50 years (Wang et al., 2022). Widespread conventional pesticide use has become ecotoxic to plants, animals, and microorganisms, and emerging nano-pesticides have been used without proper environmental assessment (Ale et al., 2023). In this regard, Song et al. (2023) designed a micro/nanorobot using magnetotropic bacteria (Magnetospirillum AMB-1) along with organic matter to effectively remove chlorpyrifos (a widely used organophosphate pesticide in agriculture) from various aqueous solutions. The robot can be precisely controlled under a magnetic field. When subjected to a clockwise magnetic field, the swarm exhibits circular swarming behavior. The micro-mixing during this process improved pesticide removal efficiency. The controllable magnet AMB-1 can be propelled under a magnetic field to efficiently remove pesticides dynamically. Authors suggest a potential approach for practical application by placing permanent magnets on water pipes in treatment plants to operate a swarm of machines inside pipes for toxin treatment.

(iii) Psychoactive drugs. Various psychoactive compounds (e.g., carbamazepine, pesticides, *etc.*) have accumulated in the environment, directly affecting freshwater systems, soils, and organisms. These compounds are found in plants through soil accumulation and in animals through the food chain. Exotic psychoactive substances have even been discovered in fish brains (Vejvodova et al., 2023). Pacheco et al. (2022) developed a PEI@PCL/Fe_3O_4 microrobot to remove nitroxide Sulphur ions (neurotoxic agents within pesticides) from real water samples. In experiments, the robot effectively removed the target from complex water samples such as tap water, when subjected to a magnetic field. The robot achieved about 60% removal of the nerve agent in a short time. Notably, the researchers used real water samples instead of idealized samples, enhancing the credibility of their results. To us, this work provides a reference sample for the large-scale removal of nerve agents from water bodies.

(iv) Phenol. Due to its high toxicity and limited biodegradability, phenol can act as a pollutant even at very low concentrations. It is toxic, carcinogenic, mutagenic and teratogenic. Several methods have been developed for the removal of phenolic compounds from wastewater, including common chemisorption and oxidation techniques, which however, come with high energy and maintenance costs (Saputera et al., 2021). Recently, Ma et al. (2020) designed a micromotor for efficient phenol degradation using a Fenton-like reaction on iron zeolite (Figure 10B). The micromotor featured a porous structure with enhanced catalytic properties. The process employed an asymmetric Pt layer to catalyze the decomposition of H_2O_2, enabling the self-propulsion of the robot. The self-propelled motion, along with the formation of bubbles, enhanced fluid mixing and improved the degradation efficiency. The iron zeolite micromotor can be collected and reused to prevent secondary pollution and waste.

(v)Therapeutic drugs. The most commonly found drugs in groundwater include anti-inflammatory medications such as diclofenac, paracetamol (PTM) and ibuprofen. Prolonged exposure to these compounds can have harmful effects on biota, such as gill changes in fish and kidney problems in birds. Antibiotics are another group of drugs widely present, which greatly favor the emergence of drug-resistant bacteria and have been identified as significant water pollutants (Sacco et al., 2023). Rayaroth et al. (2021) developed a Janus Fe/C_3N_4 microrobot driven by a chromate-hydrogen peroxide (Cr^{6+}/H_2O_2) redox system, with its kinematic attributes analyzed. The findings indicated that Cr^{6+} alone cannot effectively drive the Fe/C_3N_4-based microrobot, and it was the Cr^{6+}/H_2O_2 redox system generating oxygen bubbles that significantly propel the C_3N_4 robot. Here the formation of active substance ROS was confirmed by electron spin resonance experiments to effectively degrade sulfamethoxazole (SMX) (Figure 10C). Ye et al. (2022) designed a Fe-MnO_2 microrobot to remove tetracycline antibiotic contaminants. Their simple design, easy fabrication, good kinematic performance, magnetic recovery capability, and excellent decontamination effectiveness across a wide pH range served as a valuable reference for the degradation of antibiotics in water.

3.3 Water monitoring

In the previous section, this paper focused on water treatment and purification. However, complete pollution clean-up cannot be quickly achievable, and water bodies face potential secondary pollution risks. Hence, long-term monitoring of water quality is necessary. Water quality monitoring entails identifying and quantifying pollutants, serving as an important tool for decision-making and improving water quality. Furthermore, traditional techniques for monitoring water are often costly, requiring skilled professionals and complex equipment, and in many cases do not allow for direct analyses and immediate results in polluted areas. Presently, the emphasis in water monitoring technology lies in developing low-cost, convenient and user-friendly devices and sensors, aiming to make significant strides in this domain (Silva et al., 2022).

Traditional methods for real-time water monitoring involve utilizing various spectroscopic detection techniques and molecular methods (Zolkefli et al., 2020). These instruments are not only cumbersome but also inevitably introduce data errors for water bodies that cannot be preserved over extended periods in water quality classification. *In situ* measurements help to reduce costs by eliminating the need for sampling, sample preservation, transportation and laboratory analyses, which is where the advantage of micro/nanorobots lies. Due to current technological constraints, micro/nanorobot systems and platforms are not yet capable of full-scale water quality monitoring, only water quality testing. However, the use of micro/nanorobot systems for water quality analysis offers the advantages of cost-effectiveness and immediate on-site results. These systems can already serve as an alternative means of gathering data to improve water quality. In other words, while micro-nano robotic systems cannot entirely replace the water monitoring process, they can effectively substitute for several important testing stages.

In addition to the colorimetric method mentioned above, fluorescence methods offer an alternative approach to water monitoring. Fluorescence techniques address two main challenges. Firstly, integrating all target substances into a single

micro/nanorobot platform remains unfeasible, which means that there is a possibility of using multiple robots simultaneously in the water body, necessitating rapid identification using fluorescence methods. Moric et al. (2020) have developed highly stable fluorescent markers based on chemically modified 2D germanium compounds, available in a variety of different marker colors such as blue, violet and red, facilitating the tracking of specific robots within intricate swarms of micromachines. The efficacy of these markers was demonstrated through experiments, where robots carrying target substances were labelled with blue markers, while naked robots were marked with a red substance (Figure 10D). These robots exhibited strong and distinct fluorescence signals, thus offering a potential avenue for imaging. Secondly, the water column is cluttered with contaminants, demanding distinct responses for different contaminants. Wang et al. (2021) demonstrated a nanorobot equipped with a fluorescent 'switch' for detecting explosive substances in water (Figure 10E), and by combining the change of fluorescence with the work of Maric et al. (2020), differentiated responses to different substances can be achieved.

Based on the method of water monitoring using micro/nanorobots, there is a requirement to develop and design evaluation metrics and engineering systems for micro/nanorobot-assisted water monitoring systems. The existing metric employed for water quality assessment is the Water Quality Index (WQI), which encompasses various physicochemical parameters of water such as dissolved oxygen, total bacterial flora, pH, temperature, nitrogen, phosphorus, and turbidity (Shen et al., 2016). The WQI, which first appeared in 1960 (Horton's Index), enables the quantification of water quality in diverse contexts, including recreational, irrigation, and public water supply. Therefore, developing WQI indicators based on micro/nanorobots presents a significant avenue for integrating these systems into long-term monitoring of water quality. This involves identifying pertinent physicochemical parameters with superior performance for micro/nanorobots, establishing parameter ranges through extensive experimentation, and ultimately setting industry standards.

Finally, the integration of micro/nanorobots with emerging technologies can also be accelerated. The main technologies in progress encompass colorimetric methods or electrochemical sensors for assessing water bodies like drinking water, rivers and lakes. Nevertheless, there are well-established micro/nano-robotic systems, technologies and approaches that can simplify and improve existing water monitoring technologies while also reducing costs. Additionally, the integration of water monitoring links with the Internet can also accelerate data collection abilities, which is relevant for real-time, online water quality monitoring.

4 Conclusion and future perspective

This paper reviews the progress made in the past 5 years regarding micro/nanorobots in addressing water pollution. Although micro/nanorobots have exhibited several benefits, including high efficiency, precise motion control, targeted pollutant removal, and recyclability, challenges remain to be addressed within this field.

(i) Costly

Apart from employing basic chemical methods like hydrothermal methods for manufacturing micro/nanorobots, several of these approaches can be costly, potentially impacting the feasibility of mass production and industrial implementation. The incorporation of precious metals like platinum, gold, and silver in micro/nanorobots also raises material expenses. Reducing the utilization of precious metals to enhance cost-effectiveness has become a mainstream development in the industry.

(ii) Capture without degradation

According to the literature collected and analyzed, it is evident that not all micro/nanorobots can successfully attain the ultimate objective of pollutant degradation. Presently, numerous robots are limited to merely removing contaminants from the water column, which is mainly caused by insufficient available oxidation techniques and the absence of integration of functional modules within the robot.

(iii) Utility in open water bodies

The direct decontamination of open water bodies using micro/nanorobots remains unrealized. On one hand, the stability of robot movement is not yet high enough to resist the various unpredictable factors present in the natural environment. On the other hand, the mechanisms of capture and degradation, along with the excessively large movement space may not be suitable for water bodies exposed to nature. It has been suggested that the application of micro/nanorobots for water purification should not be aimed at open water bodies, but rather confined within specific containment units, which would serve as the basic modules for water purification, and then can be replicated to achieve industrialization and factorization (Urso et al., 2023).

(iv) Idealization Experiments

The current laboratory-based advancements often remain highly theoretical, with limited experimentation involving actual water samples. Meanwhile, target substances are often overly idealized, such as replacing dyes with methylene blue and rhodamine B, or employing *E. coli* as a proxy for harmful bacteria. These factors contribute to a disconnection between the existing outcomes and practical real-world applications.

(v) Secondary Pollution

Micro/nanorobots could potentially contribute to secondary water pollution. Firstly, the biochemical reactions occurring during the operation of these robots must be thoroughly assessed to prevent the generation of potentially bio-toxic substances. Additionally, the widespread deployment of micro/nanorobots may lead to their accumulation in the ecosystem, transforming them into environmental pollutants. To address this concern, the use of biodegradable materials should be prioritized in the design of micro/nanorobots.

(vi) Better evaluation indexes are needed

Currently, there is a lack of standard evaluation indexes for the experiments on water pollution treatment of micro/nanorobots. For example, the pollutant removal effect, the removal time needed, *etc.* Most of the indicators used now are based on the experience of the experimenters. Scholars, including Mihail N. Popescu, have recognized this issue, proposing qualitative analyses of small samples over quantitative analyses in resource-poor environments (Popescu and Gaspar, 2023). In the future, the establishment of complete engineering metrics is essential to facilitate the widespread adoption of micro/nanorobots for addressing water pollution challenges.

(vii) Further performance improvements

While this paper frequently employs the term "micro/nanorobots", it is important to note that the existing research may not fully encompass the capabilities of a genuine "robot". Until now, the terms "micro/nano-swimmers" or "micro/nano-motors" offer a more accurate depiction of these entities. Micro/nano-robotic systems still need further exploration of diverse propulsion methods, in-depth studies on multifunctional integration, exploration of potential collective effects, and addressing important issues such as robot signal processing, self-repair, and human-robot interaction. These efforts are imperative for comprehensively improving performance and expediting the industrialization of this field.

Author contributions

HW: Writing–original draft. YJ: Writing–original draft. JY: Data curation, Writing–original draft. BM: Conceptualization, Writing–original draft. MS: Methodology, Writing–original draft. YZ: Formal Analysis, Writing–original draft. LD: Investigation, Writing–original draft. SY: Writing–review and editing. ML: Writing–review and editing. LW: Funding acquisition, Writing–review and editing.

Funding

The author(s) declare financial support was received for the research, authorship, and/or publication of this article. This work was supported by the National key research and development program (2022YFB4701700), National Excellent Youth Science Fund Project of National Natural Science Foundation of China (Grant no. 52322502), National Outstanding Youth Science Fund Project of National Natural Science Foundation of China (Grant no. 52025054) National Nature Science Foundation of China (Grant No.52175009), Heilongjiang Providence Nature Science Foundation of China (Grant No. YQ 2022E022), Interdisciplinary Research Foundation of HIT (IR20211219) and Fundamental Research Funds for Central Universities. China Postdoctoral Science Foundation Grant (2023M733341), Postdoctoral Innovative Talents in Shandong Province (SDBX2023011), Qingdao Postdoctoral Project Funding (QDBSH20230202102).

Conflict of interest

Author JY was employed by PetroChina Changqing Oilfield Company.

The remaining authors declare that the research was conducted in the absence of any commercial or financial relationships that could be construed as a potential conflict of interest.

Publisher's note

References

Abu Bakar, N., Othman, N., Yunus, Z. M., Altowayti, W. A. H., Al-Gheethi, A., Asharuddin, S. M., et al. (2021). Nipah (Musa Acuminata Balbisiana) banana peel as a lignocellulosic precursor for activated carbon: characterization study after carbonization process with phosphoric acid impregnated activated carbon. *Biomass Convers. Biorefinery* 13, 11085–11098. doi:10.1007/s13399-021-01937-5

Aguiar, T., Baumann, L., Albuquerque, A., Teixeira, L., Gil, E. D., and Scalize, P. (2023). Application of electrocoagulation for the removal of transition metals in water. *Sustainability* 15 (2), 1492. doi:10.3390/su15021492

Ale, A., Andrade, V. S., Gutierrez, M. F., Bacchetta, C., Rossi, A. S., Santo Orihuela, P., et al. (2023). Nanotechnology-based pesticides: environmental fate and ecotoxicity. *Toxicol. Appl. Pharmacol.* 471, 116560. doi:10.1016/j.taap.2023.116560

Altowayti, W. A. H., Shahir, S., Othman, N., Eisa, T. A. E., Yafooz, W. M. S., Al-Dhaqm, A., et al. (2022). The role of conventional methods and artificial intelligence in the wastewater treatment: a comprehensive review. *Processes* 10 (9), 1832. doi:10.3390/pr10091832

Bayabil, H. K., Teshome, F. T., and Li, Y. C. C. (2022). Emerging contaminants in soil and water. *Front. Environ. Sci.* 10, 873499. doi:10.3389/fenvs.2022.873499

Bing, X. M., Zhang, X. L., Li, J., Ng, D. H. L., Yang, W. N., and Yang, J. (2020). 3D hierarchical tubular micromotors with highly selective recognition and capture for antibiotics. *J. Mater. Chem. A* 8 (5), 2809–2819. doi:10.1039/c9ta11730j

Casado-Rivera, E., Gal, Z., Angelo, A. C. D., Lind, C., DiSalvo, F. J., and Abruna, H. D. (2003). Electrocatalytic oxidation of formic acid at an ordered intermetallic PtBi surface. *Chemphyschem* 4 (2), 193–199. doi:10.1002/cphc.200390030

Chen, X., Ding, X. Y., Liu, Y. L., Li, J., Liu, W. J., Lu, X. L., et al. (2021). Highly efficient visible-light-driven Cu2O@CdSe micromotors adsorbent. *Appl. Mater. Today* 25, 101200. doi:10.1016/j.apmt.2021.101200

Debata, S., Kherani, N. A., Panda, S. K., and Singh, D. P. (2022). Light-driven microrobots: capture and transport of bacteria and microparticles in a fluid medium. *J. Mater. Chem. B* 10 (40), 8235–8243. doi:10.1039/d2tb01367c

Deng, D., Aryal, N., Ofori-Boadu, A., and Jha, M. K. (2018). Textiles wastewater treatment. *Water Environ. Res.* 90 (10), 1648–1662. doi:10.2175/106143018x15289915807353

Denniss, A. R., Gorochowski, T. E., and Hauert, S. (2022). An open platform for high-resolution light-based control of microscopic collectives. *Adv. Intell. Syst.* 4 (7), 9. doi:10.1002/aisy.202200009

Dilpazeer, F., Munir, M., Baloch, M. Y. J., Shafiq, I., Iqbal, J., Saeed, M., et al. (2023). A comprehensive review of the latest advancements in controlling arsenic contaminants in groundwater. *Water* 15 (3), 478. doi:10.3390/w15030478

Dong, S. Y., Mu, Y., and Sun, X. H. (2019). Removal of toxic metals using ferrate(VI): a review. *Water Sci. Technol.* 80 (7), 1213–1225. doi:10.2166/wst.2019.376

Eumann, M., and Schildbach, S. (2012). 125th Anniversary Review: water sources and treatment in brewing. *J. Inst. Brew.* 118 (1), 12–21. doi:10.1002/jib.18

Fan, X. J., Hu, Q. H., Zhang, X., Sun, L. N., and Yang, Z. (2023). Solitary and collective motion behaviors of TiO2 microrobots under the coupling of multiple light fields. *Micromachines* 14 (1), 89. doi:10.3390/mi14010089

Feng, P. P., Du, X. L., Guo, J., Wang, K., and Song, B. T. (2021). Light-responsive nanofibrous motor with simultaneously precise locomotion and reversible deformation. *Acs Appl. Mater. Interfaces* 13 (7), 8985–8996. doi:10.1021/acsami.0c22340

Fu, Z. Y., Liang, D., Jiang, S. L., Zhao, P. D., Han, K. X., and Xu, Z. (2019). Effects of radius and length on the nanomotor rotors in aqueous solution driven by the rotating electric field. *J. Phys. Chem. C* 123 (50), 30649–30656. doi:10.1021/acs.jpcc.9b07345

Fuller, R., Landrigan, P. J., Balakrishnan, K., Bathan, G., Bose-O'Reilly, S., Brauer, M., et al. (2022). Pollution and health: a progress update. *Lancet Planet. Health* 6 (6), E535–E547. doi:10.1016/s2542-5196(22)00090-0

Gkika, D. A., Mitropoulos, A. C., Lambropoulou, D. A., Kalavrouziotis, I. K., and Kyzas, G. Z. (2022). Cosmetic wastewater treatment technologies: a review. *Environ. Sci. Pollut. Res.* 29 (50), 75223–75247. doi:10.1007/s11356-022-23045-1

Glaze, W. H., Kang, J. W., and Chapin, D. H. (1987). THE CHEMISTRY OF WATER-TREATMENT PROCESSES INVOLVING OZONE, HYDROGEN-PEROXIDE AND ULTRAVIOLET-RADIATION. *Ozone-Science Eng.* 9 (4), 335–352. doi:10.1080/01919518708552148

Gong, D., Li, B., Celi, N., Cai, J., and Zhang, D. Y. (2021). Efficient removal of Pb(II) from aqueous systems using spirulina-based biohybrid magnetic helical microrobots. *Acs Appl. Mater. Interfaces* 13 (44), 53131–53142. doi:10.1021/acsami.1c18435

Gude, V. G. (2017). Desalination and water reuse to address global water scarcity. *Rev. Environ. Sci. Bio-Technology* 16 (4), 591–609. doi:10.1007/s11157-017-9449-7

Hou, Y. Z., Wang, H. P., Fu, R. X., Wang, X., Yu, J. F., Zhang, S. L., et al. (2023a). A review on microrobots driven by optical and magnetic fields. *Lab a Chip* 23 (5), 848–868. doi:10.1039/d2lc00573e

Hou, Y. Z., Wang, H. P., Zhong, S. H., Qiu, Y. K., Shi, Q., Sun, T., et al. (2023b). Design and control of a surface-dimple-optimized helical microdrill for motions in high-viscosity fluids. *Ieee-Asme Trans. Mechatronics* 28 (1), 429–439. doi:10.1109/tmech.2022.3201012

Ji, F. T., Li, T. L., Yu, S. M., Wu, Z. G., and Zhang, L. (2021). Propulsion gait analysis and fluidic trapping of swinging flexible nanomotors. *ACS Nano* 15 (3), 5118–5128. doi:10.1021/acsnano.0c10269

Ji, F. T., Wu, Y. L., Pumera, M., and Zhang, L. (2023). Collective behaviors of active matter learning from natural taxes across scales. *Adv. Mater.* 35 (8), 2203959. doi:10.1002/adma.202203959

Ji, Y. X., Lin, X. K., Zhang, H. Y., Wu, Y. J., Li, J. B., and He, Q. (2019). Thermoresponsive polymer brush modulation on the direction of motion of phoretically driven Janus micromotors. *Angew. Chemie-International Ed.* 58 (13), 4184–4188. doi:10.1002/anie.201812860

Kim, M. S., Lee, H. T., and Ahn, S. H. (2019). Laser controlled 65 micrometer long microrobot made of Ni-Ti shape memory alloy. *Adv. Mater. Technol.* 4 (12), 583. doi:10.1002/admt.201900583

Kochergin, Y. S., Villa, K., Novotny, F., Plutnar, J., Bojdys, M. J., and Pumera, M. (2020). Multifunctional visible-light powered micromotors based on semiconducting sulfur- and nitrogen-containing donor-acceptor polymer. *Adv. Funct. Mater.* 30 (38), 2701. doi:10.1002/adfm.202002701

Kong, L., Ambrosi, A., Nasir, M. Z. M., Guan, J. G., and Pumera, M. (2019). Self-propelled 3D-printed "aircraft carrier" of light-powered smart micromachines for large-volume nitroaromatic explosives removal. *Adv. Funct. Mater.* 29 (39), 3872. doi:10.1002/adfm.201903872

Kumar, S., Nehra, M., Mehta, J., Dilbaghi, N., Marrazza, G., and Kaushik, A. (2019). Point-of-Care strategies for detection of waterborne pathogens. *Sensors* 19 (20), 4476. doi:10.3390/s19204476

Lai, J. L., Meng, Q. F., Tian, M. Y., Zhuang, X. Y., Pan, P., Du, L. A., et al. (2022). A decoy microrobot that removes SARS-CoV-2 and its variants in wastewater. *Cell. Rep. Phys. Sci.* 3 (10), 101061. doi:10.1016/j.xcrp.2022.101061

Leslie, H. A., van Velzen, M. J. M., Brandsma, S. H., Vethaak, A. D., Garcia-Vallejo, J. J., and Lamoree, M. H. (2022). Discovery and quantification of plastic particle pollution in human blood. *Environ. Int.* 163, 107199. doi:10.1016/j.envint.2022.107199

Li, D. M., Wang, Z. Y., Yang, Y. X., Liu, H., Fang, S., and Liu, S. L. (2023a). Research status and development trend of wastewater treatment technology and its low carbonization. *Appl. Sciences-Basel* 13 (3), 1400. doi:10.3390/app13031400

Li, J. J., He, X. L., Jiang, H. D., Xing, Y., Fu, B., and Hu, C. Z. (2022). Enhanced and robust directional propulsion of light-activated Janus micromotors by magnetic spinning and the magnus effect. *Acs Appl. Mater. Interfaces* 14 (31), 36027–36037. doi:10.1021/acsami.2c08464

Li, T. L., Li, J. X., Morozov, K. I., Wu, Z. G., Xu, T. L., Rozen, I., et al. (2017). Highly efficient freestyle magnetic nanoswimmer. *Nano Lett.* 17 (8), 5092–5098. doi:10.1021/acs.nanolett.7b02383

Li, T. L., Li, L. Q., Song, W. P., Wang, L., Shao, G. B., and Zhang, G. Y. (2015). Self-propelled multilayered microrockets for pollutants purification. *Ecs J. Solid State Sci. Technol.* 4 (10), S3016–S3019. doi:10.1149/2.0041510jss

Li, T. L., Yu, S. M., Sun, B., Li, Y. L., Wang, X. L., Pan, Y. L., et al. (2023b). Bioinspired claw-engaged and biolubricated swimming microrobots creating active retention in blood vessels. *Sci. Adv.* 9 (18), eadg4501. doi:10.1126/sciadv.adg4501

Li, T. L., Zhang, A. N., Shao, G. B., Wei, M. S., Guo, B., Zhang, G. Y., et al. (2018). Janus microdimer surface walkers propelled by oscillating magnetic fields. *Adv. Funct. Mater.* 28 (25). doi:10.1002/adfm.201706066

Li, T. T., Lyu, Y. S., Li, J., Wang, C. Y., Xing, N. N., Yang, J., et al. (2021). Micromotor-assisted fluorescence detection of Hg^{2+} with bio-inspired AO–Mn_2O_3/γ-AlO(OH). *Environ. Science-Nano* 8 (12), 3833–3845. doi:10.1039/d1en00796c

Li, X. J., Zhao, Y. M., Luan, Y., Wang, D., and Du, X. (2023c). Near-infrared light-propelled Janus metal-phenolic@Au micromotors for enhanced removal of organic pollutants. *Mater. Lett.* 346, 134538. doi:10.1016/j.matlet.2023.134538

Liu, J., Wu, X. Y., Huang, C. Y., Manamanchaiyaporn, L., Shang, W. F., Yan, X. H., et al. (2021). 3-D autonomous manipulation system of helical microswimmers with online compensation update. *Ieee Trans. Automation Sci. Eng.* 18 (3), 1380–1391. doi:10.1109/tase.2020.3006131

Liu, W. J., Ge, H. B., Chen, X., Lu, X. L., Gu, Z. W., Li, J. X., et al. (2019). Fish-scale-like intercalated metal oxide-based micromotors as efficient water remediation agents. *Acs Appl. Mater. Interfaces* 11 (17), 16164–16173. doi:10.1021/acsami.9b01095

Liu, W. J., Ge, H. B., Ding, X. Y., Lu, X. L., Zhang, Y. N., and Gu, Z. W. (2020). Cubic nano-silver-decorated manganese dioxide micromotors: enhanced propulsion and antibacterial performance. *Nanoscale* 12 (38), 19655–19664. doi:10.1039/d0nr06281b

Liu, Y., Wang, H., Cui, Y., and Chen, N. (2023). Removal of copper ions from wastewater: a review. *Int. J. Environ. Res. public health* 20 (5), 3885. doi:10.3390/ijerph20053885

Lou, X., Yu, N., Chen, K., Zhou, X., Podgornik, R., and Yang, M. C. (2021). A composite micromotor driven by self-thermophoresis and Brownian rectification. *Chin. Phys. B* 30 (11), 114702. doi:10.1088/1674-1056/ac2727

Lu, X. L., Shen, H., Wei, Y., Ge, H. B., Wang, J., Peng, H. M., et al. (2020). Ultrafast growth and locomotion of dandelion-like microswarms with tubular micromotors. *Small* 16 (38), e2003678. doi:10.1002/smll.202003678

Lu, X. L., Zhao, K. D., Liu, W. J., Yang, D. X., Shen, H., Peng, H. M., et al. (2019). A human microrobot interface based on acoustic manipulation. *Acs Nano* 13 (10), 11443–11452. doi:10.1021/acsnano.9b04930

Lyu, X. L., Chen, J. Y., Liu, J. Y., Peng, Y. X., Duan, S. F., Ma, X., et al. (2022). Reversing a platinum micromotor by introducing platinum oxide. *Angew. Chemie-International Ed.* 61 (24), e202201018. doi:10.1002/anie.202201018

Ma, H. L., Shen, M. H., Tong, Y., and Wang, X. (2023). Radioactive wastewater treatment technologies: a review. *Molecules* 28 (4), 1935. doi:10.3390/molecules28041935

Ma, W., and Wang, H. (2019). Magnetically driven motile superhydrophobic sponges for efficient oil removal. *Appl. Mater. Today* 15, 263–266. doi:10.1016/j.apmt.2019.02.004

Ma, W., Wang, K., Pan, S. H., and Wang, H. (2020). Iron-exchanged zeolite micromotors for enhanced degradation of organic pollutants. *Langmuir* 36 (25), 6924–6929. doi:10.1021/acs.langmuir.9b02137

Maric, T., Nasir, M. Z. M., Webster, R. D., and Pumera, M. (2020). Tailoring metal/TiO2 interface to influence motion of light-activated Janus micromotors. *Adv. Funct. Mater.* 30 (9), 8614. doi:10.1002/adfm.201908614

Mayorga-Burrezo, P., Mayorga-Martinez, C. C., and Pumera, M. (2023). Photocatalysis dramatically influences motion of magnetic microrobots: application to removal of microplastics and dyes. *J. Colloid Interface Sci.* 643, 447–454. doi:10.1016/j.jcis.2023.04.019

Moghazy, R. M., Bakr, A. M., El-Wakeel, S. T., and El Hotaby, W. (2023). Porous cellulose microspheres loaded with dry Nile water algae for removal of MB dye and copper ions from aqueous media. *Polym. Eng. Sci.* 63 (7), 2002–2014. doi:10.1002/pen.26341

Moric, T., Beladi-Mousavi, S. M., Khezri, B., Sturala, J., Nasir, M. Z. M., Webster, R. D., et al. (2020). Functional 2D germanene fluorescent coating of microrobots for micromachines multiplexing. *Small* 16 (27), e1902365. doi:10.1002/smll.201902365

Nicomel, N. R., Leus, K., Folens, K., Van der Voort, P., and Du Laing, G. (2016). Technologies for arsenic removal from water: current status and future perspectives. *Int. J. Environ. Res. Public Health* 13 (1), 62. doi:10.3390/ijerph13010062

Orozco, J., Garcia-Gradilla, V., D'Agostino, M., Gao, W., Cortes, A., and Wang, J. (2013). Artificial enzyme-powered microfish for water-quality testing. *Acs Nano* 7 (1), 818–824. doi:10.1021/nn305372n

Othman, N. H., Alias, N. H., Fuzil, N. S., Marpani, F., Shahruddin, M. Z., Chew, C. M., et al. (2022). A review on the use of membrane technology systems in developing countries. *Membranes* 12 (1), 30. doi:10.3390/membranes12010030

Pacheco, M., Mayorga-Martinez, C. C., Escarpa, A., and Pumera, M. (2022). Micellar polymer magnetic microrobots as efficient nerve agent microcleaners. *Acs Appl. Mater. Interfaces* 14 (22), 26128–26134. doi:10.1021/acsami.2c02926

Palacios-Corella, M., Rojas, D., and Pumera, M. (2023). Photocatalytic Pt/Ag3VO4 micromotors with inherent sensing capabilities for corroding environments. *J. Colloid Interface Sci.* 631, 125–134. doi:10.1016/j.jcis.2022.10.169

Park, C. W., Kim, T., Yang, H. M., Lee, Y., and Kim, H. J. (2021). Active and selective removal of Cs from contaminated water by self-propelled magnetic illite microspheres. *J. Hazard. Mater.* 416, 126226. doi:10.1016/j.jhazmat.2021.126226

Popescu, M. N., and Gaspar, S. (2023). Analyte sensing with catalytic micromotors. *Biosensors-Basel* 13 (1), 45. doi:10.3390/bios13010045

Qi, P. F., Luo, R., Pichler, T., Zeng, J. Q., Wang, Y., Fan, Y. H., et al. (2019). Development of a magnetic core-shell Fe3O4@TA@UiO-66 microsphere for removal of arsenic(III) and antimony(III) from aqueous solution. *J. Hazard. Mater.* 378, 120721. doi:10.1016/j.jhazmat.2019.05.114

Raha, A., Rao, I. S., Srivastava, V. K., and Tewari, P. K. (2008). R&D areas for next-generation desalination and water purification technologies. *Int. J. Nucl. Desalination* 3 (1), 33–55. doi:10.1504/ijnd.2008.018928

Rahman, T. U., Roy, H., Islam, M. R., Tahmid, M., Fariha, A., Mazumder, A., et al. (2023). The advancement in membrane bioreactor (MBR) technology toward sustainable industrial wastewater management. *Membranes* 13 (2), 181. doi:10.3390/membranes13020181

Rayaroth, M. P., Oh, D., Lee, C. S., Kumari, N., Lee, I. S., and Chang, Y. S. (2021). Carbon-nitride-based micromotor driven by chromate-hydrogen peroxide redox system: application for removal of sulfamethaxazole. *J. Colloid Interface Sci.* 597, 94–103. doi:10.1016/j.jcis.2021.03.164

Ren, Y. Q., Li, H., Liu, J. X., Zhou, M. D., and Pan, J. M. (2022). Crescent-shaped micromotor sorbents with sulfonic acid functionalized convex surface: the synthesis by A Janus emulsion strategy and adsorption for Li+. *J. Hazard. Mater.* 422, 126870. doi:10.1016/j.jhazmat.2021.126870

Ribeiro, F., Pavlaki, M. D., Loureiro, S., Sarmento, R. A., Soares, A., and Tourinho, P. S. (2023). Systematic review of nano- and microplastics' (NMP) influence on the bioaccumulation of environmental contaminants: Part II-freshwater organisms. *Toxics* 11 (6), 474. doi:10.3390/toxics11060474

Rojas, D., Jurado-Sanchez, B., and Escarpa, A. (2016). Shoot and sense" Janus micromotors-based strategy for the simultaneous degradation and detection of persistent organic pollutants in food and biological samples. *Anal. Chem.* 88 (7), 4153–4160. doi:10.1021/acs.analchem.6b00574

Sacco, N. A., Marchesini, F. A., Gamba, I., and Garcia, G. (2023). Photoelectrochemical degradation of contaminants of emerging concern with special attention on the removal of acetaminophen in water-based solutions. *Catalysts* 13 (3), 524. doi:10.3390/catal13030524

Sambaza, S. S., and Naicker, N. (2023). Contribution of wastewater to antimicrobial resistance: a review article. *J. Glob. Antimicrob. Resist.* 34, 23–29. doi:10.1016/j.jgar.2023.05.010

Saputera, W. H., Putrie, A. S., Esmailpour, A. A., Sasongko, D., Suendo, V., and Mukti, R. R. (2021). Technology advances in phenol removals: current progress and future perspectives. *Catalysts* 11 (8), 998. doi:10.3390/catal11080998

Shang, Y. X., Cai, L. J., Liu, R., Zhang, D. G., Zhao, Y. J., and Sun, L. Y. (2022). Self-propelled structural color cylindrical micromotors for heavy metal ions adsorption and screening. *Small* 18 (46), e2204479. doi:10.1002/smll.202204479

Shemer, H., Wald, S., and Semiat, R. (2023). Challenges and solutions for global water scarcity. *Membranes* 13 (6), 612. doi:10.3390/membranes13060612

Shen, C., Jiang, Z. Y., Li, L. F., Gilchrist, J. F., and Ou-Yang, H. D. (2020). Frequency response of induced-charge electrophoretic metallic Janus particles. *Micromachines* 11 (3), 334. doi:10.3390/mi11030334

Shen, Z. Y., Liu, J., Aini, G., and Gong, Y. W. (2016). A comparative study of the grain-size distribution of surface dust and stormwater runoff quality on typical urban roads and roofs in Beijing, China. *Environ. Sci. Pollut. Res.* 23 (3), 2693–2704. doi:10.1007/s11356-015-5512-5

Shimizu, N., Oda, H., Morimoto, Y., and Takeuchi, S. (2021). "BIOHYBRID MICRO PINWHEEL POWERED BY TRAPPED MICROALGAE," in 34th IEEE International Conference on Micro Electro Mechanical Systems (MEMS), Gainesville, FL, USA, 25-29 January 2021 (IEEE), 533–535.

Silva, G. M. E., Campos, D. F., Brasil, J. A. T., Tremblay, M., Mendiondo, E. M., and Ghiglieno, F. (2022). Advances in technological research for online and *in situ* water quality monitoring-A review. *Sustainability* 14 (9), 5059. doi:10.3390/su14095059

Singh, A. K., Bhuyan, T., Maity, S., Mandal, T. K., and Bandyopadhyay, D. (2020). Magnetically actuated carbon soot nanoparticle-based catalytic CARBOts coated with Ni/Pt nanofilms for water detoxification and oil-spill recovery. *Acs Appl. Nano Mater.* 3 (4), 3459–3470. doi:10.1021/acsanm.0c00199

Siri, Y., Precha, N., Sirikanchana, K., Haramoto, E., and Makkaew, P. (2023). Antimicrobial resistance in southeast Asian water environments: a systematic review of current evidence and future research directions. *Sci. total Environ.* 896, 165229. doi:10.1016/j.scitotenv.2023.165229

Song, S. J., Mayorga-Martinez, C. C., Vyskocil, J., Castoralova, M., Ruml, T., and Pumera, M. (2023). Precisely navigated biobot swarms of bacteria magnetospirillum magneticum for water decontamination. *Acs Appl. Mater. Interfaces* 15, 7023–7029. doi:10.1021/acsami.2c16592

Soto, F., Lopez-Ramirez, M. A., Jeerapan, I., de Avila, B. E. F., Mishra, R. K., Lu, X. L., et al. (2019). Rotibot: use of rotifers as self-propelling biohybrid microcleaners. *Adv. Funct. Mater.* 29 (22). doi:10.1002/adfm.201900658

Sun, B. A., Sun, M. M., Zhang, Z. F., Jiang, Y. H., Hao, B., Wang, X., et al. (2023). Magnetic hydrogel micromachines with active release of antibacterial agent for biofilm eradication. *Adv. Intell. Syst.* 2300092 doi:10.1002/aisy.202300092

Sun, M. M., Chen, W. N., Fan, X. J., Tian, C. Y., Sun, L. N., and Xie, H. (2020). Cooperative recyclable magnetic microsubmarines for oil and microplastics removal from water. *Appl. Mater. Today* 20, 100682. doi:10.1016/j.apmt.2020.100682

Sun, Y. Y., Liu, Y., Song, B., Zhang, H., Duan, R. M., Zhang, D. F., et al. (2019). A light-driven micromotor with complex motion behaviors for controlled release. *Adv. Mater. Interfaces* 6 (4), 1965. doi:10.1002/admi.201801965

Ullattil, S. G., and Pumera, M. (2023). Light-powered self-adaptive mesostructured microrobots for simultaneous microplastics trapping and fragmentation via *in situ* surface morphing. *Small* 19, e2301467. doi:10.1002/smll.202301467

Urso, M., Ussia, M., and Pumera, M. (2023). Smart micro- and nanorobots for water purification. *Nat. Rev. Bioeng.* 1 (4), 236–251. doi:10.1038/s44222-023-00025-9

Uygun, M., de la Asuncion-Nadal, V., Evli, S., Uygun, D. A., Jurado-Sanchez, B., and Escarpa, A. (2021). Dye removal by laccase-functionalized micromotors. *Appl. Mater. Today* 23, 101045. doi:10.1016/j.apmt.2021.101045

Vejvodova, K., Kodesova, R., Horky, P., Boruvka, L., and Tlustos, P. (2023). Psychoactive substances in soils, plants, freshwater and fish: a mini review. *Soil Water Res.* 18, 139–157. doi:10.17221/58/2023-swr

Villa, K., Novotny, F., Zelenka, J., Browne, M. P., Ruml, T., and Pumera, M. (2019). Visible-light-driven single-component BiVO4 micromotors with the autonomous ability for capturing microorganisms. *Acs Nano* 13 (7), 8135–8145. doi:10.1021/acsnano.9b03184

Wang, D., Zhao, G., Chen, C. H., Zhang, H., Duan, R. M., Zhang, D. F., et al. (2019). One-step fabrication of dual optically/magnetically modulated walnut-like micromotor. *Langmuir* 35 (7), 2801–2807. doi:10.1021/acs.langmuir.8b02904

Wang, H. C., Yu, S. M., Liao, J. J., Qing, X. D., Sun, D. X., Ji, F. T., et al. (2022a). A robot platform for highly efficient pollutant purification. *Front. Bioeng. Biotechnol.* 10, 903219. doi:10.3389/fbioe.2022.903219

Wang, K., Ma, E. H., Hu, Z. Q., and Wang, H. (2021a). Rapid synthesis of self-propelled tubular micromotors for "ON-OFF" fluorescent detection of explosives. *Chem. Commun.* 57 (81), 10528–10531. doi:10.1039/d1cc03899k

Wang, L., Fan, G. L., Xu, X. F., Chen, D. M., Wang, L., Shi, W., et al. (2017). Detection of polychlorinated benzenes (persistent organic pollutants) by a luminescent sensor based on a lanthanide metal-organic framework. *J. Mater. Chem. A* 5 (11), 5541–5549. doi:10.1039/c7ta00256d

Wang, Q. L., Dong, R. F., Yang, Q. X., Wang, J. J., Xu, S. Y., and Cai, Y. P. (2020a). Highly efficient visible-light-driven oxygen-vacancy-based Cu2+1O micromotors with biocompatible fuels. *Nanoscale Horizons* 5 (2), 325–330. doi:10.1039/c9nh00592g

Wang, Q. Q., Chan, K. F., Schweizer, K., Du, X. Z., Jin, D. D., Yu, S. C. H., et al. (2021b). Ultrasound Doppler-guided real-time navigation of a magnetic microswarm for active endovascular delivery. *Sci. Adv.* 7 (9), eabe5914. doi:10.1126/sciadv.abe5914

Wang, Q. Q., Du, X. Z., Jin, D. D., and Zhang, L. (2022b). Real-time ultrasound Doppler tracking and autonomous navigation of a miniature helical robot for accelerating thrombolysis in dynamic blood flow. *Acs Nano* 16 (1), 604–616. doi:10.1021/acsnano.1c07830

Wang, Q. Q., Xiang, N., Lang, J., Wang, B., Jin, D. D., and Zhang, L. (2023a). Reconfigurable liquid-bodied miniature machines: magnetic control and microrobotic applications. *Adv. Intell. Syst.* 2300108 doi:10.1002/aisy.202300108

Wang, Q. Q., Yang, L. D., Yu, J. F., Chiu, P. W. Y., Zheng, Y. P., and Zhang, L. (2020b). Real-time magnetic navigation of a rotating colloidal microswarm under ultrasound guidance. *Ieee Trans. Biomed. Eng.* 67 (12), 3403–3412. doi:10.1109/tbme.2020.2987045

Wang, Q. Q., Zhang, J. C., Yu, J. F., Lang, J., Lyu, Z., Chen, Y. F., et al. (2023b). Untethered small-scale machines for microrobotic manipulation: from individual and multiple to collective machines. *Acs Nano* 17 (14), 13081–13109. doi:10.1021/acsnano.3c05328

Wang, Q. Q., and Zhang, L. (2021). External power-driven microrobotic swarm: from fundamental understanding to imaging-guided delivery. *Acs Nano* 15 (1), 149–174. doi:10.1021/acsnano.0c07753

Wang, Y., Tian, J., Wang, Z. H., Li, C. N., and Li, X. G. (2022c). Crop-safe pyraclostrobin-loaded multiwalled carbon nanotube delivery systems: higher fungicidal activity and lower acute toxicity. *Acs Agric. Sci. Technol.* 2 (3), 534–545. doi:10.1021/acsagscitech.1c00293

Wu, D., Hu, Y. L., Cheng, H., and Ye, X. Q. (2023). Detection techniques for lead ions in water: a review. *Molecules* 28 (8), 3601. doi:10.3390/molecules28083601

Xiao, Z. Y., Chen, J. Y., Duan, S. F., Lv, X. L., Wang, J. Z., Ma, X., et al. (2020). Bimetallic coatings synergistically enhance the speeds of photocatalytic TiO2 micromotors. *Chem. Commun.* 56 (34), 4728–4731. doi:10.1039/d0cc00212g

Xie, S. X., Jiao, N. D., Xue, Y. X., Dai, L. G., Dai, L. G., and Chen, F. (2021). "Transporting and rotating of microstructures actuated by algal microrobots," in Annual IEEE International Conference on Manipulation, Manufacturing and Measurement on the Nanoscale (3M-NANO), Xi'an, China, 02-06 August 2021 (IEEE), 86–89.

Xing, Y., Zhou, M. Y., Xu, T. L., Tang, S. S., Fu, Y., Du, X., et al. (2020). Core@Satellite Janus nanomotors with pH-responsive multi-phoretic propulsion. *Angew. Chemie-International Ed.* 59 (34), 14368–14372. doi:10.1002/anie.202006421

Xiong, X. Y., Huang, X., Liu, Y., Feng, A., Wang, Z. M., Cheng, X., et al. (2022). Azobenzene-bearing polymer engine powered organic nanomotors for light-driven cargo transport. *Chem. Eng. J.* 445, 136576. doi:10.1016/j.cej.2022.136576

Xu, S., Liu, J., Yang, C. G., Wu, X. Y., and Xu, T. T. (2022a). A learning-based stable servo control strategy using broad learning system applied for microrobotic control. *Ieee Trans. Cybern.* 52 (12), 13727–13737. doi:10.1109/tcyb.2021.3121080

Xu, T. T., Huang, C. Y., Lai, Z. Y., and Wu, X. Y. (2022b). Independent control strategy of multiple magnetic flexible millirobots for position control and path following. *Ieee Trans. Robotics* 38 (5), 2875–2887. doi:10.1109/tro.2022.3157147

Xu, Z. Y., Chen, M. J., Lee, H., Feng, S. P., Park, J. Y., Lee, S., et al. (2019). X-ray-Powered micromotors. *Acs Appl. Mater. Interfaces* 11 (17), 15727–15732. doi:10.1021/acsami.9b00174

Yang, K. W., Wu, F., Yan, X. C., and Pan, J. M. (2023a). Self-locomotive composites based on asymmetric micromotors and covalently attached nanosorbents for selective uranium recovery. *Sep. Purif. Technol.* 308, 122844. doi:10.1016/j.seppur.2022.122844

Yang, Y. Y., Shi, L., Lin, J. K., Zhang, P. P., Hu, K. S., Meng, S., et al. (2023b). Confined tri-functional FeO*x*@MnO_2@SiO_2 flask micromotors for long-lasting motion and catalytic reactions. *Small* 19 (23), e2207666. doi:10.1002/smll.202207666

Ye, H., Wang, S. N., Wang, Y., Guo, P. T., Wang, L. Y., Zhao, C. K., et al. (2022). Atomic H* mediated fast decontamination of antibiotics by bubble-propelled magnetic iron-manganese oxides core-shell micromotors. *Appl. Catal. B-Environmental* 314, 121484. doi:10.1016/j.apcatb.2022.121484

Ye, H., Wang, Y., Liu, X. J., Xu, D. D., Yuan, H., Sun, H. Q., et al. (2021). Magnetically steerable iron oxides-manganese dioxide core-shell micromotors for organic and microplastic removals. *J. Colloid Interface Sci.* 588, 510–521. doi:10.1016/j.jcis.2020.12.097

Ying, Y. L., Plutnar, J., and Pumera, M. (2021). Six-Degree-of-Freedom steerable visible-light-driven microsubmarines using water as a fuel: application for explosives decontamination. *Small* 17 (23), e2100294. doi:10.1002/smll.202100294

Ying, Y. L., Pourrahimi, A. M., Sofer, Z., Matejkova, S., and Pumera, M. (2019). Radioactive uranium preconcentration via self-propelled autonomous microrobots based on metal-organic frameworks. *Acs Nano* 13 (10), 11477–11487. doi:10.1021/acsnano.9b04960

Ying, Y. L., and Pumera, M. (2019). Micro/nanomotors for water purification. *Chemistry-a Eur. J.* 25 (1), 106–121. doi:10.1002/chem.201804189

Yoshida, K., Yamawaki, S., and Onoe, H. (2021). "ETHANOL DRIVEN MICRO-ROBOTS WITH PHOTONIC COLLOIDAL CRYSTAL HYDROGEL FOR EXPLORING AND SENSING STIMULI," in 34th IEEE International Conference on Micro Electro Mechanical Systems (MEMS), Gainesville, FL, USA, 25-29 January 2021 (IEEE), 47–50.

Yu, S., Li, T., Ji, F., Zhao, S., Liu, K., Zhang, Z., et al. (2022). Trimer-like microrobots with multimodal locomotion and reconfigurable capabilities. *Mater. Today Adv.* 14, 100231. doi:10.1016/j.mtadv.2022.100231

Yusuf, A., Sodiq, A., Giwa, A., Eke, J., Pikuda, O., De Luca, G., et al. (2020). A review of emerging trends in membrane science and technology for sustainable water treatment. *J. Clean. Prod.* 266, 121867. doi:10.1016/j.jclepro.2020.121867

Zhang, F. Y., Li, Z. X., Yin, L., Zhang, Q. Z., Askarinam, N., Mundaca-Uribe, R., et al. (2021a). ACE2 receptor-modified algae-based microrobot for removal of SARS-CoV-2 in wastewater. *J. Am. Chem. Soc.* 143 (31), 12194–12201. doi:10.1021/jacs.1c04933

Zhang, X. L., Xie, W. Q., Wang, H. G., and Zhang, Z. X. (2021b). Magnetic matchstick micromotors with switchable motion modes. *Chem. Commun.* 57 (31), 3797–3800. doi:10.1039/d1cc00773d

Zhao, G. J., Sanchez, S., Schmidt, O. G., and Pumera, M. (2013). Poisoning of bubble propelled catalytic micromotors: the chemical environment matters. *Nanoscale* 5 (7), 2909–2914. doi:10.1039/c3nr34213a

Zhao, H., Zeng, H. R., Chen, T., Huang, X. Y., Cai, Y. P., and Dong, R. F. (2023). Catalytic micromotors as self-stirring microreactors for efficient dual-mode colorimetric detection. *J. Colloid Interface Sci.* 643, 196–204. doi:10.1016/j.jcis.2023.03.144

Zhao, Z. W., Si, T. Y., Kozelskaya, A. I., Akimchenko, I. O., Tverdokhlebov, S. I., Rutkowski, S., et al. (2022). Biodegradable magnesium fuel-based Janus micromotors with surfactant induced motion direction reversal. *Colloids Surfaces B-Biointerfaces* 218, 112780. doi:10.1016/j.colsurfb.2022.112780

Zheng, Z. Q., Wang, H. P., Demir, S. O., Huang, Q., Fukuda, T., and Sitti, M. (2022). Programmable aniso-electrodeposited modular hydrogel microrobots. *Sci. Adv.* 8 (50), eade6135. doi:10.1126/sciadv.ade6135

Zheng, Z. Q., Wang, H. P., Dong, L. X., Shi, Q., Li, J. N., Sun, T., et al. (2021). Ionic shape-morphing microrobotic end-effectors for environmentally adaptive targeting, releasing, and sampling. *Nat. Commun.* 12 (1), 411. doi:10.1038/s41467-020-20697-w

Zhou, H. J., Mayorga-Martinez, C. C., Pane, S., Zhang, L., and Pumera, M. (2021b). Magnetically driven micro and nanorobots. *Chem. Rev.* 121 (8), 4999–5041. doi:10.1021/acs.chemrev.0c01234

Zhou, H. J., Mayorga-Martinez, C. C., and Pumera, M. (2021a). Microplastic removal and degradation by mussel-inspired adhesive magnetic/enzymatic microrobots. *Small Methods* 5 (9), e2100230. doi:10.1002/smtd.202100230

Zolkefli, N., Sharuddin, S. S., Yusoff, M. Z. M., Hassan, M. A., Maeda, T., and Ramli, N. (2020). A review of current and emerging approaches for water pollution monitoring. *Water* 12 (12), 3417. doi:10.3390/w12123417

frontiers | Frontiers in Bioengineering and Biotechnology

TYPE Original Research
PUBLISHED 05 December 2023
DOI 10.3389/fbioe.2023.1296832

OPEN ACCESS

EDITED BY
Fengtong Ji,
University of Cambridge, United Kingdom

REVIEWED BY
Ke Yuan,
Beijing Genomics Institute (BGI), China
Ben Wang,
Shenzhen University, China

*CORRESPONDENCE
Hae-Jin Hu,
haejinhu@goendomics.com
Jung-Hwan Park,
pa90201@gachon.ac.kr

RECEIVED 19 September 2023
ACCEPTED 17 November 2023
PUBLISHED 05 December 2023

CITATION
Kim J, Moon J-W, Kim GR, Kim W, Hu H-J, Jo W-J, Baek S-K, Sung G-H, Park JH and Park J-H (2023), Safety tests and clinical research on buccal and nasal microneedle swabs for genomic analysis. *Front. Bioeng. Biotechnol.* 11:1296832. doi: 10.3389/fbioe.2023.1296832

Safety tests and clinical research on buccal and nasal microneedle swabs for genomic analysis

JeongHyeon Kim[1], Jae-Woo Moon[2], Gyeong Ryeong Kim[2], Wonsub Kim[2], Hae-Jin Hu[2]*, Won-Jun Jo[3], Seung-Ki Baek[3], Gil-Hwan Sung[3], Jung Ho Park[4] and Jung-Hwan Park[1]*

[1]Department of Bionano Technology and Gachon BioNano Research Institute, Gachon University, Seongnam, Republic of Korea, [2]Endomics Inc, Seongnam, Republic of Korea, [3]QuadMedicine R&D Centre, QuadMedicine Co. Ltd., Seongnam, Republic of Korea, [4]Department of Medicine, Kangbuk Samsung Hospital, Sungkyunkwan University School of Medicine, Seoul, Republic of Korea

Conventional swabs have been used as a non-invasive method to obtain samples for DNA analysis from the buccal and the nasal mucosa. However, swabs may not always collect pure enough genetic material. In this study, buccal and nasal microneedle swab is developed to improve the accuracy and reliability of genomic analysis. A cytotoxicity test, a skin sensitivity test, and a skin irritation test are conducted with microneedle swabs. Polymer microneedle swabs meet the safety requirements for clinical research and commercial use. When buccal and nasal microneedle swabs are used, the amount of genetic material obtained is greater than that from commercially available swabs, and DNA purity is also high. The comparatively short microneedle swab (250 μm long) cause almost no pain to all 25 participants. All participants also report that the microneedle swabs are very easy to use. When genotypes are compared at five SNP loci from blood of a participant and from that person's buccal or nasal microneedle swab, the buccal and nasal microneedle swabs show 100% concordance for all five SNP genotypes. Microneedle swabs can be effectively used for genomic analysis and prevention through genomic analysis, so the utilization of microneedle swabs is expected to be high.

KEYWORDS

buccal microneedle swab, nasal microneedle swab, genomic analysis, safety test, clinical research

1 Introduction

Genetic analysis is a powerful tool to identify gene function and control, disease classification, biomarker identification and drug discovery (International, 2004; Chen et al., 2009). DNA sequence variation can occur within species, often in the form of single nucleotide polymorphisms (SNPs). SNPs are single base-pair changes that occur at specific positions along the DNA strand, representing genetic variations within a population. They can influence various traits, including susceptibility to diseases, physical attributes, and drug responses (Manolio et al., 2008; Chen et al., 2009).

There are two common methods of collecting DNA for genetic analysis: using a syringe to draw blood, and using a swab to retrieve samples of saliva or mucosal tissue (Walker et al., 1999; Lee and Ladd, 2001). Blood collection is commonly used because blood circulates throughout tissues and biomarkers such as DNA are abundant in blood (Yip et al., 2017; Donohue et al., 2019). However, this method has several disadvantages: significant pain caused by the syringe, difficulty in collecting blood from the elderly, the risk of infection, and the necessity of medical

expertise (Vagnoli et al., 2015; Cheng et al., 2016; Fukuroku et al., 2016; Chen et al., 2022). Swabs, on the other hand, are easy use, cause less pain, and thus facilitate greater patient compliance (Walker et al., 1999; McBride et al., 2010). Samples of saliva and tissues separated from mucosal tissue can be collected easily, mainly from the buccal mucosa, by using a swab (Theda et al., 2018; Kam et al., 2020). However, swabs have the disadvantages of greater difficulty in collecting a sufficient amount of DNA and the resulting lower DNA purity (Lee and Ladd, 2001).

Microneedles are used to deliver drugs or to extract body fluid from the skin with little pain (Park et al., 2005). Microneedles have been reported to be clinically safe, although minor problems such as skin irritation and erythema have been reported (Chen et al., 2019; Santos et al., 2021). However, the pain caused by microneedles depends on the length of the microneedle (Gill et al., 2008; Jeong et al., 2017). Shorter microneedles with length less than 500 μm cause very little pain and skin was resealed within about 20 min after insertion (Bal et al., 2008; Haq et al., 2009; Gupta et al., 2011; Chen et al., 2019). Thus, shorter microneedles have been manufactured for commercial use in fields such as the cosmetics industry (Kim et al., 2012).

Currently, microneedles are used diagnostically to detect metabolites such as glucose and cholesterol or cell-free nucleic acids present in the interstitial fluid by absorbing interstitial fluid or by delivering interstitial fluid through the microchannel of hollow microneedles (Al Sulaiman et al., 2019). However, microneedles have not been used to directly collect tissue samples. In particular, microneedles have not been used to collect biomarkers from mucous membranes, including the oral and nasal cavity. In a previous study, we developed and optimized a polymeric microneedle swab for sampling buccal mucosa noninvasively. *Ex-vivo* and *in-vivo* studies resulted in the development of a microneedle swab that can retrieve a greater amount of DNA and also provide greater DNA purity compared to commercially available cotton swabs. In addition, animal experiments have shown that a microneedle swab enables the analysis of biomarkers in the buccal mucosa that contain genetic information (Kim et al., 2022).

In the current study, two types of microneedle swabs, buccal and nasal microneedle swab, were fabricated in established way from the results of previous studies. Clinical efficacy was observed in four areas when these microneedle swabs were applied to the buccal and nasal cavities: (International, 2004): medical grade buccal and nasal microneedle swabs were produced for safety and clinical research, (Chen et al., 2009), the amount and purity of DNA collected from buccal and nasal mucosa were evaluated, (Manolio et al., 2008), the genotypes of the five SNP loci in the obtained DNA were compared with the corresponding genotypes obtained from DNA in blood, and (Walker et al., 1999) the safety of a microneedle swab was evaluated. Through this clinical study, the safety and clinical efficacy of nasal and buccal microneedle swabs were verified.

2 Materials and methods

2.1 Characteristics of microneedle swab

Buccal and nasal microneedle swabs consist of a head and a handle connected to the head (Kim et al., 2022). Microneedles are on both sides of the head. There is a breakpoint on the handle so that the head can be separated and put into a 1.5-mL tube after the sample is obtained. The difference between microneedles for the buccal swab and for the nasal swab is the size of the head and the number of microneedles. However, the number of microneedles per unit area is the same for both swabs.

The buccal microneedle swab has a total of 890 microneedles, 445 per side. The nasal microneedle swab has a total of 502 microneedles, 251 on each side. In both swabs, microneedles are arranged in a zigzag pattern. The height of the microneedles is 250 μm, and the distance between the microneedles is 200 μm. The sharpness of the tip is 20 μm (Table 1A). The total length of the buccal microneedle swab is 14 cm, and the breakpoint of the handle is 3 cm below end of the head. The length and breakpoint of the nasal microneedle swab are 10.5 cm and 2.5 cm, respectively. The head of the buccal microneedle is 6 mm wide by 15 mm long by 2 mm thick. The head of the nasal microneedle swab is 5 mm wide by 10 mm long by 2 mm thick (Table 1B).

Polymeric microneedle swabs were manufactured by injection molding obtained from Cyclic Olefin Copolymer (COC) in Quad Medicine's medical device GMP (good manufacturing practice) facility (Seongnam-si, Gyeonggi-do, Korea) (Supplementary Figure S1, S2). Polymeric microneedle swabs were prepared using injection molding. Molds for buccal swabs and nasal swabs were made of stainless steel using a computer numerical control (CNC) machine. The stainless steel mold can also be used to mold other thermoplastic polymers. The injection temperature was 200°C–250°C, and the injection pressure was 80–110 MPa. Commercial buccal swabs were SK-2S (rayon swabs) from Isohelix, and commercial nasal swabs were NFS-1 (flocked nylon swabs) from Noblebio. The geometries of microneedle swabs and commercial swabs were observed using a mirrorless camera (Canon EOS RP, Japan), a stereo microscope (Leica M205, Wetzlar, Germany), and a scanning electron microscope.

2.2 Safety tests of microneedle swab

Prior to clinical tests, cytotoxicity, skin sensitivity, and skin irritation tests were performed to confirm the safety of the microneedle swab.

2.2.1 Cytotoxicity test

Mouse fibroblast NCTC clone 929 (L-929; American Type Culture Collection, United States) was used to evaluate the toxicity of the microneedle swab. The test substance was eluted using minimum essential medium (MEM; liquid, gibco) with 10% (v/v) horse serum (gibco) and 1% (v/v) penicillin-streptomycin (gibco). The elute was brought into direct contact with the cells, and the reaction was observed under a microscope. MEM medium containing no substance was used as a solvent control (Reagent control), and high-density polyethylene film and ZDEC polyurethane film (Hatano Research Institute, Food and Drug Safety Center, Japan) were used as negative and positive control materials, respectively. The head of the microneedle swab was broken at the breakpoint (6 cm^2/1 mL 10% MEM medium), placed in the medium, and stirred for 24 h in a 37 °C 5% CO_2 incubator. Negative and positive controls were eluted at a rate of 1 mL of 1× MEM medium per 0.1 g at 37 °C for 24 h in a 5% CO2 incubator with stirring. All eluates were not pH adjusted, stored

TABLE 1 Geometric characteristics. (A) Microneedles of buccal swab and nasal swab. (B) Geometric characteristics of commercial swabs (Isohelix, Noblebio) and buccal and nasal microneedle swabs.

(A) MN swab	Height [μm]	Number [ea]	Interval [μm]	Width [μm]	Sharpness [μm]
Buccal	250	890	200	200	20
Nasal	250	502	200	200	20

(B) Swab characteristics		Total	Head			Shaft	
		Length [cm]	Length [cm]	Width [cm]	Thickness [cm]	Length [cm]	Breakpoint [cm]
Buccal	Isohelix	16	1.5	0.75	0.3	14.5	4
	MN swab	14	1.5	0.6	0.2	12.5	3
Nasal	Noblebio	15	1.5	0.3	0.3	13.5	9
	MN swab	10.5	1	0.5	0.2	9.5	2.5

at room temperature, and used within 4 h. The monolayer of cultured cells was treated with trypsin (trypsin/EDTA, gibco) to adjust the cell concentration to 10^5 per 1 mL, and the cultured cells were injected (2 mL each) into about 10 cm^2 wells (6-well tissue culture plate, Φ 35 mm/well). After culturing for more than 24 h in a 37 ˚C, 5% CO_2 incubator, monolayer of cultured wells was selected, marked as either a test substance treatment group or a control group (a solvent control group, a negative control group, and a positive control group), and then the medium was removed. The test substance treatment group, a solvent control group, a negative control group, and a positive control group were dispensed into selected wells and incubated for 48 h in a 37 C 5% CO_2 incubator. After culturing, cell lysis and morphology were observed under a microscope (Nikon, Japan). The presence of a uniform monolayer of cells was expressed as (+), and the absence of a confluent monolayer was expressed as (−). When the color of the medium changed to yellow after elution, it was determined that the medium was changed to acidic by the eluted material, and when it turned crimson or purple, it was determined that the medium was changed to basic. To demonstrate the validity of the test, the solvent control group and the negative control group should not show cytotoxicity (Grade 0), and the positive control group should show moderate to high cytotoxicity (> Grade 2).

2.2.2 Skin sensitivity test

In order to evaluate the skin sensitivity of microneedle swabs, sensitization was induced by intradermal injection and topical application of polar and non-polar solvent eluates with 300–370 g Dunkin Hartley guinea pigs (Samtako Bio Korea, Gyeonggi-do, Korea). The mortality, general symptoms, and skin sensitivity of the guinea pigs were evaluated. This test was approved by the Animal Ethics Committee (approval number: IAC 2022-2242) and carried out in accordance with the Law on Laboratory Animals [Law No. 18969 (2020-06-10, partially amended)] and standard operating guidelines.

Sterile saline (Daihan Pharm. Co., Seoul, Korea) was used as a polar elution solvent and cottonseed oil (Junsei Chemical Co., Tokyo, Japan) was used as a non-polar elution solvent. The elution rate was 6 cm^2/mL (surface area of the test substance: 4.88 cm^2/ea) and eluted by stirring in a shaking water bath (50 ˚C, 72 h). The solvent control group was eluted under the same conditions. The test groups for each elution solvent (G2, G4) consisted of 10 guinea pigs each, and the control group (G1, G3) consisted of 5 guinea pigs each. Intradermal induction and local induction were carried out by shaving the intrascapular region, and induction and skin reaction evaluation were performed by shaving the upper flank.

In the intradermal induction step, three samples of solvent, solvent and Freund's complete adjuvant (FCA; Sigma-Aldrich) (1:1), and solvent, FCA, and extract (1:1:1) were intradermally injected into the left and right sides of the skin of the scapula, respectively (Supplementary Figure S3A,B).

For the topical induction step, 0.5 mL of 10% sodium dodecyl sulfate (SDS; BIONEER) was applied 5 days after completion of intradermal induction. A filter paper (2 cm × 4 cm) was wetted with the test substance (0.4 mL) and applied to the intradermal injection site for 48 h The control substance (0.4 mL) was applied in the same manner.

In the induction phase, at 13 days after the local induction phase, filter papers (2 cm × 2 cm) wetted with the test substance (left, 0.2 mL) and the control substance (right, 0.2 mL) were placed for 24 h using Coban (TM, 3M) and then removed.

The skin reaction was evaluated according to the table (Supplementary Figure S3C). If the control group's grade is less than 1 grade and the test group's grade is 1 or higher, it is considered to indicate skin sensitization of the test group.

2.2.3 Skin irritation test

The eluate from the microneedle swab was administered intradermally to NZWnl rabbits (Pizhou Dongfang Breeding, China) to evaluate skin irritation. This was approved by the Animal Ethics Committee (approval number: IAC 2022-2133) and performed in accordance with the Law on Laboratory Animals [Law No. 18969 (2020-06-10, partially amended)] and standard operating guidelines.

The head of the microneedle swab was separated at the breakpoint, and the head was put in sterile saline solution (Daihan Pharm. Co., Ltd) and cottonseed oil (Junsei Chemical Co., Ltd). The skin irritation test was performed in the same manner as the skin sensitivity test.

After the rabbits' body weight was measured, hair was removed from the back before administration of the test substance, and three

healthy rabbits weighing 2.0 kg or more with clean skin were selected. On the day of administration, 0.2 mL each of the extracts of sterile physiological saline and cottonseed oil and each solvent control material were administered intradermally to 5 sites near the rabbit's spine (Supplementary Figure S4A).

Changes in general symptoms and the death of any animals were observed for all animals once a day for 3 days. Body weight change was measured three times. Immediately after administration, the presence of abnormalities at the administration site was checked, and erythema, crust formation, and degree of edema formation were observed and recorded according to grade at 24, 48, and 72 h after administration (Supplementary Figure S4B). Immediately after intradermal administration, photographs were taken to record the shape of the injection site.

Skin irritation was evaluated by adding up all grades of erythema observed at 24, 48, and 72 h after administration, and then dividing the total number of observations by 15 (3 scoring time points × 5 test injection sites). The values calculated for each animal were added together and divided by 3. When the difference between the scores of the test substance and the control substance was 1.0 or less, it was considered that there was no skin irritation.

2.3 Clinical test of microneedle swabs

2.3.1 Sterilization of microneedle swabs

Sterilization and validation of sterilization of the microneedle swab were confirmed by Greenpia Technology Co., Ltd. (Yeoju-si, Gyeonggi-do, Korea). Buccal and nasal microneedle swabs were treated with 15.0 kGy gamma sterilization for clinical study. Sterility validation was performed according to the validation protocol described in ISO11137-2:2013.

2.3.2 Clinical research and subjects

The clinical research was conducted by randomly recruiting 25 healthy subjects from Kangbuk Samsung Hospital. The participants were between 19 and 70 years old, and informed consent was obtained from all participants. This study was approved by the Kangbuk Samsung Hospital Clinical Review Board (IRB File No: KBSMC 2022-10-001-001).

2.3.3 Sampling method

Commercial swabs were used as controls. A commercially available rayon swab (SK-2S, Isohelx) was used for the buccal swab, and a flocked nylon swab (NFS-1, Noblebio) was used for the nasal swab.

SK-2S buccal swab sampling was carried out according to the manufacturer's instructions. For buccal microneedle swab, buccal samples were collected by rubbing each side of the swab 5 times for a total of 10 times of wiping both sides (Supplementary Figure S5A). Samples were collected by rubbing the inside of the cheek vigorously 10 times for at least 20 s. Only one side of the cheek was used for each swab. That is, when taking a microneedle swab from the left cheek, SK-2S should be applied only on the opposite right cheek.

When collecting a sample using a nasal microneedle swab, inside of the one nostril and its surroundings are wiped in a circular motion 3 times for a total of 6 times with both side of the swab (Supplementary Figure S5B). NFS-1 nasal swab sampling was also carried out in the opposite nostril according to the manufacturer's instructions.

After buccal and nasal samples were collected, the swab handle was cut at the breakpoint, placed in a 1.5-mL tube, and stored in the refrigerator (Supplementary Figure S5A,B). Blood samples were collected using a 5-mL Streck tube and stored at freezer before the experiments.

2.3.4 DNA extraction, concentration, and purity measurement

The collected buccal, nasal swabs and blood samples were subjected to a DNA extraction process using a HiGene™ gDNA Prep kit (Biofact, Daejeon, Korea) according to the manufacturer's protocol. The experiment was conducted in two ways depending on the sample.

1) Buccal and nasal swab samples were processed as described below.

The swab was put into the tube, 450 uL of GD1 Buffer was added, and the solution was mixed by vortexing for 1 min. After vortexing, the solution was immediately transferred to a new 1.5-mL tube to prevent cell sedimentation. After 5uL of Proteinase K (20 mg/mL) and 2uL of RNase A (4 mg/mL) was dispensed, the solution was mixed by vortexing for 1 min and incubated at 56°C for 10 min. After incubation, 200uL of GD2 Buffer was added, vortexed for 10 s, and incubated at 70°C for 10 min. After incubation, centrifugation was performed at 13,000 rpm for 5 min. The supernatant of the centrifuged sample was transferred to a new 1.5-mL tube and inverted 20 times by adding 200 uL of GB buffer. After 200ul of Help B Buffer was added to a spin column equipped with a collection tube, the solution was centrifuged at 7,000 rpm for 1 min. The sample solution containing GB buffer was added to the spin column and centrifuged at 7,000 rpm for 1 min 500 uL of 80% ethanol was added to the spin column and then centrifuged at 13,000 rpm for 30 s. This process was repeated one more time. After the washing process, the spin column was idling at 13,000 rpm for 3 min. The spin column was inserted into a new 1.5-mL tube, and 50 uL of DNA Hydration Solution was added for DNA elution and incubated at room temperature for 1 min. The spin column was removed after centrifugation at 13,000 rpm for 2 min. Finally, DNA is obtained in the 1.5 mL tube for use in downstream applications.

2) Blood samples were processed as described below.

Whole blood (200ul), GD2 buffer (400 uL), and Proteinase K (20 uL, 20 mg/mL) were added into the tube and mixed by vortexing for 1 min. After incubation at 56°C for 10 min, 200 uL of GB buffer was added and inverted 20 times. Help B Buffer (200 ul) was added to the spin column equipped with a collection tube, and the column was centrifuged at 7000 rpm for 1 min. The sample solution containing GB buffer was added to the spin column. The column was centrifuged at 7,000 rpm for 1 min. The rest of the steps are the same as the process described above for buccal and nasal swab samples.

The concentration and purity of the extracted DNA samples were measured at a wavelength of 260 nm using a NanoDrop® ND-

1000 spectrophotometer (Nanodrop Technologies Inc., NC, United States).

2.3.5 Genotyping

Genotyping was performed with 22 DNA samples, which satisfied the purity criteria (1.6–2.1). Five SNPs (rs1065757, rs3752752, rs921115, rs1009480, rs1009480, rs1820795) were randomly selected among the SNPs with a minor allele frequency in the range of approximately 0.4–0.5 in Koreans. Since SNPs are biallelic, genotyping can be more definitive when selecting SNPs among evenly distributed alleles. Genotyping was performed using the Sanger sequencing method (ABI 3500XL Sequencer®, Applied Biosystems, United States).

2.3.6 Visual Analogue Scale (VAS)

The pain caused by the buccal and nasal microneedle swab was investigated using the Visual Analogue Scale (VAS) for the 25 subjects who participated in the clinical trial. The VAS pain index was expressed as a number from 1 (*no pain at all*) to 10 (*very painful*), and the values were interpreted through a table (Supplementary Figure S6) (Wewers and Lowe, 1990; Caffarel-Salvador et al., 2021). Bleeding was checked when the buccal and nasal microneedle swab was used, and satisfaction was expressed as a number from 1 (*very uncomfortable*) to 10 (*very satisfied*).

2.4 Statistical analysis

For statistical analysis of microneedle swabs and commercial swabs, we set a effect size ($f = 0.4$) (Cohen, 2013), power 80% and an alpha error probability of 0.05. Under these conditions, the total sample size needed was 66, and the sample size for each group was 22.

DNA concentrations from buccal and nasal microneedle swabs and commercial swabs were tested by paired *t*-test. The test was performed at the significance level of 0.05 (95% confidence level), and $p \leq .05$ was considered significant.

The five SNPs were selected to compare the genotypes of DNA obtained from buccal and nasal microneedle swabs and those obtained from blood. The concordance rate (%) of genotypes from each person's blood and buccal or nasal microneedle swab and Kappa statistics were calculated. Kappa statistics evaluate the degree of concordance between measurement methods, and it is a statistical method that measures whether the results from the two methods coincide with each other by chance.

Concordance rates and kappa statistics were calculated using only genotypes called simultaneously by both methods. If missing data occurred at any locus of the five SNP loci in the blood sample, the locus was excluded from calculation. When missing data occurred at any locus of the five SNP loci in a buccal or nasal swab sample, the locus was considered a genotype mismatch. This is because it is considered that the sampling performance through the swab has degraded.

The lower the kappa value, the lower the degree of concordance, and the closer the value is to 1, the higher the degree of agreement. Kappa values were interpreted according to the criteria (Supplementary Figure S7) (McHugh, 2012).

3 Results

3.1 Characteristics of microneedle swab

The dimensions of the head of the buccal microneedle swab used in clinical trials were 6 mm × 15 mm × 2 mm (W × L × T), and the size of the head of the nasal microneedle swab was 5 mm × 10 mm × 2 mm (W × L × T). The size of the microneedle swab head was determined based on the size of the commercial buccal and nasal swabs (Figures 1, 2). One thousand samples were prepared in a single process, and when the deviation in the length of the microneedles ($n = 100$) was measured, the relative standard deviation (RSD) among the samples was less than 1%. For the buccal microneedle swab, the accessibility of the swab to the buccal mucosa was considered. The head size of the of nasal microneedle swab and the commercial swab was determined by the fact that the location of the nasal sample was 2-3 cm from the entrance of the human nose.

Considering user convenience and potential error in use, microneedles were placed on both sides of the swab head. Because the length of the microneedles is 250 μm, it is not easy to find the side where the microneedles are located. Therefore, microneedles were placed on both sides of the swab head so that the user could obtain a reproducible amount of sample from both sides with same number of repetitions of swabbing.

3.2 Safety of microneedle swab

3.2.1 Cytotoxicity test

Cells were treated with the eluate of the polymer microneedle swab made of cyclic olefin copolymer (COC). A uniform monolayer of cells was formed during culture, but mild inhibition of cell proliferation (10% of total cells) was observed. The solvent control and negative control showed no toxicity (Grade 0) to the cultured cells, and the positive control caused cytotoxicity (Grade 4) to 75% of the total cell. Since the color of the culture medium did not change, the eluate from the microneedle swab did not change acidity. Therefore, there was very weak cytotoxicity to mouse fibroblasts. The microneedle swab showed Grade 1 (slight) cytotoxicity according to the cytotoxicity criteria of ISO 10993-5, and meets the cytotoxicity test criteria for medical devices that must be Grade 2 (mild) cytotoxicity or lower (Table 2).

3.2.2 Skin sensitivity test

A skin sensitivity test was conducted for 24 days. During the experimental period, the mortality rate due to test substance administration was 0% in polar (G2) solvent test and non-polar (G4) solvent test groups, and no general symptoms appeared in test groups (Supplementary Figure S8A). When skin reactions were observed at 24 h and 48 h after the challenge, skin reactions such as erythema and edema were not observed in the test group compared to the control group. In both G2 and G4 solvent test groups, the skin response score and sensitization rate were 0.0% and 0.0%. In both the polar (G1) and non-polar (G3) solvent control groups, the skin response score and sensitization rate were 0.0% and 0.0%, respectively, indicating that there was no solvent sensitization. As a positive control test using dinitrochlorobenzene (DNCB)

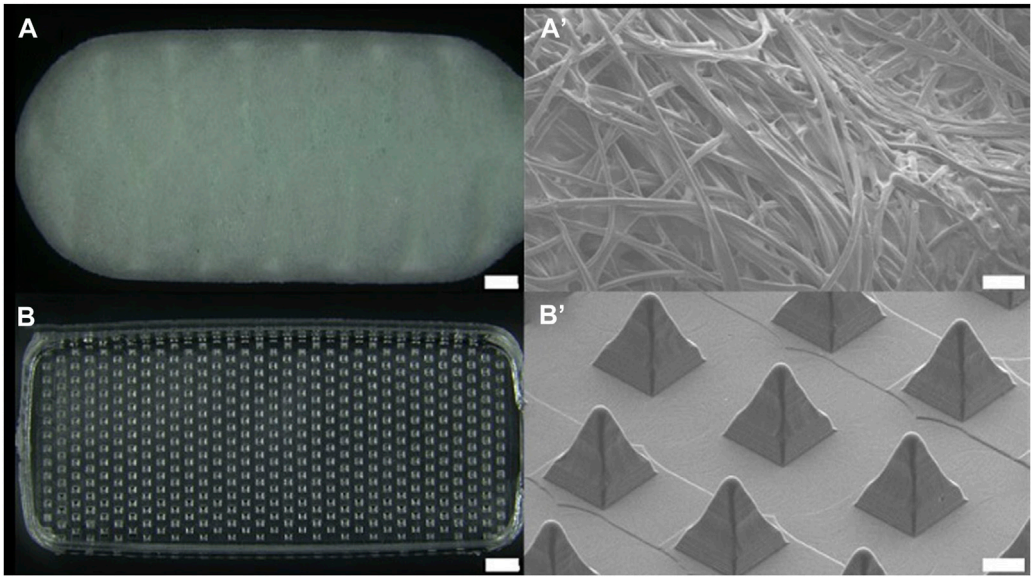

FIGURE 1
Optical image of **(A)** buccal commercial swab head (SK-2S, Isohelix, scale bar 1 mm) and **(B)** buccal microneedle swab head. Scanning electron microscopic images of **(A')** commercial swab and **(B')** microneedle swab (scale bar 100 μm).

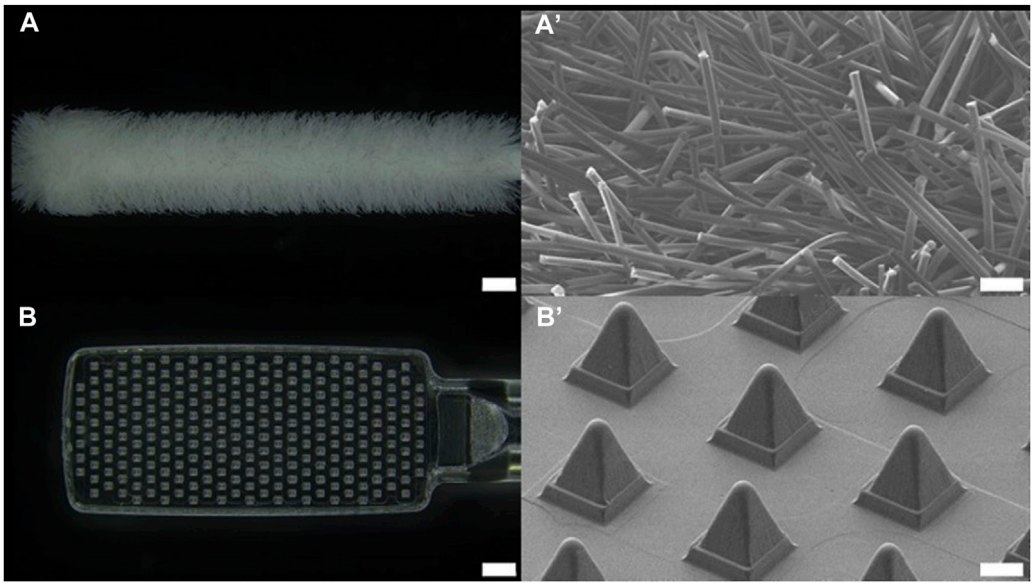

FIGURE 2
Optical image of **(A)** nasal commercial swab head (NFS-1, Noblebio, scale bar 1 mm) and **(B)** nasal microneedle swab head. Scanning electron microscopic images of **(A')** commercial swab and **(B')** microneedle swab (scale bar 100 μm).

according to ISO 1993-10, skin reactions such as erythema and edema were observed in the same manner. The skin response scores were calculated as 1.4, 1.7 and the sensitization rates were 100% (Supplementary Figure S8B). In addition, test groups G2 and G4 and control groups G1 and G3 showed no weight loss (Supplementary Figure S9). Therefore, the microneedle swab does not cause skin irritation, and it is made of a material that does not cause skin sensitization.

3.2.3 Skin irritation test

For 3 days after administration, general symptoms and weight loss were not observed in all rabbits, and no rabbits died (Table 3). The difference between the test substance and the control substance was calculated as 0.00 for both sterile saline and cottonseed oil extracts (Supplementary Figure S10A,B). As a result of a positive control test using 0.5% SDS according to ISO 10993-23, well-defined to severe (dark red) erythema (grade 2–4) was observed at 24, 48,

TABLE 2 Qualitative analysis results of cytotoxicity test. Grade 0: none, Grade 1: slight, Grade 2: mild, Grade 3: moderate, Grade 4: severe.

Well	Confluent monolayer	% Growth inhibition	%Cells without intracellular granulation	% Rounding	% lysis	Reactivity	Grade
Test 1	(+)	10	0	0	0	Slight	1
Test 2	(+)	10	0	0	0	Slight	1
Test 3	(+)	10	0	0	0	Slight	1
N.C. 1	(+)	0	0	0	0	None	0
N.C. 2	(+)	0	0	0	0	None	0
N.C. 3	(+)	0	0	0	0	None	0
R.C. 1	(+)	0	0	0	0	None	0
R.C. 2	(+)	0	0	0	0	None	0
R.C. 3	(+)	0	0	0	0	None	0
P.C. 1	(−)	100	N/A	N/A	100	Severe	4
P.C. 2	(−)	100	N/A	N/A	100	Severe	4
P.C. 3	(−)	100	N/A	N/A	100	Severe	4

Note. Test = microneedle swab extraction; N.C., negative control; R.C., reagent control; P.C., positive control. (+) = present, (−) = absent, N/A = not applicable.

TABLE 3 Skin irritation test results of clinical signs and mortality for eluent from microneedle swab.

Number of rabbits	Day(s) after application				Mortality (%)
	0	1	2	3	
n = 3	Normal	Normal	Normal	Normal	0

and 72 h after intradermal administration. Finally, the difference between the test substance and the positive control substance was 6.22, and it is a value greater than 1.0 (Supplementary Figure S10C). In the skin irritation test, each eluate from the microneedle swab satisfied the safety requirements because the difference in scores between the negative control substance and the sample is less than 1.0. Thus, the material constituting the microneedle swab was proven to be safe.

3.3 Clinical study of microneedle swab

3.3.1 Sterilization efficacy of microneedle swab

The result of the sterilization validation test of the microneedle swab showed that a dose of at least 15 kGy was allowed as a regular sterilization dose according to the ISO 11137 VD_{max}^{15} method for the sterilization assurance level. The maximum permissible dose for the product was properly investigated through the gamma irradiation process of Greenpia Technology Co., Ltd., and the effect on product performance or packaging was confirmed to be suitable by the manufacturer.

3.3.2 DNA yield and purity

The clinical research was conducted with randomly recruited 25 people from Kangbuk Samsung Hospital. The study consisted of healthy subjects between the ages of 19 and 80 years with the informed consent of all them (Table 4).

TABLE 4 Characteristics of the study participants.

Subject characteristics		Count	Percentage(%)
Gender	Male	18	72
	Female	7	28
Age (years)	19–25	13	52
	26–30	9	36
	60–70	3	12
Total participation		25	100

The amount of DNA obtained from a buccal microneedle swab was 33 ± 14 ng/μL, and the amount of DNA obtained with a commercial buccal swab (SK-2S, Isohelix) was 16 ± 18 ng/μL. Thus the buccal microneedle swab retrieved twice the amount of DNA as the commercial swab ($p < .001$) (Figure 3A). The DNA purity of the buccal microneedle swab was 1.75 ± 0.08, and the DNA purity of the commercial swab was 2.12 ± 0.37. Thus the DNA purity of the sample obtained by the buccal microneedle swab was within the appropriate range (1.6–2.1) for genetic analysis (Figure 3B) (Ahmed et al., 2013).

The amount of DNA obtained from the nasal cavity by the nasal microneedle swab was 9 ± 3 ng/μL, and the amount of DNA obtained by the commercial nasal swab (NFS-1, Noblebio) was 5 ± 2 ng/μL. Therefore, the amount of DNA obtained by the

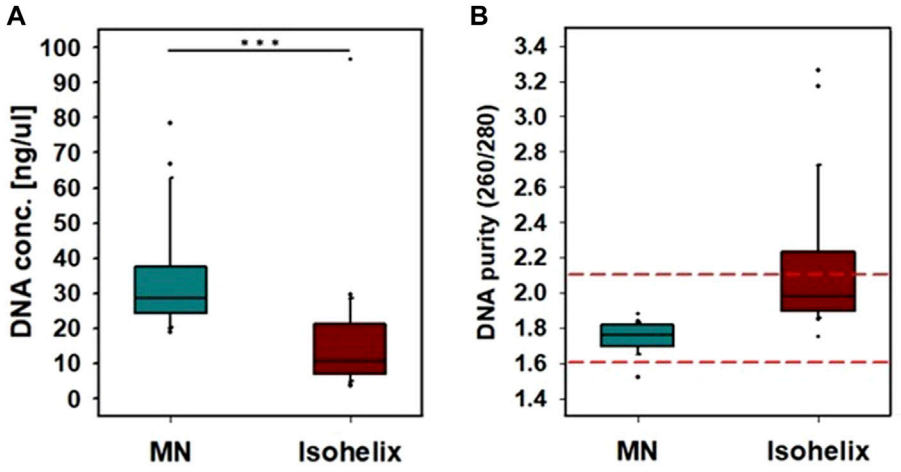

FIGURE 3
Comparison of buccal microneedle swab with Isohelix buccal swab. A sample was collected by rubbing each side of the swab 5 times for a total of 10 times wiping both sides of the microneedle swab. **(A)** DNA concentration, **(B)** DNA purity. (***: $p < 0.001$).

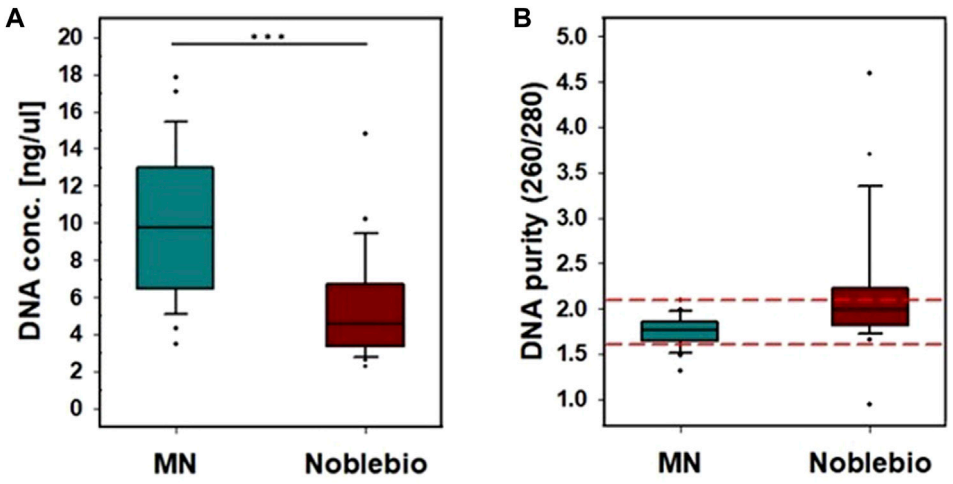

FIGURE 4
Comparison of nasal microneedle swab with Noblebio nasal swab. The inside of one nostril and its surroundings were wiped in a circular motion 3 times for a total of 6 times wiping both sides of the microneedle swab. **(A)** DNA concentration obtained, **(B)** DNA purity. (***: $p < 0.001$).

nasal microneedle swab was two times greater than that by the commercially available nasal swab (Figure 4A). The amount of DNA obtained is affected by how many times a swab is wiped and the pressure used when swabbing (Kim et al., 2022). The deviation in DNA amount can be caused by individual differences in the swabs used to collect samples, as shown in the variance in DNA amount in Figure 4A. The DNA purity was 1.75 ± 0.17 for the nasal microneedle swab and 2.16 ± 0.71 for NFS-1 (Noblebio), indicating that the purity of microneedle swabs was within the appropriate range (1.6–2.1) for genetic analysis (Figure 4B).

In the *ex-vivo* porcine buccal tissue experiment in our previous study, the microneedle swab showed twice as much DNA yield as the commercial rayon swab and the nylon flocked swab, and in the *in-vivo* experiment with pigs, the DNA yield of the microneedle swab was greater than that of the nylon flocked swab (Kim et al., 2022). Similar to the previous results, in the clinical trials of this study, microneedle swabs showed higher DNA yields than the commercial cotton swabs in both the buccal and the nasal samples, and the microneedle swabs showed a purity suitable for downstream genomic analysis.

3.3.3 Genotype concordance

Genotype concordance was assessed with DNA samples, satisfying the DNA concentration and purity criteria. Genotypes were compared at five SNP loci from the blood of the same person, buccal, nasal microneedle swabs, and commercial swabs. The buccal and nasal microneedle swab showed a Kappa value of 1.0 for all five SNP genotypes, and the concordance rate was 100%. The SK-2S swabs (Isohelix) also showed a Kappa value of 1.0 and a concordance

TABLE 5 Kappa statistics and genotype concordance rate.

Sampling	Buccal				Nasal			
Comparison target	Blood - MN (n = 22)		Blood - Isohelix (n = 22)		Blood - MN (n = 22)		Blood - Noblebio (n = 22)	
SNP	Kappa	Concordance rate (%)	Kappa	Concordance rate (%)	Kappa	Concordance rate (%)	Kappa	Concordance rate (%)
rs1065757	1.0	100	1.0	100	1.0	100	1.0	100
rs3752752	1.0	100	1.0	100	1.0	100	1.0	100
rs921115	1.0	100	1.0	100	1.0	100	0.9	95
rs1009480	1.0	100	1.0	100	1.0	100	1.0	100
rs1820795	1.0	100	1.0	100	1.0	100	1.0	100

[a]Kappa: Kappa result ranges from 0 to 1. The higher the value of Kappa, the stronger the agreement.

rate of 100%. Only one sample collected from a commercial nasal swab (NFS-1, Noblebio) in the nasal cavity showed a mismatched genotype for one SNP (rs921115) between the blood and the nasal swab, which resulted in a concordance rate of 95% and a Kappa value of 0.9 for commercial cotton swab (Table 5).

This observation suggests that both the commercial buccal swabs and the buccal or nasal microneedle swabs in this study are suitable for use in downstream genetic analysis. Even though one discrepant genotype was found, the commercial nasal swabs may also be considered suitable for analysis. This discrepancy may be caused by weak frictional strength during nasal swabs, depending on the participant.

For accurate genetic analysis, a sufficient amount of DNA should be obtained and it must have sufficient purity. Commercial cotton swabs pick up fragments of epithelial cells present in saliva. When the buccal tissue is swabbed, bacteria or food present on the mucosal surface and saliva affect sample collection and analysis (Brownlow et al., 2012). In addition, cotton swabs showed low extraction efficiency and low recovery efficiency of less than 50% even though they had high absorption capacity in sample collection (Bruijns et al., 2018). Compared to conventional rayon swabs and nylon flocked swabs, microneedle swabs showed improved release efficiency because microneedles were exposed to the extraction medium (Wise et al., 2021; Kim et al., 2022). Therefore, the microneedle swab has advantages not only in sample collection but also in analysis.

3.3.4 VAS measurement of pain caused by microneedle swabs

Since microneedle swabs contact with the buccal surface, pain caused by the swabs is a major consideration. The VAS pain scale of the buccal microneedle swab was 1.0 ± 0.2 and the nasal microneedle swab was 1.0 ± 0.4 (Figure 5A). A value of VAS 1 is very low pain perception (Supplementary Figure S6; scale of VAS pain scale). Also, none of the participants in the clinical study reported any bleeding and pain during the swabbing process.

As the microneedle length increases, pain increases proportionally (Gill et al., 2008; Jeong et al., 2017). In an *ex-vivo* experiment in a previous study, a microneedle swab with a length of 250 μm caused a scratch of about 20 μm (Kim et al., 2022). In other clinical studies, when 250 μm long microneedles pierced the skin, the pain was too low to feel (Griffin et al., 2017; Fernando et al., 2018; Samant et al., 2020). For a microneedle swab, since only the surface of the buccal mucosa is swabbed, a scratch 20 μm deep is much less than the insertion depth of a 250 μm long microneedle. As the length of the microneedle increases, more sample can be obtained, but the risk of pain or infection can also increase. Thus, the 250 μm long microneedle has an optimal geometry for obtaining samples from the mucosal surface safely and efficaciously (Kaushik et al., 2001; Gupta et al., 2011; Jeong et al., 2017).

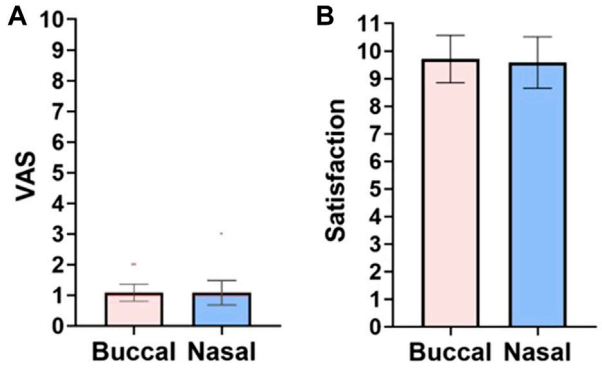

FIGURE 5
Survey results. **(A)** VAS pain scale: 0, no pain; 10, pain as bad as it could possibly be. **(B)** Satisfaction scores for buccal and nasal microneedle swabs: 0, very uncomfortable; 10, very satisfied. Pink: buccal; blue: nasal.

When study participants were asked about the satisfaction and convenience of the microneedle swab, the average satisfaction reported for the buccal swab and the nasal swab was 9.7 ± 0.8 points and 9.5 ± 0.9 points (out of 10 points), respectively (Figure 5B). This means that buccal and nasal microneedle swabs are easy to use and have high accessibility because they are non-invasive and thus have excellent user accessibility.

4 Discussion

Buccal and nasal microneedle swabs have the advantage of obtaining a large amount of high-purity cells with less force than

the previous sampling method using a cotton swab. Thus, using buccal or nasal swabs is expected to increase the accuracy of the genomic analysis. None of the participants in the clinical study reported any bleeding or pain during the swabbing process. However, there is a risk of irritation to the mucous membrane if the user does not follow the sampling guidelines. In the future, we will continue to evaluate the safety of microneedle swabs in a wider range of areas and suggest directions for use through additional clinical studies.

As we go through the COVID-19 pandemic era, the medical community is gradually moving toward a non–face-to-face testing system. Therefore, in the future, rather than visiting a hospital to collect blood and test for disease, it is expected that there will be a method of collecting samples at home using a diagnostic kit and sending the sample to be tested for disease. In addition, for large-scale genomic analysis, such as the study of population genetics, sampling methods using buccal or nasal swabs will facilitate the recruitment of many participants. In other words, individuals can easily participate in large-scale research by filling out a consent form online and collecting samples using a sampling kit delivered to their home without having to visit a hospital.

In this study, we examined the applicability of buccal and nasal microneedle swabs by comparing their performance (DNA concentration and purity) and analyzed genotype concordance with commercial swabs in a limited number of participants. In addition, safety tests (e.g., cytotoxicity test, skin sensitivity test, skin irritation test) were conducted based on guidelines established by the Korean Minister of Food and Drug Safety. Moreover, buccal and nasal microneedle swabs met the safety requirements for clinical study and commercial use. Finally, the microneedle swab for clinical study was registered as a Grade 2 medical device by the Korean Minister of Food and Drug Safety.

However, additional research is needed to apply buccal and nasal microneedle swabs in large-scale genomic analysis. That is, the reproducibility of these swabs must be evaluated under various conditions (e.g., between samplers, between sampling times, etc.). In addition, a large number of samples should be used to compare the genetic analysis performance of buccal and nasal microneedle swab samples with existing sampling methods and to verify their reliability. We plan to pursue this research in the future.

Genetic data obtained through buccal or nasal microneedle swabs is very sensitive personal information. The data contain a variety of information about an individual's health, ancestry, and potential predisposition to various diseases. Therefore, it is important to keep these data secure to prevent unauthorized access and misuse. In addition, when a company or organization uses an individual's genetic data for research, participants must fully understand the implications of sharing their genetic data and give prior consent for use of the data. The company or organization is also obligated to protect personal information by anonymizing such information, and the data must be used ethically.

To harness the full potential of genomics in long-term research and medical practice, it is essential to continue advancing technology and computational tools for genomics, ensuring the privacy and ethical use of genetic data, and integrating genomic data into routine medical care. In that respect, continual improvement of buccal and nasal microneedle swab sampling techniques is important to secure reliable genetic data. For example, it is necessary to evaluate how reproducible genotypes obtained based on samples collected at different times for various genetic loci for the same person are obtained. In addition, it is necessary to evaluate whether a sufficient amount of DNA is consistently obtained with high purity and whether genotyping results are error-free when using the buccal or nasal microneedle swab sampling kit in a test group consisting of a larger number of people.

5 Conclusion

This study was conducted to confirm the safety of the microneedle swab and to evaluate its clinical performance. The microneedle swab manufactured in good manufacturing practice (GMP) satisfied all safety test standards regarding cytotoxicity, skin sensitivity, and skin irritation. It also passed the sterilization efficacy test. Buccal and nasal microneedle swabs showed two times higher DNA yields and greater purity than commercial cotton swabs. When the genotypes of SNPs were compared between samples collected by microneedle swabs and blood samples, all genotypes tested were concordant, confirming that microneedle swabs were suitable for clinical use. The VAS pain index during sampling was 1, which is difficult to perceive, and user convenience also showed satisfactory characteristics.

For large-scale genomic analysis in areas such as population genetics, buccal or nasal microneedle swab sampling methods allow for easy recruitment of many participants. Although this study evaluated the performance and safety of the buccal or nasal microneedle swab using a small number of samples, such evaluations should be conducted with a larger number of samples in the future.

Therefore, the newly developed microneedle swab can effectively and easily collect DNA from the buccal and nasal mucosa. Microneedle swabs can be used for DTC tests as well as disease diagnosis and prevention through genomic analysis, so its utilization is expected to be high.

Data availability statement

The datasets presented in this study can be found in online repositories. The names of the repository/repositories and accession number(s) can be found in the article/Supplementary Material.

Ethics statement

The studies involving humans were approved by Clinical trial was approved by the Kangbuk Samsung Hospital Clinical Review Board (IRB File No: KBSMC 2022-10-001-001). The studies were conducted in accordance with the local legislation and institutional requirements. Written informed consent for participation in this study was provided by the participant's legal guardians/next of kin. The animal studies were approved by Skin sensitivity test of the guinea pigs was approved by the Animal Ethics Committee (approval number: IAC 2022-2242) and carried out in accordance with the Law on Laboratory Animals [Law No. 18969 (2020-06-10, partially amended)] of Korea Testing and Research Institute for Chemical Industry (KOTRIC) and standard operating

guidelines. Skin irritation test of the NZWnl rabbits was approved by the Animal Ethics Committee (approval number: IAC2022-2133) and performed in accordance with the Law on Laboratory Animals [Law No. 18969 (2020-06-10, partially amended)] of Korea Testing and Research Institute for Chemical Industry (KOTRIC) and standard operating guidelines. The studies were conducted in accordance with the local legislation and institutional requirements. Written informed consent was obtained from the owners for the participation of their animals in this study.

Author contributions

JK: Software, Writing–original draft, Writing–review and editing. J-WM: Software, Writing–review and editing. GK: Investigation, Methodology, Writing–review and editing. WK: Software, Writing–review and editing. H-JH: Conceptualization, Data curation, Supervision, Writing–original draft, Writing–review and editing. W-JJ: Investigation, Methodology, Writing–review and editing. S-KB: Formal Analysis, Funding acquisition, Writing–review and editing. G-HS: Investigation, Methodology, Writing–review and editing. J-HP: Conceptualization, Data curation, Supervision, Writing–original draft, Writing–review and editing.

Funding

The author(s) declare financial support was received for the research, authorship, and/or publication of this article. This work was supported by the Gachon University research fund of 2021 (GCU-202110370001) and supported by the Technology development Program(S2956928) funded by the Ministry of SMEs and Startups (MSS, Korea).

Conflict of interest

H.H. is an inventor of patent related to microneedle based swab. Authors J-WM, GK, WK, and H-JH were employed by Endomics Inc. Authors W-JJ, S-KB, and G-HS were employed by QuadMedicine Co, Ltd.

The remaining authors declare that the research was conducted in the absence of any commercial or financial relationships that could be construed as a potential conflict of interest.

Publisher's note

All claims expressed in this article are solely those of the authors and do not necessarily represent those of their affiliated organizations, or those of the publisher, the editors and the reviewers. Any product that may be evaluated in this article, or claim that may be made by its manufacturer, is not guaranteed or endorsed by the publisher.

Supplementary material

The Supplementary Material for this article can be found online at: https://www.frontiersin.org/articles/10.3389/fbioe.2023.1296832/full#supplementary-material

References

Ahmed, N., Nawaz, S., Iqbal, A., Mubin, M., Butt, A., Lightfoot, D. A., et al. (2013). Extraction of high-quality intact DNA from okra leaves despite their high. *Biosci. Methods* 4. doi:10.5376/bm.2013.04.0004

Al Sulaiman, D., Chang, J. Y., Bennett, N. R., Topouzi, H., Higgins, C. A., Irvine, D. J., et al. (2019). Hydrogel-coated microneedle arrays for minimally invasive sampling and sensing of specific circulating nucleic acids from skin interstitial fluid. *ACS Nano* 13 (8), 9620–9628. doi:10.1021/acsnano.9b04783

Bal, S. M., Caussin, J., Pavel, S., and Bouwstra, J. A. (2008). *In vivo* assessment of safety of microneedle arrays in human skin. *Eur. J. Pharm. Sci.* 35 (3), 193–202. doi:10.1016/j.ejps.2008.06.016

Brownlow, R. J., Dagnall, K. E., and Ames, C. E. (2012). A comparison of DNA collection and retrieval from two swab types (cotton and nylon flocked swab) when processed using three QIAGEN extraction methods. *J. forensic Sci.* 57 (3), 713–717. doi:10.1111/j.1556-4029.2011.02022.x

Bruijns, B. B., Tiggelaar, R. M., and Gardeniers, H. (2018). The extraction and recovery efficiency of pure DNA for different types of swabs. *J. forensic Sci.* 63 (5), 1492–1499. doi:10.1111/1556-4029.13837

Caffarel-Salvador, E., Kim, S., Soares, V., Tian, R. Y., Stern, S. R., Minahan, D., et al. (2021). A microneedle platform for buccal macromolecule delivery. *Sci. Adv.* 7 (4), eabe2620. doi:10.1126/sciadv.abe2620

Chen, B. Z., Liu, J. L., Li, Q. Y., Wang, Z. N., Zhang, X. P., Shen, C. B., et al. (2019). Safety evaluation of solid polymer microneedles in human volunteers at different application sites. *ACS Appl. Bio Mater.* 2 (12), 5616–5625. doi:10.1021/acsabm.9b00700

Chen, C.-H., Tsai, Y.-T., Chou, C.-A., Weng, S.-J., Lee, W.-C., Hsiao, L.-W., et al. (2022). Evaluating different strategies on the blood collection counter settings to improve patient waiting time in outpatient units. *Inq. J. Health Care Organ. Provis. Financing* 59, 004695802210957. doi:10.1177/00469580221095797

Chen, X., Jorgenson, E., and Cheung, S. T. (2009). New tools for functional genomic analysis. *Drug Discov. Today* 14 (15-16), 754–760. doi:10.1016/j.drudis.2009.05.005

Cheng, H.-Y., Lu, C.-Y., Huang, L.-M., Lee, P.-I., Chen, J.-M., and Chang, L.-Y. (2016). Increased frequency of peripheral venipunctures raises the risk of central-line associated bloodstream infection in neonates with peripherally inserted central venous catheters. *J. Microbiol. Immunol. Infect.* 49 (2), 230–236. doi:10.1016/j.jmii.2014.06.001

Cohen, J. (2013). *Statistical power analysis for the behavioral sciences*. New York: Academic Press.

Donohue, D. E., Gautam, A., Miller, S.-A., Srinivasan, S., Abu-Amara, D., Campbell, R., et al. (2019). Gene expression profiling of whole blood: a comparative assessment of RNA-stabilizing collection methods. *PloS one* 14 (10), e0223065. doi:10.1371/journal.pone.0223065

Fernando, G. J., Hickling, J., Flores, C. M. J., Griffin, P., Anderson, C. D., Skinner, S. R., et al. (2018). Safety, tolerability, acceptability and immunogenicity of an influenza vaccine delivered to human skin by a novel high-density microprojection array patch (Nanopatch™). *Vaccine* 36 (26), 3779–3788. doi:10.1016/j.vaccine.2018.05.053

Fukuroku, K., Narita, Y., Taneda, Y., Kobayashi, S., and Gayle, A. A. (2016). Does infrared visualization improve selection of venipuncture sites for indwelling needle at the forearm in second-year nursing students? *Nurse Educ. Pract.* 18, 1–9. doi:10.1016/j.nepr.2016.02.005

Gill, H. S., Denson, D. D., Burris, B. A., and Prausnitz, M. R. (2008). Effect of microneedle design on pain in human volunteers. *Clin. J. pain* 24 (7), 585–594. doi:10.1097/ajp.0b013e31816778f9

Griffin, P., Elliott, S., Krauer, K., Davies, C., Skinner, S. R., Anderson, C. D., et al. (2017). Safety, acceptability and tolerability of uncoated and excipient-coated high density silicon micro-projection array patches in human subjects. *Vaccine* 35 (48), 6676–6684. doi:10.1016/j.vaccine.2017.10.021

Gupta, J., Gill, H. S., Andrews, S. N., and Prausnitz, M. R. (2011). Kinetics of skin resealing after insertion of microneedles in human subjects. *J. Control. release* 154 (2), 148–155. doi:10.1016/j.jconrel.2011.05.021

Haq, M. I., Smith, E., John, D. N., Kalavala, M., Edwards, C., Anstey, A., et al. (2009). Clinical administration of microneedles: skin puncture, pain and sensation. *Biomed. Microdevices* 11 (1), 35–47. doi:10.1007/s10544-008-9208-1

International, C. (2004). Human Genome Sequencing: finishing the euchromatic sequence of the human genome. *Nature* 431 (7011), 931–945. doi:10.1038/nature03001

Jeong, H.-R., Lee, H.-S., Choi, I.-J., and Park, J.-H. (2017). Considerations in the use of microneedles: pain, convenience, anxiety and safety. *J. drug Target.* 25 (1), 29–40. doi:10.1080/1061186x.2016.1200589

Kam, K.-q., Yung, C. F., Maiwald, M., Chong, C. Y., Soong, H. Y., Loo, L. H., et al. (2020). Clinical utility of buccal swabs for severe acute respiratory syndrome coronavirus 2 detection in coronavirus disease 2019–infected children. *J. Pediatr. Infect. Dis. Soc.* 9 (3), 370–372. doi:10.1093/jpids/piaa068

Kaushik, S., Hord, A. H., Denson, D. D., McAllister, D. V., Smitra, S., Allen, M. G., et al. (2001). Lack of pain associated with microfabricated microneedles. *Anesth. Analgesia* 92 (2), 502–504. doi:10.1097/00000539-200102000-00041

Kim, Y.-C., Park, J.-H., and Prausnitz, M. R. (2012). Microneedles for drug and vaccine delivery. *Adv. drug Deliv. Rev.* 64 (14), 1547–1568. doi:10.1016/j.addr.2012.04.005

Kim, Y.-S., Kim, J., Na, W., Sung, G.-H., Baek, S.-K., Kim, Y. K., et al. (2022). Development of a microneedle swab for acquisition of genomic DNA from buccal cells. *Front. Bioeng. Biotechnol.* 10, 829648. doi:10.3389/fbioe.2022.829648

Lee, H. C., and Ladd, C. (2001). Preservation and collection of biological evidence. *Croat. Med. J.* 42 (3), 225–228.

Manolio, T. A., Brooks, L. D., and Collins, F. S. (2008). A HapMap harvest of insights into the genetics of common disease. *J. Clin. Invest.* 118 (5), 1590–1605. doi:10.1172/jci34772

McBride, C. M., Wade, C. H., and Kaphingst, K. A. (2010). Consumers' views of direct-to-consumer genetic information. *Annu. Rev. Genomics Hum. Genet.* 11 (1), 427–446. doi:10.1146/annurev-genom-082509-141604

McHugh, M. L. (2012). Interrater reliability: the kappa statistic. *Biochem. medica* 22 (3), 276–282. doi:10.11613/bm.2012.031

Park, J.-H., Allen, M. G., and Prausnitz, M. R. (2005). Biodegradable polymer microneedles: fabrication, mechanics and transdermal drug delivery. *J. Control. release* 104 (1), 51–66. doi:10.1016/j.jconrel.2005.02.002

Samant, P. P., Niedzwiecki, M. M., Raviele, N., Tran, V., Mena-Lapaix, J., Walker, D. I., et al. (2020). Sampling interstitial fluid from human skin using a microneedle patch. *Sci. Transl. Med.* 12 (571), eaaw0285. doi:10.1126/scitranslmed.aaw0285

Santos, S. D. C., Fávaro-Moreira, N. C., Abdalla, H. B., Augusto, G. G. X., Costa, Y. M., Volpato, M. C., et al. (2021). A crossover clinical study to evaluate pain intensity from microneedle insertion in different parts of the oral cavity. *Int. J. Pharm.* 592, 120050. doi:10.1016/j.ijpharm.2020.120050

Theda, C., Hwang, S. H., Czajko, A., Loke, Y. J., Leong, P., and Craig, J. M. (2018). Quantitation of the cellular content of saliva and buccal swab samples. *Sci. Rep.* 8 (1), 6944. doi:10.1038/s41598-018-25311-0

Vagnoli, L., Caprilli, S., Vernucci, C., Zagni, S., Mugnai, F., and Messeri, A. (2015). Can presence of a dog reduce pain and distress in children during venipuncture? *Pain Manag. Nurs.* 16 (2), 89–95. doi:10.1016/j.pmn.2014.04.004

Walker, A. H., Najarian, D., White, D. L., Jaffe, J., Kanetsky, P. A., and Rebbeck, T. R. (1999). Collection of genomic DNA by buccal swabs for polymerase chain reaction-based biomarker assays. *Environ. health Perspect.* 107 (7), 517–520. doi:10.1289/ehp.99107517

Wewers, M. E., and Lowe, N. K. (1990). A critical review of visual analogue scales in the measurement of clinical phenomena. *Res. Nurs. Health* 13 (4), 227–236. doi:10.1002/nur.4770130405

Wise, N. M., Wagner, S. J., Worst, T. J., Sprague, J. E., and Oechsle, C. M. (2021). Comparison of swab types for collection and analysis of microorganisms. *MicrobiologyOpen* 10 (6), e1244. doi:10.1002/mbo3.1244

Yip, L., Fuhlbrigge, R., Atkinson, M. A., and Fathman, C. G. (2017). Impact of blood collection and processing on peripheral blood gene expression profiling in type 1 diabetes. *BMC Genomics* 18 (1), 636. doi:10.1186/s12864-017-3949-2

frontiers | Frontiers in Bioengineering and Biotechnology

TYPE Review
PUBLISHED 08 January 2024
DOI 10.3389/fbioe.2023.1327441

OPEN ACCESS

EDITED BY
Tianlong Li,
Harbin Institute of Technology, China

REVIEWED BY
Zhijie Huan,
Xiamen University of Technology, China
Junyang Li,
Ocean University of China, China

*CORRESPONDENCE
Hao Yang,
yhao@suda.edu.cn
Fuzhou Niu,
fzniu@usts.edu.cn

†These authors have contributed equally to this work

RECEIVED 25 October 2023
ACCEPTED 04 December 2023
PUBLISHED 08 January 2024

CITATION
Bo Y, Wang H, Niu H, He X, Xue Q, Li Z, Yang H and Niu F (2024), Advancements in materials, manufacturing, propulsion and localization: propelling soft robotics for medical applications.
Front. Bioeng. Biotechnol. 11:1327441.
doi: 10.3389/fbioe.2023.1327441

Advancements in materials, manufacturing, propulsion and localization: propelling soft robotics for medical applications

Yunwen Bo[1†], Haochen Wang[1†], Hui Niu[2†], Xinyang He[1], Quhao Xue[1], Zexi Li[1], Hao Yang[3*] and Fuzhou Niu[1*]

[1]School of Mechanical Engineering, Suzhou University of Science and Technology, Suzhou, China, [2]Department of Pathology, Second Affiliated Hospital of Soochow University, Suzhou, China, [3]Robotics and Microsystems Center, School of Mechanical and Electrical Engineering, Soochow University, Suzhou, China

Soft robotics is an emerging field showing immense potential for biomedical applications. This review summarizes recent advancements in soft robotics for *in vitro* and *in vivo* medical contexts. Their inherent flexibility, adaptability, and biocompatibility enable diverse capabilities from surgical assistance to minimally invasive diagnosis and therapy. Intelligent stimuli-responsive materials and bioinspired designs are enhancing functionality while improving biocompatibility. Additive manufacturing techniques facilitate rapid prototyping and customization. Untethered chemical, biological, and wireless propulsion methods are overcoming previous constraints to access new sites. Meanwhile, advances in tracking modalities like computed tomography, fluorescence and ultrasound imaging enable precision localization and control enable *in vivo* applications. While still maturing, soft robotics promises more intelligent, less invasive technologies to improve patient care. Continuing research into biocompatibility, power supplies, biomimetics, and seamless localization will help translate soft robots into widespread clinical practice.

KEYWORDS

soft robotics, medical applications, intelligent materials, manufacturing methods, localization technology

1 Introduction

The definition of soft robotics has been continuously evolving since the first prototypes were developed in the late 1990s, as relevant materials, actuation technologies, fabrication procedures, and applications have adapted to new scientific advances (Suzumori et al., 1992; Tondu and Lopez, 2000). One of the most important yet simplest definitions uses Young's modulus, ranging from 10^4 to 10^9 Pascals, to define "Soft" (Majidi, 2014; Rus and Tolley, 2015; Hartmann et al., 2021). This definition is well-suited to characterize the majority of early bio-inspired soft robot samples, but excludes many later developed robots that incorporate embedded rigid components. An additional advancing definition is that if a robot is constructed from materials that are relatively soft and safe compared to its operating environment, it can be classified as a soft robot, even if it is of some rigid components or structures (Cheney et al., 2015; Chen et al., 2017). To date, numerous soft robotics studies have incorporated rigid components within their actuation modules or internal structures with variable stiffness, enabling adaptation to surroundings and safe interaction with

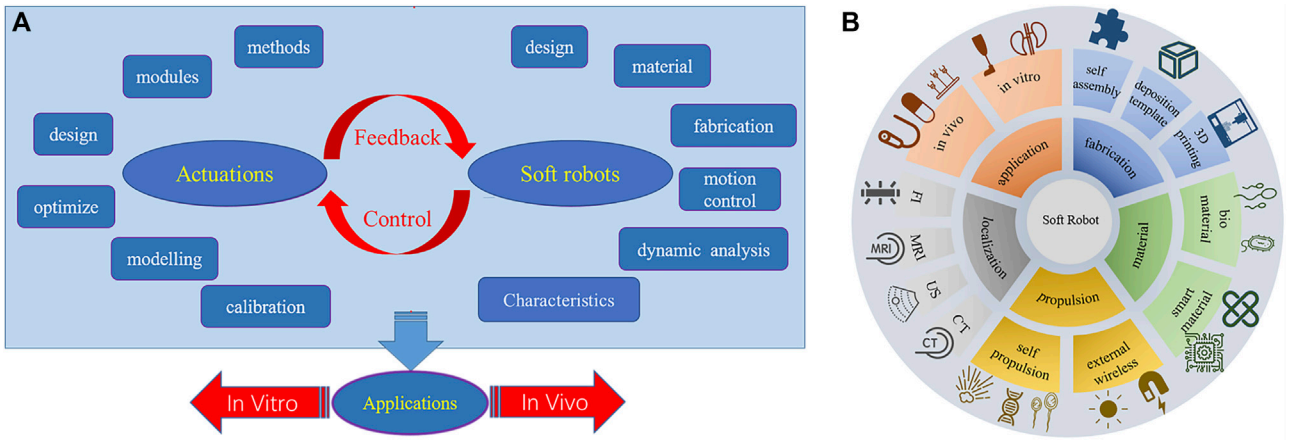

FIGURE 1
(A) considerations in the design and construction of soft robots. **(B)** summarized aspects in this paper.

organisms (Lee et al., 2017; Medina-Sánchez et al., 2018; Thalman and Artemiadis, 2020). Potential applications for soft robots span industrial to medical scenarios, including but not limited to grasping, targeted drug delivery, monitoring, rehabilitation, function verification, diagnosis, and treatment (Rao et al., 2015; Al-Fahaam et al., 2016; Li et al., 2016a; Chen X.-Z. et al., 2017; Yang G.-Z. et al., 2019; Kim H. et al., 2020; Terzopoulou et al., 2020; Dupont et al., 2021; Zhou and Alici, 2022; Kortman et al., 2023). In particular, the possibility of using soft robots in minimally invasive therapies may represent a paradigm shift in medical treatments. Their high accessibility, adaptability, and safety when operating in the complex *in vivo* environment with multiphase physics offers significant benefits (Chautems et al., 2019; Wang C. et al., 2022).

Soft robotics has emerged as a transformative technology in the field of biomedicine, offering promising solutions for both *in vitro* and *in vivo* applications. *In vitro* (Hui and Régnier, 2011; Li et al., 2020; Zhang S. et al., 2022; Li et al., 2022), soft robots have played a pivotal role in advancing disease modeling, cell and tissue culture engineering, environmental monitoring, surgical assistance, and rehabilitation therapies. These platforms empower researchers to investigate disease processes, screen drugs, and optimize treatment plans, particularly in disease models involving the rectum, respiratory system, heart, and other vital organs. In the domain of *in vivo* applications (Li et al., 2017; Xing et al., 2020; Law et al., 2022; Ma et al., 2022; Wang et al., 2023), soft robots offer distinct advantages such as minimally invasive capabilities, compact dimensions, remote controllability, biocompatibility, and adaptability to complex fluidic environments. They hold tremendous potential in targeted drug delivery, biopsy sampling, thrombus dissolution, and minimally invasive procedures spanning various medical disciplines, including cardiology and oncology. Recent advancements have yielded innovative solutions, including magnetically actuated robotic capsules designed for site-specific drug delivery (Shimanovich et al., 2014), soft robotic capsules with fine needle biopsy capabilities for precise tissue sampling, and untethered flexible manipulators for challenging *in vivo* biopsies (Rehan et al., 2020). Soft catheters, among the most promising soft architectural designs for practical applications, are playing a pivotal role in thrombus treatment and cardiac arrhythmia intervention by facilitating direct drug delivery, cardiac tissue modulation, and even *in vivo* bioprinting. They offer minimally invasive, highly efficient solutions for addressing these critical cardiovascular conditions.

To harness the potential applications of soft robotics, several critical factors must be taken into accounts. While soft robots can manifest in various forms, two fundamental considerations in the construction of a soft robotic system are the robot's design and actuation, with control strategy serving as an integrative bridge between these components, illustrated in Figure 1A. The design of the robot encompasses various facets, including structural considerations, material selection, fabrication techniques, functional specifications, physicochemical characterization, kinematic properties, and biocompatibility. Materials can span a spectrum from hydrogels to elastomers, tailored to achieve desired attributes such as stiffness, haptic feedback, and biodegradability (Wang X. et al., 2022; Middelhoek et al., 2022; Chen et al., 2023). The fabrication process benefits from the use of rapid prototyping techniques like three dimensional (3D) printing and molding (Liu et al., 2015; Yang et al., 2015; Wu et al., 2016; Li J. et al., 2018; Yang et al., 2020). The second pivotal factor is actuation (Xuan et al., 2016; Gao et al., 2019; Hou et al., 2023; Tang et al., 2023), which spans options such as pneumatic systems, hydraulic systems, and smart materials like shape memory alloys (SMA) or dielectric elastomers (DE). Proper actuation involves selecting the appropriate actuation mechanism and medium, modeling and calibrating the dynamic actuation field, and precisely regulating the magnitude and distribution of forces and motions. Closed-loop feedback control connects the robot to the actuator by modulating the actuation field based on sensory inputs that monitor the robot's state and its environment. This control mechanism facilitates the realization of the robot's predetermined motions and functions.

Soft robotics is an emerging field that holds significant potential for medical applications due to the inherent flexibility, adaptability, and biocompatibility of soft robots compared to traditional rigid robots. This review summarizes recent advancements in soft robotics for diagnostic, therapeutic,

and rehabilitative purposes, overing aspects such as applications, materials and fabrication, actuation and localization, illustrated in Figure 1B, as well as addressing challenges and prospects for the future. *In vitro* applications of soft robots outside the body include disease modeling, drug screening, surgical assistance, rehabilitation, and medical imaging. For *in vivo* applications, soft robots enable minimally invasive capabilities like targeted drug delivery, biopsy sampling, and precision surgery by navigating narrow spaces inside the body. Soft robot materials and manufacturing methods are also discussed, with a focus on intelligent materials like stimuli-responsive hydrogels and self-healing biomaterials that enhance functionality. Rapid fabrication techniques including 3D printing and self-assembly facilitate iterative design. For *in vivo* navigation systems, propulsion mechanisms can be categorized into two primary categories based on their energy sources: self-contained and external wireless propulsion. Self-contained relies on internal energy sources within the device itself, such as tendon-driven, chemical fuels, and biomechanical motion. External wireless propulsion refers to the wireless driving of the device through externally generated sources such as magnetics, acoustics, or optics. Precise localization during *in vivo* operation is enabled by tracking modalities such as fluorescence imaging (FI), magnetic resonance imaging (MRI), ultrasound (US), and computed tomography (CT) scans. Key challenges for translating soft robots into clinical practice include biocompatibility, degradability, biomimetic design, and tracking/visualization capabilities. Furthermore, with continuing research into intelligent materials, bioinspired design, propulsion, and localization, soft robots can enable the next-generation of diagnostic, therapeutic, and rehabilitative technologies.

2 Medical applications

Soft robots can offer several benefits over traditional rigid robots in terms of usages in medical applications. They are often more flexible and can conform to complex surfaces, and are also safer to interact with delicate tissues and organs, as they do not cause physical damage or trauma. The development of advanced soft robotics technology will likely lead to even more innovative applications in medicine. As materials science and engineering continue to advance, soft robots may become increasingly adaptable to various environments and able to perform more complex tasks. As a rapidly evolving field, robotic surgery (Li et al., 2010) not only reduces the workload for medical staffs and alleviates patients' suffering but also finds extensive application in both *in vivo* and *in vitro* medical tasks. Soft robots exhibit substantial promise in medical applications, due to their remarkable flexibility, adaptability, and safety features. Soft robots are proficient in tasks such as precise lesion localization, minimally invasive tissue resection, targeted drug delivery, and various surgical procedures. They also hold the potential to evolve into exoskeletons for rehabilitation purposes, with a wide range of potential applications (Ding et al., 2017). This chapter will focus on summarizing the potential medical applications of soft robots.

2.1 In vitro

In vitro medical applications of soft robots include but not limit to: environmental monitoring (Rao et al., 2015; Chen X.-Z. et al., 2017), surgical assistance (Kim H. et al., 2020), rehabilitation therapy (Al-Fahaam et al., 2016), targeted delivery (Li et al., 2022), developing disease models (Roche et al., 2017; Zrinscak et al., 2023), functional structures (Calderon et al., 2019; Pang et al., 2021; Ying et al., 2021) and tissue engineering (Zhou Y. et al., 2021). Solovev et al. (2010) wirelessly controlled microrobots using external magnets to assist with loading, transport, delivery, and assembly of microparticles and nanosheets in fuel solutions, shown in Figure 2A. Given ethical constraints, direct *in vivo* experimentation with humans can be highly complex, so establishing accurate *in vitro* disease models is crucial for furthering soft robotics in biomedicine. In Zrinscak et al. (2023), the authors introduce disease models of the gastrointestinal tract, respiratory system, cardiovascular system, and other organs amenable to soft robotics research. Adams et al. (2017) fabricated a kidney using diverse materials, illustrated in Figure 2B. Roche et al. (2017) developed a device to enhance cardiac function and performed *in vitro* experiments shown in Figure 2C. Zhou C. et al. (2021) achieved direct ink writing of flexible, stretchable conductive traces via ferromagnetic soft catheter robot (FSCR), shown in Figure 2D. Rehan et al. (2020) conceptualized a computer aided design (CAD) based capsule robot design comprised of an actuation mechanism and sampling mechanism shown in Figure 2E. With soft robotic cell culture platforms, clinicians and scientists can better study disease processes, screen pharmacological agents, and optimize therapeutic regimens. Another promising exterior application is wearable devices to provide ambulatory assistance and gait rehabilitation for patients with mobility impairments (Li et al., 2018). Compared to rigid exoskeletons, soft exoskeletons are lighter, more compliant, and less restrictive of the user's natural movements, promising greater comfort. As one example, Yang X. et al. (2019) developed a soft, continuous exoskeleton mimicking the spine to aid with bending and lifting activities, designed to conform to human anatomy and reduce forces on the back. Ying et al. (2021) designed artificial ionic skins with multifunctional strong adhesives that exhibit high stretchability, anti-freezing ability, and environmental stability in Figure 2F. Moreover, soft robotics can enhance imaging techniques. A novel soft robotic effector was proposed aiming at safely obtain standard views required for prenatal diagnostic fetal US exams. Its adjustable shape conforms to varied maternal anatomies, enabling more flexible and reliable fatal imaging (Lindenroth et al., 2020). In summary, while soft robots demonstrate immense potential in *ex vivo* contexts, their *in vivo* applications are more anticipated. However, at present, this field is still in its infancy, experiencing both laboratory demonstrations and industrial development. It still leaves a last step for being truly utilized in medical applications. Currently, for achieving *in vivo* applications, there often lack sufficient strength, stability, and precision to perform complex surgical tasks. Additionally, their sensors and control systems require further improvement to achieve more accurate and reliable operation.

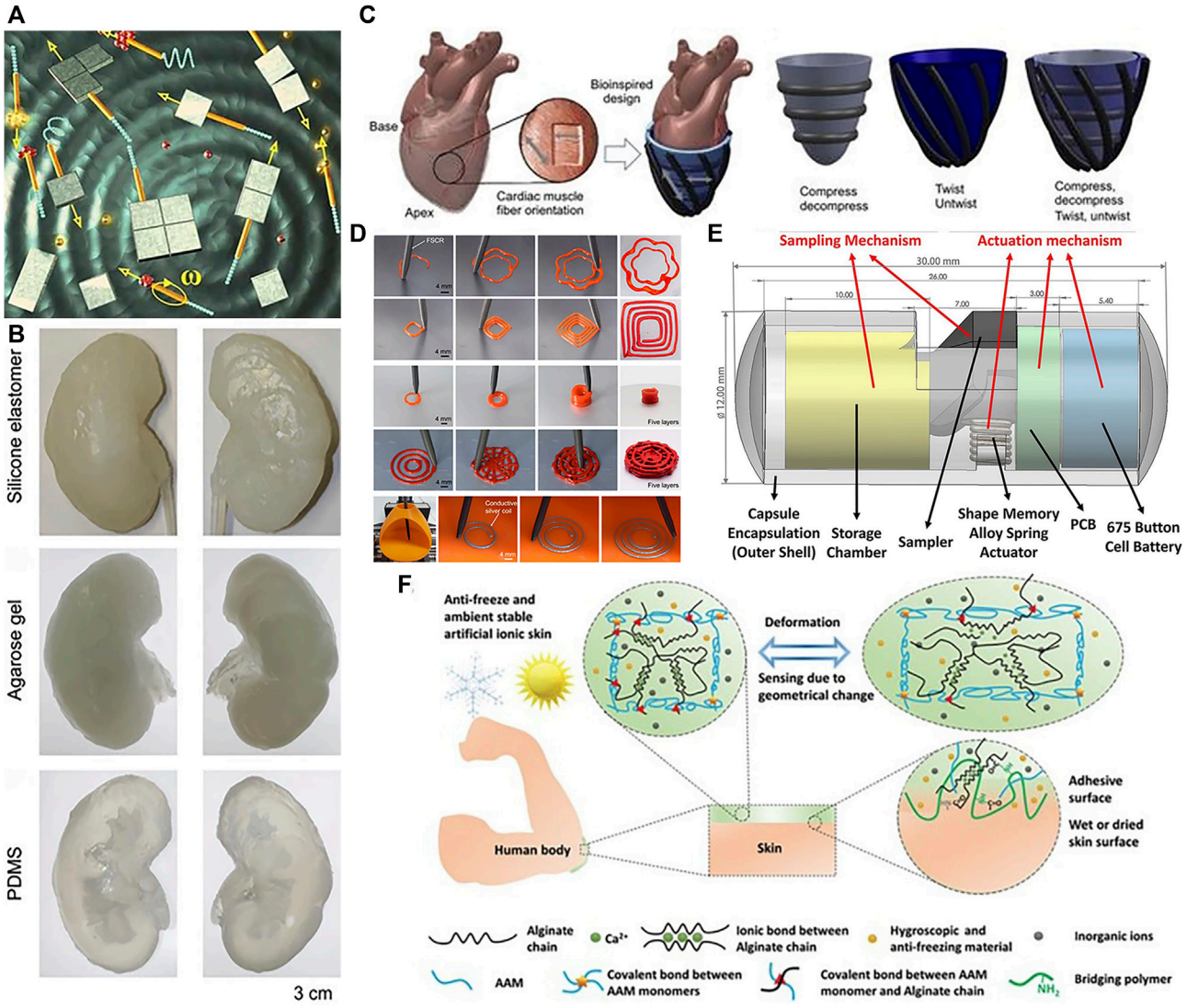

FIGURE 2
In vitro applications of soft robots. **(A)** Microsurgery. Reproduced with permission (Solovev et al., 2010). Copyright 2010, Wiley. **(B)** Kidney organoid. Reproduced with permission (Adams et al., 2017). Copyright 2016, ABE. **(C)** Enhance cardiac. Reproduced with permission (Roche et al., 2017). Copyright 2017, AAAS. **(D)** Ink writing. Reproduced with permission (Zhou C. et al., 2021). Copyright 2021, Springer Nature. **(E)** Capsule robots that can perform biopsy sampling. Reproduced with permission (Rehan et al., 2020). Copyright 2020, Wiley. **(F)** Artificial ionic skins. Reproduced with permission (Ying et al., 2021). Copyright 2021, Wiley.

2.2 In vivo

Soft robots enable unique capabilities for minimally invasive endoscopic surgeries (Gifari et al., 2019), permitting direct puncturing, cutting, or extracting of cells and tissues with extreme precision down to the cellular scale. Compared to bulky rigid robots, soft robots can traverse narrow blood vessels and anatomical tracts to access lesions at hard-to-reach interior locations. Advantages like small sizes (Ren et al., 2021), remote controllability (Zhou C. et al., 2021), biocompatibility, adaptability to low Reynolds number fluid environments (Digumarti et al., 2018), and facile conversion of external power to motion make soft robots well-suited for *in vivo* use. Consequently, soft robots hold tremendous potential for targeted drug delivery, biopsy sampling, thrombus dissolution and other minimally invasive procedures (Wang et al., 2017), while continuing to break new ground in cardiology (Chautems et al., 2019), oncology (Forbes, 2010; Luo et al., 2016) and other medical fields. Current *in vivo* soft robotic systems mainly take the forms of capsules (Basar et al., 2018), catheters, microgrippers, and micro/nanomotors that harness nanotechnology for precise motion control. Pokki et al. (2017) validated the potential of soft robots, which can be injected into rabbit, for ocular disease diagnosis, therapy, and drug delivery, shown in Figure 3A. Achieving localized targeted drug delivery (Shimanovich et al., 2014) can effectively avoid these pitfalls, spurring intense research in biomedicine. Zhou and Alici (2022) proposed a magnetically actuated robotic capsule for site-specific drug release in the gastrointestinal tract. The capsule contains an extendable needle to directly inject drugs into diseased tissues, enabling rapid absorption and enhanced delivery efficacy.

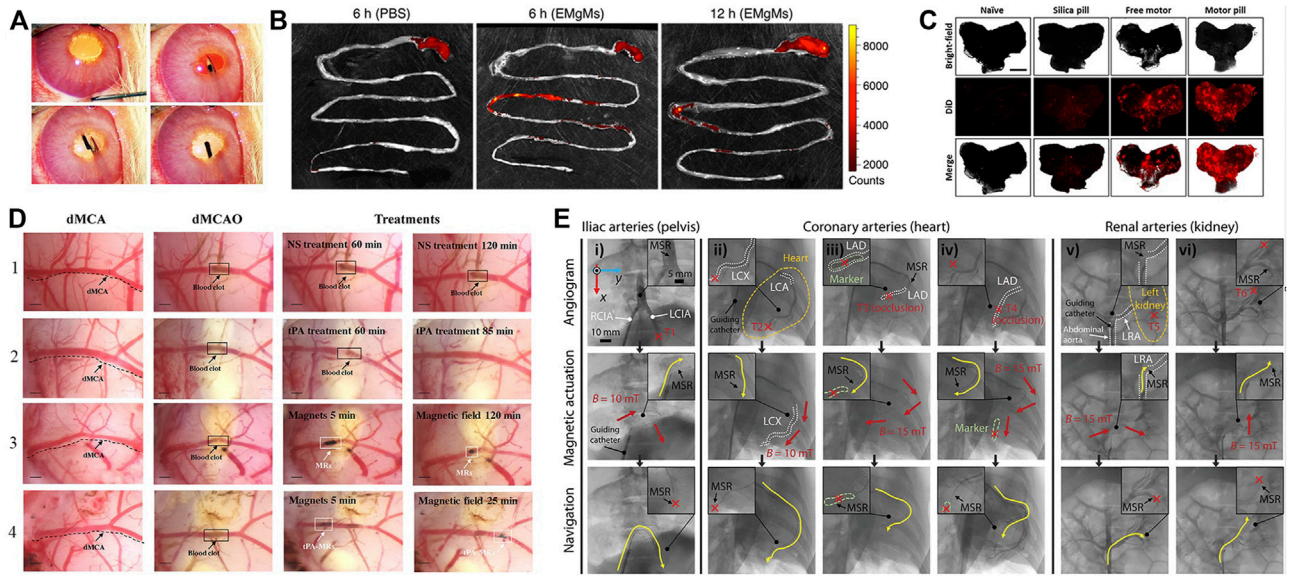

FIGURE 3
In vivo applications of soft robots. **(A)** Work in vitreous. Reproduced with permission (Pokki et al., 2017). Copyright 2016, Wiley. **(B)** Targeted delivery in Gastrointestinal. Reproduced with permission (Li et al., 2016b). Copyright 2016, ACS. **(C)** Targeted delivery in stomach. Reproduced with permission (Karshalev et al., 2018). Copyright 2018, ACS. **(D)** Thrombolysis by tissue plasminogen activator (tPA) microrods. Reproduced with permission (Hu et al., 2018). Copyright 2018, ACS. **(E)** Navigation of microrobotic guidewire. Reproduced with permission (Hwang et al., 2022). Copyright 2022, Wiley.

Lu et al. (2018) designed soft robots capable of rapid locomotion in environments like the stomach, enabling targeted drug delivery via cargo capsules. Additionally, a multilayered microrobot termed metal-organic framework (MOF) to qualify as small-scale robot was developed, with each layer providing distinct functionality (Terzopoulou et al., 2020), it enables targeted drug delivery by loading therapeutics into biodegradable drug carriers. Preliminary depictions have emerged for future integrated application scenarios of 3D printing *in vivo* and biodegradable microrobotic swimmers (Ceylan et al., 2019). Li et al. (2016b) proposed an intestinal micromotor system using micromotors coated with an enteric polymer layer to convey payloads to specific locations. Propulsion activated at the target site enabled local tissue penetration and retention, as shown in Figure 3B, achieving directional transportation in the jejunum. Similarly, Karshalev et al. (2018) proposed micromotor pills for cargo delivery focused on the stomach, achieving higher retention compared to other methods as shown in Figure 3C.

Common tissue sampling techniques like surgery, needle aspiration, and biopsy carry procedural risks while often yielding insufficient or inaccurate samples affected by surrounding tissues. With advances in *in vivo* soft robotics, soft robots guided by imaging can access tumor or lesion sites to perform tissue and cell sampling in a safer, more efficient, and thorough manner, significantly enhancing diagnostic accuracy and utility. For example, a magnetically-driven soft robotic capsule for fine oligonucleotide analogs can capture and isolate proteins. Additionally, antibody-coated microrockets allow selective capture and separation of cancer cells for diagnosis and therapy (Li et al., 2016a). Diller and Sitti (2014) proposed untethered, precisely manipulative microgrippers capable of non-invasive access to confined spaces for executing out-of-plane 3D operations and assembly tasks to create complex 3D materials and structures.

Medical catheters can administer thrombolytic drugs or physically intervene in cardiac tissues to enable treatment of thrombosis and cardiac arrhythmias. Thrombosis, characterized by clot formation obstructing blood vessels, is a high-incidence cardiovascular disease warranting novel therapies. As a high-incidence cardiovascular disease, thrombus treatment has attracted much attention. Thrombi are solid clotted masses formed from components in the blood that block blood vessel lumens, disrupt blood flow and thus cause other cardiovascular diseases. Conventional treatments like anticoagulants, thrombolytics, aspiration, surgical removal, or stenting each have limitations in invasiveness, efficacy, or recurrence risk. Ideal thrombosis treatment should rapidly and thoroughly dissolve clots in a minimally invasive manner without increasing bleeding risk. Hu et al. (2018) overcame limitations of standalone tPA thrombolysis using modified tPA-loaded microrobots, significantly improving thrombolytic efficacy in Figure 3D. Intravenously injected microrobots could be renally excreted without damaging kidneys or liver, enabling effective treatment for ischemic stroke. Soft robotic catheters hold great potential for *in vivo* thrombolytic interventions. In Figure 3E, Hwang et al. (2022) proposed a microrobotic system for real-time remote manipulation of micro-guidewires by physicians. The multifunctional soft robot catheter put forward (Rogatinsky et al., 2023) can achieve stable, dexterous, and efficacious performance within the heart, surmounting core impediments stemming from dimensional disparities, maneuverability requirements, and remote operability, while concurrently expanding possibilities for minimally invasive intracardiac procedures. Clinical studies in coronary, iliac, and renal arteries demonstrated feasibility and effectiveness. Similarly,

arrhythmias arising from irregular cardiac electrical patterns can be addressed by soft cardiac ablation devices capable of precise electrophysiology modulation. Beyond drug delivery and tissue intervention, soft robotic catheters also demonstrate promise for *in vivo* bioprinting. For example, Zhou C. et al. (2021) utilized a magnetically-driven soft catheter to conduct minimally invasive bioprinting inside the body.

3 Materials and manufacturing

A crucial distinction between soft robots and traditional rigid robots is the utilization of highly stretchable, flexible materials. The most common materials used in soft robotics are silicone, elastomers, and hydrogels. Silicone robots are made from a flexible and durable silicone material, while elastomer robots are made from a viscoelastic material that can be stretched and compressed. Hydrogel robots are composed of a water-based gel that can be easily molded and shaped. Ideal materials possess high elongation (>200%) and low Young's modulus (0.1–10 MPa) (Rus and Tolley, 2015; Hartmann et al., 2021; Zhu et al., 2023), while Polydimethylsiloxane (PDMS) (Shepherd et al., 2011; Gossweiler et al., 2015; Lu et al., 2018) and Ecoflex (Shepherd et al., 2011; Rusu et al., 2023) are prevalent in existing soft robots. We highlight emerging smart materials that could enhance soft robotic performance and efficacy in this chapter. In particular, stimuli-responsive hydrogels (Panda et al., 2023) capable of altering their shape or mechanical properties on demand could enable soft robots to adapt to dynamic *in vivo* environments. We summarized the materials involved in this paper in Supplementary Table S1.

3.1 Materials

Smart materials capable of sensing and responding to external stimuli are enabling new paradigms in soft robotics. As novel materials that can respond to external stimuli such as temperature, light, US, pH, ions, and magnetic fields by changing their properties or functions accordingly. Common smart materials include poly(N-isopropylacrylamide) (PNIPAM), liquid crystal elastomers (LCE), SMA (Song et al., 2016), MOF (Ikezoe et al., 2015), macromolecules (Tang et al., 2020), etc. Hydrogels are a versatile responsive material, exhibiting significant volume change under temperature, pH, light, and other triggers. Composite hydrogels confined with other materials can direct strain to targeted regions or directions, imparting multifunctional responsiveness (Jeon et al., 2017; Banerjee et al., 2018). The incorporation of conductive fillers can impart conductivity to hydrogels. Conductive nanofillers can provide resistivity-based tactile sensing and, via composite formation, stimulate actuation. Moreover, doping with other materials in the hydrogel matrix can enable actuation capabilities (Zhou et al., 2018). In order to enhance biocompatibility more effectively, efforts have been made to optimize biocompatibility, biocompatible hydrogels like gelatin methacryloyl (GelMA), derived from enzymatically degradable gelatin, represent a promising alternative to poly(ethylene glycol) diacrylate (PEGDA) for fabricating soft microrobotics. GelMA polymer is derived by functionalizing gelatin (a denatured and partially hydrolyzed polypeptide mixture) and can substitute PEGDA for fabricating helical microstructures. Gelatin can be digested by proteases like matrix metalloproteinase-2 (MMP-2). Compared to PEGDA, GelMA exhibits lower toxicity (Wang et al., 2018; Ceylan et al., 2019). MOFs are highly porous crystalline coordination polymers possessing desired traits for motile micro/nanodevices including high payload capacity, biodegradability, biocompatibility, and stimulatory responsiveness, can efficiently transduce stimuli into micro/nanorobot motion. Zhang X. et al. (2022) reported a near-infrared light-driven, shape-programmable hydrogel actuator by loading MOFs on a PDMS film, achieving distinct shape changes under near-infrared irradiation, and demonstrated how to fabricate MOF. Tang et al. (2020) introduced a deoxyribonucleic acid (DNA) nanorobot where DNA molecules can self-assemble and self-organize into stable structures through interactions. Moreover, the programmability of DNA allows specific functions via sequence synthesis and modification. This DNA hydrogel robot exhibits ultrasoftness and supertoughness, enabling shape adaptivity and magnetically-driven navigation in confined, unstructured spaces in Figure 4A. In addition, Ahn et al. (2019) fabricated liquid crystal elastomer-carbonate/carbon nanotube (LCE-CNT) composite films capable of reversible photoinduced bending shown in Figure 4B. Sun et al. (2022) demonstrated magnetically driven mucus microrobots using non-Newtonian fluids, which can achieve functions including grasping solid objects, swallowing and transporting harmful substances, monitoring human body movement, as well as circuit switching and repairing.

Further advancements in smart materials may enable additional capabilities, such as bio-inspired designs or self-healing functions. For example, Rogóż et al. (2016) harnessed the photosensitivity of LCE to create a soft, caterpillar-like robot driven by asymmetric illumination. The robot's segmented body deforms under patterned light to inch forward through peristaltic motion. In another demonstration, Mao et al. (2014) activated flexible SMA rays in a starfish-inspired soft robot capable of multi-modal locomotion and obstacle clearance twice its height. By combining responsive materials with bioinspired designs, these robots exemplify how smart material actuation can achieve lifelike motion in soft-bodied systems. In particular, self-healing materials hold particular promise for enhancing soft robot robustness during prolonged *in vivo* operation (Terryn et al., 2021). Polyimide (PI) is a high-performance polymer renowned for its outstanding thermal stability, mechanical robustness, and chemical resistance. The Young's modulus of PI is typically between 2.5 and 6 GPa, depending on factors like polymer structure, manufacturing technique, and temperature. When incorporated into composites, PI's excellent mechanical properties and deformability enable its use in developing soft robots that can function for prolonged periods *in vivo* (Rubehn and Stieglitz, 2010; Dong et al., 2013). Zhu et al. (2023) introduced a novel dynamic covalent PI with softness, stretchability, recoverability, rapid room-temperature self-healing, and multimodal actuation capabilities. By reducing crosslink density and utilizing intermolecular hydrogen bonding, the polymer matrix achieved softness, stretchability, recoverability, and rapid self-healing at room temperature. Through the addition of magnetic particles, wireless magnetically-controlled actuation was realized in soft robots under external magnetic fields shown in Figure 4C.

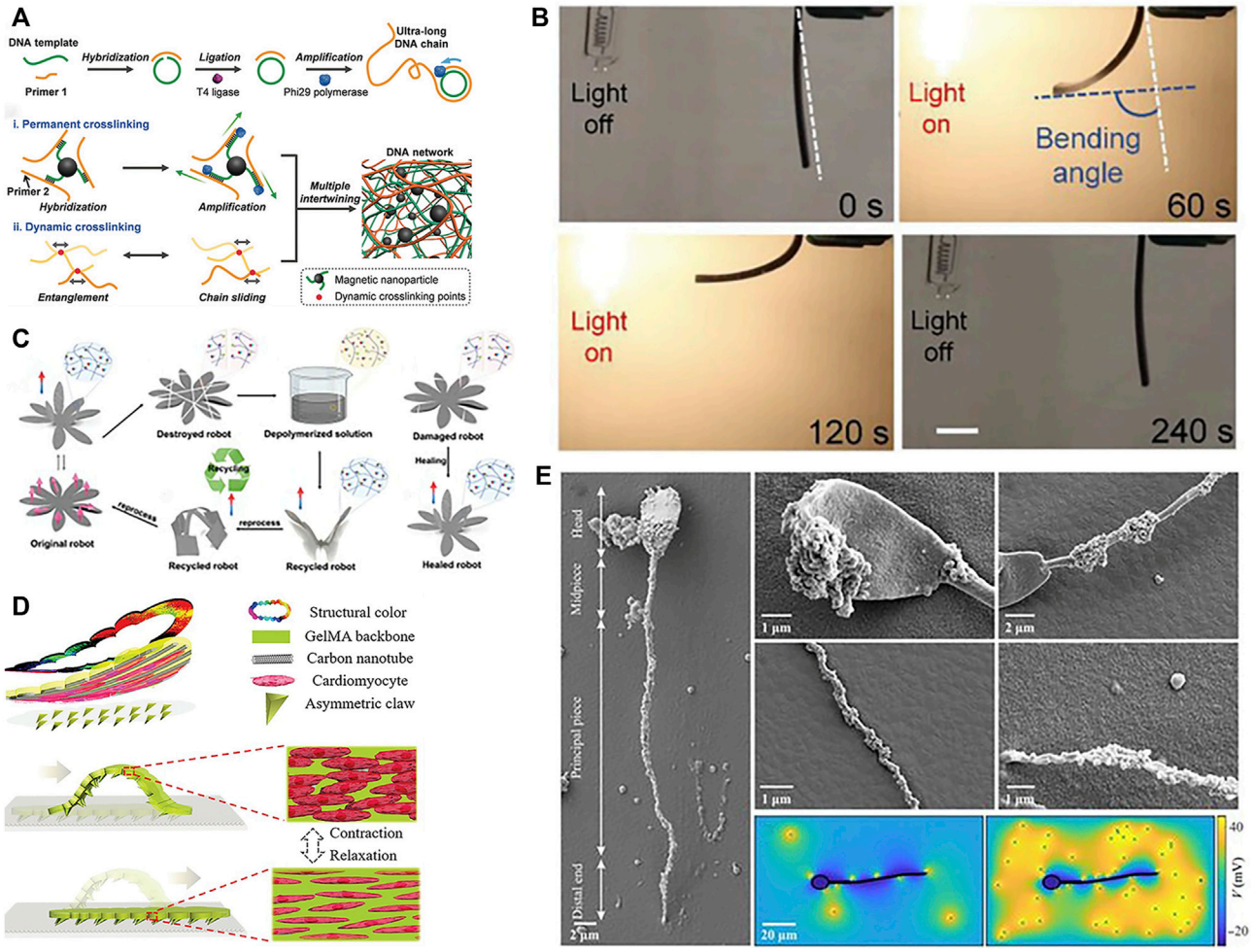

FIGURE 4
Materials of soft robots. **(A)** DNA. Reproduced with permission (Tang et al., 2020). Copyright 2019, Wiley. **(B)** Optical-stimulated material. Reproduced with permission (Ahn et al., 2019). Copyright 2019, Wiley. **(C)** Self-healing material. Reproduced with permission (Zhu et al., 2023). Copyright 2023, Wiley. **(D)** Cardiomyocytes. Reproduced with permission (Sun et al., 2019). Copyright 2019, Wiley. **(E)** Sperm. Reproduced with permission (Magdanz et al., 2020). Copyright 2020, AAAS.

In addition, biomaterials with good biocompatibility and degradability are also gradually being studied by scholars. Common biological materials that can be used for soft robot fabrication include algae, bacteria, sperm, cardiomyocytes (Sun et al., 2019), spores, etc. Sun et al. (2019) achieved crawling of soft robots driven by cardiomyocytes in Figure 4D. Sareh et al. (2013) mimicked the flagella of the alga Volvox to develop planar actuators. By optimizing the segmentation patterns and bioinspired driving signals, they successfully replicated the motion of natural cilia in artificial cilia. These exhibited good performance in low Reynolds number environments. Magdanz et al. (2020) introduced a hybrid magnetic microrobot using self-assembled non-motile sperm cells and magnetic nanoparticles. These function as biocompatible, controllable, and detectable biohybrid tools with potential for targeted *in vivo* therapies shown in Figure 4E. Justus et al. (2019) engineered a soft gripper containing engineered bacteria, a flexible light-emitting diode (LED) circuit, and a soft pneumatic actuator. Their study demonstrated that the bio-LED-actuator module can detect chemical signals by pressurizing and releasing contents of a hydrogel injected with chemicals. It can also make viable decisions using chemical sensing and feedback during pick-and-place operations, and integrating chemically responsive synthetic cells and soft materials for biosensing soft robots. As these cases illustrate, harnessing biological building blocks and bioinspired designs can impart unique capabilities to soft robots while ensuring biocompatibility.

3.2 Manufacturing methodologies

Rapid fabrication technologies like 3D printing (Joyee and Pan, 2019) and shape deposition modeling enable accelerated design iterations compared to conventional manufacturing. Wang et al. (2018) printed helical microstructures using two-photon polymerization (2PP). Next, incubating these microstructures in an aqueous suspension of magnetic iron oxide (Fe_3O_4) nanoparticles imparted magnetism, yielding biodegradable GelMA helical microrobotic swimmers shown in Figure 5A. Yin et al. (2021)

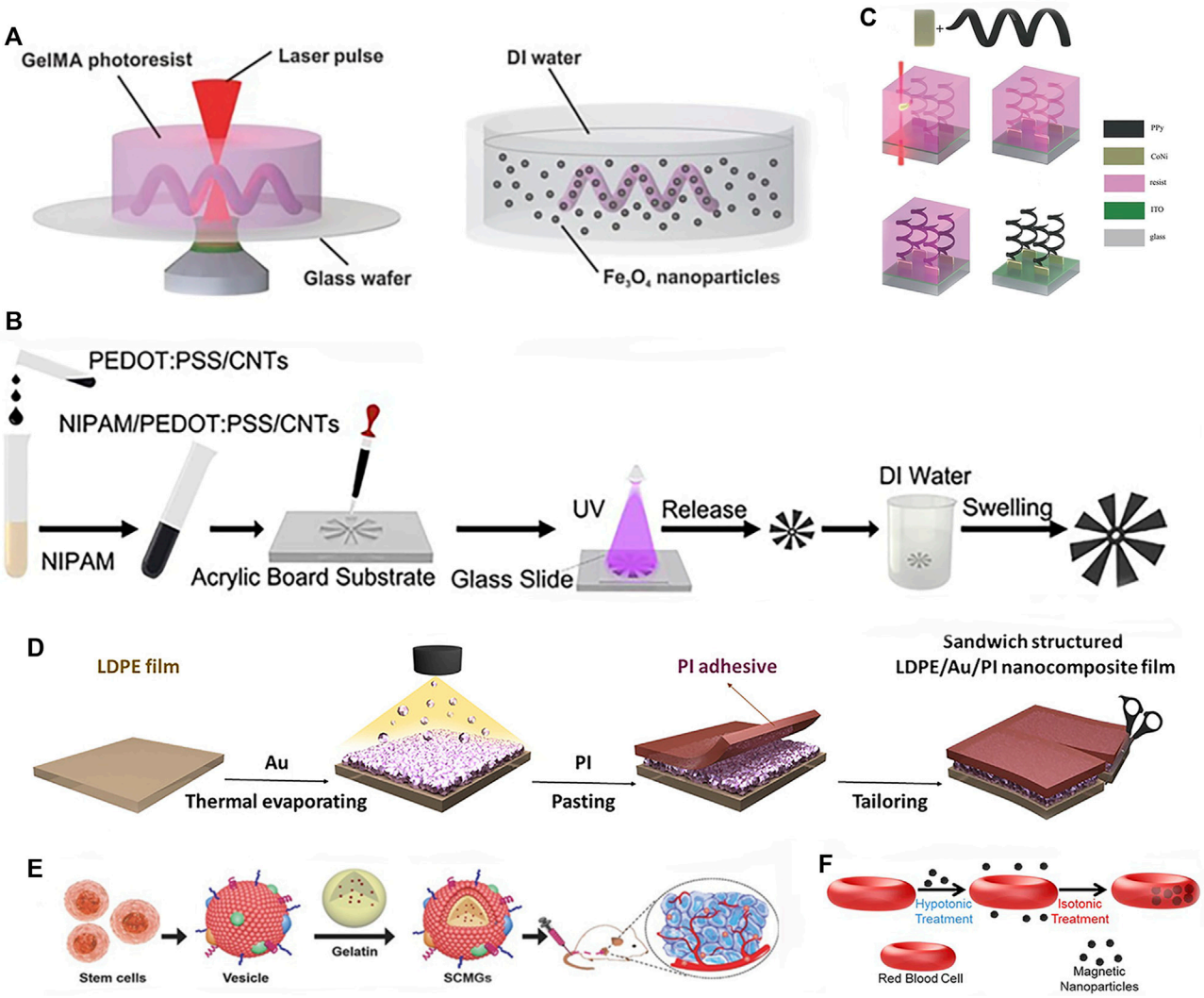

FIGURE 5
Fabrications methods of soft robots. **(A)** 2PP. Reproduced with permission (Wang et al., 2018). Copyright 2018, Wiley. **(B)** Photopolymerized and template. Reproduced with permission (Yin et al., 2021). Copyright 2021, ACS. **(C)** Template, electrodeposition and electropolymerization. Reproduced with permission (Zeeshan et al., 2014). Copyright 2013, Wiley. **(D)** Deposition. Reproduced with permission (Yu et al., 2021). Copyright 2021, Wiley. **(E)** Assembly. Reproduced with permission (Gao et al., 2016). Copyright 2016, Wiley. **(F)** Self-assembly. Reproduced with permission (Wu et al., 2014). Copyright 2014, ACS.

fabricated visible light-driven jellyfish-like miniature soft robot (JMSR) robots using molds and ultraviolet (UV) light shown in Figure 5B. By facilitating agile modification of product categories and dimensions, these advanced techniques are well-suited for iteratively prototyping soft robots with complex geometries and functionalities. The rapid prototyping of soft robots is being facilitated by numerous techniques, including 3D printing, templated deposition, and self-assembly methods. These approaches allow for the expedited fabrication of soft robot prototypes while also creating new opportunities for customized medical devices. In the following sections, we review recent advances in these promising fabrication paradigms.

3D printing enables multi-material fabrication to achieve complex structures and geometries, while providing high degrees of freedom and design flexibility. By avoiding complex machining and assembly in traditional manufacturing methods, Zhou et al. (2022) successfully printed an intermediate skeleton for a continuous robot with rigid-soft-rigid structures. Photolithography holds great promise in the fabrication of soft robots. This advanced light-based manufacturing technique demonstrates remarkable precision, scalability, material compatibility, integration of functionalities, and design flexibility, making it particularly suitable for soft robot manufacturing (Qin et al., 2014). The recent advancements in laser lithography technology and molecular alignment engineering have enabled the arbitrary 3D pattern design of LCE. By harnessing predetermined driving characteristics, these engineered LCE structures can exhibit a diverse range of motions as a cohesive unit (Rogóż et al., 2016). In addition to the aforementioned techniques, there are other manufacturing methods. The fabrication of soft robots can also be achieved through templated deposition or assembly/self-assembly approaches. Templated deposition utilizes a sacrificial mold or template to guide the structured build-up of materials, enabling

precise control over the resulting structure. Meanwhile, assembly or self-assembly methods can be used to construct soft robots by integrating and joining components either manually or automatically. Utilization of electrodeposition and electropolymerization technique in conjunction with 3D template assistance resulted in the fabrication of hybrid helical microrobots shown in Figure 5C (Zeeshan et al., 2014). Yu et al. (2021) proposed a light-responsive nanocomposite thin film that can be used for mass production of sandwich-structured devices, as shown in Figure 5D. To improve biocompatibility for better *in vivo* application, incorporating biomaterials through assembly/self-assembly approaches can effectively enhance bio-compatibility. Gao et al. (2016) developed bone marrow-derived mesenchymal stem cell membrane cloaked gelatin nanogels as an efficient tumor-targeting drug delivery platform, as shown in Figure 5E. Wu et al. (2014) fabricated red blood cell micromotors using a self-assembly approach, as depicted in Figure 5F. A novel approach is presented for the development of a bio-hybrid magnetic microrobot utilizing electrostatic self-assembly of non-motile sperm cells and magnetic nanoparticles (Magdanz et al., 2020). A method combining ordered self-assembly and sol-gel reaction was introduced to fabricate bio-inspired silica honeycomb membranes with controlled structural and chemical characteristics (Aynard et al., 2020). Overall, these advanced fabrication paradigms are overcoming traditional manufacturing limitations to unlock new horizons in soft robot design and performance.

4 Propulsion and localization

Appropriate soft robotic actuation and localization depend on the intended *in vivo* versus *in vitro* application. For external devices like exoskeletons, tethered fluidic or tendon-driven actuators suffice (In et al., 2015). However, for *in vivo* applications, traditional tethered soft robots are gradually being replaced by untethered propulsion methods due to invasiveness concerns. Untethered actuation can be further classified as self-contained or external wireless, depending on whether the power source is internal or external to the body. Unlike *ex vivo* soft robots, determining position and orientation is critical for *in vivo* soft robots. Current imaging modalities explored for soft robot localization include US, MRI, FI, CT scans, etc. In particular, swarm robotics with multiple miniature soft robots can enhance localization through collective imaging. In summary, choosing suitable energy sources and imaging techniques based on the intended environment will maximize functionality and biocompatibility of soft robots for practical applications ranging from drug delivery to minimally invasive surgery.

4.1 Propulsion methodologies

Actuating soft robots externally using fluids and tendons has matured considerably. Roche et al. (2017) utilized compressed air to actuate silicone artificial muscles for compression and twisting, mimicking normal cardiac motions to assist failing hearts. Phan et al. (2022) presented hydraulically actuated artificial muscle fibers for smart textiles with high plasticity, adaptivity, and mechanical programmability for multimodal motion and shape shifting. The focus now shifts towards internal propulsion mechanisms. Self-contained is the ability to produce on-board thrust for autonomous motion. Initially studied for microparticles via chemical reactions or external field excitation, self-contained has recently been applied in biomedicine with nanotechnology and microrobotic advancements. For soft robots, internal propulsion can be categorized into chemically-driven, biologically-driven self-contained or wireless propulsion. Chemical driving involves asymmetric bubble release from reactions, self-electrophoresis, or diffusiophoresis from local concentration and potential gradients at the surface (Moran and Posner, 2017). Comprised of a chemical catalyst surface and a narrow channel holding chemical fuel, reactions occur as fuel flows over the catalyst, generating bubbles that asymmetrically emit from a wider outlet to produce thrust. By tuning conditions like the reaction and channel geometry, microrocket motion can be controlled in Figure 6A (Li et al., 2016a).

Biological driving integrates biological and non-biological materials, exploiting innate or environmental taxis for propulsion. Commonly used bio-components include sperm, bacteria, algae, and cardiomyocytes. Singh et al. (2020) developed a sperm-propelled microrobot that harnesses flagellar beating for thrust with inherent biocompatibility and high speeds, overcoming propulsion and compatibility challenges. Bacterial motility is highly efficient and controllable at the microscale, enabling autonomous navigation in complex fluids (Carlsen and Sitti, 2014). Exploiting bacterial taxis and extracellular responses enables precise drug release in tumor microenvironments for cancers like hepatocellular carcinoma, colorectal cancer, and prostate cancer (Forbes, 2010). Careful concentration control prevents toxic immune reactions (Hosseinidoust et al., 2016). Zhuang et al. (2015) utilized bacterial pH taxis for propulsion. Like bacteria, algae exhibit taxis. Weibel et al. (2005) attached payloads (1–6 μm polystyrene microparticles) to phototactic Chlamydomonas reinhardtii and steered the loaded swimming cells via phototaxis for light-triggered cargo release. Sun et al. (2019) fabricated a cardiomyocyte-powered robot where cardiomyocytes interacted with carbon nanotube layers to generate directional motion via asymmetric leg designs. Shown in Figure 6B, Morimoto et al. (2020) encapsulated skeletal muscle tissue in collagen structures, achieving locomotion through contraction of the muscle tissue in the collagen. Skeletal muscle actuation is also possible (Morimoto and Takeuchi, 2022).

External wireless propulsion is an active research area focusing on magnetic (Frutiger et al., 2009; You et al., 2021), optical (Ahn et al., 2019; Yin et al., 2021), and acoustic (Xu et al., 2017; Zhou Y. et al., 2021) actuation. Magnetic driving generates forces or torques using magnetic field gradients or alternating fields, which can modulate velocity and trajectories through changes in field strength and direction. This enables motions like rolling, tumbling, precession, corkscrewing, and travelling-wave propulsion (Nelson et al., 2010). Hua et al. (2022) proposed a novel magnetically actuated FSCR for intragastric diagnosis and therapy. The FSCR uses a composite shell of ferrofluid, permanent magnets, and soft elastomers remotely actuated by external permanent magnets, the key features include: 1) The composite shell has a soft outer surface to reduce tissue damage while improving magnetic circuits for controlled, safe motion via the ferrofluid-magnet combination. 2) The FSCR integrates an oscillation module for advanced functions like drug release.

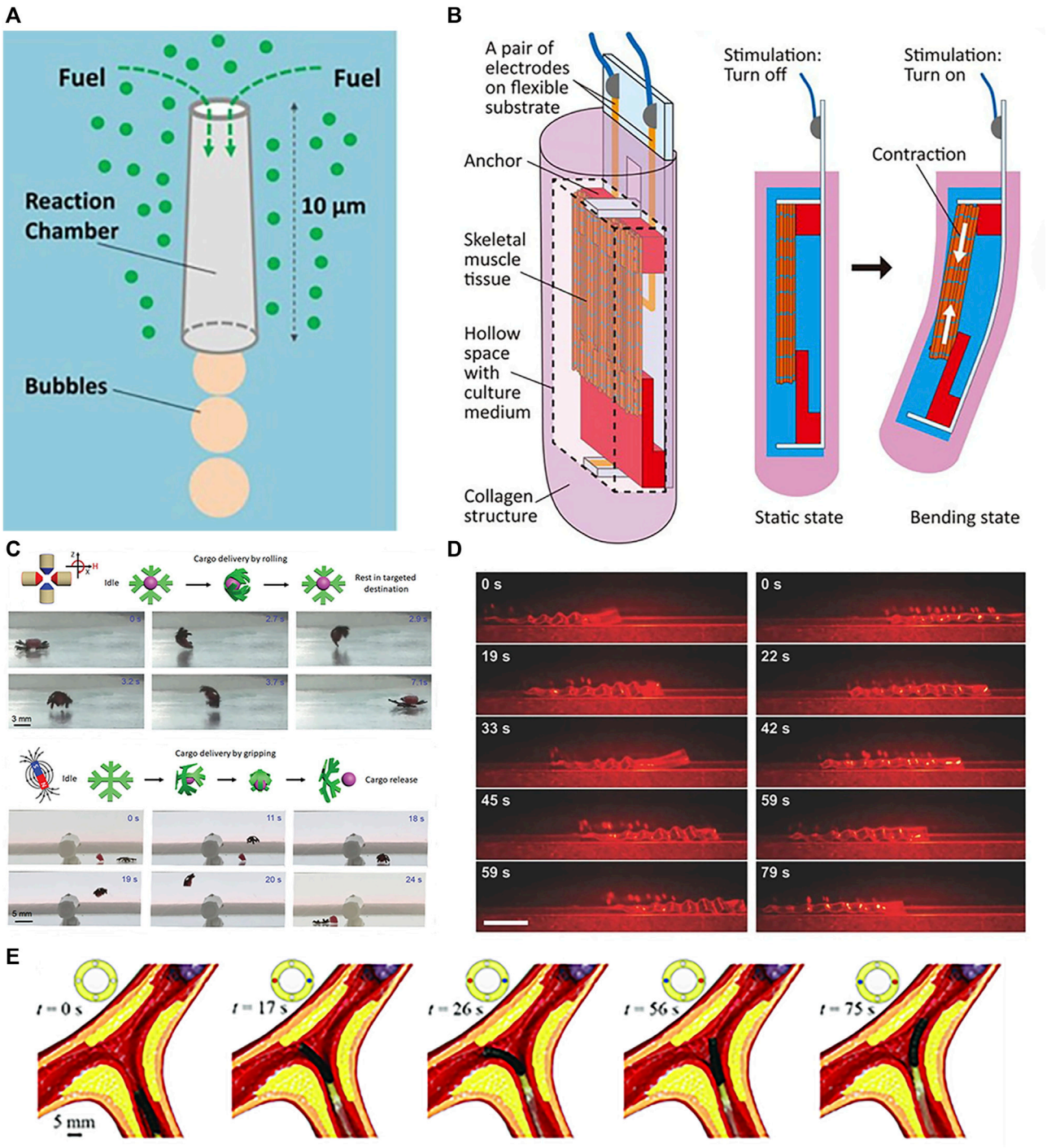

FIGURE 6
Propulsions of soft robots. **(A)** Propulsion by chemical. Reproduced with permission (Li et al., 2016a). Copyright 2016, ACS. **(B)** Propulsion by muscle tissue. Reproduced with permission (Morimoto et al., 2020). Copyright 2020, APL. **(C)** Propulsion by magnetic. Reproduced with permission (Goudu et al., 2020). Copyright 2020, Wiley. **(D)** Propulsion by optical. Reproduced with permission (Rogóż et al., 2016). Copyright 2016, Wiley. **(E)** Propulsion by tendon. Reproduced with permission (Zhang et al., 2021). Copyright 2020, Wiley.

Acoustic waves oscillate microswimmers via applied ultrasonic forces. Goudu et al. (2020) demonstrated magnetic actuation of untethered hydrogel microrobots for grasp, transport, and release of cargo shown in Figure 6C. Ultrasound propulsion offers excellent controllability and tunability by modulating parameters like frequency, amplitude, and duration to precisely control speed and direction (Rao et al., 2015). Real-time control, longevity, non-invasiveness, wireless, and biocompatibility enable precise drug delivery and imaging via micro/nanorobotic manipulation, including ultrasonic excitation and oscillations in acoustic suspensions (Xu et al., 2017). Terzopoulou et al. (2020) alternately activated/deactivated UV-vis light to produce walking

motions of a ribbon-like MOF film through cyclic swelling and shrinking. Rogóż et al. (2016) fabricated LCE soft robots capable of photo-driven actuation shown in Figure 6D. Light can also generate secondary effects like photothermal responses (Terzopoulou et al., 2020).

In addition to individual approaches, hybrid actuation combines multiple integrated mechanisms for enhanced versatility (Kim D.-I. et al., 2020; Hu et al., 2022). Zhang et al. (2021) demonstrated active steering of tendon-magnetically driven soft continuum robots through tendon actuation in a vascular model shown in Figure 6E. For example, Laschi et al. (2012) coupled tendons with SMA to achieve both longitudinal and lateral driving in a robotic arm. Yuan et al. (2020) created Janus micromotors with two dimensional (2D) nanomaterial coatings responsive to chemical fuels, light, and magnetism. Selective coating of the hemispherical motors enabled a bubble propulsion engine powered by catalytic nanoparticles, a magnetic engine propelled by iron oxides, and an optical engine driven by quantum dot illumination. Such multifunctional hybrid systems overcome limitations of individual actuation modes for more robust soft robotic control.

4.2 Localization and tracking

Unlike *ex vivo* settings, determining soft robot position and orientation is critical for *in vivo* targeting and navigation. Currently pursued medical imaging modalities for soft robot localization include FI (Luo et al., 2016; Singh et al., 2017), MRI (Böll et al., 2019), US (Wang and Zhang, 2020), and CT (Masamune et al., 2001). Each approach has tradeoffs in factors like resolution, field-of-view, accessibility, and compatibility with soft materials that guide appropriate matching to the clinical application. For instance, while MRI provides excellent soft tissue contrast, the magnetic fields may interfere with soft robots incorporating ferromagnetic components.

FI provides high detection sensitivity for tracking soft robots labeled with appropriate fluorescent markers. It allows real-time monitoring of dynamic changes in target substances (Singh et al., 2017) and facilitates the acquisition of multi-channel image information by simultaneously utilizing multiple fluorescence dyes with different excitation wavelengths and emission filters. However, the presence of intrinsic fluorescence can interfere with the fluorescence signal of the target substance. Similarly, the imaging capability in deep tissues is constrained by attenuation and scattering, and heavily relies on the efficiency and specificity of fluorescence dye selection and labeling. Servant et al. (2015) monitored magnetic navigation of microswimmers using near-infrared probes (NIR-797) dye-labeled artificial bacterial flagella (ABFs). FI is a versatile localization modality, but optimal dye selection and tissue depth constraints warrant consideration.

MRI is a technique that utilizes magnetic fields and radio waves to generate images of the internal tissues of the human body. Its greatest advantage lies in the absence of ionizing radiation, eliminating the risk of radiation-induced harm to the human body. Additionally, MRI exhibits high tissue contrast, enabling clear visualization of soft tissue structures, facilitating disease diagnosis and anatomical observations. Moreover, MRI can generate multi-planar images to provide comprehensive anatomical information. However, there are limitations due to the underlying imaging principles. Patients with implanted cardiac pacemakers, for example, are unable to undergo MRI scans, and the presence of other metallic implants may result in thermal injuries or adverse reactions. Furthermore, the high cost of MRI equipment and the need for specialized personnel for maintenance and operation restrict its widespread availability. Additionally, MRI scans are time-consuming, making long-duration procedures challenging to undertake. MRI was utilized to track porous iron-based MOF nanocarriers as integrated theranostic drug delivery systems (Böll et al., 2019).

US imaging employs the propagation and reflection characteristics of US waves to generate images of internal tissues in the human body. After being generated by an US transducer, US waves propagate through the tissue via a conductive medium, undergoing refraction, scattering, and absorption. Due to inconsistencies in the reflection of sound waves at different tissue structures and interfaces, images can be generated based on the reflected waves captured by the receiver (Boda-Heggemann et al., 2008). It allows high frame-rate, real-time imaging at relatively low cost without radiation, accurately capturing morphology and positional information of soft robots, making it well-suited for clinical applications. Recently, de Oliveira et al. (2022) proposed and validated a magnetically controlled bioinspired soft robot system based on US tracking and closed-loop control. Camera and US feedback enabled motion planning and control with small tracking errors. Wang et al. (2020) utilized US imaging to guide magnetic nanoparticles and tPA to blood clots and induce deformation for optimal thrombolysis, thus achieving thrombolytic therapy. Thus, US imaging is a versatile, accessible option for soft robot localization.

CT scanning offers rapid image acquisition, generating images within a few seconds. It is well-suited for emergency situations and urgent assessments, providing high resolution to visualize anatomical details and abnormalities. CT can generate multi-planar images, offering comprehensive anatomical information and is applicable to various body regions for diagnosing diseases and injuries. However, due to the use of X-rays in CT scanning, exposure to radiation increases the patient's radiation dose. Consequently, frequent CT scans are not advisable, and it is contraindicated for pregnant women or patients with allergies to contrast agents. Shahriari et al. (2017) developed a CT-compatible remotely actuated needle-guiding robot that fuses CT and electromagnetic sensor data for needle tip localization and steering, enabling targeting of >5 mm lung nodules to reduce complications. While advantageous for anatomical delineation, judicious use of CT is warranted given radiation concerns.

5 Challenges and prospects

Soft robots, as an emerging robotic technology, hold vast promise for medical applications due to their flexible and compliant nature. Compared to conventional rigid robots, soft robots have gained preliminary usage in surgical assistance, targeted drug delivery, rehabilitation training and demonstrated great potential by virtue of their biomimetic properties. In order to optimize the clinical implementation of soft robots, they still face

challenges related to the biocompatibility and degradability of materials, the extension of biomimetic approaches, and modeling.

The biocompatibility of soft robots is primarily influenced by the materials and components used in their construction. There are two common strategies in this regard. The first involves constructing the entire soft robot using materials that exhibit high biocompatibility. The second is creating an external "shell" that encapsulates materials and components with lower biocompatibility. For instance, this can be achieved by sputtering a layer of "biometal" titanium on the robot's surface (Li N. et al., 2018), or by encapsulating the entire robot with hydrogels (Nasseri et al., 2023), PDMS (Niu et al., 2022), chitosan (Niu et al., 2017), etc. Furthermore, if the operational duration of the robot is brief and it can be degraded or expelled from the body afterwards, the requirements for biocompatibility can be moderately reduced. An example of this is the magnetically controlled capsule endoscope, which can be expelled from the body after completing its diagnostic function (Hua et al., 2022).

Most biological materials degrade over time, thus medical devices designed for temporary interventions should have degradable, integrative, or minimally disruptive clearance capabilities after completing specific tasks. Biodegradable robots that can be metabolized *in vivo* or *ex vivo* can serve as transient diagnostic and therapeutic tools to minimize harm to the body. Currently, aliphatic polyesters including poly(lactic-co-glycolic acid) (PLGA), poly(L-lactic acid) (PLLA), poly(D,L-lactic acid) (PDLLA), and poly(caprolactone) (PCL) are popular due to their biocompatibility and hydrolytic degradability. Furthermore, introducing bio-cleavable bonds into hydrogel structures enables degradable soft robotics using composite matrix precursor polymerization or helical microstructures from hydrogels. PEGDA and GelMA can serve as hydrogel precursors. Additionally, naturally-derived alginate and chitosan are useful for degradable robots. Compared to conventional approaches, biodegradable robots can enable cheaper, safer, and more efficient surgeries (Llacer-Wintle et al., 2021). Goudu et al. (2020) developed fully degradable soft millimetric robots with encoded 3D magnetic anisotropy for static and dynamic shape control. As a proof of concept, reversible deformations were demonstrated in hydrogel millimetric grippers in glycerol and biologically-relevant media. The grippers executed cargo grabbing, rolling transport, and release through magnetic field modulation. Complete degradation of the grippers by MMP-2 was achieved at physiologically-relevant concentrations. Additionally, biocompatibility testing of the degradation products using human umbilical vein endothelial cells showed no acute toxicity.

As natural systems have evolved over billions of years, bio-inspired designs can be leveraged to enhance soft robotics. By mimicking the structures, morphologies, functions, and processes of biological organisms, the stability, adaptability, and capabilities of soft robots can be improved. Through biomimetic designs of structure and form, soft robots can achieve increased robustness and adaptability to complex environments. Functional biomimesis, such as replicating locomotion, sensing, and control schemes from nature, can enable more efficient energy conversion, flexible movements, and intelligent control. By studying biological self-assembly and self-healing, soft robots can possess desirable resilience and self-repairing abilities. The applications of bionics in soft robotics extend beyond morphological designs to algorithmic control as well, for example, through ant colony optimization, neural networks, and other bio-inspired control schemes to augment the autonomous mobility and adaptability of soft robots (Wang and Chortos, 2022).

When soft robots are utilized for biomedical applications, accurate modeling is highly desired to minimize adverse impacts on the human body. However, unlike traditional robots made of rigid components, soft robots employ materials that often exhibit nonlinear characteristics such as viscoelasticity, large strains, or deformations, making kinematic and dynamic modeling extremely challenging. Moreover, soft robots possess near infinite degrees of freedom, necessitating novel control approaches tailored for soft robots. Currently, finite element analysis (FEA) can provide relatively precise models. To further enhance control accuracy of soft robot motion, future work may integrate deep learning artificial intelligence (AI) to optimize modeling and control from large datasets, while developing more sophisticated sensors for feedback of soft robot states to enable more precise closed-loop control. In summary, precise modeling and control of soft robot dynamics and interactions remain open challenges vital for advancing biomedical applications of soft robotics. Advanced numerical methods, data-driven modeling, AI-enabled control algorithms, and real-time state feedback through innovative sensory solutions will likely play key roles in realizing the immense promise of soft robots to safely augment human capabilities and improve wellbeing.

6 Conclusion

This review has provided a comprehensive overview of recent advancements in soft robotics for biomedical applications. Significant progress has been made in in vitro and *in vivo* contexts owing to the unique capabilities of soft robots including flexibility, biocompatibility, adaptability, and miniaturization. For *in vitro* applications, soft robots show potential for cell culture engineering, surgical assistance, drug screening, and wearable assistive devices. *In vivo*, they enable minimally invasive diagnosis, targeted drug delivery, biopsy sampling, and catheter interventions by safely navigating the body.

Several key aspects were highlighted that are propelling soft robot development. Intelligent stimuli-responsive materials and bioinspired designs are enhancing functionality while ensuring biocompatibility. Rapid manufacturing techniques like 3D printing facilitate iterative prototyping and customization. Untethered propulsion methods utilizing chemical fuels, biological motility, or external wireless actuation overcome previous constraints, expanding the range of accessible sites. Precision navigation and localization are enabled by tracking modalities like FI and US imaging. Algorithmic control further augments soft robotic capabilities.

While still an emerging field, soft robotics holds immense clinical promise. With continuing advances in materials, manufacturing, propulsion, and localization, soft robots are poised to revolutionize minimally invasive diagnosis and therapies. Areas warranting further research include biocompatibility, biomimetic designs, degradability, and on-board power supplies. Seamless integration with medical

imaging for localization and control also remains an open challenge. As these capabilities mature, soft robotics could enable the next-generation of intelligent diagnostic and therapeutic technologies to improve patient outcomes.

Author contributions

YB: Conceptualization, Methodology, Visualization, Writing–original draft. HW: Conceptualization, Methodology, Visualization, Writing–original draft. HN: Software, Validation, Formal analysis, Investigation, Resources, Writing and Visualization. XH: Methodology, Visualization, Writing–original draft. QX: Formal Analysis, Investigation, Methodology, Resources, Software, Validation, Visualization, Writing–original draft. ZL: Formal Analysis, Investigation, Resources, Software, Validation, Writing–original draft. HY: Funding acquisition, Supervision, Writing–review and editing. FN: Data curation, Funding acquisition, Project administration, Supervision, Writing–review and editing.

Funding

The authors declare financial support was received for the research, authorship, and/or publication of this article. This work was support in part by the National Natural Science Foundation of China under Grant 61903269 and 62073230, in part by the Outstanding Youth Natural Science Foundation of Jiangsu Province under Grant BK20230072, in part by the Suzhou City Industry Foresight and Key Core Technology Project under Grant SYC2022044, in part by the China Postdoctoral Science Foundation under Grant 2020M681517, in part by the Jiangsu Postdoctoral Science Foundation under Grant 2020Z063, and in part by Natural Science Foundation of Higher Education of Jiangsu Province under Grant 22KJB460036, in part by jiangsu 'QingLan' project, and in part by Doctoral Innovation and Entrepreneurship Program of Jiangsu Province.

Conflict of interest

The authors declare that the research was conducted in the absence of any commercial or financial relationships that could be construed as a potential conflict of interest.

Publisher's note

All claims expressed in this article are solely those of the authors and do not necessarily represent those of their affiliated organizations, or those of the publisher, the editors and the reviewers. Any product that may be evaluated in this article, or claim that may be made by its manufacturer, is not guaranteed or endorsed by the publisher.

Supplementary material

The Supplementary Material for this article can be found online at: https://www.frontiersin.org/articles/10.3389/fbioe.2023.1327441/full#supplementary-material

References

Adams, F., Qiu, T., Mark, A., Fritz, B., Kramer, L., Schlager, D., et al. (2017). Soft 3D-printed phantom of the human kidney with collecting system. *Ann. Biomed. Eng.* 45, 963–972. doi:10.1007/s10439-016-1757-5

Ahn, C., Liang, X., and Cai, S. (2019). Bioinspired design of light-powered crawling, squeezing, and jumping untethered soft robot. *Adv. Mater. Technol.* 4. doi:10.1002/admt.201900185

Al-Fahaam, H., Davis, S., and Nefti-Meziani, S. (2016). "Wrist rehabilitation exoskeleton robot based on pneumatic soft actuators," in 2016 international Conference for Students on applied engineering (ICSAE)*: ieee)*, 491–496.

Aynard, A., Pessoni, L., and Billon, L. (2020). Directed self-assembly in "breath figure" templating of block copolymers followed by soft hydrolysis-condensation: one step towards synthetic bio-inspired silica diatoms exoskeleton. *Polymer* 210, 123047. doi:10.1016/j.polymer.2020.123047

Banerjee, H., Suhail, M., and Ren, H. (2018). Hydrogel actuators and sensors for biomedical soft robots: brief overview with impending challenges. *Biomimetics (Basel)*, 3. doi:10.3390/biomimetics3030015

Basar, M. R., Ahmad, M. Y., Cho, J., and Ibrahim, F. (2018). An improved wearable resonant wireless power transfer system for biomedical capsule endoscope. *IEEE Trans. Industrial Electron.* 65, 7772–7781. doi:10.1109/tie.2018.2801781

Boda-Heggemann, J., Köhler, F. M., Küpper, B., Wolff, D., Wertz, H., Mai, S., et al. (2008). Accuracy of ultrasound-based (bat) prostate-repositioning: a three-dimensional on-line fiducial-based assessment with cone-beam computed tomography. *Int. J. Radiat. Oncology*Biology*Physics* 70, 1247–1255. doi:10.1016/j.ijrobp.2007.12.003

Böll, K., Zimpel, A., Dietrich, O., Wuttke, S., and Peller, M. (2019). Clinically approved MRI contrast agents as imaging labels for a porous iron-based MOF nanocarrier: a systematic investigation in a clinical MRI setting. *Adv. Ther.* 3. doi:10.1002/adtp.201900126

Calderon, A. A., Ugalde, J. C., Chang, L., Cristobal Zagal, J., and Perez-Arancibia, N. O. (2019). An earthworm-inspired soft robot with perceptive artificial skin. *Bioinspir Biomim.* 14, 056012. doi:10.1088/1748-3190/ab1440

Carlsen, R. W., and Sitti, M. (2014). Bio-hybrid cell-based actuators for microsystems. *Small* 10, 3831–3851. doi:10.1002/smll.201400384

Ceylan, H., Yasa, I. C., Yasa, O., Tabak, A. F., Giltinan, J., and Sitti, M. (2019). 3D-Printed biodegradable microswimmer for theranostic cargo delivery and release. *ACS Nano* 13, 3353–3362. doi:10.1021/acsnano.8b09233

Chautems, C., Tonazzini, A., Boehler, Q., Jeong, S. H., Floreano, D., and Nelson, B. J. (2019). Magnetic continuum device with variable stiffness for minimally invasive surgery. *Adv. Intell. Syst.* 2. doi:10.1002/aisy.201900086

Chen, A., Yin, R., Cao, L., Yuan, C., Ding, H., and Zhang, W. (2017). "Soft robotics: definition and research issues," in *2017 24th international conference on mechatronics and machine vision in practice (M2VIP)* (IEEE), 366–370.

Chen, S., Tan, Z., Liao, P., Li, Y., Qu, Y., Zhang, Q., et al. (2023). Biodegradable microrobots for DNA vaccine delivery. *Adv. Healthc. Mater.* 12, e2202921. doi:10.1002/adhm.202202921

Chen, X.-Z., Hoop, M., Mushtaq, F., Siringil, E., Hu, C., Nelson, B. J., et al. (2017b). Recent developments in magnetically driven micro- and nanorobots. *Appl. Mater. Today* 9, 37–48. doi:10.1016/j.apmt.2017.04.006

Cheney, N., Bongard, J., and Lipson, H. (2015). "Evolving soft robots in tight spaces," in *Proceedings of the 2015 annual conference on genetic and evolutionary computation*, 935–942.

De Oliveira, A. J. A., Batista, J., Misra, S., and Venkiteswaran, V. K. (2022). "Ultrasound tracking and closed-loop control of a magnetically-actuated biomimetic soft robot," in *2022 IEEE/RSJ international conference on intelligent robots and systems (IROS)*.

Digumarti, K. M., Conn, A. T., and Rossiter, J. (2018). EuMoBot: replicating euglenoid movement in a soft robot. *J. R. Soc. Interface* 15, 20180301. doi:10.1098/rsif.2018.0301

Diller, E., and Sitti, M. (2014). Three-dimensional programmable assembly by untethered magnetic robotic micro-grippers. *Adv. Funct. Mater.* 24, 4397–4404. doi:10.1002/adfm.201400275

Ding, Y., Galiana, I., Asbeck, A. T., De Rossi, S. M., Bae, J., Santos, T. R., et al. (2017). Biomechanical and physiological evaluation of multi-joint assistance with soft exosuits. *IEEE Trans. Neural Syst. Rehabil. Eng.* 25, 119–130. doi:10.1109/tnsre.2016.2523250

Dong, J., Yin, C., Zhao, X., Li, Y., and Zhang, Q. (2013). High strength polyimide fibers with functionalized graphene. *Polymer* 54, 6415–6424. doi:10.1016/j.polymer.2013.09.035

Dupont, P. E., Nelson, B. J., Goldfarb, M., Hannaford, B., Menciassi, A., O'malley, M. K., et al. (2021). A decade retrospective of medical robotics research from 2010 to 2020. *Sci. Robot.* 6, eabi8017. doi:10.1126/scirobotics.abi8017

Forbes, N. S. (2010). Engineering the perfect (bacterial) cancer therapy. *Nat. Rev. Cancer* 10, 785–794. doi:10.1038/nrc2934

Frutiger, D. R., Vollmers, K., Kratochvil, B. E., and Nelson, B. J. (2009). Small, fast, and under control: wireless resonant magnetic micro-agents. *Int. J. Robotics Res.* 29, 613–636. doi:10.1177/0278364909353351

Gao, C., Lin, Z., Jurado-Sánchez, B., Lin, X., Wu, Z., and He, Q. (2016). Stem cell membrane-coated nanogels for highly efficient *in vivo* tumor targeted drug delivery. *Small* 12, 4056–4062. doi:10.1002/smll.201600624

Gao, C., Lin, Z., Wang, D., Wu, Z., Xie, H., and He, Q. (2019). Red blood cell-mimicking micromotor for active photodynamic cancer therapy. *ACS Appl. Mater. Interfaces* 11, 23392–23400. doi:10.1021/acsami.9b07979

Gifari, M. W., Naghibi, H., Stramigioli, S., and Abayazid, M. (2019). A review on recent advances in soft surgical robots for endoscopic applications. *Int. J. Med. Robot.* 15, e2010. doi:10.1002/rcs.2010

Gossweiler, G. R., Brown, C. L., Hewage, G. B., Sapiro-Gheiler, E., Trautman, W. J., Welshofer, G. W., et al. (2015). Mechanochemically active soft robots. *ACS Appl. Mater Interfaces* 7, 22431–22435. doi:10.1021/acsami.5b06440

Goudu, S. R., Yasa, I. C., Hu, X., Ceylan, H., Hu, W., and Sitti, M. (2020). Biodegradable untethered magnetic hydrogel milli-grippers. *Adv. Funct. Mater.* 30. doi:10.1002/adfm.202004975

Hartmann, F., Baumgartner, M., and Kaltenbrunner, M. (2021). Becoming sustainable, the new frontier in soft robotics. *Adv. Mater* 33, e2004413. doi:10.1002/adma.202004413

Hosseinidoust, Z., Mostaghaci, B., Yasa, O., Park, B. W., Singh, A. V., and Sitti, M. (2016). Bioengineered and biohybrid bacteria-based systems for drug delivery. *Adv. Drug Deliv. Rev.* 106, 27–44. doi:10.1016/j.addr.2016.09.007

Hou, Y., Wang, H., Fu, R., Wang, X., Yu, J., Zhang, S., et al. (2023). A review on microrobots driven by optical and magnetic fields. *Lab a Chip* 23, 848–868. doi:10.1039/d2lc00573e

Hu, J., Huang, S., Zhu, L., Huang, W., Zhao, Y., Jin, K., et al. (2018). Tissue plasminogen activator-porous magnetic microrods for targeted thrombolytic therapy after ischemic stroke. *ACS Appl. Mater Interfaces* 10, 32988–32997. doi:10.1021/acsami.8b09423

Hu, X., Ge, Z., Wang, X., Jiao, N., Tung, S., and Liu, L. (2022). Multifunctional thermo-magnetically actuated hybrid soft millirobot based on 4D printing. *Compos. Part B Eng.* 228, 109451. doi:10.1016/j.compositesb.2021.109451

Hua, D., Liu, X., Lu, H., Sun, S., Sotelo, M. A., Li, Z., et al. (2022). Design, fabrication, and testing of a novel ferrofluid soft capsule robot. *IEEE/ASME Trans. Mechatronics* 27, 1403–1413. doi:10.1109/tmech.2021.3094213

Hui, X., and Régnier, S. (2011). Development of a flexible robotic system for multiscale applications of micro/nanoscale manipulation and assembly. *IEEE/ASME Trans. Mechatronics* 16, 266–276. doi:10.1109/tmech.2010.2040483

Hwang, J., Jeon, S., Kim, B., Kim, J. Y., Jin, C., Yeon, A., et al. (2022). An electromagnetically controllable microrobotic interventional system for targeted, real-time cardiovascular intervention. *Adv. Healthc. Mater* 11, e2102529. doi:10.1002/adhm.202102529

Ikezoe, Y., Fang, J., Wasik, T. L., Shi, M., Uemura, T., Kitagawa, S., et al. (2015). Peptide-metal organic framework swimmers that direct the motion toward chemical targets. *Nano Lett.* 15, 4019–4023. doi:10.1021/acs.nanolett.5b00969

In, H., Kang, B. B., Sin, M., and Cho, K.-J. (2015). Exo-glove: a wearable robot for the hand with a soft tendon routing system. *IEEE Robotics Automation Mag.* 22, 97–105. doi:10.1109/mra.2014.2362863

Jeon, S. J., Hauser, A. W., and Hayward, R. C. (2017). Shape-morphing materials from stimuli-responsive hydrogel hybrids. *Acc. Chem. Res.* 50, 161–169. doi:10.1021/acs.accounts.6b00570

Joyee, E. B., and Pan, Y. (2019). A fully three-dimensional printed inchworm-inspired soft robot with magnetic actuation. *Soft Robot.* 6, 333–345. doi:10.1089/soro.2018.0082

Justus, K. B., Hellebrekers, T., Lewis, D. D., Wood, A., Ingham, C., Majidi, C., et al. (2019). A biosensing soft robot: autonomous parsing of chemical signals through integrated organic and inorganic interfaces. *Sci. Robotics* 4, eaax0765. doi:10.1126/scirobotics.aax0765

Karshalev, E., Esteban-Fernandez De Avila, B., Beltran-Gastelum, M., Angsantikul, P., Tang, S., Mundaca-Uribe, R., et al. (2018). Micromotor pills as a dynamic oral delivery platform. *ACS Nano* 12, 8397–8405. doi:10.1021/acsnano.8b03760

Kim, D.-I., Song, S., Jang, S., Kim, G., Lee, J., Lee, Y., et al. (2020a). Untethered gripper-type hydrogel millirobot actuated by electric field and magnetic field. *Smart Mater. Struct.* 29, 085024. doi:10.1088/1361-665x/ab8ea4

Kim, H., Sung, C. M., Ju, H., Park, H., Jeong, J., Nam, K. I., et al. (2020b). Soft magnetic pillars to secure an upper airway for the relief of obstructive sleep apnea. *Adv. Mater. Technol.* 5. doi:10.1002/admt.202000695

Kortman, V. G., Sakes, A., Endo, G., and Breedveld, P. (2023). A bio-inspired expandable soft suction gripper for minimal invasive surgery-an explorative design study. *Bioinspir Biomim.* 18, 046004. doi:10.1088/1748-3190/accd35

Laschi, C., Cianchetti, M., Mazzolai, B., Margheri, L., Follador, M., and Dario, P. (2012). Soft robot arm inspired by the Octopus. *Adv. Robot.* 26, 709–727. doi:10.1163/156855312x626343

Law, J., Wang, X., Luo, M., Xin, L., Du, X., Dou, W., et al. (2022). Microrobotic swarms for selective embolization. *Sci. Adv.* 8, eabm5752. doi:10.1126/sciadv.abm5752

Lee, C., Kim, M., Kim, Y. J., Hong, N., Ryu, S., Kim, H. J., et al. (2017). Soft robot review. *Int. J. Control, Automation Syst.* 15, 3–15. doi:10.1007/s12555-016-0462-3

Li, J., Li, X., Luo, T., Wang, R., Liu, C., Chen, S., et al. (2018a). Development of a magnetic microrobot for carrying and delivering targeted cells. *Sci. Robotics* 3, eaat8829. doi:10.1126/scirobotics.aat8829

Li, J., Rozen, I., and Wang, J. (2016a). Rocket science at the nanoscale. *ACS Nano* 10, 5619–5634. doi:10.1021/acsnano.6b02518

Li, J., Thamphiwatana, S., Liu, W., Esteban-Fernandez De Avila, B., Angsantikul, P., Sandraz, E., et al. (2016b). Enteric micromotor can selectively position and spontaneously propel in the gastrointestinal tract. *ACS Nano* 10, 9536–9542. doi:10.1021/acsnano.6b04795

Li, M., Li, H., Li, X., Zhu, H., Xu, Z., Liu, L., et al. (2017). A bioinspired alginate-gum Arabic hydrogel with micro-/nanoscale structures for controlled drug release in chronic wound healing. *ACS Appl. Mater. Interfaces* 9, 22160–22175. doi:10.1021/acsami.7b04428

Li, M., Wu, J., Lin, D., Yang, J., Jiao, N., Wang, Y., et al. (2022). A diatom-based biohybrid microrobot with a high drug-loading capacity and pH-sensitive drug release for target therapy. *Acta Biomater.* 154, 443–453. doi:10.1016/j.actbio.2022.10.019

Li, N., Yang, T., Yang, Y., Yu, P., Xue, X., Zhao, X., et al. (2020). Bioinspired musculoskeletal model-based soft wrist exoskeleton for stroke rehabilitation. *J. Bionic Eng.* 17, 1163–1174. doi:10.1007/s42235-020-0101-9

Li, N., Yang, T., Yu, P., Chang, J., Zhao, L., Zhao, X., et al. (2018b). Bio-inspired upper limb soft exoskeleton to reduce stroke-induced complications. *Bioinspir Biomim.* 13, 066001. doi:10.1088/1748-3190/aad8d4

Li, Q. H., Zamorano, L., Pandya, A., Perez, R., Gong, J., and Diaz, F. (2010). The application accuracy of the NeuroMate robot—a quantitative comparison with frameless and frame-based surgical localization systems. *Comput. Aided Surg.* 7, 90–98. doi:10.3109/10929080209146020

Lindenroth, L., Housden, R. J., Wang, S., Back, J., Rhode, K., and Liu, H. (2020). Design and integration of a parallel, soft robotic end-effector for extracorporeal ultrasound. *IEEE Trans. Biomed. Eng.* 67, 2215–2229. doi:10.1109/tbme.2019.2957609

Liu, N., Wei, F., Liu, L., Lai, H. S. S., Yu, H., Wang, Y., et al. (2015). Optically-controlled digital electrodeposition of thin-film metals for fabrication of nano-devices. *Opt. Mater. Express* 5, 838. doi:10.1364/ome.5.000838

Llacer-Wintle, J., Rivas-Dapena, A., Chen, X. Z., Pellicer, E., Nelson, B. J., Puigmartí-Luis, J., et al. (2021). Biodegradable small-scale swimmers for biomedical applications. *Adv. Mater.* 33, e2102049. doi:10.1002/adma.202102049

Lu, H., Zhang, M., Yang, Y., Huang, Q., Fukuda, T., Wang, Z., et al. (2018). A bioinspired multilegged soft millirobot that functions in both dry and wet conditions. *Nat. Commun.* 9, 3944. doi:10.1038/s41467-018-06491-9

Luo, C. H., Huang, C. T., Su, C. H., and Yeh, C. S. (2016). Bacteria-Mediated hypoxia-specific delivery of nanoparticles for tumors imaging and therapy. *Nano Lett.* 16, 3493–3499. doi:10.1021/acs.nanolett.6b00262

Ma, X., Wang, L., Wang, P., Liu, Z., Hao, J., Wu, J., et al. (2022). An electromagnetically actuated magneto-nanozyme mediated synergistic therapy for destruction and eradication of biofilm. *Chem. Eng. J.* 431, 133971. doi:10.1016/j.cej.2021.133971

Magdanz, V., Khalil, I. S., Simmchen, J., Furtado, G. P., Mohanty, S., Gebauer, J., et al. (2020). IRONSperm: sperm-templated soft magnetic microrobots. *Sci. Adv.* 6, eaba5855. doi:10.1126/sciadv.aba5855

Majidi, C. (2014). Soft robotics: a perspective—current trends and prospects for the future. *Soft Robot.* 1, 5–11. doi:10.1089/soro.2013.0001

Mao, S., Dong, E., Jin, H., Xu, M., Zhang, S., Yang, J., et al. (2014). Gait study and pattern generation of a starfish-like soft robot with flexible rays actuated by SMAs. *J. Bionic Eng.* 11, 400–411. doi:10.1016/s1672-6529(14)60053-6

Masamune, K., Fichtinger, G., Patriciu, A., Susil, R. C., Taylor, R. H., Kavoussi, L. R., et al. (2001). System for robotically assisted percutaneous procedures with computed tomography guidance. *Comput. Aided Surg.* 6, 370–383. doi:10.3109/10929080109146306

Medina-Sánchez, M., Magdanz, V., Guix, M., Fomin, V. M., and Schmidt, O. G. (2018). Swimming microrobots: soft, reconfigurable, and smart. *Adv. Funct. Mater.* 28. doi:10.1002/adfm.201707228

Middelhoek, K. I. N. A., Magdanz, V., Abelmann, L., and Khalil, I. S. M. (2022). Drug-Loaded IRONSperm clusters: modeling, wireless actuation, and ultrasound imaging. *Biomed. Mater.* 17, 065001. doi:10.1088/1748-605x/ac8b4b

Moran, J. L., and Posner, J. D. (2017). Phoretic self-propulsion. *Annu. Rev. Fluid Mech.* 49, 511–540. doi:10.1146/annurev-fluid-122414-034456

Morimoto, Y., Onoe, H., and Takeuchi, S. (2020). Biohybrid robot with skeletal muscle tissue covered with a collagen structure for moving in air. *Apl. Bioeng.* 4, 026101. doi:10.1063/1.5127204

Morimoto, Y., and Takeuchi, S. (2022). Biohybrid soft robots driven by contractions of skeletal muscle tissue. *J. Robotics Mechatronics* 34, 260–262. doi:10.20965/jrm.2022.p0260

Nasseri, R., Bouzari, N., Huang, J., Golzar, H., Jankhani, S., Tang, X. S., et al. (2023). Programmable nanocomposites of cellulose nanocrystals and zwitterionic hydrogels for soft robotics. *Nat. Commun.* 14, 6108. doi:10.1038/s41467-023-41874-7

Nelson, B. J., Kaliakatsos, I. K., and Abbott, J. J. (2010). Microrobots for minimally invasive medicine. *Annu. Rev. Biomed. Eng.* 12, 55–85. doi:10.1146/annurev-bioeng-010510-103409

Niu, D., Li, D., Chen, J., Zhang, M., Lei, B., Jiang, W., et al. (2022). SMA-based soft actuators with electrically responsive and photoresponsive deformations applied in soft robots. *Sensors Actuators A Phys.* 341, 113516. doi:10.1016/j.sna.2022.113516

Niu, F., Li, J., Ma, W., Yang, J., and Sun, D. (2017). Development of an enhanced electromagnetic actuation system with enlarged workspace. *IEEE/ASME Trans. Mechatronics* 22, 2265–2276. doi:10.1109/tmech.2017.2743021

Panda, S., Hajra, S., Rajaitha, P. M., and Kim, H. J. (2023). Stimuli-responsive polymer-based bioinspired soft robots. *Micro Nano Syst. Lett.* 11, 2. doi:10.1186/s40486-023-00167-w

Pang, G., Yang, G., Heng, W., Ye, Z., Huang, X., Yang, H.-Y., et al. (2021). CoboSkin: soft robot skin with variable stiffness for safer human–robot collaboration. *IEEE Trans. Industrial Electron.* 68, 3303–3314. doi:10.1109/tie.2020.2978728

Phan, P. T., Thai, M. T., Hoang, T. T., Davies, J., Nguyen, C. C., Phan, H. P., et al. (2022). Smart textiles using fluid-driven artificial muscle fibers. *Sci. Rep.* 12, 11067. doi:10.1038/s41598-022-15369-2

Pokki, J., Ergeneman, O., Chatzipirpiridis, G., Luhmann, T., Sort, J., Pellicer, E., et al. (2017). Protective coatings for intraocular wirelessly controlled microrobots for implantation: corrosion, cell culture, and *in vivo* animal tests. *J. Biomed. Mater Res. B Appl. Biomater.* 105, 836–845. doi:10.1002/jbm.b.33618

Qin, X.-H., Ovsianikov, A., Stampfl, J., and Liska, R. (2014). Additive manufacturing of photosensitive hydrogels for tissue engineering applications. *BioNanoMaterials* 15. doi:10.1515/bnm-2014-0008

Rao, K. J., Li, F., Meng, L., Zheng, H., Cai, F., and Wang, W. (2015). A force to be reckoned with: a review of synthetic microswimmers powered by ultrasound. *Small* 11, 2836–2846. doi:10.1002/smll.201403621

Rehan, M., Al-Bahadly, I., Thomas, D. G., and Avci, E. (2020). Capsule robot for gut microbiota sampling using shape memory alloy spring. *Int. J. Med. Robot.* 16, 1–14. doi:10.1002/rcs.2140

Ren, Z., Zhang, R., Soon, R. H., Liu, Z., Hu, W., Onck, P. R., et al. (2021). Soft-bodied adaptive multimodal locomotion strategies in fluid-filled confined spaces. *Sci. Adv.* 7, eabh2022. doi:10.1126/sciadv.abh2022

Roche, E. T., Horvath, M. A., Wamala, I., Alazmani, A., Song, S.-E., Whyte, W., et al. (2017). Soft robotic sleeve supports heart function. *Sci. Transl. Med.* 9, eaaf3925. doi:10.1126/scitranslmed.aaf3925

Rogatinsky, J., Recco, D., Feichtmeier, J., Kang, Y., Kneier, N., Hammer, P., et al. (2023). A multifunctional soft robot for cardiac interventions. *Sci. Adv.* 9, eadi5559. eadi5559. doi:10.1126/sciadv.adi5559

Rogóż, M., Zeng, H., Xuan, C., Wiersma, D. S., and Wasylczyk, P. (2016). Light-driven soft robot mimics caterpillar locomotion in natural scale. *Adv. Opt. Mater.* 4, 1689–1694. doi:10.1002/adom.201600503

Rubehn, B., and Stieglitz, T. (2010). *In vitro* evaluation of the long-term stability of polyimide as a material for neural implants. *Biomaterials* 31, 3449–3458. doi:10.1016/j.biomaterials.2010.01.053

Rus, D., and Tolley, M. T. (2015). Design, fabrication and control of soft robots. *Nature* 521, 467–475. doi:10.1038/nature14543

Rusu, D. M., Mandru, S. D., Biris, C. M., Petrascu, O. L., Morariu, F., and Ianosi-Andreeva-Dimitrova, A. (2023). Soft robotics: a systematic review and bibliometric analysis. *Micromachines (Basel)*, 14. doi:10.3390/mi14020359

Sareh, S., Rossiter, J., Conn, A., Drescher, K., and Goldstein, R. (2013). Swimming like algae: biomimetic soft artificial cilia. *J. R. Soc. Interface* 10, 20120666. doi:10.1098/rsif.2012.0666

Servant, A., Qiu, F., Mazza, M., Kostarelos, K., and Nelson, B. J. (2015). Controlled *in vivo* swimming of a swarm of bacteria-like microrobotic flagella. *Adv. Mater* 27, 2981–2988. doi:10.1002/adma.201404444

Shahriari, N., Heerink, W., Van Katwijk, T., Hekman, E., Oudkerk, M., and Misra, S. (2017). Computed tomography (CT)-compatible remote center of motion needle steering robot: fusing CT images and electromagnetic sensor data. *Med. Eng. Phys.* 45, 71–77. doi:10.1016/j.medengphy.2017.04.009

Shepherd, R. F., Ilievski, F., Choi, W., Morin, S. A., Stokes, A. A., Mazzeo, A. D., et al. (2011). Multigait soft robot. *Proc. Natl. Acad. Sci. U. S. A.* 108, 20400–20403. doi:10.1073/pnas.1116564108

Shimanovich, U., Bernardes, G. J., Knowles, T. P., and Cavaco-Paulo, A. (2014). Protein micro- and nano-capsules for biomedical applications. *Chem. Soc. Rev.* 43, 1361–1371. doi:10.1039/c3cs60376h

Singh, A. V., Ansari, M. H. D., Mahajan, M., Srivastava, S., Kashyap, S., Dwivedi, P., et al. (2020). Sperm cell driven microrobots-emerging opportunities and challenges for biologically inspired robotic design. *Micromachines (Basel)*, 11. doi:10.3390/mi11040448

Singh, A. V., Hosseinidoust, Z., Park, B. W., Yasa, O., and Sitti, M. (2017). Microemulsion-based soft bacteria-driven microswimmers for active cargo delivery. *ACS Nano* 11, 9759–9769. doi:10.1021/acsnano.7b02082

Solovev, A. A., Sanchez, S., Pumera, M., Mei, Y. F., and Schmidt, O. G. (2010). Magnetic control of tubular catalytic microbots for the transport, assembly, and delivery of micro-objects. *Adv. Funct. Mater.* 20, 2430–2435. doi:10.1002/adfm.200902376

Song, S. H., Kim, M. S., Rodrigue, H., Lee, J. Y., Shim, J. E., Kim, M. C., et al. (2016). Turtle mimetic soft robot with two swimming gaits. *Bioinspir Biomim.* 11, 036010. doi:10.1088/1748-3190/11/3/036010

Sun, L., Chen, Z., Bian, F., and Zhao, Y. (2019). Bioinspired soft robotic caterpillar with cardiomyocyte drivers. *Adv. Funct. Mater.* 30. doi:10.1002/adfm.201907820

Sun, M., Tian, C., Mao, L., Meng, X., Shen, X., Hao, B., et al. (2022). Reconfigurable magnetic slime robot: deformation, adaptability, and multifunction. *Adv. Funct. Mater.* 32. doi:10.1002/adfm.202112508

Suzumori, K., Iikura, S., and Tanaka, H. (1992). Applying a flexible microactuator to robotic mechanisms. *IEEE Control Syst. Mag.* 12, 21–27. doi:10.1109/37.120448

Tang, J., Yao, C., Gu, Z., Jung, S., Luo, D., and Yang, D. (2020). Super-soft and super-elastic DNA robot with magnetically driven navigational locomotion for cell delivery in confined space. *Angew. Chem. Int. Ed. Engl.* 59, 2490–2495. doi:10.1002/anie.201913549

Tang, X., Yang, Y., Zheng, M., Yin, T., Huang, G., Lai, Z., et al. (2023). Magnetic–acoustic sequentially actuated CAR T cell microrobots for precision navigation and *in situ* antitumor immunoactivation. *Adv. Mater.* 35, e2211509. doi:10.1002/adma.202211509

Terryn, S., Langenbach, J., Roels, E., Brancart, J., Bakkali-Hassani, C., Poutrel, Q.-A., et al. (2021). A review on self-healing polymers for soft robotics. *Mater. Today* 47, 187–205. doi:10.1016/j.mattod.2021.01.009

Terzopoulou, A., Nicholas, J. D., Chen, X. Z., Nelson, B. J., Pane, S., and Puigmarti-Luis, J. (2020). Metal-organic frameworks in motion. *Chem. Rev.* 120, 11175–11193. doi:10.1021/acs.chemrev.0c00535

Thalman, C., and Artemiadis, P. (2020). A review of soft wearable robots that provide active assistance: trends, common actuation methods, fabrication, and applications. *Wearable Technol.* 1, e3. doi:10.1017/wtc.2020.4

Tondu, B., and Lopez, P. (2000). Modeling and control of McKibben artificial muscle robot actuators. *IEEE control Syst. Mag.* 20, 15–38. doi:10.1109/37.833638

Wang, C., Puranam, V. R., Misra, S., and Venkiteswaran, V. K. (2022a). A snake-inspired multi-segmented magnetic soft robot towards medical applications. *IEEE Robotics Automation Lett.* 7, 5795–5802. doi:10.1109/lra.2022.3160753

Wang, H., Zhang, R., Chen, W., Wang, X., and Pfeifer, R. (2017). A cable-driven soft robot surgical system for cardiothoracic endoscopic surgery: preclinical tests in animals. *Surg. Endosc.* 31, 3152–3158. doi:10.1007/s00464-016-5340-9

Wang, J., and Chortos, A. (2022). Control strategies for soft robot systems. *Adv. Intell. Syst.* 4. doi:10.1002/aisy.202100165

Wang, Q., Wang, B., Yu, J., Schweizer, K., Nelson, B. J., and Zhang, L. (2020). "Reconfigurable magnetic microswarm for thrombolysis under ultrasound imaging," in *2020 IEEE international conference on robotics and automation (ICRA)* (IEEE), 10285–10291.

Wang, Q., and Zhang, L. (2020). Ultrasound imaging and tracking of micro/nanorobots: from individual to collectives. *IEEE Open J. Nanotechnol.* 1, 6–17. doi:10.1109/ojnano.2020.2981824

Wang, X., Gong, Z., Wang, T., Law, J., Chen, X., Wanggou, S., et al. (2023). Mechanical nanosurgery of chemoresistant glioblastoma using magnetically controlled carbon nanotubes. *Sci. Adv.* 9, eade5321. doi:10.1126/sciadv.ade5321

Wang, X., Lin, D., Zhou, Y., Jiao, N., Tung, S., and Liu, L. (2022b). Multistimuli-responsive hydroplaning superhydrophobic microrobots with programmable motion and multifunctional applications. *ACS Nano* 16, 14895–14906. doi:10.1021/acsnano.2c05783

Wang, X., Qin, X. H., Hu, C., Terzopoulou, A., Chen, X. Z., Huang, T. Y., et al. (2018). 3D printed enzymatically biodegradable soft helical microswimmers. *Adv. Funct. Mater.* 28. doi:10.1002/adfm.201804107

Weibel, D. B., Garstecki, P., Ryan, D., Diluzio, W. R., Mayer, M., Seto, J. E., et al. (2005). Microoxen: microorganisms to move microscale loads. *Proc. Natl. Acad. Sci.* 102, 11963–11967. doi:10.1073/pnas.0505481102

Wu, Z., Li, T., Li, J., Gao, W., Xu, T., Christianson, C., et al. (2014). Turning erythrocytes into functional micromotors. *Acs Nano* 8, 12041–12048. doi:10.1021/nn506200x

Wu, Z., Lin, X., Si, T., and He, Q. (2016). Recent progress on bioinspired self-propelled micro/nanomotors via controlled molecular self-assembly. *Small* 12, 3080–3093. doi:10.1002/smll.201503969

Xing, J., Yin, T., Li, S., Xu, T., Ma, A., Chen, Z., et al. (2020). Sequential magneto-actuated and optics-triggered biomicrorobots for targeted cancer therapy. *Adv. Funct. Mater.* 31. doi:10.1002/adfm.202008262

Xu, T., Xu, L.-P., and Zhang, X. (2017). Ultrasound propulsion of micro-/nanomotors. *Appl. Mater. Today* 9, 493–503. doi:10.1016/j.apmt.2017.07.011

Xuan, M., Wu, Z., Shao, J., Dai, L., Si, T., and He, Q. (2016). Near infrared light-powered Janus mesoporous silica nanoparticle motors. *J. Am. Chem. Soc.* 138, 6492–6497. doi:10.1021/jacs.6b00902

Yang, G.-Z., Full, R. J., Jacobstein, N., Fischer, P., Bellingham, J., Choset, H., et al. (2019a). *Ten robotics technologies of the year*. American Association for the Advancement of Science.

Yang, W., Cai, S., Chen, Y., Liang, W., Lai, Y., Yu, H., et al. (2020). Modular and customized fabrication of 3D functional microgels for bottom-up tissue engineering and drug screening. *Adv. Mater. Technol.* 5. doi:10.1002/admt.201900847

Yang, W., Yu, H., Liang, W., Wang, Y., and Liu, L. (2015). Rapid fabrication of hydrogel microstructures using UV-induced projection printing. *Micromachines* 6, 1903–1913. doi:10.3390/mi6121464

Yang, X., Huang, T.-H., Hu, H., Yu, S., Zhang, S., Zhou, X., et al. (2019b). Spine-inspired continuum soft exoskeleton for stoop lifting assistance. *IEEE Robotics Automation Lett.* 4, 4547–4554. doi:10.1109/lra.2019.2935351

Yin, C., Wei, F., Fu, S., Zhai, Z., Ge, Z., Yao, L., et al. (2021). Visible light-driven jellyfish-like miniature swimming soft robot. *ACS Appl. Mater Interfaces* 13, 47147–47154. doi:10.1021/acsami.1c13975

Ying, B., Chen, R. Z., Zuo, R., Li, J., and Liu, X. (2021). An anti-freezing, ambient-stable and highly stretchable ionic skin with strong surface adhesion for wearable sensing and soft robotics. *Adv. Funct. Mater.* 31. doi:10.1002/adfm.202104665

You, T. L., Philamore, H., and Matsuno, F. (2021). A magneto-active elastomer crawler with peristaltic and caterpillar locomotion patterns. *Actuators* 10, 74. doi:10.3390/act10040074

Yu, Y., Peng, R., Chen, Z., Yu, L., Li, J., Wang, J., et al. (2021). Photoresponsive biomimetic soft robots enabled by near-infrared-driven and ultrarobust sandwich-structured nanocomposite films. *Adv. Intell. Syst.* 3. doi:10.1002/aisy.202170067

Yuan, K., De La Asunción-Nadal, V., Jurado-Sánchez, B., and Escarpa, A. (2020). 2D nanomaterials wrapped Janus micromotors with built-in multiengines for bubble, magnetic, and light driven propulsion. *Chem. Mater.* 32, 1983–1992. doi:10.1021/acs.chemmater.9b04873

Zeeshan, M. A., Grisch, R., Pellicer, E., Sivaraman, K. M., Peyer, K. E., Sort, J., et al. (2014). Hybrid helical magnetic microrobots obtained by 3D template-assisted electrodeposition. *Small* 10, 1284–1288. doi:10.1002/smll.201302856

Zhang, S., Xu, B., Elsayed, M., Nan, F., Liang, W., Valley, J. K., et al. (2022a). Optoelectronic tweezers: a versatile toolbox for nano-/micro-manipulation. *Chem. Soc. Rev.* 51, 9203–9242. doi:10.1039/d2cs00359g

Zhang, T., Yang, L., Yang, X., Tan, R., Lu, H., and Shen, Y. (2021). Millimeter-scale soft continuum robots for large-angle and high-precision manipulation by hybrid actuation. *Adv. Intell. Syst.* 3, 2000189. doi:10.1002/aisy.202000189

Zhang, X., Xue, P., Yang, X., Valenzuela, C., Chen, Y., Lv, P., et al. (2022b). Near-infrared light-driven shape-programmable hydrogel actuators loaded with metal-organic frameworks. *ACS Appl. Mater Interfaces* 14, 11834–11841. doi:10.1021/acsami.1c24702

Zhou, C., Yang, Y., Wang, J., Wu, Q., Gu, Z., Zhou, Y., et al. (2021a). Ferromagnetic soft catheter robots for minimally invasive bioprinting. *Nat. Commun.* 12, 5072. doi:10.1038/s41467-021-25386-w

Zhou, H., and Alici, G. (2022). A magnetically actuated novel robotic capsule for site-specific drug delivery inside the gastrointestinal tract. *IEEE Trans. Syst. Man, Cybern. Syst.* 52, 4010–4020. doi:10.1109/tsmc.2021.3088952

Zhou, P., Yao, J., Zhang, S., Wei, C., Zhang, H., and Qi, S. (2022). A bioinspired fishbone continuum robot with rigid-flexible-soft coupling structure. *Bioinspir Biomim.* 17, 066012. doi:10.1088/1748-3190/ac8c10

Zhou, Y., He, B., Yan, Z., Shang, Y., Wang, Q., and Wang, Z. (2018). Touch locating and stretch sensing studies of conductive hydrogels with applications to soft robots. *Sensors (Basel)* 18, 569. doi:10.3390/s18020569

Zhou, Y., Liu, J., Yan, J., Guo, S., and Li, T. (2021b). Soft-contact acoustic microgripper based on a controllable gas-liquid interface for biomicromanipulations. *Small* 17, e2104579. doi:10.1002/smll.202104579

Zhu, G., Hou, Y., Xia, N., Wang, X., Zhang, C., Zheng, J., et al. (2023). Fully recyclable, healable, soft, and stretchable dynamic polymers for magnetic soft robots. *Adv. Funct. Mater.* 33. doi:10.1002/adfm.202300888

Zhuang, J., Wright Carlsen, R., and Sitti, M. (2015). pH-taxis of biohybrid microsystems. *Sci. Rep.* 5, 11403. doi:10.1038/srep11403

Zrinscak, D., Lorenzon, L., Maselli, M., and Cianchetti, M. (2023). Soft robotics for physical simulators, artificial organs and implantable assistive devices. *Prog. Biomed. Eng.* 5, 012002. doi:10.1088/2516-1091/acb57a

frontiers | Frontiers in Bioengineering and Biotechnology

TYPE Review
PUBLISHED 19 January 2024
DOI 10.3389/fbioe.2024.1353660

OPEN ACCESS

EDITED BY
Tianlong Li,
Harbin Institute of Technology, China

REVIEWED BY
Hao Yang,
Soochow University, China
Peipei Jin,
University of Science and Technology of China, China

*CORRESPONDENCE
Haoran Mu,
dr_muhaoran@163.com
Zhonghua Xu,
xuzhonghua1985@163.com
Jin He,
18961118686@189.cn

†These authors have contributed equally to this work

RECEIVED 11 December 2023
ACCEPTED 09 January 2024
PUBLISHED 19 January 2024

CITATION
Pu R, Yang X, Mu H, Xu Z and He J (2024), Current status and future application of electrically controlled micro/nanorobots in biomedicine.
Front. Bioeng. Biotechnol. 12:1353660.
doi: 10.3389/fbioe.2024.1353660

Current status and future application of electrically controlled micro/nanorobots in biomedicine

Ruochen Pu[1,2†], Xiyu Yang[2,3†], Haoran Mu[2,3*], Zhonghua Xu[1,3*] and Jin He[1,3*]

[1]Jintan Hospital Affiliated to Jiangsu University, Changzhou, Jiangsu Province, China, [2]Shanghai Bone Tumor Institution, Shanghai, China, [3]Department of Orthopedics, Shanghai General Hospital, Shanghai Jiao Tong University School of Medicine, Shanghai, China

Using micro/nanorobots (MNRs) for targeted therapy within the human body is an emerging research direction in biomedical science. These nanoscale to microscale miniature robots possess specificity and precision that are lacking in most traditional treatment modalities. Currently, research on electrically controlled micro/nanorobots is still in its early stages, with researchers primarily focusing on the fabrication and manipulation of these robots to meet complex clinical demands. This review aims to compare the fabrication, powering, and locomotion of various electrically controlled micro/nanorobots, and explore their advantages, disadvantages, and potential applications.

KEYWORDS

electrically-controlled MNRs, MNRs, application, fabrication, Janus 1

1 Introduction

Micro/nanomotors (MNRs), characterized by their small size and precise control capabilities, represent a class of intelligent robots operating in the micro- and nanoscale dimensions. These robots possess the ability to navigate freely within the microscopic world and harness external environmental energy for propulsion and manipulation (Feng et al., 2023). As a result, MNRs have found extensive applications in the field of modern medicine, including targeted drug delivery, precision healthcare, biosensing, and waste removal (Vujacic Nikezic and Grbovic Novakovic, 2022; Zhou et al., 2022). Current research endeavors predominantly focus on magnetic (Diller et al., 2013; Peyer et al., 2013; Servant et al., 2015; Li et al., 2019; Xie et al., 2019; Fang et al., 2023), optical (Wang J. et al., 2019; Dai et al., 2022; Wang et al., 2023), acoustic (Abbas et al., 2020; Das et al., 2022; Wu et al., 2023), thermal (Tu et al., 2017), and biohybrid MNRs (Park et al., 2013; Han et al., 2016; Wang X. et al., 2019; Magdanz et al., 2021; Song et al., 2022). In contrast, studies pertaining to electro-controlled MNRs remain limited, considering the intricate balance between fabrication complexity, cost-effectiveness, feasibility of energy supply, and existing clinical demands. From a technological standpoint, the materials employed in electro-controlled MNRs are often constrained by the limitations imposed by their motion mechanisms, necessitating a certain level of conductivity or charge-carrying capability. Consequently, the development of novel materials for electro-controlled MNRs is hindered (Demirörs et al., 2018). In terms of energy

supply, the storage and transmission of energy at the micro- and nanoscale are inherently limited, thus rendering electro-controlled MNRs reliant on external power sources or wireless energy transfer for their energy needs. This complexity and dependence on external sources impose significant constraints on the feasibility of electro-controlled MNRs in practical applications (Fath et al., 2022).

However, compared to other MNRs, electro-controlled MNRs still possess several advantages. Firstly, electric fields offer high energy efficiency and a wide range of modulation, enabling efficient propulsion of MNRs at extremely low voltages while exhibiting different motion capabilities and patterns at various voltage levels (Kim et al., 2017; Shen et al., 2020; Lee et al., 2021). Secondly, electro-controlled MNRs can alter their shape and mechanical properties through the adjustment of electric fields, allowing adaptation to diverse application requirements (Jang et al., 2021; Liu et al., 2021; Zheng et al., 2022). Moreover, in drug delivery, electro-controlled MNRs offer unique advantages. As carriers, they not only achieve precise motion but also enable precise drug release through external electric fields, facilitating ideal drug administration. This review summarizes the fabrication, energy supply, and motion mechanisms of electro-controlled MNRs, compares their relative advantages, and emphasizes the need for further research in terms of biocompatibility and propulsion. By evaluating existing studies, the review provides insights into the future clinical applications of electro-controlled MNRs (Figure 1).

2 Fabrication of electro-controlled MNRS

The primary challenge in the fabrication of micro-motors lies in achieving robust locomotion of robots in low Reynolds number fluids, such as blood, at the nanoscale (Zheng L. et al., 2023). In such fluids, inertial forces are exceedingly small, while MNRs often require precise control, necessitating continuous power input (Wang, 2009; Soto et al., 2020). Furthermore, conventional fuels like chemical propellants are typically biologically harmful (Lv et al., 2023), prompting biomedical researchers to demand more compatible propulsion methods. In addition to these considerations, researchers must also address cost and fabrication complexity to meet the growing practical demands of clinical applications.

During the fabrication process of MNRs, several factors significantly influence the design. i) Energy sources for MNRs: These robots can be broadly categorized into externally propelled and self-propelled types. For externally propelled MNRs, precise control of the external field on the robot particles is crucial, encompassing both collective and individual configurations (Zheng L. et al., 2023). The external field can also serve as a means of recharging the robots, for instance, through wireless charging techniques (Kim et al., 2017). Conversely, self-propelled MNRs often rely on chemical and biological energy sources, with common catalytic media including light (Dong et al., 2018; He et al., 2021), electricity (Seh et al., 2017; Suen et al., 2017), and chemical

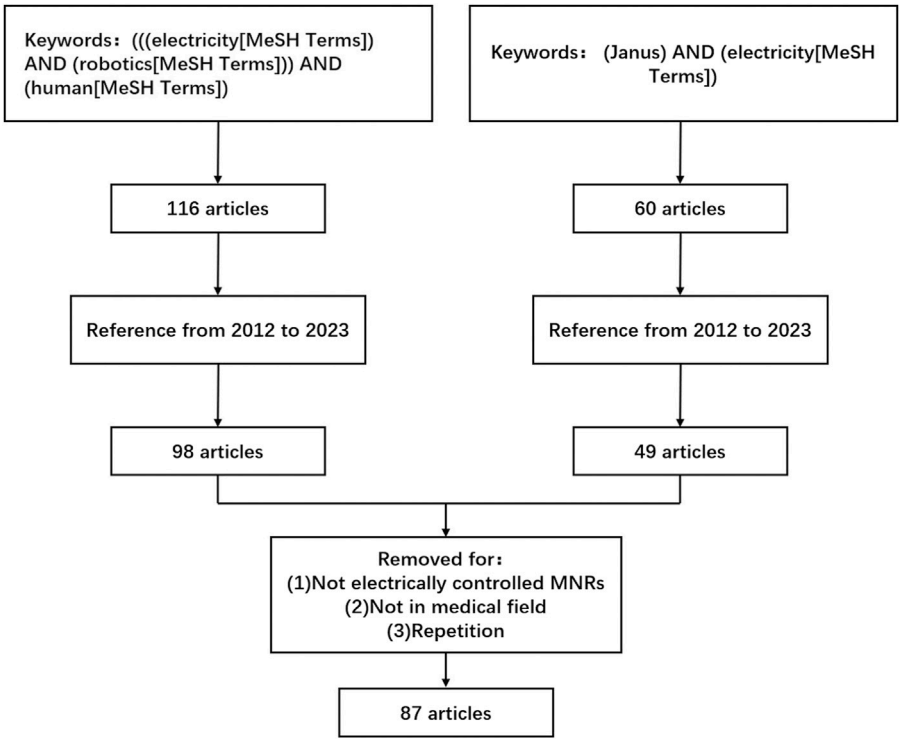

FIGURE 1
A Review strategy.

environments (Lyu et al., 2021). Consequently, the fabrication process must consider not only the MNRs themselves but also the design of their accompanying external fields. ii) Modes of motion for MNRs: In addition to conventional field-guided motion, MNRs can exhibit a diverse range of motion patterns based on their design. Under external field stimulation, these robots can achieve rotation, translation, and helical propulsion, among other modes (Lee et al., 2023). For electro-controlled self-propelled MNRs, specific motion behaviors can be achieved through the design of structures such as Janus particles, which exploit distinct hemisphere configurations (Shen et al., 2020). Additionally, biomimetic structures, including flagella-like structures (Ma et al., 2012), sperm-like structures (Celi et al., 2021; Mayorga-Martinez et al., 2021), and cilia-like structures (Wang W. et al., 2022), offer the ability to facilitate flexible forward and backward motion and directional changes. In the context of electro-controlled MNRs, careful consideration must also be given to the manipulation methods, such as the selection between alternating and direct current fields, as well as the design of microfluidic chips.

Currently, common methods for the fabrication of MNRs include Photolithography (Iacovacci et al., 2019; Mu et al., 2021), Template-guided electrodeposition (Ji et al., 2021; Li et al., 2021; Lu et al., 2022), Additive manufacturing (Otuka et al., 2014; Li and Pumera, 2021; Liu et al., 2022), and Glancing angle deposition (Cohen and Walt, 2019; Ghosh and Ghosh, 2020; Dasgupta et al., 2022). Photolithography involves the use of photosensitive materials and a photomask. The light emitted by a photolithography machine passes through the patterned mask and exposes a thin film coated with photoresist. The photoresist undergoes a change in properties upon exposure, allowing the pattern from the mask to be replicated onto the film, resulting in the formation of corresponding protruding structures (del Barrio and Sánchez-Somolinos, 2019). Template-guided electrodeposition utilizes electric current to reduce metal ions (or conductive polymers) onto the surface of an electrode covered with a porous membrane (Medina-Sánchez et al., 2018). In this process, adjusting the pore size of the membrane enables control over the size of the robot, and the porous membrane can be dissolved after fabrication to release the robot. Currently, there are five main additive manufacturing (also known as 3D printing) techniques used for the fabrication of MNRs: Direct laser writing (DLW), Stereolithography, Microscale continuous optical printing, Inkjet printing, and PolyJet (Zheng L. et al., 2023). Glancing angle deposition is a novel thin film deposition technique that involves controlling the tilt and rotation of the substrate to obtain nanostructured porous films different from traditional dense films. With the assistance of a rotating substrate, it is possible to achieve nanopores with various diameters and shapes (Wang Z. et al., 2022).

The fabrication of electrically controlled MNRs primarily focuses on the preparation of Janus particles. Given material constraints, common techniques for fabricating electrically controlled Janus particles include electron beam deposition (Demirörs et al., 2018; Zhang et al., 2019). Demirörs et al. Demirörs et al. (2018) used 4.64 μm diameter silica particles to prepare sub-monolayer structures. They coated a suspension of these particles onto a glass substrate and formed a sub-monolayer after drying. Subsequently, they employed the Plassys II (Plassys Bestek) electron beam deposition technique to vertically deposit a 15 nm thick layer of platinum onto the sub-monolayer. The researchers then subjected the samples to ultrasonication in deionized water to collect the particles, which were subsequently collected by centrifugal concentration. Similarly, by depositing a 15 nm nickel layer and a 15 nm platinum layer onto a dried colloidal sub-monolayer, Janus particles with magnetic responsiveness can be prepared. Similarly, Zhang et al. Zhang et al. (2019) used drop casting to prepare 3 nm single-layer SiO2, which was then suspended in 20 μL of ethanol and dispersed by ultrasonication (Figure 2B). After drying, a 50 nm titanium film was deposited onto the silica microspheres using electron beam deposition, followed by ultrasonic collection. Building upon these fabrication methods, Lee et al. (2019) employed glancing angle deposition to deposit size- and shape-tunable 10 nm chromium and 30 nm gold onto polystyrene microspheres at small angles of $0^{\circ} < \varphi < 20^{\circ}$ (Figures 2A, 3B). These nearly symmetric mirror-like triangular structures endowed the particles with unique motion capabilities and trajectories.

For electrically controlled MNRs in forms other than Janus particles, electron beam deposition and photolithography techniques are also commonly used for their fabrication. Fennimore et al. Fennimore et al. (2003), for example, used photolithography to attach multiwalled carbon nanotubes with 10 nm chromium and 90 nm gold, creating rotatable nanoscale motors.

Overall, the fabrication of electro-controlled MNRS does not differ significantly from other types of micro- and nanomotors. Rather, the fabrication of electro-controlled MNRS tends to be relatively limited due to the constraints of material properties (Figure 2C). MNRs driven by electric fields require materials with good conductivity, while electrically controlled MNRs based on Janus particles require specific electrically responsive materials. However, research on conventional polymers and metals for these applications is relatively mature. Currently, research on the fabrication of electro-controlled MNRS should focus on two directions: i) Optimizing existing fabrication methods and material performance to achieve the production of conventional robots through lower cost and lower complexity approaches. ii) Integrating MNRs with biological structures to create artificial muscles, bio-hybrid electrically responsive robots, and so on, and conducting in-depth research on biocompatibility and autonomous locomotion.

3 Energy acquisition of electro-controlled MNRS

The energy for electro-controlled MNRS primarily originates from external electric fields and self-propulsion (Wang and Zhang, 2021). Electro-controlled MNRS powered by external electric fields can be categorized into two types: i) Direct external field-driven motors (Kim et al., 2017; Lee et al., 2019; Zhang et al., 2019; Shen et al., 2020; Demirörs et al., 2021; Zheng Y. et al., 2023; Haque et al., 2023). This method of energy supply is the most prevalent and offers advantages such as simplicity, contactless operation, and minimal waste generation. ii) External field-powered motors (Guanying et al., 2007; Lv et al., 2022). This non-contact power supply mode avoids the need for intricate wiring connections and finds promising applications in human environments. Once charged, these micro- and nanomotors acquire the ability for autonomous motion within a certain time

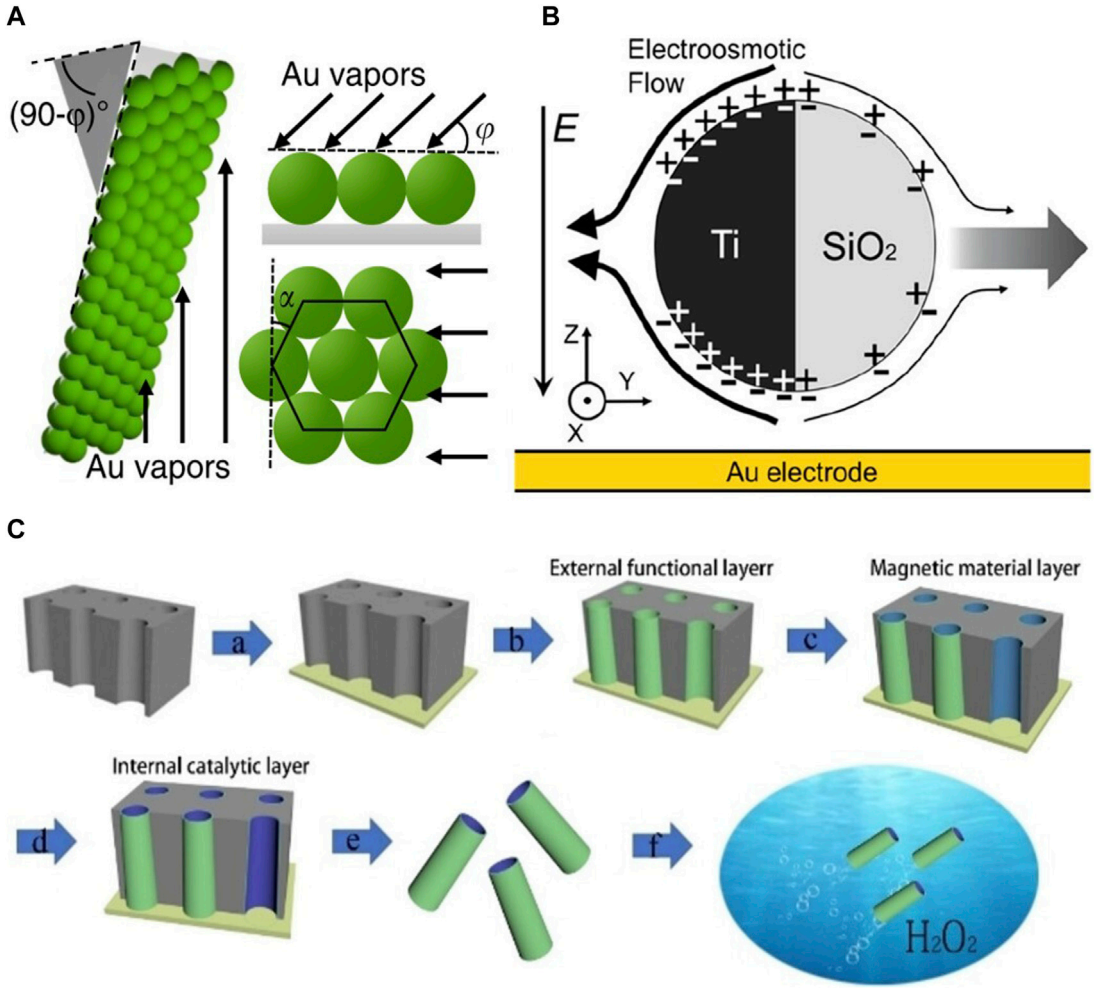

FIGURE 2
(A) A schematic of metal (Au) deposition using glancing angle deposition onto a substrate coated with a monolayer of polystyrene (PS) microspheres. The arrows indicate the direction of incident metal vapors (Lee et al., 2019). 2019, The Author (s). **(B)** Schematic of a SiO_2–Ti particle undergoing induced charge electrophoresis (IECP) (Zhang et al., 2019). 2019 American Chemical Society. **(C)** Schematic diagram of the steps involved in the preparation of microtubules by template-assisted electrodeposition (Li et al., 2021). 2021 The Authors. Published by Wiley-VCH GmbH.

frame, enabling them to perform more precise movements in complex environments. Self-propelled electro-controlled MNRS primarily exist in the form of electrochemical Janus particles (Nie et al., 2018; Lee et al., 2021; Liu et al., 2021; Yang et al., 2022; Liao et al., 2023), which will be discussed further in subsequent sections.

3.1 Electrically controlled MNRs operated by direct external fields

To respond to external electric fields, electric field-driven MNRs require materials that possess inherent conductivity. Two types of electric fields, alternating current (AC) and direct current (DC) can be employed for remote control of MNRs' propulsion. Common propulsion mechanisms include electrostatic tweezers (Fan et al., 2011), induced charge electrophoresis (ICEP) (Gangwal et al., 2008), electrophoretic flow (Calvo-Marzal et al., 2010), electrohydrodynamic flow (EHD) (Ma et al., 2015), and self-electrophoresis (sDEP) (Boymelgreen et al., 2016).

3.1.1 MNRs manipulated by electrostatic tweezers

Electrostatic tweezers are a technique that employs an alternating electric field applied to patterned electrodes to manipulate suspended nanoparticles. This technique allows for controlled rotation, positioning, and cargo release of nanowires, among other functionalities (Fan et al., 2011). Xu et al. Xu et al. (2015) demonstrated the polarization effect of electrostatic tweezers on a specific type of micro- and nanorobot composed of plasma-sensitive nanorods as rotors, patterned nanomagnets as bearings, and microelectrodes as stators (Figure 3A). They systematically validated the polarization effect of electrostatic tweezers on this type of micro- and nanorobot, which can be utilized to modulate the release rate of biochemical substances on the surface of nanoparticles, demonstrating its potential for drug loading and release applications. Furthermore, the alternating magnetic field required for electrostatic tweezers can also be generated under optical induction. Zhang et al. (2022) provided a detailed overview of the working mechanism and experimental setup of optoelectronic tweezers, along with its applications in non-

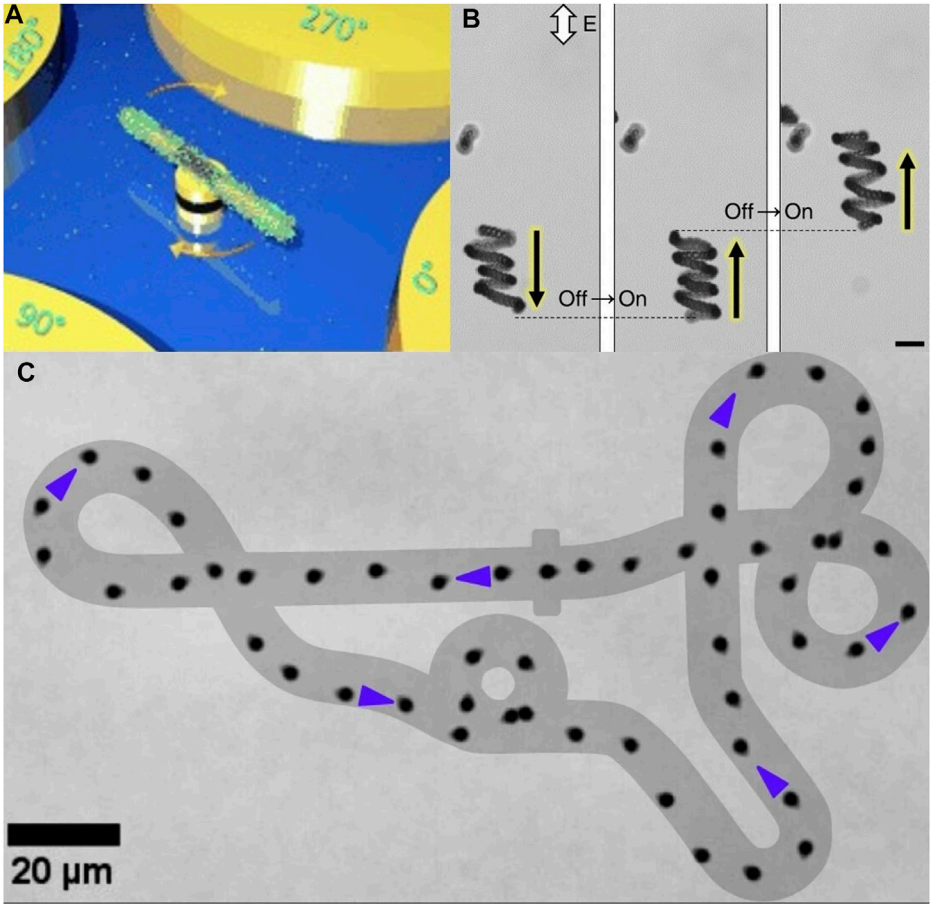

FIGURE 3
(A) Nanomotors accomplish rotation and drug release due to polarisation in the presence of electric tweezers (Xu et al., 2015). 2015 WILEY-VCH Verlag GmbH and Co. KGaA, Weinheim **(B)** Under an alternating electric field, particles exhibit helical motion and undergo chiral turnover (Lee et al., 2019). 2019, The Author (s) **(C)** Under concentration polarisation electrophoresis (CPEP), Janus particles move along predetermined orbits (Katzmeier and Simmel, 2023). 2023, The Author (s).

biological and biological fields, indicating the future directions of electrostatic tweezers.

3.1.2 MNRs manipulated by electrophoretic flow

Another method for manipulating MNRs using an AC electric field is electrophoretic flow. Electrophoretic flow is the fluid motion induced by applying a voltage across porous media, microchannels, and other fluidic conduits, relying on the generated dipole moment (Alizadeh et al., 2021). The advantages of electrophoretic driving include a simple system architecture, ease of operation, and a planar flow profile. However, electrophoretic driving is susceptible to factors such as applied electric field strength, channel surface, microfluidic properties, and heat transfer efficiency, resulting in relatively poor stability. Additionally, this driving mechanism is only applicable to electrolyte solutions, limiting its range of applications. Calvo-Marzal et al. (2010) utilized an AC electric field to drive PPy-Cd/CdSe-Au-CdSe hybrid fuel-free semiconductor diode nanowires based on the electrophoretic flow mechanism, enabling motion along the direction parallel to the electric field axis. This structure can easily attach drugs, biosensing structures, and other entities, making it promising for biomedical applications.

3.1.3 MNRs manipulated by electrohydrodynamic flow

By applying a high voltage between two electrodes, an electric field is formed in an electrolyte solution. When the applied voltage exceeds a certain threshold, corona discharge occurs, causing ions of the same polarity as the electrode to move towards the other electrode, creating space charges. The resulting current induces Coulombic forces between the ions, leading to electrohydrodynamic flow (Peng et al., 2023). Ni et al. (2017) employed sequential capillary-assisted particle assembly (sCAPA) to connect microspheres of different materials into defined-shaped mixed clusters, referred to as "colloidal molecules." These clusters can actively translate, circulate, and rotate under the driving force of asymmetric electrohydrodynamic flow. Clustered particles possess motion characteristics and cargo-loading capabilities that individual nanoparticles lack, making them advantageous for targeted drug delivery.

Comparing electrophoretic flow and electrohydrodynamic flow, both involve electrokinetic phenomena that induce fluid motion through an applied electric potential. Electrophoretic flow offers high efficiency, controllability, low diffusion, and

simple devices but has relatively low flow velocities, sensitivity to interfering charges, and complex control requirements (Slater et al., 2010). On the other hand, electrohydrodynamic flow can enhance mixing at the microscale and has the potential for electrochemical-driven self-propulsion, but its research is still in its early stages, and control techniques are lacking. Further research is needed to address the limitations and explore the full potential of electrohydrodynamic flow.

3.1.4 MNRs manipulated by induced charge electrophoresis

Induced charge electrophoresis (ICEP) is a special nonlinear electrokinetic phenomenon (Gangwal et al., 2008). Generally, in a non-uniform alternating current field, net electrostatic forces induce particle motion, a phenomenon known as dielectrophoresis. Building upon this, Murtsovkin, (1996) discovered that the polarization of the ion double layer can also cause nonlinear electro-osmotic flow at low frequencies (kHz). Based on this, Bazant and Squires, (2004) introduced the term induced charge electrophoresis to describe the collective motion resulting from the action of an externally applied electric field on the self-induced diffusive charges near a polarizable surface.

Unlike electrophoretic flow, ICEP is a driving method commonly used for Janus particles. The direction of particle motion is perpendicular to the field direction. This is because, in an electric field, the metal hemisphere of a Janus particle polarizes more strongly than the dielectric hemisphere, resulting in a higher electro-osmotic strength on the metal side. Lee et al. Lee et al. (2023) applied an external alternating electric field to a cluster of Janus particles and demonstrated the diverse motion modes generated by ICEP, showcasing its rich potential.

This manipulation method of MNRs distinguishes itself from electrophoretic flow and electrohydrodynamic flow by directly acting on the particles themselves, with the particle motion direction typically different from the electric field lines (Figure 3C). Compared to traditional electrophoresis, this electrophoresis mode has more limited applications but provides higher precision, making it highly valuable in the field of electrically controlled microactuators.

3.2 MNRs manipulated by electrohydrodynamic flow

With the increasing demand for painless diagnosis, high security, and accurate detection, wirelessly powered MNRs have become a hot research area (Gao C. et al., 2021). Guanying et al. (2007) proposed an inductively coupled wireless power transfer system employing two coils. The coupling coefficient between these coils was measured based on axial, transversal, and spacing deviations. By selecting suitable tuning capacitors and transmission frequencies, the researchers derived and optimized the power transfer efficiency. Compared to the parallel resonant circuit topology, the series resonant circuit (SRC) demonstrated greater adaptability on the receiving end. To address the uncertainty in the direction of the receiving coil, the researchers also proposed and studied a multi-coil receiving structure. Experimental results showed that when the receiving coil was positioned at the center of the transmitting coil, the system could stably receive up to 170 mW of direct current power with an efficiency of 1.3%, meeting the power requirements of certain microsystems. Although researchers have made significant progress in miniaturizing the structure, the design and fabrication of nanoscale wirelessly powered robots remain relatively unexplored territory.

3.3 MNRs manipulated by other methods

In addition to external field powering, converting other forms of energy into electricity is also a common method of energy supply for MNRs. Fan et al. introduced the concept of Triboelectric Nanogenerators (TENG) in 2012, which can directly convert mechanical energy from our daily activities into electricity and has found extensive applications in engineering (Zhong et al., 2013; Wang et al., 2017). TENG exhibits high output voltage and low output current characteristics. The short-circuit current is typically in the milliampere or microampere range, while the open-circuit voltage can reach several kilovolts (Lee et al., 2015; Seung et al., 2015). Lv et al. (2022) designed a TENG that can be driven by ultra-weak mechanical stimuli. The study found that by adjusting the driving frequency, separation distance, and motion amplitude, a maximum energy conversion efficiency of 73.6% and an energy output of 48 pJ can be achieved. This work holds significant importance in expanding the applications of TENG in the field of biomicrorobotics. Furthermore, Nie et al. (2018) combined TENG with electrowetting techniques to achieve self-powered manipulation of microfluidics. They developed a miniature car with four droplets as wheels, limiting its volume to tens of nanoliters, and accomplished precise stepping motion and cargo loading.

Moreover, the idea of converting mechanical energy into electricity can potentially be integrated with other micro/nanorobot designs. Lee et al. (2021) designed a nanobiological supercapacitor (nBSC) catalyzed by redox reactions, which has a volume of only 1 nL and operates at high potentials ranging from 1V to 1.6V. To withstand the pressure and temperature variations in blood flow, the research team utilized a planar structure that self-assembles into a compact three-dimensional tubular geometry. Combining this tubular structure with energy conversion systems like TENG may potentially enable the development of MNRs with high energy storage capacity and continuous motion/supply.

Bubble propulsion is an important mode of propulsion in liquid environments. In electrochemistry, there are various methods to generate a large number of bubbles, which provides an exciting theoretical basis for the integration of electrically controlled micro/nanorobots with bubble propulsion. Zhan et al. (2023) have developed a photopyroelectric slippery surface (PESS) based on the photopolymerization-electric effect to achieve versatile manipulation of bubbles. Under near-infrared light irradiation, the PESS generates dielectric wetting and nonuniform electric fields, resulting in the simultaneous application of the Laplace force and dielectrophoresis force on the bubbles, enabling high-speed movement. These bubbles can be efficiently and precisely guided along arbitrarily designed paths, covering a wide range of volumes. More importantly, PESS allows for the splitting, merging, and detachment of underwater bubbles, offering a promising

approach for selective chemical reactions, self-assembly, and cargo transportation.

4 Motion modes of electrically controlled MNRs

As mentioned earlier, electrically controlled MNRs generally move under the influence of electric fields or electric field-induced fluid flow. This mode of motion typically relies on the direction and strength of the electric field, making the motion of MNRs predictable and highly controllable (Yang et al., 2020; Wang et al., 2021). In addition to linear and curved motion, common motion modes include rotation, vibration, and spiral movement. Individual MNRs often exhibit limited motion states, such as linear motion or controllable motion under orbital confinement. Brooks et al. achieved the spiral motion of spherical colloids with low-symmetry metal patches in an alternating current electric field (Lee et al., 2019). However, when MNRs move collectively, they can demonstrate a wider range of motion patterns. Lee et al. (2023) utilized asymmetric Janus particle clusters to achieve five different states of motion: translation, rotation, butterfly pattern, spiral, and orbital motion. This enables electrically controlled MNRs to have enhanced motion capabilities in complex three-dimensional environments.

In different modes of motion, electrochemically-controlled micro/nano robots can adapt to different environments to demonstrate multitasking capabilities. Here are some basic motion modes and their application: i) Rolling: Electrically controlled MNRs that can roll have potential applications in targeted drug delivery within the bloodstream. Their rolling motion enables them to navigate through blood vessels, reaching specific target sites for drug release. ii) Swimming: MNRs capable of swimming can be used for tasks such as clearing clogged arteries or delivering therapeutic agents to specific organs or tissues. Their swimming motion allows them to propel through fluids, facilitating navigation within the body. Some special swimming pattern like spiral render them ability to navigate complex environments such as vascular networks and tumor microenvironments. iii) Crawling: MNRs with crawling capabilities can be employed for tasks like tissue exploration or wound healing. Their crawling motion enables them to navigate through intricate structures, such as the digestive tract or damaged tissue, for diagnostic or therapeutic purposes.

5 Applications of electrically controlled MNRs

5.1 Overall application scenarios of electrically controlled MNRs

Electrically controlled MNRs have made significant advancements in design and fabrication. Compared to other manipulation methods, the major advantage of electrically controlled MNRs is their low cost and non-contact manipulation capability (Wang et al., 2021). Although magnetically controlled MNRs possess similar properties, they fall slightly behind in terms of manipulation ability, precision, and real-time responsiveness (Han et al., 2018; Wang et al., 2021). MNRs with conductive or semiconductive properties can be precisely controlled and exhibit multidirectional movement or rotation in three-dimensional space through changes in external electric fields (Fan et al., 2005; Guo et al., 2018; Han et al., 2018). Kim et al. (2014) designed an ordered array of nanoscale motors through bottom-up assembly, where nanowires act as rotors, patterned nanomagnets serve as bearings, and quadrupole microelectrodes function as stators. Under the influence of an electric field, the nanomotor array can perform chiral rotations with controllable angles and speeds (exceeding 18,000 r.p.m.). This research demonstrates the significant implications for nanoelectromechanical systems, nanomedicine, microfluidics, and on-chip laboratory architectures. However, the application of electrically controlled MNRs is still limited in the human body, especially in complex environments such as the bloodstream, due to the rapid decay of electric fields with distance and their instability in high-particle environments (Wang and Gao, 2012). Currently, mainstream research suggests that electrically controlled MNRs have a unique advantage in size control. Due to dielectrophoretic forces, electric fields can achieve precise control at the microscale (Velev et al., 2003; Han et al., 2018), whereas the size of magnetically controlled MNRs is typically limited by magnetic materials (Gao Y. et al., 2021). It can be expected that, once the challenges of interference resistance and sustained operation of electrically controlled MNRs are addressed, they will demonstrate promising performance in targeted tumor therapy, drug delivery, nucleic acid biomarker detection, diagnostics, sensing, microsurgery, blood clot ablation, and wound healing.

On the other hand, research on MNRs propelled by electrochemical reactions has reached relatively mature stages. The electrochemical reactions occurring in asymmetric particles provide a strong theoretical foundation for self-propelled electrically controlled MNRs (Paxton et al., 2004; Paxton et al., 2005; Wang et al., 2013). The electrochemical and fluidic properties resulting from redox reactions (Luo et al., 2019) enable MNRs with electrochemical capabilities to exhibit good performance in self-propulsion and sustained propulsion (Paxton et al., 2005; Calvo-Marzal et al., 2010; Kümmel et al., 2013; Dai et al., 2016). Sun et al. (2023) combined MNRs with nano-catalytic medicine to achieve deep tumor penetration induced by self-propulsion and catalytic reaction-triggered tumor therapy *in vivo* (Figures 4A, C). They utilized self-propelled Janus nano-catalytic robots (JNCR) guided by magnetic resonance imaging (MRI) for enhanced tumor treatment inside the body. JNCR exhibited active mobility in the H2O2 solution. Compared to passive nanoparticles, these self-propelled JNCRs could penetrate deeper into tumors after intratumoral injection, thereby improving tumor treatment efficacy. These robots demonstrated biocompatibility in mouse models and hold the potential for integrating MNRs with nano-catalytic medicine, thereby improving tumor therapy and achieving clinical translation. However, H2O2 exhibits certain biological toxicity in the body (Wang et al., 2021), and further exploration is needed for the *in vivo* application of related electro-catalytic-driven microelectric motors. Conversely, non-contact electric fields have a greater advantage in terms of safety. Chen et al. (2014) proposed a wireless-powered microrobot based on an Archimedean spiral, which possesses a highly integrated active motion module.

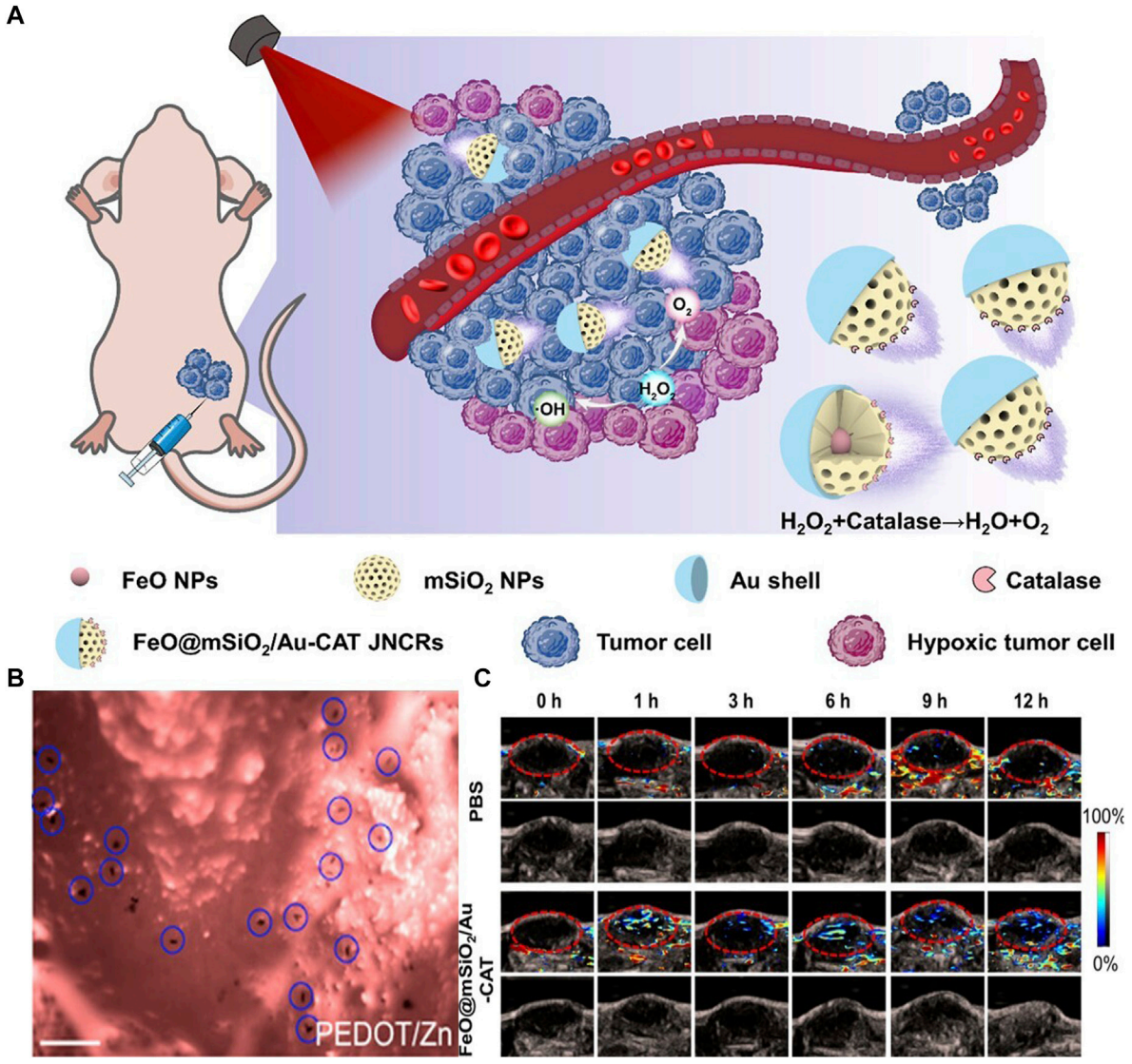

FIGURE 4
(A) Mechanisms of Self-Propelled Janus Nanocatalytic Robots for 4T1 tumor-bearing mice (Sun et al., 2023). 2023 American Chemical Society **(B)** Retention of PEDOT/Zn micromotors on mouse gastric mucosal tissues. Scale bars, 100 μm (Gao et al., 2015b). 2014 American Chemical Society **(C)** Saturated oxygen (sO2) levels in the tumour vasculature after saline or Janus nanocatalytic robots injections at 0, 1, 3, 6, 9 and 12 h (Sun et al., 2023). 2023 American Chemical Society.

The researchers fabricated and tested a prototype for wireless capsule endoscopy (WCE) using radiofrequency-based power transfer. Through design modifications, a cylindrical ferrite core was added to the receiving coil array, significantly improving the coupling efficiency (up to 12%). Such designs can also achieve functionalities such as targeted propulsion and integration with imaging techniques, while significantly enhancing safety.

5.2 Applications of Janus particles in electrically controlled MNRs

Janus particles with distinct dielectric properties have emerged as a highly promising choice for electrically controlled MNRs. These particles possess induced charges and an asymmetric distribution of electric dipole s (Demirörs et al., 2018), enabling their propulsion and manipulation through ICEP (Lee et al., 2023), Lee et al. (2023) discovered that magnetic locking assemblies of metallic-dielectric Janus particles exhibit five distinct motion states under the influence of ICEP, with four of them achievable using Janus dimers alone. Furthermore, the asymmetric nature of Janus particles leads to an imbalanced electrokinetic flow on both sides of the particle (Ma et al., 2015), endowing them with self-propulsion capabilities. With this combination of characteristics, Janus particles have demonstrated significant potential in biomedical applications such as drug delivery, cell manipulation, and targeted transport. In all these applications, precise positioning and navigation of Janus particles are often crucial initial steps.

Current mainstream MNRs employ various methods for localization and guidance, including magnetic (Diller et al., 2013;

Peyer et al., 2013; Servant et al., 2015; Li et al., 2019; Xie et al., 2019; Fang et al., 2023), optical/thermal (Wang J. et al., 2019; Xie et al., 2019; Dai et al., 2022; Wang et al., 2023), and acoustic (Abbas et al., 2020; Das et al., 2022; Wu et al., 2023) methods, as well as physical constraints through microstructure fabrication and microfluidic manipulation (Katuri et al., 2016; Patteson et al., 2016). However, these approaches are often limited by the physical structures of the materials themselves or the complex interactions between materials and microfluidic channels, making it challenging to explore new directions and optimize their performance. Despite these limitations, the development of electrically controlled Janus particles, particularly those controlled by ICEP, has been relatively limited until the introduction of a self-powered microelectromotor by Yoshizumi et al. (2015). This microelectromotor utilizes alternating-current electroosmosis (ACEO) and positive dielectrophoresis (pDEP) for control and is capable of simple, low-cost two-dimensional motion. The micro electromotor is composed of a gold/platinum bilayer Janus particle and can be individually controlled for self-propulsion using grid electrodes formed at the bottom and top of microchannels, eliminating the need for external guiding devices such as multi-axis manipulators. The behavior of 5 μm PS/Pt/Au microelectromotors was investigated in deionized water and 1M H2O2 solution. Experimental results revealed that the MNRs possessed a negative zeta potential in the water solution. When immersed in a fuel solution, the electrochemical reactions of gold and platinum induced an electric field resulting from charge separation, causing electrophoretic fluid to flow along the surface of the microelectromotor towards the negative electrode, thereby enabling its motion. However, similar to the design by Sun et al., the self-propelled motion of the Janus particle microelectromotor was observed only in the presence of H2O2 solution, with an average velocity of approximately 7 μm/s. Additionally, Clausius-Mossotti factor (CMF) measurements conducted on PS, PS/Pt, and PS/Pt/Au particles revealed that PS particles exhibited behavior similar to negative dielectrophoresis at higher frequencies, while PS/Pt and PS/Pt/Au particles exhibited negative dielectrophoresis-like behavior at all frequencies, attributed to enhanced polarization from the metal shell structure. At low frequencies, PS, PS/Pt, and PS/Pt/Au particles were dragged toward the center of the ITO electrode due to ACEO effects, and pDEP effectively attracted the MNRs to the edge of the electrode. Such structural and design considerations provide novel ideas for the two-dimensional motion of electrically controlled Janus particle microelectromotors. Building upon this research, Zhang et al. (2019) proposed a similar collection and anchoring mechanism for Janus particles under the propulsion of ICEP. The team reported a universal strategy for propelling, constraining, and collecting metal-dielectric Janus microspheres using an interdigitated microelectrode design. Interdigitated microelectrodes exhibit rich alternating-current electrodynamic characteristics and are widely employed in applications such as the detection and separation of biological samples, as well as biochemical and electrochemical sensing. It was observed that particles could be propelled along the center of the electrode towards both ends via ICEP and subsequently trapped by electroosmosis, without the need for additional fuel. Furthermore, the particles rotated at the closed end of the electrode, decelerated, and accumulated at the open end. By simply modifying the electrode configuration, a maze pattern composed of serpentine chains could be formed. This study presents a versatile electrode-based strategy for controlling one-dimensional transport and aggregation of MNRs in a configurable, switchable, and non-contact manner, offering potential benefits for fundamental research and applications such as sensing, sorting, and transport.

Compared to static positioning, the control of Janus particles' motion holds greater clinical value. Lee et al. (2019) discovered that asymmetric metallic patches on the surface of spherical colloids can be driven by an alternating electric field, guiding the colloids to move along nonlinear helical trajectories. By altering the size and shape of the patches, the details of particle motion, such as trajectory speed and radius, can be adjusted. Particles with approximately mirror-symmetric triangular patches can perform helical motion rather than linear propulsion. In porous membranes, helical trajectories offer functional advantages for particle navigation compared to linear propulsion. This implies that Janus particles propelled in a helical manner are an ideal modality in complex environments such as the human body. Moreover, as particle symmetry is further reduced, the motion patterns become increasingly complex. By comparing particles with complex helical trajectory motion to particles with ordinary linear motion, the research team found that particles with complex trajectories are more likely to find and traverse channels in porous matrices, further demonstrating the advantages of helical motion for *in vivo* applications. Similarly, Demirörs et al. (2021) found that Janus particles are influenced by external electric fields and the chemical properties of their contact surfaces, allowing the particles to be coupled to rolling motion in orthogonal electric fields under certain conditions, and estimating the contact surface friction properties using derived mathematical ratios. Rolling motion mimics migration behaviors observed in leukocytes and macrophages, indicating that electrically controlled Janus particles' motion is not limited to pure fluidic environments but can also occur at the fluid-substrate interface. Furthermore, the rolling response of Janus microrobots can be utilized for reversible cargo capture and release using electric fields, enabling the manipulation of cargo particles at the microscale. By combining functional molecules, Janus microrobots can be used to create microscale chemical gradients or achieve programmable release with spatiotemporal control, applying to bioanalytical platforms for drug screening, medical diagnostics, or fundamental biological research.

Another key feature of Janus particles is their self-propulsion ability. Compared to external field manipulation, self-propelled Janus particles offer the following advantages: i) better mobility in complex environments such as high ionic environments like blood, ii) spontaneous emergence of collective behaviors, and iii) potential for self-assembly. This is due to the generation of surface forces upon breaking symmetry, resulting in a phenomenon known as self-electrophoresis (Boymelgreen et al., 2016) Similar concepts have been demonstrated in early zinc-based micromotors. Gao et al. (2015a) conducted *in vivo* studies of artificial micromotors in mice through oral administration (Figure 4B). The results showed that propulsion forces driven by gastric acid could effectively enhance the binding and retention of micromotors and their payloads on the gastric wall. The micromotor body gradually dissolves in gastric acid and autonomously releases the carried payload without leaving any

toxic residues. In addition to drug delivery, self-propelled micromotors also assist in detoxification (Orozco et al., 2013) and self-healing systems (Li et al., 2015). Building upon such research, asymmetric self-propelled Janus particles with more complex structures naturally hold greater development potential. Das and Yossifon, (2023)employed optoelectric tweezers to achieve simultaneous manipulation of Janus active particles and electrically driven self-propulsion while discretizing the external field space. Microscopic objects were manipulated using optically induced dielectrophoresis, generating and controlling multiple beams of light through a digital micromirror device (DMD) in a dynamic and programmable manner. Additionally, by controlling the number and types of illuminated regions, the self-assembly of active particles into specific configurations can be guided. Compared to random assembly, this system allows for deterministic combination of non-active particles, forming complex hybrid structures. The study demonstrates that sufficiently large active particles can uniformly manipulate synthetic/biological cargo particles. Moreover, the photoelectric effects generated by manipulating particles can also induce effects like electroporation on cells, indicating the potential realization of gene transfection, cell fusion, and cell separation for individual target cells using this approach. Similarly, Peng et al. (2020), inspired by the motion patterns of *Escherichia coli*, developed a photothermal-electrically driven Janus particle that exhibits rotation within a plane under a temperature gradient-induced electric field, in addition to conventional photoelectric effects. By adjusting the rotation laser beam's timing, the particle can be positioned in any desired direction, enabling efficient active control of the swimming direction. Through dark-field optical imaging and feedback control algorithms, autonomous propulsion and navigation of MNRs have been achieved. This approach overcomes the disorder in long-timescale motion direction caused by random Brownian motion of Janus particles.

As research progresses, an increasing number of scientists recognize the limitations of single-driven MNRs, especially Janus particles, in complex application environments due to strict energy and environmental constraints (Xu et al., 2017). MNRs with different responses often require different asymmetric materials, such as magnetic Janus particles composed of Fe2O3/ZnFe2O4/Mn2O3 (Yang et al., 2023), asymmetrically sound-pressure-driven Au nanowires (Wang et al., 2012), and electrochemically catalyzed Pt/Au microparticles (Paxton et al., 2004). Zheng et al. [116] developed a double-layered bowl-shaped structure consisting of platinum and α-Fe2O3, integrating five driving engines: light, sound, magnetic, electric, and chemical. Under an alternating electric field, the inner platinum and outer α-Fe2O3 layers exhibit asymmetric polarization, inducing motion through charge-induced electroosmosis (ICEO). The other four propulsion mechanisms enhance the performance of the micro-robot in specific applications. These multi-driven Janus particles may possess unique adaptability and advantages in complex biological environments.

Overall, Janus particles with asymmetric chemical structures are excellent materials for electric field-driven and self-propelled systems, offering the following advantages: i) Multifunctionality: The two different surfaces of Janus particles can exhibit distinct functionalities. For example, one side may possess biocompatibility for drug binding or act as a biosensor, while the other side may have conductivity for power generation or catalytic activity. In future developments, these surfaces could be interchangeable to adapt to different biological environments such as blood, blood vessel walls, and tissue structures. ii) Controllability: Under certain conditions, such as various external fields and electron tweezers microfluidic chip control, Janus particles can be precisely positioned and manipulated within a certain range. The influence of external field-driven and self-propelled Janus particles has significant implications for applications such as targeted tumor therapy and precise cell manipulation. iii) Aggregability: Janus particles can be precisely positioned and aggregated under certain electrical field stimulations, such as discrete electric fields and optoelectric chips, leading to cluster effects and unexpected functionalities and motion patterns. This offers limitless possibilities and surprises in the future development of biomedical applications.

However, Janus particles also face some challenges: i) Difficulty in preparation: The synthesis of Janus particles often requires special methods and conditions, which may increase complexity and cost. ii) Biocompatibility: Some Janus particles require biologically harmful environments such as H2O2, and most of the research on Janus particles is limited to *in vitro* studies, lacking validation for biocompatibility. iii) Stability: Janus particles composed of inert materials like Au/Pt exhibit relatively high stability, but the stability and durability of other active materials such as iron and zinc need further consideration.

5.3 Electrophysiological processes in bionic electro-controlled MNRs

To address the issues of large size, complex manufacturing, low efficiency, high frictional losses, and generation of hazardous waste associated with traditional rigid MNRs (Wang, 2009; Alizadeh et al., 2020; Soto et al., 2020; Huang et al., 2022), in addition to artificial micro/nanoparticles, bionic micro motors have also rapidly developed in the past decade. Bionic micromotors can be broadly categorized into three types: MNRs that mimic/utilize bacteria/algae (Ma et al., 2012; Park et al., 2013; Rogowski et al., 2020; Rogowski et al., 2021; Xie et al., 2021; Gwisai et al., 2022), those that mimic/utilize sperm (Magdanz et al., 2013; Medina-Sánchez et al., 2016; Chen et al., 2021), and bionic micro motors that mimic muscles. Shi and Yeatman (2021) defined a class of responsive materials or devices that are small in scale, low in stiffness, and capable of replicating the core functionality of natural muscles as artificial muscles. These artificial muscles exhibit various modes of response, including electrical (Jang et al., 2021), pressure-based (Jang et al., 2015; Jang et al., 2017) chemical environment-based (Mashayekhi Mazar et al., 2019), thermal (Haines et al., 2014; Mirvakili and Hunter, 2017), and magnetic (Lee et al., 2018) responses. In this review, electrically stimulated artificial muscles are considered as part of electrically controlled MNRs.

Electrically stimulated artificial muscles often utilize stimulation signals directly to achieve contraction. Jang et al. (2021), inspired by skeletal muscle myofibrils, developed a bundle-shaped biohybrid artificial muscle (Figure 5A). By integrating skeletal muscle cells with hydrophilic polyurethane and carbon nanotube nanofibers, they created a structure resembling natural skeletal muscle fibers. The

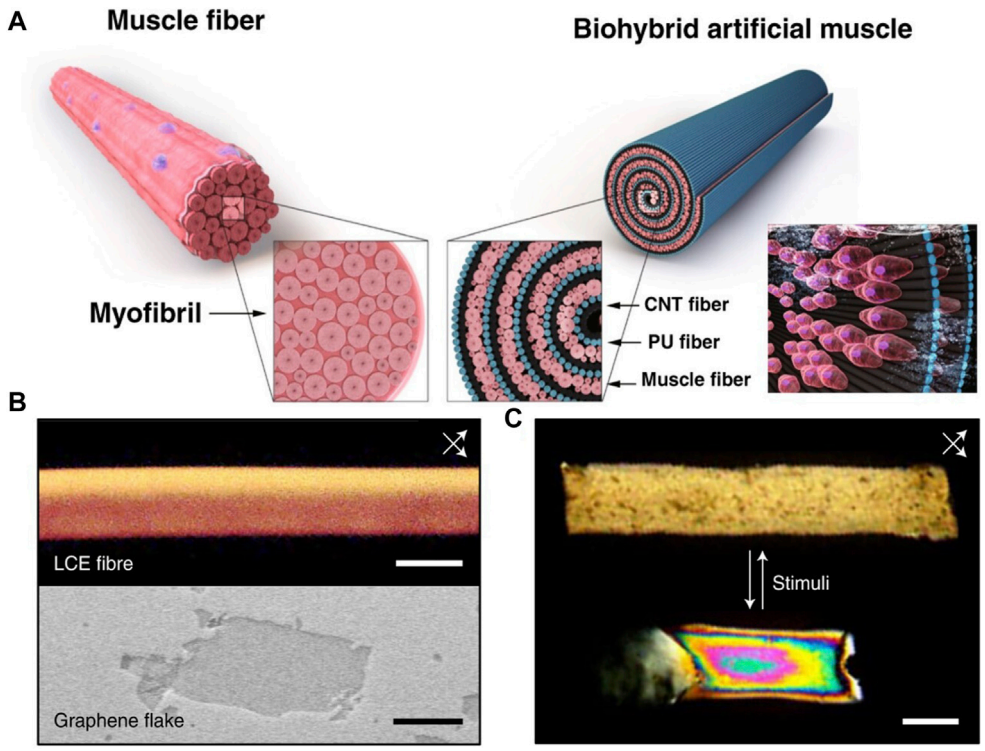

FIGURE 5
(A) The structural similarities and differences between natural muscles and artificial muscles (Jang et al., 2021) 2021, The Author (s). **(B)** Polarized Optical Microscope of Liquid Crystal Formation observed at 45° angles with respect to cross-polarizers (top) and Scanning Electron Microscope image of an Electrographite flake (bottom) (Kim et al., 2022). 2022, The Author (s). **(C)** The shape deformation of artificial muscles during relaxation and contraction (Kim et al., 2022) 2022, The Author (s).

nanofibers provided a stretchable scaffold, similar to the framework of actin and myosin, while the incorporation of skeletal muscle fibers helped drive the biohybrid artificial muscle. Reversible contraction of the biohybrid artificial muscle can be achieved through electric field stimulation. This electrically driven artificial muscle holds tremendous potential for driving motion and drug delivery systems in implantable medical robots. Furthermore, the integration of biohybrid artificial muscles controlled by motor neurons is of significant importance for brain-machine interfaces.

In addition to bionic muscles prepared through biohybrid approaches, ion polymer actuators made of electrically lightweight, low-power, active polymers have also received attention (Shahinpoor and Kim, 2005; Khan et al., 2015). These actuators are flexible, lightweight, low-power, and can be processed at the nanoscale, making them ideal for artificial muscles. Khan et al. (2019) synthesized ion-exchange polymer films based on polypyrrole/polyvinyl alcohol (PPy/PVA), incorporating PEDOT:PSS/SWNT/IL electrodes that can change conformation through externally applied voltage. To investigate size-dependent electromechanical actuation performance, the researchers fabricated ion polymer actuator films with four different sizes of PPy nanoparticles. Compared to other expensive perfluorinated polymer-based actuators, the PPy/PVA polymer composite films showed enhanced electrical performance and tip deflection performance, with the electrodes utilizing a hybrid PEDOT:PSS/SWNT/IL electrode film. Based on this, a microgripper device with two fingers composed of PPy/PVA/EL ion-exchange polymer films was developed. MNRs designed with this approach exhibit electrophysiological functionality similar to natural muscles, and their ability to change conformation through externally applied voltage provides additional functional potential beyond natural muscles. In the field of implantable medical robots, such bionic muscles can meet macro-scale requirements with a micro-scale configuration, enabling tasks such as object grasping and precision surgery.

Building upon artificial muscles, researchers believe that the piezoelectric properties of artificial muscles can be effectively extended to artificial cochlea. Jang et al. (2015) developed a piezoelectric artificial basilar membrane (ABM) composed of a microelectromechanical system (MEMS) cantilever array, which emulates the tonotopic characteristics of the cochlea and produces clear tones within the audible frequency range. Through experiments conducted on animal models, the characteristics of ABM as a potential front-end for cochlear implant applications were validated. The frequency selectivity of ABM was confirmed by measuring electrically evoked auditory brainstem responses (EABR).

Overall, the advantages of bionic artificial muscles are evident. As an ideal microactuator mechanism, they possess the following features: i) Soft and resilient mechanical characteristics: Artificial muscles exhibit flexibility and elasticity similar to natural muscles, enabling highly deformable motions (Figures 5B, C). ii) Flexible driving mechanisms: Microactuators provide precise control and adjustment, allowing fine movements and power output of artificial muscles. iii) Small size and high efficiency: Microactuator-driven

artificial muscles demonstrate acceptable efficiency at the micrometer to sub-centimeter scale, making them highly suitable for microsystem applications. This potential opens up avenues for development in the following areas: i) Robotics and human-machine interaction: Microactuator-driven artificial muscles can be employed in the motion and operation of robots, enabling more natural and flexible human-machine interaction. ii) Prosthetics and rehabilitation devices: Artificial muscles can be utilized in the production of lightweight and efficient prosthetics and rehabilitation devices, offering improved movement and functional recovery. iii) Medical instruments: Microactuator-driven artificial muscles can be employed in microscale medical instruments such as endoscopes and minimally invasive surgical devices, enabling precise manipulation and control. iv) Flexible electronic products: Artificial muscles can be integrated into flexible electronic products, such as wearable devices and smart textiles, for a more comfortable and adaptive user experience. v) Biomedical research: Artificial muscles can be utilized in biomedical research, including biomimetic models and tissue engineering, aiding in the understanding and simulation of biological system movements and functions.

6 Discussion

In conclusion, although the clinical application of electrically controlled MNRs is still in its early stages, their complex motion patterns, self-propulsion capabilities, and deformability have shown promising potential. However, the practicality and stability of electrically controlled MNRs are still subject to exploration due to fabrication challenges and the highly ionic environment within the human body.

In the future, qualified electrically controlled MNRs should possess the following characteristics: i) Good biocompatibility to avoid recognition as foreign objects and clearance by the immune system; ii) Dual control of external fields and self-propulsion to accomplish tasks in complex environments; iii) Strong deformability allowing a single robot to perform multiple tasks; iv) Low-cost fabrication with streamlined production.

As research progresses, the applications of electrically controlled MNRs will become increasingly diverse and suitable for various purposes. With the help of the aforementioned characteristics, electrically controlled MNRs hold tremendous potential for applications in the following areas: i) Targeted drug delivery: This form of targeted delivery based on electrically controlled MNRs can enhance the efficacy of drugs, reduce side effects, and enable more effective treatment methods. ii) Diagnostic monitoring of biomarkers and pathological changes: By performing monitoring within the body, these MNRs can provide more accurate, sensitive, and real-time diagnostic results. iii) Minimally invasive surgery and interventional therapy: Electrically controlled MNRs can be utilized for minimally invasive surgical procedures and interventional therapies, thereby reducing surgical trauma and recovery time. iv) Cancer treatment: In the fields of early cancer detection, targeted drug delivery to tumors, and precise radiotherapy, electrically controlled MNRs can improve treatment efficacy and reduce side effects.

Author contributions

RP: Writing–original draft, Writing–review and editing. YX: Writing–review and editing. HM: Writing–review and editing. ZX: Writing–review and editing. JH: Writing–review and editing.

Funding

The author(s) declare financial support was received for the research, authorship, and/or publication of this article. Jiangsu Provincial Health Commission Project (z2022077).

Conflict of interest

The authors declare that the research was conducted in the absence of any commercial or financial relationships that could be construed as a potential conflict of interest.

Publisher's note

References

Abbas, M., Alqahtani, M., Algahtani, A., Kessentini, A., Loukil, H., Parayangat, M., et al. (2020). Validation of nanoparticle response to the sound pressure effect during the drug-delivery process. *Polym. (Basel)* 12 (1), 186. doi:10.3390/polym12010186

Alizadeh, A., Hsu, W.-L., Wang, M., and Daiguji, H. (2021). Electroosmotic flow: from microfluidics to nanofluidics. *ELECTROPHORESIS* 42 (7-8), 834–868. doi:10.1002/elps.202000313

Alizadeh, S., Esmaeili, A., Barzegari, A., Rafi, M. A., and Omidi, Y. (2020). Bioengineered smart bacterial carriers for combinational targeted therapy of solid tumours. *J. Drug Target* 28 (7-8), 700–713. doi:10.1080/1061186X.2020.1737087

Bazant, M. Z., and Squires, T. M. (2004). Induced-charge electrokinetic phenomena: theory and microfluidic applications. *Phys. Rev. Lett.* 92 (6), 066101. doi:10.1103/PhysRevLett.92.066101

Boymelgreen, A., Yossifon, G., and Miloh, T. (2016). Propulsion of active colloids by self-induced field gradients. *Langmuir* 32 (37), 9540–9547. doi:10.1021/acs.langmuir.6b01758

Calvo-Marzal, P., Sattayasamitsathit, S., Balasubramanian, S., Windmiller, J. R., Dao, C., and Wang, J. (2010). Propulsion of nanowire diodes. *Chem. Commun.* 46 (10), 1623–1624. doi:10.1039/B925568K

Celi, N., Gong, D., and Cai, J. (2021). Artificial flexible sperm-like nanorobot based on self-assembly and its bidirectional propulsion in precessing magnetic fields. *Sci. Rep.* 11 (1), 21728. doi:10.1038/s41598-021-00902-6

Chen, Q., Tang, S., Li, Y., Cong, Z., Lu, D., Yang, Q., et al. (2021). Multifunctional metal-organic framework exoskeletons protect biohybrid sperm microrobots for active drug delivery from the surrounding threats. *ACS Appl. Mater Interfaces* 13 (49), 58382–58392. doi:10.1021/acsami.1c18597

Chen, W., Yan, G., Wang, Z., Jiang, P., and Liu, H. (2014). A wireless capsule robot with spiral legs for human intestine. *Int. J. Med. Robot.* 10 (2), 147–161. doi:10.1002/rcs.1520

Cohen, L., and Walt, D. R. (2019). Highly sensitive and multiplexed protein measurements. *Chem. Rev.* 119 (1), 293–321. doi:10.1021/acs.chemrev.8b00257

Dai, B., Wang, J., Xiong, Z., Zhan, X., Dai, W., Li, C.-C., et al. (2016). Programmable artificial phototactic microswimmer. *Nat. Nanotechnol.* 11 (12), 1087–1092. doi:10.1038/nnano.2016.187

Dai, B., Zhou, Y., Xiao, X., Chen, Y., Guo, J., Gao, C., et al. (2022). Fluid field modulation in mass transfer for efficient photocatalysis. *Adv. Sci. (Weinh)* 9 (28), e2203057. doi:10.1002/advs.202203057

Das, S. S., Erez, S., Karshalev, E., Wu, Y., Wang, J., and Yossifon, G. (2022). Switching from chemical to electrical micromotor propulsion across a gradient of gastric fluid via magnetic rolling. *ACS Appl. Mater Interfaces* 14 (26), 30290–30298. doi:10.1021/acsami.2c02605

Das, S. S., and Yossifon, G. (2023). Optoelectronic trajectory reconfiguration and directed self-assembly of self-propelling electrically powered active particles. *Adv. Sci. (Weinh)* 10 (16), e2206183. doi:10.1002/advs.202206183

Dasgupta, D., Peddi, S., Saini, D. K., and Ghosh, A. (2022). Mobile nanobots for prevention of root canal treatment failure. *Adv. Healthc. Mater.* 11 (14), 2200232. doi:10.1002/adhm.202200232

del Barrio, J., and Sánchez-Somolinos, C. (2019). Light to shape the future: from photolithography to 4D printing. *Adv. Opt. Mater.* 7 (16), 1900598. doi:10.1002/adom.201900598

Demirörs, A. F., Akan, M. T., Poloni, E., and Studart, A. R. (2018). Active cargo transport with Janus colloidal shuttles using electric and magnetic fields. *Soft Matter* 14 (23), 4741–4749. doi:10.1039/c8sm00513c

Demirörs, A. F., Stauffer, A., Lauener, C., Cossu, J., Ramakrishna, S. N., de Graaf, J., et al. (2021). Magnetic propulsion of colloidal microrollers controlled by electrically modulated friction. *Soft Matter* 17 (4), 1037–1047. doi:10.1039/d0sm01449d

Diller, E., Giltinan, J., and Sitti, M. (2013). Independent control of multiple magnetic microrobots in three dimensions. *Int. J. Robotics Res.* 32 (5), 614–631. doi:10.1177/0278364913483183

Dong, R., Cai, Y., Yang, Y., Gao, W., and Ren, B. (2018). Photocatalytic micro/nanomotors: from construction to applications. *Acc. Chem. Res.* 51 (9), 1940–1947. doi:10.1021/acs.accounts.8b00249

Fan, D. L., Zhu, F. Q., Cammarata, R. C., and Chien, C. L. (2005). Controllable high-speed rotation of nanowires. *Phys. Rev. Lett.* 94 (24), 247208. doi:10.1103/PhysRevLett.94.247208

Fan, D. L., Zhu, F. Q., Cammarata, R. C., and Chien, C. L. (2011). Electric tweezers. *Nano Today* 6 (4), 339–354. doi:10.1016/j.nantod.2011.05.003

Fang, R. H., Gao, W., and Zhang, L. (2023). Targeting drugs to tumours using cell membrane-coated nanoparticles. *Nat. Rev. Clin. Oncol.* 20 (1), 33–48. doi:10.1038/s41571-022-00699-x

Fath, A., Xia, T., and Li, W. (2022). Recent advances in the application of piezoelectric materials in microrobotic systems. *Micromachines (Basel)* 13 (9), 1422. doi:10.3390/mi13091422

Feng, A., Cheng, X., Huang, X., Liu, Y., He, Z., Zhao, J., et al. (2023). Engineered organic nanorockets with light-driven ultrafast transportability for antitumor therapy. *Small* 19 (21), 2206426. doi:10.1002/smll.202206426

Fennimore, A. M., Yuzvinsky, T. D., Han, W.-Q., Fuhrer, M. S., Cumings, J., and Zettl, A. (2003). Rotational actuators based on carbon nanotubes. *Nature* 424 (6947), 408–410. doi:10.1038/nature01823

Gangwal, S., Cayre, O. J., Bazant, M. Z., and Velev, O. D. (2008). Induced-charge electrophoresis of metallodielectric particles. *Phys. Rev. Lett.* 100 (5), 058302. doi:10.1103/PhysRevLett.100.058302

Gao, C., Huang, J., Xiao, Y., Zhang, G., Dai, C., Li, Z., et al. (2021a). A seamlessly integrated device of micro-supercapacitor and wireless charging with ultrahigh energy density and capacitance. *Nat. Commun.* 12 (1), 2647. doi:10.1038/s41467-021-22912-8

Gao, W., Dong, R., Thamphiwatana, S., Li, J., Gao, W., Zhang, L., et al. (2015a). Artificial micromotors in the mouse's stomach: a step toward *in vivo* use of synthetic motors. *ACS Nano* 9 (1), 117–123. doi:10.1021/nn507097k

Gao, W., Dong, R., Thamphiwatana, S., Li, J., Gao, W., Zhang, L., et al. (2015b). Artificial micromotors in the mouse's stomach: a step toward *in vivo* use of synthetic motors. *ACS Nano* 9 (1), 117–123. doi:10.1021/nn507097k

Gao, Y., Wei, F., Chao, Y., and Yao, L. (2021b). Bioinspired soft microrobots actuated by magnetic field. *Biomed. Microdevices* 23 (4), 52. doi:10.1007/s10544-021-00590-z

Ghosh, S., and Ghosh, A. (2020). Design considerations for effective thermal management in mobile nanotweezers. *J. Micro-Bio Robotics* 16 (1), 33–42. doi:10.1007/s12213-020-00123-6

Guanying, M., Guozheng, Y., and Xiu, H. (2007). Power transmission for gastrointestinal microsystems using inductive coupling. *Physiol. Meas.* 28 (3), N9–N18. doi:10.1088/0967-3334/28/3/n01

Guo, J., Gallegos, J. J., Tom, A. R., and Fan, D. (2018). Electric-field-guided precision manipulation of catalytic nanomotors for cargo delivery and powering nanoelectromechanical devices. *ACS Nano* 12 (2), 1179–1187. doi:10.1021/acsnano.7b06824

Gwisai, T., Mirkhani, N., Christiansen, M. G., Nguyen, T. T., Ling, V., and Schuerle, S. (2022). Magnetic torque-driven living microrobots for increased tumor infiltration. *Sci. Robot.* 7 (71), eabo0665. doi:10.1126/scirobotics.abo0665

Haines, C. S., Lima, M. D., Li, N., Spinks, G. M., Foroughi, J., Madden, J. D., et al. (2014). Artificial muscles from fishing line and sewing thread. *Science* 343 (6173), 868–872. doi:10.1126/science.1246906

Han, J., Zhen, J., Du Nguyen, V., Go, G., Choi, Y., Ko, S. Y., et al. (2016). Hybrid-actuating macrophage-based microrobots for active cancer therapy. *Sci. Rep.* 6, 28717. doi:10.1038/srep28717

Han, K., Shields IV, C. W., and Velev, O. D. (2018). Engineering of self-propelling microbots and microdevices powered by magnetic and electric fields. *Adv. Funct. Mater.* 28 (25), 1705953. doi:10.1002/adfm.201705953

Haque, M. A., Zhu, X., Uyanga, N., and Wu, N. (2023). Propulsion of homonuclear colloidal chains based on orientation control under combined electric and magnetic fields. *Langmuir* 39 (7), 2751–2760. doi:10.1021/acs.langmuir.2c03221

He, X., Jiang, H., Li, J., Ma, Y., Fu, B., and Hu, C. (2021). Dipole-moment induced phototaxis and fuel-free propulsion of ZnO/Pt Janus micromotors. *Small* 17 (31), e2101388. doi:10.1002/smll.202101388

Huang, S., Gao, Y., Lv, Y., Wang, Y., Cao, Y., Zhao, W., et al. (2022). Applications of nano/micromotors for treatment and diagnosis in biological lumens. *Micromachines (Basel)* 13 (10), 1780. doi:10.3390/mi13101780

Iacovacci, V., Blanc, A., Huang, H., Ricotti, L., Schibli, R., Menciassi, A., et al. (2019). High-resolution SPECT imaging of stimuli-responsive soft microrobots. *Small* 15 (34), 1900709. doi:10.1002/smll.201900709

Jang, J., Jang, J. H., and Choi, H. (2017). Biomimetic artificial basilar membranes for next-generation cochlear implants. *Adv. Healthc. Mater* 6 (21). doi:10.1002/adhm.201700674

Jang, J., Lee, J., Woo, S., Sly, D. J., Campbell, L. J., Cho, J. H., et al. (2015). A microelectromechanical system artificial basilar membrane based on a piezoelectric cantilever array and its characterization using an animal model. *Sci. Rep.* 5, 12447. doi:10.1038/srep12447

Jang, Y., Kim, S. M., Kim, E., Lee, D. Y., Kang, T. M., and Kim, S. J. (2021). Biomimetic cell-actuated artificial muscle with nanofibrous bundles. *Microsyst. Nanoeng.* 7, 70. doi:10.1038/s41378-021-00280-z

Ji, F., Li, T., Yu, S., Wu, Z., and Zhang, L. (2021). Propulsion gait analysis and fluidic trapping of swinging flexible nanomotors. *ACS Nano* 15 (3), 5118–5128. doi:10.1021/acsnano.0c10269

Katuri, J., Seo, K. D., Kim, D. S., and Sánchez, S. (2016). Artificial micro-swimmers in simulated natural environments. *Lab a Chip* 16 (7), 1101–1105. doi:10.1039/C6LC90022D

Katzmeier, F., and Simmel, F. C. (2023). Microrobots powered by concentration polarization electrophoresis (CPEP). *Nat. Commun.* 14 (1), 6247. doi:10.1038/s41467-023-41923-1

Khan, A., Alamry, K. A., and Jain, R. K. (2019). Polypyrrole nanoparticles-based soft actuator for artificial muscle applications. *RSC Adv.* 9 (68), 39721–39734. doi:10.1039/c9ra06900c

Khan, A., Inamuddin, Jain, R. K., and Naushad, M. (2015). Fabrication of a silver nano powder embedded kraton polymer actuator and its characterization. *RSC Adv.* 5 (111), 91564–91573. doi:10.1039/C5RA17776F

Kim, D., Hwang, K., Park, J., Park, H. H., and Ahn, S. (2017). Miniaturization of implantable micro-robot propulsion using a wireless power transfer system. *Micromachines (Basel)* 8 (9), 269. doi:10.3390/mi8090269

Kim, I. H., Choi, S., Lee, J., Jung, J., Yeo, J., Kim, J. T., et al. (2022). Human-muscle-inspired single fibre actuator with reversible percolation. *Nat. Nanotechnol.* 17 (11), 1198–1205. doi:10.1038/s41565-022-01220-2

Kim, K., Xu, X., Guo, J., and Fan, D. L. (2014). Ultrahigh-speed rotating nanoelectromechanical system devices assembled from nanoscale building blocks. *Nat. Commun.* 5, 3632. doi:10.1038/ncomms4632

Kümmel, F., ten Hagen, B., Wittkowski, R., Buttinoni, I., Eichhorn, R., Volpe, G., et al. (2013). Circular motion of asymmetric self-propelling particles. *Phys. Rev. Lett.* 110 (19), 198302. doi:10.1103/PhysRevLett.110.198302

Lee, D. W., Kim, S. H., Kozlov, M. E., Lepró, X., Baughman, R. H., and Kim, S. J. (2018). Magnetic torsional actuation of carbon nanotube yarn artificial muscle. *RSC Adv.* 8 (31), 17421–17425. doi:10.1039/c8ra01040d

Lee, J. G., Brooks, A. M., Shelton, W. A., Bishop, K. J. M., and Bharti, B. (2019). Directed propulsion of spherical particles along three dimensional helical trajectories. *Nat. Commun.* 10 (1), 2575. doi:10.1038/s41467-019-10579-1

Lee, J. G., Thome, C. P., Cruse, Z. A., Ganguly, A., Gupta, A., and Shields, C. W. (2023). Magnetically locked Janus particle clusters with orientation-dependent motion in AC electric fields. *Nanoscale* 15 (40), 16268–16276. doi:10.1039/D3NR03744D

Lee, K. Y., Gupta, M. K., and Kim, S. W. (2015). Transparent flexible stretchable piezoelectric and triboelectric nanogenerators for powering portable electronics. *Nano Energy* 14, 139–160. doi:10.1016/j.nanoen.2014.11.009

Lee, Y., Bandari, V. K., Li, Z., Medina-Sánchez, M., Maitz, M. F., Karnaushenko, D., et al. (2021). Nano-biosupercapacitors enable autarkic sensor operation in blood. *Nat. Commun.* 12 (1), 4967. doi:10.1038/s41467-021-24863-6

Li, D., Niu, F., Li, J., Li, X., and Sun, D. (2019). Gradient-enhanced electromagnetic actuation system with a new core shape design for microrobot manipulation. *IEEE Trans. Industrial Electron.* 67, 4700–4710. doi:10.1109/TIE.2019.2928283

Li, J., and Pumera, M. (2021). 3D printing of functional microrobots. *Chem. Soc. Rev.* 50 (4), 2794–2838. doi:10.1039/D0CS01062F

Li, J., Shklyaev, O. E., Li, T., Liu, W., Shum, H., Rozen, I., et al. (2015). Self-propelled nanomotors autonomously seek and repair cracks. *Nano Lett.* 15 (10), 7077–7085. doi:10.1021/acs.nanolett.5b03140

Li, Z., Xie, Z., Lu, H., Wang, Y., and Liu, Y. (2021). Cargo transportation and methylene blue degradation by using fuel-powered micromotors. *ChemistryOpen* 10 (9), 861–866. doi:10.1002/open.202100064

Liao, J., Majidi, C., and Sitti, M. (2023). Liquid metal actuators: a comparative analysis of surface tension controlled actuation. *Adv. Mater* 36, e2300560. doi:10.1002/adma.202300560

Liu, Q., Wang, W., Reynolds, M. F., Cao, M. C., Miskin, M. Z., Arias, T. A., et al. (2021). Micrometer-sized electrically programmable shape-memory actuators for low-power microrobotics. *Sci. Robot.* 6 (52), eabe6663. doi:10.1126/scirobotics.abe6663

Liu, Z., Li, M., Dong, X., Ren, Z., Hu, W., and Sitti, M. (2022). Creating three-dimensional magnetic functional microdevices via molding-integrated direct laser writing. *Nat. Commun.* 13 (1), 2016. doi:10.1038/s41467-022-29645-2

Lu, X., Ou, H., Wei, Y., Ding, X., Wang, X., Zhao, C., et al. (2022). Superfast fuel-free tubular hydrophobic micromotors powered by ultrasound. *Sensors Actuators B Chem.* 372, 132667. doi:10.1016/j.snb.2022.132667

Luo, M., Zhao, Z., Zhang, Y., Sun, Y., Xing, Y., Lv, F., et al. (2019). PdMo bimetallene for oxygen reduction catalysis. *Nature* 574 (7776), 81–85. doi:10.1038/s41586-019-1603-7

Lv, Y., Bu, T., Zhou, H., Liu, G., Chen, Y., Wang, Z., et al. (2022). An ultraweak mechanical stimuli actuated single electrode triboelectric nanogenerator with high energy conversion efficiency. *Nanoscale* 14 (21), 7906–7912. doi:10.1039/d2nr01530g

Lv, Y., Pu, R., Tao, Y., Yang, X., Mu, H., Wang, H., et al. (2023). Applications and future prospects of micro/nanorobots utilizing diverse biological carriers. *Micromachines* 14 (5), 983. doi:10.3390/mi14050983

Lyu, X., Liu, X., Zhou, C., Duan, S., Xu, P., Dai, J., et al. (2021). Active, yet little mobility: asymmetric decomposition of H(2)O(2) is not sufficient in propelling catalytic micromotors. *J. Am. Chem. Soc.* 143 (31), 12154–12164. doi:10.1021/jacs.1c04501

Ma, F., Yang, X., Zhao, H., and Wu, N. (2015). Inducing propulsion of colloidal dimers by breaking the symmetry in electrohydrodynamic flow. *Phys. Rev. Lett.* 115 (20), 208302. doi:10.1103/PhysRevLett.115.208302

Ma, Q., Chen, C., Wei, S., Chen, C., Wu, L. F., and Song, T. (2012). Construction and operation of a microrobot based on magnetotactic bacteria in a microfluidic chip. *Biomicrofluidics* 6 (2), 24107–2410712. doi:10.1063/1.3702444

Magdanz, V., Sanchez, S., and Schmidt, O. G. (2013). Development of a sperm-flagella driven micro-bio-robot. *Adv. Mater* 25 (45), 6581–6588. doi:10.1002/adma.201302544

Magdanz, V., Vivaldi, J., Mohanty, S., Klingner, A., Vendittelli, M., Simmchen, J., et al. (2021). Impact of segmented magnetization on the flagellar propulsion of sperm-templated microrobots. *Adv. Sci. (Weinh)* 8 (8), 2004037. doi:10.1002/advs.202004037

Mashayekhi Mazar, F., Martinez, J. G., Tyagi, M., Alijanianzadeh, M., Turner, A. P. F., and Jager, E. W. H. (2019). Artificial muscles powered by glucose. *Adv. Mater* 31 (32), e1901677. doi:10.1002/adma.201901677

Mayorga-Martinez, C. C., Zelenka, J., Grmela, J., Michalkova, H., Ruml, T., Mareš, J., et al. (2021). Swarming aqua sperm micromotors for active bacterial biofilms removal in confined spaces. *Adv. Sci. (Weinh)* 8 (19), e2101301. doi:10.1002/advs.202101301

Medina-Sánchez, M., Magdanz, V., Guix, M., Fomin, V. M., and Schmidt, O. G. (2018). Swimming microrobots: soft, reconfigurable, and smart. *Adv. Funct. Mater.* 28 (25), 1707228. doi:10.1002/adfm.201707228

Medina-Sánchez, M., Schwarz, L., Meyer, A. K., Hebenstreit, F., and Schmidt, O. G. (2016). Cellular cargo delivery: toward assisted fertilization by sperm-carrying micromotors. *Nano Lett.* 16 (1), 555–561. doi:10.1021/acs.nanolett.5b04221

Mirvakili, S. M., and Hunter, I. W. (2017). Multidirectional artificial muscles from nylon. *Adv. Mater* 29 (4). doi:10.1002/adma.201604734

Mu, X., Zhong, Y., Jiang, T., and Cheang, U. K. (2021). Effect of solvation on the synthesis of MOF-based microrobots and their targeted-therapy applications. *Mater. Adv.* 2 (12), 3871–3880. doi:10.1039/D1MA00139F

Murtsovkin, V. A. (1996). Nonlinear flows near polarized disperse particles. *Colloid J. Russ. Acad. Sci.* 58, 341–349.

Ni, S., Marini, E., Buttinoni, I., Wolf, H., and Isa, L. (2017). Hybrid colloidal microswimmers through sequential capillary assembly. *Soft Matter* 13 (23), 4252–4259. doi:10.1039/C7SM00443E

Nie, J., Ren, Z., Shao, J., Deng, C., Xu, L., Chen, X., et al. (2018). Self-powered microfluidic transport system based on triboelectric nanogenerator and electrowetting technique. *ACS Nano* 12 (2), 1491–1499. doi:10.1021/acsnano.7b08014

Orozco, J., Cheng, G., Vilela, D., Sattayasamitsathit, S., Vazquez-Duhalt, R., Valdés-Ramírez, G., et al. (2013). Micromotor-based high-yielding fast oxidative detoxification of chemical threats. *Angew. Chem. Int. Ed. Engl.* 52 (50), 13276–13279. doi:10.1002/anie.201308072

Otuka, A. J. G., Corrêa, D. S., Fontana, C. R., and Mendonça, C. R. (2014). Direct laser writing by two-photon polymerization as a tool for developing microenvironments for evaluation of bacterial growth. *Mater. Sci. Eng. C* 35, 185–189. doi:10.1016/j.msec.2013.11.005

Park, S. J., Park, S. H., Cho, S., Kim, D. M., Lee, Y., Ko, S. Y., et al. (2013). New paradigm for tumor theranostic methodology using bacteria-based microrobot. *Sci. Rep.* 3, 3394. doi:10.1038/srep03394

Patteson, A. E., Gopinath, A., and Arratia, P. E. (2016). Active colloids in complex fluids. *Curr. Opin. Colloid and Interface Sci.* 21, 86–96. doi:10.1016/j.cocis.2016.01.001

Paxton, W. F., Kistler, K. C., Olmeda, C. C., Sen, A., St. Angelo, S. K., Cao, Y., et al. (2004). Catalytic nanomotors: autonomous movement of striped nanorods. *J. Am. Chem. Soc.* 126 (41), 13424–13431. doi:10.1021/ja047697z

Paxton, W. F., Sen, A., and Mallouk, T. E. (2005). Motility of catalytic nanoparticles through self-generated forces. *Chem. – A Eur. J.* 11 (22), 6462–6470. doi:10.1002/chem.200500167

Peng, X., Chen, Z., Kollipara, P. S., Liu, Y., Fang, J., Lin, L., et al. (2020). Opto-thermoelectric microswimmers. *Light Sci. Appl.* 9 (1), 141. doi:10.1038/s41377-020-00378-5

Peng, Y., Li, D., Yang, X., Ma, Z., and Mao, Z. (2023). A review on electrohydrodynamic (EHD) pump. *Micromachines* 14 (2), 321. doi:10.3390/mi14020321

Peyer, K. E., Zhang, L., and Nelson, B. J. (2013). Bio-inspired magnetic swimming microrobots for biomedical applications. *Nanoscale* 5 (4), 1259–1272. doi:10.1039/c2nr32554c

Rogowski, L. W., Oxner, M., Tang, J., and Kim, M. J. (2020). Heterogeneously flagellated microswimmer behavior in viscous fluids. *Biomicrofluidics* 14 (2), 024112. doi:10.1063/1.5137743

Rogowski, L. W., Zhang, X., Tang, J., Oxner, M., and Kim, M. J. (2021). Flagellated Janus particles for multimodal actuation and transport. *Biomicrofluidics* 15 (4), 044104. doi:10.1063/5.0053647

Seh, Z. W., Kibsgaard, J., Dickens, C. F., Chorkendorff, I., Nørskov, J. K., and Jaramillo, T. F. (2017). Combining theory and experiment in electrocatalysis: insights into materials design. *Science* 355(6321), eaad4998. doi:10.1126/science.aad4998

Servant, A., Qiu, F., Mazza, M., Kostarelos, K., and Nelson, B. J. (2015). Controlled *in vivo* swimming of a swarm of bacteria-like microrobotic flagella. *Adv. Mater* 27 (19), 2981–2988. doi:10.1002/adma.201404444

Seung, W., Gupta, M. K., Lee, K. Y., Shin, K. S., Lee, J. H., Kim, T. Y., et al. (2015). Nanopatterned textile-based wearable triboelectric nanogenerator. *ACS Nano* 9 (4), 3501–3509. doi:10.1021/nn507221f

Shahinpoor, M., and Kim, K. J. (2005). Ionic polymer–metal composites: IV. Industrial and medical applications. *Smart Mater. Struct.* 14 (1), 197–214. doi:10.1088/0964-1726/14/1/020

Shen, C., Jiang, Z., Li, L., Gilchrist, J. F., and Ou-Yang, H. D. (2020). Frequency response of induced-charge electrophoretic metallic Janus particles. *Micromachines (Basel)* 11 (3), 334. doi:10.3390/mi11030334

Shi, M., and Yeatman, E. M. (2021). A comparative review of artificial muscles for microsystem applications. *Microsyst. Nanoeng.* 7, 95. doi:10.1038/s41378-021-00323-5

Slater, G. W., Tessier, F., and Kopecka, K. (2010). The electroosmotic flow (EOF). *Methods Mol. Biol.* 583, 121–134. doi:10.1007/978-1-60327-106-6_5

Song, X., Fu, W., and Cheang, U. K. (2022). Immunomodulation and delivery of macrophages using nano-smooth drug-loaded magnetic microrobots for dual targeting cancer therapy. *iScience* 25 (7), 104507. doi:10.1016/j.isci.2022.104507

Soto, F., Wang, J., Ahmed, R., and Demirci, U. (2020). Medical micro/nanorobots in precision medicine. *Adv. Sci. (Weinh)* 7 (21), 2002203. doi:10.1002/advs.202002203

Suen, N.-T., Hung, S.-F., Quan, Q., Zhang, N., Xu, Y.-J., and Chen, H. M. (2017). Electrocatalysis for the oxygen evolution reaction: recent development and future perspectives. *Chem. Soc. Rev.* 46 (2), 337–365. doi:10.1039/C6CS00328A

Sun, Z., Wang, T., Wang, J., Xu, J., Shen, T., Zhang, T., et al. (2023). Self-propelled Janus nanocatalytic robots guided by magnetic resonance imaging for enhanced tumor penetration and therapy. *J. Am. Chem. Soc.* 145 (20), 11019–11032. doi:10.1021/jacs.2c12219

Tu, Y., Peng, F., Sui, X., Men, Y., White, P. B., van Hest, J. C. M., et al. (2017). Self-propelled supramolecular nanomotors with temperature-responsive speed regulation. *Nat. Chem.* 9 (5), 480–486. doi:10.1038/nchem.2674

Velev, O. D., Prevo, B. G., and Bhatt, K. H. (2003). On-chip manipulation of free droplets. *Nature* 426 (6966), 515–516. doi:10.1038/426515a

Vujacic Nikezic, A., and Grbovic Novakovic, J. (2022). Nano/microcarriers in drug delivery: moving the timeline to contemporary. *Curr. Med. Chem.* 30, 2996–3023. doi:10.2174/0929867329666220821193938

Wang, B., Kostarelos, K., Nelson, B. J., and Zhang, L. (2021). Trends in micro-/nanorobotics: materials development, actuation, localization, and system integration for biomedical applications. *Adv. Mater.* 33 (4), 2002047. doi:10.1002/adma.202002047

Wang, J. (2009). Can man-made nanomachines compete with nature biomotors? *ACS Nano* 3 (1), 4–9. doi:10.1021/nn800829k

Wang, J., and Gao, W. (2012). Nano/microscale motors: biomedical opportunities and challenges. *ACS Nano* 6 (7), 5745–5751. doi:10.1021/nn3028997

Wang, J., Yao, C., Shen, B., Zhu, X., Li, Y., Shi, L., et al. (2019a). Upconversion-magnetic carbon sphere for near infrared light-triggered bioimaging and photothermal therapy. *Theranostics* 9 (2), 608–619. doi:10.7150/thno.27952

Wang, Q., and Zhang, L. (2021). External power-driven microrobotic swarm: from fundamental understanding to imaging-guided delivery. *ACS Nano* 15 (1), 149–174. doi:10.1021/acsnano.0c07753

Wang, W., Castro, L. A., Hoyos, M., and Mallouk, T. E. (2012). Autonomous motion of metallic microrods propelled by ultrasound. *ACS Nano* 6 (7), 6122–6132. doi:10.1021/nn301312z

Wang, W., Chiang, T.-Y., Velegol, D., and Mallouk, T. E. (2013). Understanding the efficiency of autonomous nano- and microscale motors. *J. Am. Chem. Soc.* 135 (28), 10557–10565. doi:10.1021/ja405135f

Wang, W., Liu, Q., Tanasijevic, I., Reynolds, M. F., Cortese, A. J., Miskin, M. Z., et al. (2022a). Cilia metasurfaces for electronically programmable microfluidic manipulation. *Nature* 605 (7911), 681–686. doi:10.1038/s41586-022-04645-w

Wang, X., Cai, J., Sun, L., Zhang, S., Gong, D., Li, X., et al. (2019b). Facile fabrication of magnetic microrobots based on spirulina templates for targeted delivery and synergistic chemo-photothermal therapy. *ACS Appl. Mater Interfaces* 11 (5), 4745–4756. doi:10.1021/acsami.8b15586

Wang, X., Yin, Y., Yi, F., Dai, K., Niu, S., Han, Y., et al. (2017). Bioinspired stretchable triboelectric nanogenerator as energy-harvesting skin for self-powered electronics. *Nano Energy* 39, 429–436. doi:10.1016/j.nanoen.2017.07.022

Wang, Y., Chen, W., Wang, Z., Zhu, Y., Zhao, H., Wu, K., et al. (2023). NIR-II light powered asymmetric hydrogel nanomotors for enhanced immunochemotherapy. *Angew. Chem. Int. Ed. Engl.* 62 (3), e202212866. doi:10.1002/anie.202212866

Wang, Z., Xu, Z., Zhu, B., Zhang, Y., Lin, J., Wu, Y., et al. (2022b). Design, fabrication and application of magnetically actuated micro/nanorobots: a review. *Nanotechnology* 33 (15), 152001. doi:10.1088/1361-6528/ac43e6

Wu, D., Baresch, D., Cook, C., Ma, Z., Duan, M., Malounda, D., et al. (2023). Biomolecular actuators for genetically selective acoustic manipulation of cells. *Sci. Adv.* 9 (8), eadd9186. doi:10.1126/sciadv.add9186

Xie, H., Sun, M., Fan, X., Lin, Z., Chen, W., Wang, L., et al. (2019). Reconfigurable magnetic microrobot swarm: multimode transformation, locomotion, and manipulation. *Sci. Robot.* 4 (28), eaav8006. doi:10.1126/scirobotics.aav8006

Xie, S., Qin, L., Li, G., and Jiao, N. (2021). Robotized algal cells and their multiple functions. *Soft Matter* 17 (11), 3047–3054. doi:10.1039/d0sm02096f

Xu, T., Gao, W., Xu, L.-P., Zhang, X., and Wang, S. (2017). Fuel-free synthetic micro-/nanomachines. *Adv. Mater.* 29 (9), 1603250. doi:10.1002/adma.201603250

Xu, X., Kim, K., and Fan, D. (2015). Tunable release of multiplex biochemicals by plasmonically active rotary nanomotors. *Angew. Chem. Int. Ed.* 54 (8), 2525–2529. doi:10.1002/anie.201410754

Yang, J. F., Berrueta, T. A., Brooks, A. M., Liu, A. T., Zhang, G., Gonzalez-Medrano, D., et al. (2022). Emergent microrobotic oscillators via asymmetry-induced order. *Nat. Commun.* 13 (1), 5734. doi:10.1038/s41467-022-33396-5

Yang, Q., Xu, L., Zhong, W., Yan, Q., Gao, Y., Hong, W., et al. (2020). Recent advances in motion control of micro/nanomotors. *Adv. Intell. Syst.* 2 (8), 2000049. doi:10.1002/aisy.202000049

Yang, W., Xu, C., Lyu, Y., Lan, Z., Li, J., and Ng, D. H. L. (2023). Hierarchical hollow α-Fe(2)O(3)/ZnFe(2)O(4)/Mn(2)O(3) Janus micromotors as dynamic and efficient microcleaners for enhanced photo-Fenton elimination of organic pollutants. *Chemosphere* 338, 139530. doi:10.1016/j.chemosphere.2023.139530

Yoshizumi, Y., Honegger, T., Berton, K., Suzuki, H., and Peyrade, D. (2015). Trajectory control of self-propelled micromotors using AC electrokinetics. *Small* 11 (42), 5630–5635. doi:10.1002/smll.201501557

Zhan, H., Yuan, Z., Li, Y., Zhang, L., Liang, H., Zhao, Y., et al. (2023). Versatile bubble maneuvering on photopyroelectric slippery surfaces. *Nat. Commun.* 14 (1), 6158. doi:10.1038/s41467-023-41918-y

Zhang, L., Xiao, Z., Chen, X., Chen, J., and Wang, W. (2019). Confined 1D propulsion of metallodielectric Janus micromotors on microelectrodes under alternating current electric fields. *ACS Nano* 13 (8), 8842–8853. doi:10.1021/acsnano.9b02100

Zhang, S., Xu, B., Elsayed, M., Nan, F., Liang, W., Valley, J. K., et al. (2022). Optoelectronic tweezers: a versatile toolbox for nano-/micro-manipulation. *Chem. Soc. Rev.* 51 (22), 9203–9242. doi:10.1039/D2CS00359G

Zheng, L., Hart, N., and Zeng, Y. (2023a). Micro-/nanoscale robotics for chemical and biological sensing. *Lab a Chip* 23 (17), 3741–3767. doi:10.1039/D3LC00404J

Zheng, Y., Wang, B., Cai, Y., Zhou, X., and Dong, R. (2023b). Five in one: multi-engine highly integrated microrobot. *Small Methods* 7 (10), e2300390. doi:10.1002/smtd.202300390

Zheng, Z., Wang, H., Demir, S. O., Huang, Q., Fukuda, T., and Sitti, M. (2022). Programmable aniso-electrodeposited modular hydrogel microrobots. *Sci. Adv.* 8 (50), eade6135. doi:10.1126/sciadv.ade6135

Zhong, J., Zhong, Q., Fan, F.-R., Zhang, Y., Wang, S., Hu, B., et al. (2013). Finger typing driven triboelectric nanogenerator and its use for instantaneously lighting up LEDs. *Nano Energy* 2, 491–497. doi:10.1016/j.nanoen.2012.11.015

Zhou, H., Dong, G., Gao, G., Du, R., Tang, X., Ma, Y., et al. (2022). Hydrogel-based stimuli-responsive micromotors for biomedicine. *Cyborg Bionic Syst.* 2022. 9852853. doi:10.34133/2022/9852853

frontiers | Frontiers in Bioengineering and Biotechnology

TYPE Review
PUBLISHED 25 January 2024
DOI 10.3389/fbioe.2024.1347312

OPEN ACCESS

EDITED BY
Tianlong Li,
Harbin Institute of Technology, China

REVIEWED BY
Xinjina Fan,
Soochow University, Taiwan
Sui Ziqi,
The First People's Hospital of Linping, China

*CORRESPONDENCE
Hao Chang,
doctorhaochang@sohu.com
Jingxue Sun,
sunjingxue0205@163.com

†These authors have contributed equally to this work and share first authorship

RECEIVED 08 December 2023
ACCEPTED 02 January 2024
PUBLISHED 25 January 2024

CITATION
Sun T, Chen J, Zhang J, Zhao Z, Zhao Y, Sun J and Chang H (2024), Application of micro/nanorobot in medicine.
Front. Bioeng. Biotechnol. 12:1347312.
doi: 10.3389/fbioe.2024.1347312

Application of micro/nanorobot in medicine

Tianhao Sun[1†], Jingyu Chen[2†], Jiayang Zhang[3†], Zhihong Zhao[1], Yiming Zhao[1], Jingxue Sun[4*] and Hao Chang[1*]

[1]Department of Thoracic Surgery, The First Affiliated Hospital of Harbin Medical University, Harbin, Heilongjiang, China, [2]Department of Oncology, The Fourth Affiliated Hospital of Harbin Medical University, Harbin, Heilongjiang, China, [3]Key Laboratory of Carcinogenesis and Translational Research (Ministry of Education/Beijing), Department of Breast Oncology, Peking University Cancer Hospital and Institute, Beijing, China, [4]Department of Endocrinology and Metabolism, The Second Affiliated Hospital of Harbin Medical University, Harbin, China

The development of micro/nanorobots and their application in medical treatment holds the promise of revolutionizing disease diagnosis and treatment. In comparison to conventional diagnostic and treatment methods, micro/nanorobots exhibit immense potential due to their small size and the ability to penetrate deep tissues. However, the transition of this technology from the laboratory to clinical applications presents significant challenges. This paper provides a comprehensive review of the research progress in micro/nanorobotics, encompassing biosensors, diagnostics, targeted drug delivery, and minimally invasive surgery. It also addresses the key issues and challenges facing this technology. The fusion of micro/nanorobots with medical treatments is poised to have a profound impact on the future of medicine.

KEYWORDS

micro/nanorobot, biosensor, diagnosis, targeting drug delivery, surgery

1 Introduction

Micro/nano robots refer to robots or robotic systems whose size is on the micron or nanometer scale. These robots typically consist of micro or nano-scale components and can perform specific tasks, such as operations at the cellular level or assembly and repair at the molecular level (Xie et al., 2019). With the rapid advancement of nanotechnology and materials science, micro/nano robots find applications in various fields of biomedicine (Mohammadinejad et al., 2016). The miniaturization of robot systems to the micro/nano scale holds immense potential in the diagnosis and treatment of various diseases (Nelson et al., 2010). These diminutive robots can penetrate deep or otherwise inaccessible regions within our bodies, conducting various medical procedures, and showcasing great promise in areas such as diagnosis, drug delivery, and surgery (Soto et al., 2020; Zhao et al., 2022).

Various methods exist for constructing micro/nano robots. Initially, one needs to define the tasks the micro/nano robot is intended to perform, specifying parameters such as size, shape, materials, sensors, actuators, and more. Physical methods like photolithography, chemical methods involving the synthesis of molecular components using chemical substances, or 3D printing technology can be employed to create parts. In addition, self-assembly technology enables the automatic assembly of nanoparticles into desired structures by controlling molecular interactions. When the size of an object is reduced to the micrometer or nanometer range, the ratio of inertial force to viscous force (Reynolds number) becomes negligible, making it necessary to continuously provide power to propel small robots. The driving modes for micro/nano robots primarily include chemical

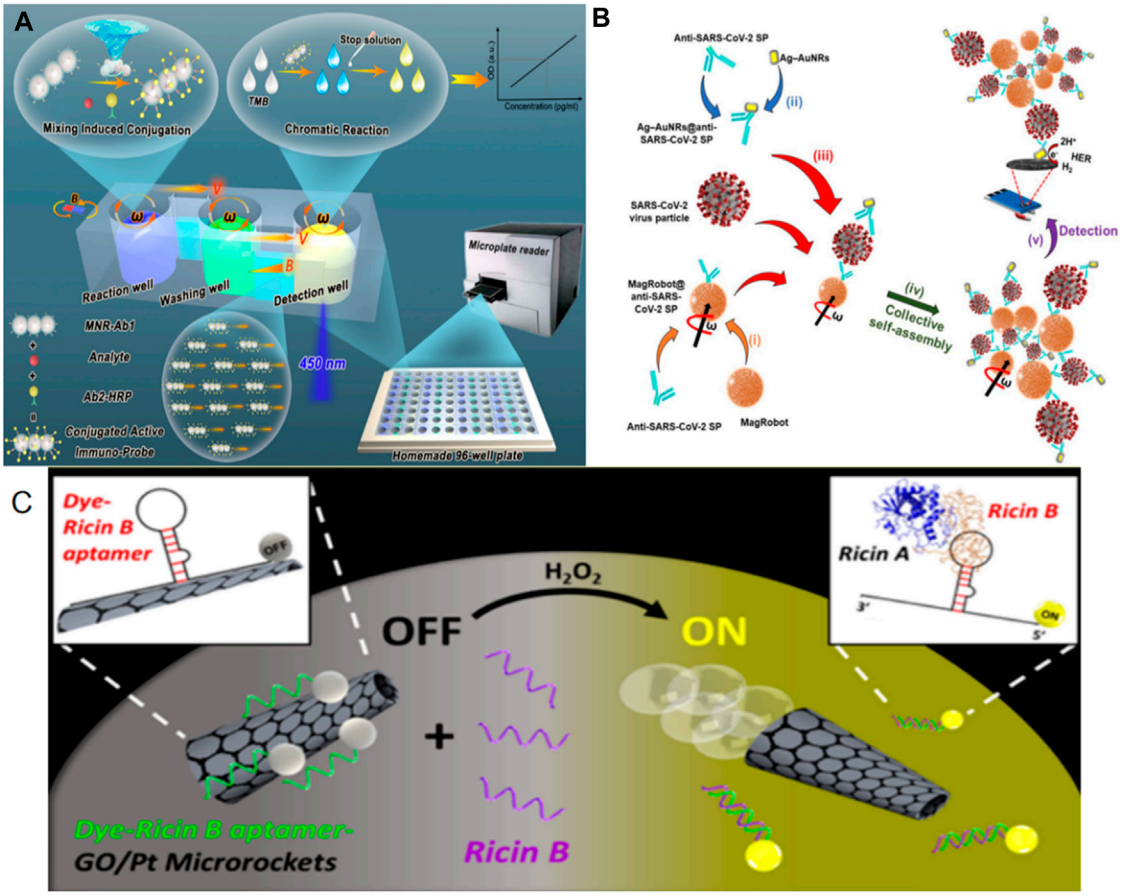

FIGURE 1
(A) Magnetic Nanorobot-Enabled Automated and Efficient ELISA (nR-ELISA) Analysis. Adapted with permission from Wang et al. (2022). Copyright 2022 American Chemical Society. **(B)** MagRobots were modified with antibody against SARS-CoV-2 spike protein. Adapted with permission from Mayorga-Martinez et al. (2022). Copyright 2022 Elsevier Science and Technology Journals. **(C)** The preparation of fluorescent magnetic spore–based (spore@Fe3O4@CDs) microrobots involves the combination of facile chemical deposition and subsequent encapsulation and functionalization techniques. Adapted with permission from de Ávila et al. (2016). Copyright 2016 American Chemical Society.

propulsion driven by local chemical and biochemical energy sources (e.g., H2O2, urea), physical field propulsion driven by external fields (e.g., light, ultrasound, or magnetic fields), and biological propulsion driven by microorganisms or cells (e.g., sperm). Building upon these propulsion methods, micro/nano robots can navigate deep or inaccessible regions of the body, performing various medical tasks and demonstrating significant potential in areas such as diagnosis, drug delivery, and surgery. For instance, in the realm of diagnostics, novel micro/nano machines are used for real-time measurements of blood glucose and lipid levels (Yu et al., 2021). These microdimmers are controlled by an applied magnetic field and exhibit distinct movement speeds and postures in response to different concentrations of glucose, cholesterol, and triglycerides, facilitating the measurement of blood glucose and lipids. In the field of surgery, micro/nano robots can access deep tissues that are beyond the reach of larger robots and human surgeons (Nguyen et al., 2021). For example, guided spiral robots have been employed for targeted thrombectomy and recanalization in small blood vessels (Nguyen et al., 2021). In the medical domain, micro/nano robots can accomplish tasks that are unattainable on a macro scale, thus enhancing the precision and refinement of medical treatments. This paper will primarily present research findings on the medical applications of micro/nano robots and elaborate on their current status and challenges in four key areas: biosensors, diagnostics, targeted drug delivery, and surgery.

2 Application of micro/nanorobot in medicine

2.1 Biosensor

Traditional medical examinations involve the analysis of human tissues using various physical and chemical methods within fields like microbiology, immunology, biochemistry, hematology, and cytology. With the advancement of precision medicine, there is a growing demand for higher levels of accuracy and specificity in these examinations. However, traditional medical examination methods have their limitations. Biosensors, as a method of inspection, can detect biological information within samples. Traditional biosensors often require strict sample environments. In contrast, micro/nanorobots used as sensors exhibit characteristics such as

sensitivity and speed, holding significant promise within the field of medicine (Deng et al., 2021; Hegde et al., 2023). One classic biochemical detection technique is the Enzyme-Linked Immunosorbent Assay (ELISA). This method quantifies analytes through enzymatic reactions, followed by chemical colorimetry. ELISA has gained widespread use in the medical field (Aydin, 2015). Wang et al. (2022) developed a micro/nano motor designed for immune probes, enhancing the efficiency of Enzyme-Linked Immunosorbent Assay (ELISA) using Fe3O4@SiO2 core-shell nanorods. These nanorods were further modified with a capture antibody (AB-1) to create a mobile analytical probe based on nanorobots (see Figure 1A). These nanorobots are propelled by a magnetic field and can be guided to target positions through the influence of gradient magnetic fields and rotating magnetic fields. Due to their one-dimensional structure, these robots can rotate and agitate liquids under the influence of a magnetic field, thereby improving the detection efficiency. In an effort to enhance the sensitivity and specificity of virus and protein detection, Mayorga-Martinez et al. (2022) developed a magnetic microrobot (see Figure 1B). This microrobot was modified with anti-SARS coronavirus type 2 spike protein and loaded with pre-concentrated spike protein. Additionally, anti-SARS coronavirus type 2 spike protein coupled with Ag-AuNRs was employed as a marker. This detection platform exhibits heightened sensitivity, reducing the detection limit for severe acute respiratory syndrome coronavirus type 2 by an order of magnitude when compared to traditional detection methods. The utilization of this microrobot platform for virus and protein detection can be applied to similar virus or protein detection scenarios.

Utilizing the microrobot platform, individuals can achieve the detection of toxins. de Ávila et al. (2016) devised a self-propelled micromotor constructed from reduced graphene oxide (RGO) and platinum (Pt). They modified this micromotor with a specialized ricin B aptamer labeled with fluorescein-amidine (FAM) dye (see Figure 1C). Through a visual "on-off" fluorescence reaction and rapid binding to toxins, this system enables quick and sensitive detection across various media. Consequently, trace amounts of ricin can be detected in complex biological samples, and the advancement of this microrobot platform holds significant promise for detecting other biological threats, making it invaluable for biological defense applications. In a separate development, Zhang et al. (2019) introduced an efficient, spore-based fluorescent magnetic robot. They integrated porous natural spores with Fe3O4 particles and coupled them with functionalized carbon dots (CDs), allowing for tracking through fluorescence emission. These microrobots can rapidly detect *Clostridium difficile* toxin, with their detection efficiency confirmed on bacterial culture medium and clinical stool specimens.

2.2 Dignosis

Traditional medical examinations primarily operate at a macro level, making it challenging to access deep tissues without causing patient discomfort or trauma, as seen in procedures like endoscopy or biopsy. Additionally, certain imaging examinations, such as those involving radiation or magnetic resonance imaging, can be impacted by metal interference or patient movement. Micro/nanorobots possess remarkable tissue-penetrating capabilities. Furthermore, they can be externally controlled to navigate through the body's internal environment, thereby enhancing the efficiency and precision of various medical applications (Aziz et al., 2020). These applications include tumor detection, enhanced imaging signal acquisition, pathological biopsy, and more (Tu et al., 2017; Yang, 2020).

Micro/nanorobots have the potential to replace conventional endoscopes in diagnosing intestinal diseases. Traditional colonoscopy, a well-established clinical practice for direct intestinal observation and biopsy, has certain drawbacks. Its larger size relative to microscopic objects can potentially cause discomfort or injury to patients during the procedure. Moreover, there are inherent limitations in observing and operating in certain blind spots within the intestine during examinations (Tapia-Siles et al., 2016; Tumino et al., 2023). In response to these challenges, technological advancements have led to the development of non-invasive endoscopic capsules and capsule endoscopes that can actively navigate within the intestinal tract under magnetic field guidance. However, these solutions also have their limitations (Bianchi et al., 2019). To address these issues, Han et al. (2020) introduced an innovative micro-robotic model for diagnosing intestinal diseases. This micro-robot, designed using principles of bionics, features a two-layer folding mechanism to anchor itself to intestinal tissue. Additionally, it includes a stretching mechanism that allows for axial motion within the intestine, with radio waves serving as the means of propulsion. Robots with this design can move both forward and backward within the intestine while securely attached to the intestinal wall. The safety and effectiveness of this microrobot have been confirmed through *in vitro* experiments conducted in pig intestines.

Micro/nanorobots offer significant advantages in enhancing medical imaging by reaching deep tissues and providing strong penetration capabilities, ultimately leading to clearer images. Photoacoustic imaging is an innovative imaging technique that combines the benefits of optical resolution and acoustic penetration, and it finds a wide range of clinical applications (Attia et al., 2019; Manohar and Gambhir, 2020; Gröhl et al., 2021). Yan et al. (2020) and others devised a microrobot made from a mixture of photoresist and nickel particles. They control the movement of this microrobot using an external magnetic field and utilize photoacoustic imaging for imaging purposes. Their verification experiments demonstrated that this microrobot exhibits high sensitivity in turbid biological tissues. Magnetic imaging is another widely used method for visualizing microrobots (Zhang et al., 2022a). In comparison to other imaging techniques, magnetic imaging offers superior resolution and penetration depth while avoiding the ionizing radiation associated with some imaging methods. During the research and development of microrobots, magnetic materials are incorporated to generate distinct signals from surrounding tissues in a magnetic field. Yan et al. (2017) prepared a spirulina micro robot coated with Fe3O4, offering superparamagnetic properties and enabling it to move in a targeted manner within biological fluids under the influence of an external magnetic field. This microrobot serves as a contrast imaging tool, enhancing imaging performance. Furthermore, it can be biodegradable and exhibits selective cytotoxicity towards cancer cells.

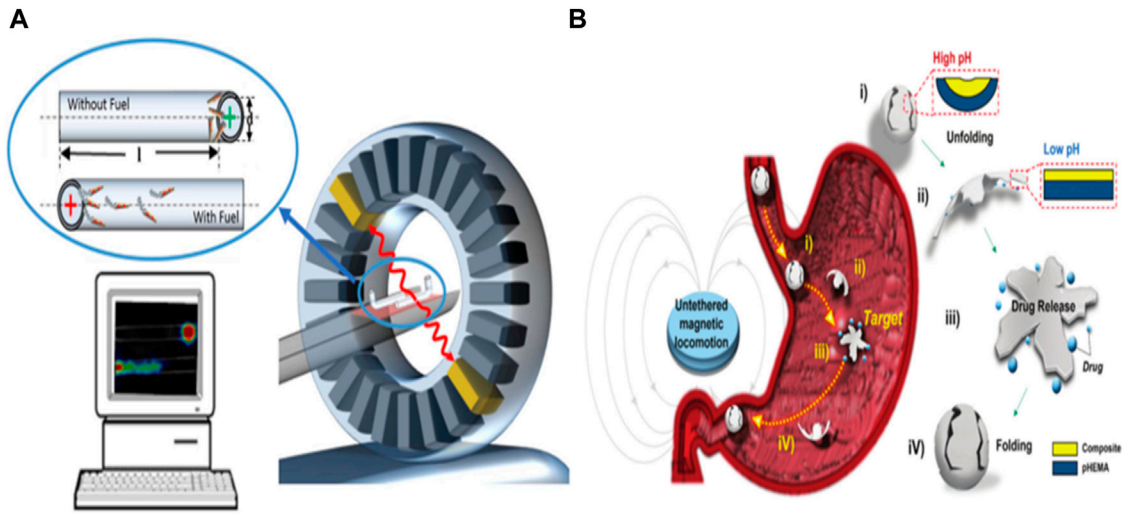

FIGURE 2
(A) PET-CT for tracking tubular Au/PEDOT/Pt micromotors. Adapted with permission from Vilela et al. (2018). Copyright 2018 American Chemical Society. **(B)** Conceptual design of the pH-responsive microrobot for targeted drug delivery, X-ray imaging, and retrieval. Reproduced with permission from Darmawan et al. (2022); published by Royal Society of Chemistry, 2022.

Micro/nanorobots also play a vital role in ionization imaging, significantly enhancing diagnostic capabilities. Ionization imaging is a prevalent method for disease diagnosis in clinical practice, and one such technique is Proton Emission Tomography (PET), which relies on radioactive nuclides. PET is particularly effective at detecting deep tissue distribution of radioactive nuclides. However, it may lack anatomical and morphological details, leading to its frequent combination with CT and MRI in clinical settings (Wållberg and Ståhl, 2013). One drawback of nuclide-based examinations is their high equipment cost, limited real-time imaging capabilities, and lengthy acquisition times. Dahroug et al. (2018) addressed this by developing a microrobot coated with an iodine isotope surface, tracked using PET-CT. Their work confirmed PET-CT's ability to image microrobot models within deep tissues, demonstrating the technique's capacity to locate microrobots (see Figure 2A). By incorporating magnetic nanoparticles and a pH-responsive design, a micro robot can be propelled by an external magnetic field while being equipped with an X-ray contrast agent for real-time X-ray imaging (see Figure 2B) (Darmawan et al., 2022). This versatile microrobot, carrying doxorubicin, can facilitate real-time imaging diagnostics and combat tumor cells in gastric cancer.

2.3 Targeting drug delivery

The traditional drug delivery route primarily involves systemic circulation, but it has limitations such as poor tissue permeability and local drug delivery capability, resulting in inefficient drug delivery. However, with the advancement of microrobot technology, these challenges can be overcome. By utilizing microrobots to transport drugs, it becomes possible to target deep tissues for precise drug delivery, leading to increased delivery efficiency and reduced drug dosages (Li et al., 2017a; Li et al., 2017b; Ji et al., 2021). Microrobots can even navigate biofilm structures to deliver drugs, and this drug delivery method has been extensively studied in conditions like inflammation and tumors (Yang et al., 2017; Lin et al., 2021). In the realm of drug delivery, there is a growing desire for microrobots to autonomously navigate to affected areas for precise treatment (Fan et al., 2022). Consequently, the means of propelling these robots is a critical challenge that requires resolution. Early solutions involved the design of micro/nanorobots driven by chemistry, which converts chemical energy into kinetic energy, enabling them to self-propel. Such robots can transport and release various substances, including drugs, nucleic acids, and microorganisms (Wu et al., 2013). Wu et al. (2014) developed a chemically driven polymer-based microrobot that can be securely released upon near-infrared light stimulation. By incorporating biological enzyme catalysis, these robots can self-propel even at lower hydrogen peroxide fuel concentrations, significantly advancing the potential of micro/nanorobots for drug delivery (see Figure 3A).

Beyond chemical propulsion, prevalent methods for actuation encompass magnetic, optical, and even pH-based approaches (Wu et al., 2016; Chen et al., 2018; Yu et al., 2018; Yu et al., 2023). Magnetic propulsion, in particular, stands out as a safer alternative, eschewing the byproducts of chemical propulsion that could potentially disrupt human circulatory and tissue systems. Numerous micro- and nanorobotic systems harnessing magnetic drive have been engineered, showcasing enhanced drug delivery efficiencies both *in vitro* and *in vivo* (Gong et al., 2022). These microrobots are often embedded with magnetic particles or affixed with permanent magnets, allowing for precision control by modulation of magnetic field direction and intensity to realize targeted therapeutic delivery. Mu et al. (2022) devised a hydrogel-based microrobot for drug delivery, utilizing a synthetic lethal drug that, while inherently cytotoxic to normal cells, is guided by genomic markers. Through magnetic manipulation, the microrobot devised by Mu and others can be steered with precision to tumor sites, thereby mitigating adverse effects and augmenting the efficacy of drug delivery. Peng et al. (2017)

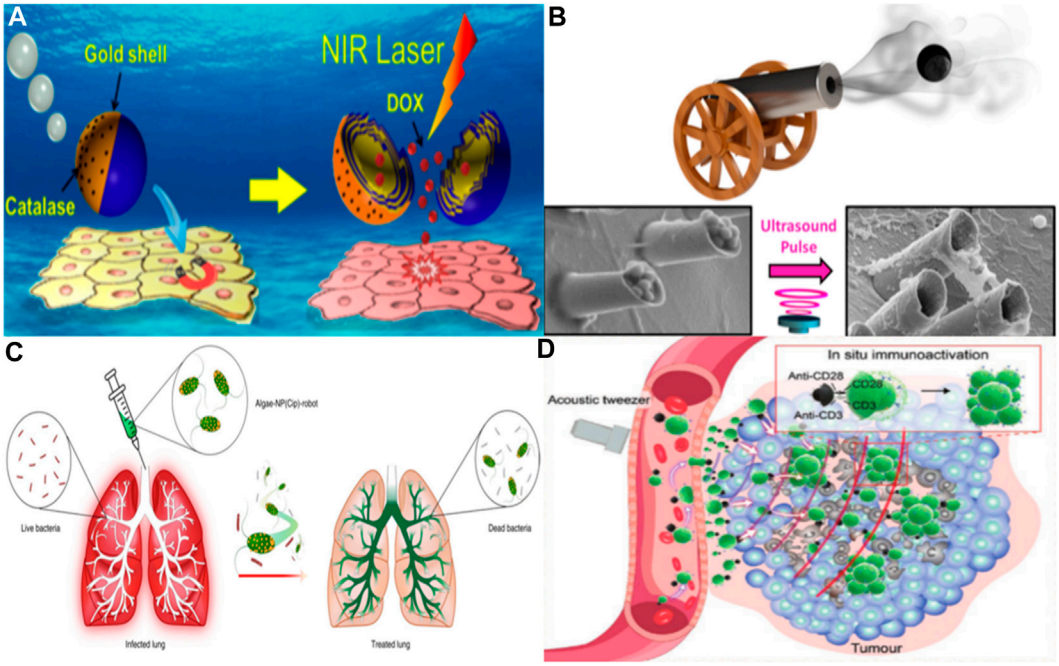

FIGURE 3
(A) Janus capsule engine navigates to the cell layer through an external magnetic field and releases drugs activated by near-infrared light. Adapted with permission from Wu et al. (2014). Copyright 2014 American Chemical Society. **(B)** Acoustic triggered micro gun, which can load and launch nano bullets, is a powerful micro ballistic tool. It can efficiently load and launch a variety of goods, and provide better target location and enhanced tissue penetration performance. Adapted with permission from Soto et al. (2016). Copyright 2016 American Chemical Society. **(C)** Schematic depicting the use of algae-NP-robot for the treatment of a bacterial lung infection. C. *reinhardtii* algae is modified with drug-loaded NPs and then administered *in vivo* for the treatment of P. *aeruginosa* lung infection. Reprinted with the permission from Zhang et al. (2022b). Copyright 2022 Nature Publishing Group. **(D)** Peritumoural-accumulated M-CAR Ts were propelled by acoustic force from tumor-fixed acoustic tweezers to migrate deeply into the deep tumor. Immunomagnetic beads modified with anti-CD3/CD28 *in situ* stimulated the proliferation and activation of CAR T cells, thus achieving a robust antitumor effect. Reproduced with permission from Tang et al. (2023); published by John Wiley and Sons, 2023.

demonstrated the capabilities of a magnetically-driven nanorobot. They ingeniously incorporated magnetic metallic nickel *in situ* into catalytic platinum nanoparticles, ensuring the synergistic coexistence of nickel and platinum. This integration enables the nanorobot to be driven in dual modes. The controllability of the nanorobot was validated using a human cervical cancer cell model, heralding significant potential for precise drug delivery applications. In targeting the digestive system for drug administration, pH-sensitive mechanisms are often employed to steer robots (Gao et al., 2012; Sattayasamitsathit et al., 2014). Gao et al. (2015) unveiled an acid-powered, zinc-based microrobot capable of efficient propulsion and targeted drug delivery within acidic environments, negating the need for conventional fuel sources. *In vivo* experiments using mice demonstrated that, unlike traditional orally administered drugs that rely on passive diffusion, these micro/nanorobots actively navigate and persist within the gastric walls. This zinc-based microrobot is designed to decompose in acidic conditions without releasing harmful substances, thereby proving non-toxic to human tissues. Further advancing the field, their team proposed a magnesium-based microrobot tailored for treating *Helicobacter pylori* infections by delivering antibiotics. This microrobot possesses a proton depletion feature, potentially reducing the reliance on proton pump inhibitors and minimizing side effects associated with their long-term usage, as compared to traditional passive drug diffusion methods (de Ávila et al., 2017).

Soto et al. (2016) introduced acoustic microcannons that harness sound wave energy for propulsion and manipulation of minute payloads. By incorporating a magnetic component, the microcannons can be precisely positioned during the drug release process. These researchers aspire to use acoustic cannons, either singly or in arrays, to transport drugs and vaccines, thus broadening their practical utility. They aim to minimize resistance by optimizing the microcannons' shape and density, enabling the "nano bullets" to penetrate target tissues efficiently without excessive energy discharge. Such microcannons have the potential for a variety of applications, including drug delivery, tissue penetration, and destruction, actualizing the concept of a "magic bullet" (see Figure 3B).

In the realm of medical applications, micro/nanorobots confront several challenges, including the penetration of biofilm structures and the navigation and drug administration within specialized tissues such as the vitreous body and the lungs. The latter organ, replete with macrophages designed to eliminate foreign entities, poses a particular challenge: evading the human immune system's clearance mechanisms to achieve targeted drug delivery remains a formidable hurdle for micro/nanorobotic technologies. Zhang et al. (2022b) have engineered a microrobot system tailored for intratracheal drug delivery (see Figure 3C). This system comprises microrobots cloaked in the cell membrane of neutrophils, with a core of algae modified with nanoparticles that

ferry therapeutic agents. In contrast to purely synthetic constructs, these biologically hybridized microrobots inherit the intrinsic properties of their biological components. They exhibit facile cultivation, self-propulsion via flagellar motion, and improved distribution and retention within pulmonary tissues. Notably, the flagellar activity has been demonstrated to decrease macrophage-mediated clearance of the microrobots. The presence of the neutrophil cell membrane not only shields the microrobots from the host's biological milieu but also facilitates targeted pathogen binding and drug delivery. Substantiated through both *in vivo* and *in vitro* studies, the efficacy of this biologically hybrid microrobot system in treating bacterial pneumonia has been confirmed. In recent years, advancements in biomimetics and micro/nanorobotics have given rise to a burgeoning array of bio-integrated microrobot systems (Middelhoek et al., 2022). These systems are designed to harness biological features to diminish the rate of immune clearance by the body and to enhance the efficiency of drug delivery (Li et al., 2016; Yu et al., 2022; Zhang et al., 2023). Li et al. (2023) have pioneered the design of a biomimetic micro-robot, which emulates the claw-like appendages of certain aquatic microorganisms. This novel design offers a significant advancement over traditional synthetic micro-robots. The claw structure enables the robot to anchor to the vascular endothelium in a manner akin to these organisms, rendering it less susceptible to the shearing forces of blood flow. Such an adaptation ensures active retention within the circulatory system. Furthermore, the researchers have ingeniously enveloped the micro-robot with a layer of red blood cell membrane, capitalizing on its role as a natural transport medium. This coating effectively camouflages the robot, mitigating immune detection and clearance. During *in vivo* trials in the rabbit jugular vein, the biomimetic robot exhibited proficient propulsive behavior and demonstrated its potential for active, targeted drug delivery. The blood-brain barrier (BBB) represents a formidable physiological barricade segregating the brain's milieu from the systemic circulation. While it serves as a protective shield against exogenous substances, potentially detrimental to neural tissue, it concurrently poses a significant challenge for delivering therapeutic agents to the brain (Kadry et al., 2020). Joseph et al. (2017) designed a synthetic vesicle with chemotaxis to cross the blood-brain barrier. This is a fully synthesized organic nanorobot that encapsulates glucose oxidase alone or together with catalase into nanoscale vesicles. These vesicles demonstrate sensitive movement toward regions with higher glucose concentrations, following the external glucose gradient. Moreover, they have exhibited that the chemotactic ability of these nanorobots, coupled with their affinity for the low-density lipoprotein receptor-related protein 1 (LRP-1), enhances their permeability across the BBB by fourfold. Nanorobots are also emerging as instrumental tools in the rapidly advancing domain of cancer immunotherapy. While Chimeric Antigen Receptor T (CAR-T) cell therapy has shown promise in treating hematological malignancies, its efficacy in solid tumors is curtailed by physical barriers and the immune microenvironment (Ma et al., 2019; Li et al., 2021). Addressing this, Tang et al. (2023) have engineered a living micro-robot using CAR-T cells, which are augmented with immune magnetic beads through click conjugation (see in Figure 3D). This construct is magnetically steerable and capable of navigating fluids and circumventing obstacles. It demonstrates the capacity for long-range travel and accumulation in tumor models, showing an impressive ability to penetrate deep into tumor tissues aided by acoustic waves, thereby enhancing the infiltration of exogenous $CD8^+$ T cells sixfold. The inclusion of anti-CD3/CD28 immune magnetic beads promotes the activation of the infiltrating CAR-T cells, substantially bolstering their anti-tumor efficacy. In conclusion, nanorobots represent a paradigm shift in enhancing the precision and efficiency of drug delivery, overcoming environmental barriers, and refining targeted therapeutic interventions. It is the collective hope of the research community that these advanced microrobot systems will soon transition into clinically viable tools for healthcare practitioners.

2.4 Surgery

As surgical methodologies evolve, particularly with the advent of minimally invasive techniques, there is an escalating demand for reduced trauma and increased precision in reaching surgical targets. Traditional approaches, whether open or minimally invasive, confront limitations in the depth of tissue accessibility and the inability to operate under significantly microscopic conditions. The emergence of micro/nanorobotics in surgical arenas promises to mitigate these challenges. These diminutive robots are designed to navigate and congregate precisely at targeted sites, directed by external stimuli. Their compact form factor enables traversal through capillary networks to locations that are otherwise inaccessible via conventional surgical methods, facilitating interventions at the cellular scale. Such capability not only reduces the scale of surgical incisions but also abbreviates the recuperation period, heralding significant prospects for clinical treatments (Nelson et al., 2010). Micro/nanorobots offer the distinct advantage of operating at considerable distances with robust tissue penetration capabilities. Xi et al. (2013) have pioneered a remotely controllable "surgical knife," a testament to the innovative strides in this field. This groundbreaking work presents a novel magnetically-guided micro drill designed for minimally invasive surgery. Fabricated from 2D nanomaterials with acutely sharp tips, these microsurgical tools can dynamically alter their orientation by modulating the frequency of an external magnetic field in tandem with the solution's viscosity. The reported experimental data suggests that these micro drills can execute precise drilling tasks in soft biological tissues and navigate through fluid mediums mirroring the viscosity of blood. Such magnetic-controlled micro drills hold immense promise for minimally invasive medical interventions, including targeted micro drug delivery and the removal of vascular plaques. Further extending the scope of microsurgical innovation, Liu et al. (2022) introduced a micro robot capable of conducting intricate surgical procedures within the confines of microscale blood vessels. This magnetic-driven, soft continuum micro robot is fabricated from a blend of polydimethylsiloxane (PDMS) and neodymium iron boron (NdFeB) particles, allowing for precision navigation and manipulation via magnetic control. Experimental demonstrations validate the soft continuum micro robot's significant flexibility and particle manipulation prowess, rendering it highly effective for operational tasks within microvascular structures. However, further improvements are required, particularly in terms of the size and control accuracy of soft continuous microrobots. Nguyen et al. (2018) also showcased a micro/nanorobot designed for intravascular surgery. This system

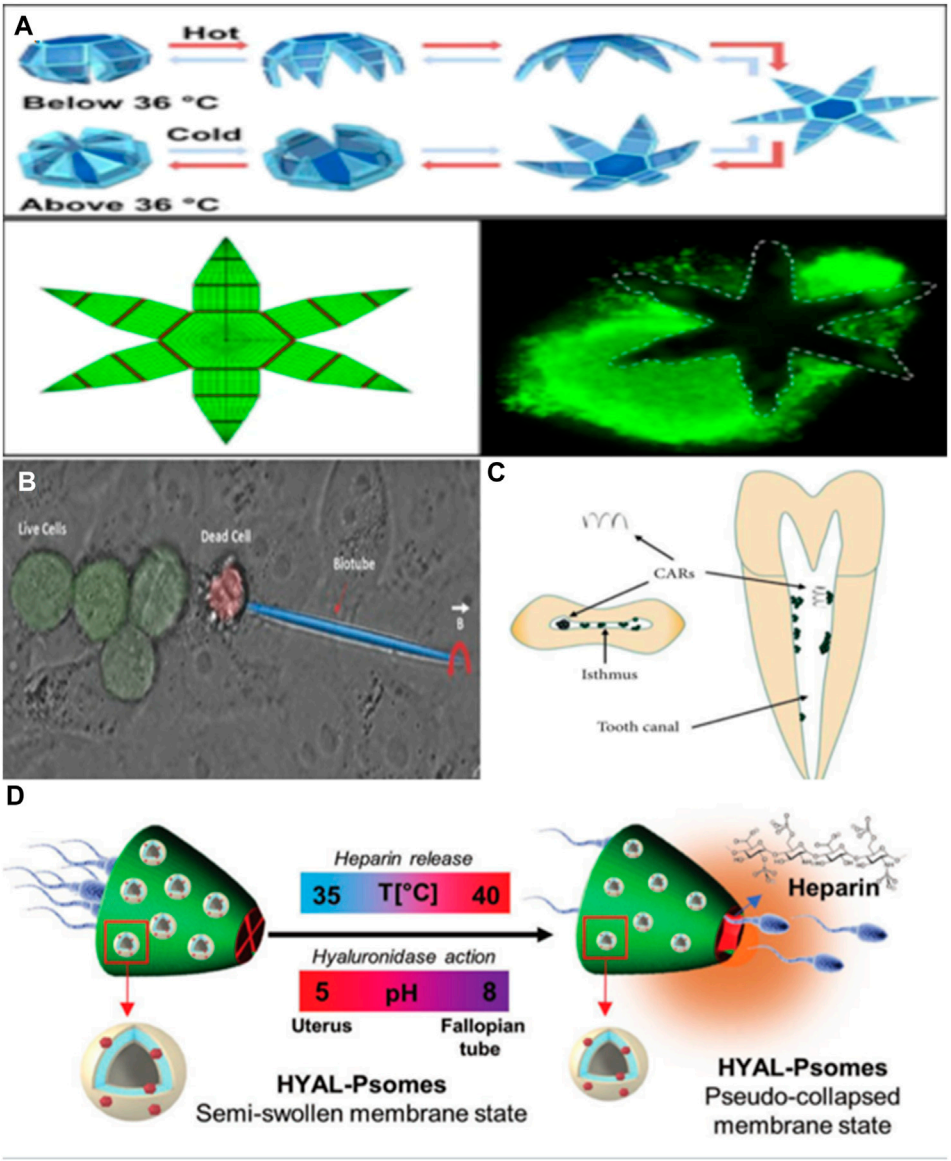

FIGURE 4
(A) A hydrogel robot can perform surgical operations. Adapted with permission from Breger et al. (2015). Copyright 2015 American Chemical Society. **(B)** A double acting micro robot that can create cell incisions. Reproduced with permission from Srivastava et al. (2016); published by John Wiley and Sons, 2016. **(C)** A magnetic microrobot for catalytic biofilm degradation. Reproduced with permission (Cheng et al., 2022). Copyright 2022, Chen Cheng. **(D)** A multifunctional microcomputer robot carrying sperm to realize utilization. Reproduced with permission from Rajabasadi et al. (2022); published by John Wiley and Sons, 2022.

comprises a spiral microrobot guided by specially manufactured wires and an enhanced electromagnetic excitation system. Experiments have demonstrated its capacity to generate a maximum magnetic field with nearly zero phase delay across a broad operating frequency range. The system offers precise motion control and cutting force, making it suitable for thrombectomy procedures within the vascular system. In the future, *in vivo* experiments can be conducted to assess the clinical effectiveness of the mechanical thrombectomy device proposed in this study.

The ability of microrobots to penetrate tissues can be harnessed for tissue and specimen biopsies. With the ongoing advancements in minimally invasive surgery technology, there is a growing need to miniaturize surgical instruments for procedures conducted through natural openings or small incisions. Currently, one of the primary features of minimally invasive surgical instruments is their reliance on connecting wires or cables to transmit energy and signals while being controlled externally. These connecting wires restrict the flexibility of surgical tools and their capacity to access hard-to-reach areas within the body. Gultepe et al. (2013) have pioneered the development of wireless and autonomous microsurgical tools designed for accessing narrow channels inside the body. These microtools can autonomously move and grasp tissues through thermal activation. Constructed from thermally sensitive materials, they can be controlled using external heat sources. The researchers demonstrated the viability of these microtools for *in vivo* pig bile duct biopsies through experiments, offering a novel

approach to *in vivo* pig bile duct biopsies. In the fields of robotics and surgery, the ability to grasp and securely hold objects is a crucial task, particularly when it comes to tissue biopsy. Breger et al. (2015) introduced a novel design and preparation method for a self-folding micro fixture that combines thermosensitive hydrogel and hard polymer. By incorporating iron oxide nanoparticles into the porous hydrogel layer, this micro fixture becomes responsive to magnetic fields, enabling remote control. The micro fixture comprises a rigid PPF segment and a soft PNIPAM AAC layer, which automatically closes when the temperature exceeds 36°C. Experimental results demonstrate that this self-folding micro clamp effectively clamps onto cell tissue, and the clamping and release times can be regulated by temperature adjustments (see Figure 4A).On the other hand, Leong et al. (2009) developed an innovative micro fixture with mobility and quality control capabilities, driven by biological signals. Utilizing the principles of thin-film strain drive and self-assembly, this micro fixture was designed, manufactured, and subjected to experimental validation. The research findings reveal that this micro fixture exhibits excellent grasping and handling capabilities, making it suitable for operation in various environments.

One of our primary objectives is the miniaturization of robots to an incredibly small scale, potentially at the cellular or even subcellular level. These miniature robots could perform surgical operations within this dimension, and even be used for tasks like transmitting or harvesting DNA and RNA. Solovev et al. (2012) developed a self-driving nanotube structure through molecular beam epitaxy. He utilized bubbles generated by the decomposition of hydroxide fuel to propel these nanotubes. By depositing a ferromagnetic layer on the nanotube, remote magnetic guidance of nanotools can also be achieved. These nanotube tools possess a small diameter and a unique asymmetric structure, allowing them to generate spiral motion and perform drilling on biomaterials. These micro/nano tools are capable of carrying multiple yeast cells for transportation. However, it's worth noting that the propellant used is toxic to mammalian cells, limiting its feasibility for applications involving living cells. In another approach, Srivastava et al. (2016) proposed a micro robot with dual functionality for targeted drug delivery and cell surgery. They extracted calcified porous microneedles from Dracaena species with drug-carrying capabilities and coated them with a magnetic layer for cell penetration under the influence of a magnetic field. The carried drugs have the potential to eliminate nearby harmful and malignant cells while also releasing supplementary drugs to enhance the body's defense against infections. The robot's ability to penetrate single cells can also serve as an anchoring mechanism for drug release, especially in secondary treatments mediated by other drugs. This robot system offers the potential to significantly reduce treatment side effects, including those associated with chemotherapy (see Figure 4B). Harder et al. (2023) introduced a microrobot constructed from alginate. This microrobot relies on a combination of photothermal drive and temperature sensing to precisely stimulate a single cell. It activates the intracellular thermosensitive ion channels, leading to changes in intracellular calcium content. While preliminary experiments were conducted on human embryonic kidney cells, and a comprehensive evaluation of toxicity and biocompatibility is yet to be performed, the emergence of this robot platform presents a novel approach for studying the thermobiology of cells and mammalian tissues.

With the ongoing development of microrobot technology, its application in surgical procedures has been gradually transitioning into clinical practice. Even though it is still primarily in the experimental stages with animal subjects, the results obtained thus far inspire confidence. Ullrich et al. (2013) introduced a microrobot designed for minimally invasive surgery in the posterior segment of the eye and presented the outcomes of activity experiments conducted in rabbit eyes. These microdevices are injected into the vitreous cavity and can be guided to the lesion site through wireless control via a magnetic field. Surgeons can then manipulate the microrobots for necessary treatments, such as mechanical procedures or targeted drug delivery. The initial application of this technology focuses on drug delivery to lesions near the retina, aiming to reduce the required drug dosage and prolong treatment duration. This approach allows for injection into the eye, manipulation, and subsequent removal of the microrobot, offering a potential adjunctive method for ophthalmic treatments. However, further research is needed to explore the interaction and impact of these microrobots on intraocular tissues. On a related note, Wu et al. (2018) designed micropropellers capable of moving within the eye under external magnetic field control, enabling precise delivery of drugs and therapeutic substances to target areas. These micropropellers feature a super-lubricated surface coating, reducing friction resistance within the vitreous of the eyeball, allowing them to move freely within the eye. Using technologies like optical coherence tomography (OCT), researchers successfully observed the movement and positioning of these micropropellers in pig eyes, providing a new technique for intraocular surgery and treatment.

Microrobots are increasingly finding applications in various surgical fields. Nguyen et al. (2018) introduced the concept and requirements for micro-robot-assisted cholesteatoma surgery. By combining microscopy, imaging technology, and laser ablation tools, residual cholesteatoma cells can be detected and removed. However, a complete robot system for clinical experiments has not yet been fully developed. Cheng et al. (2022) also summarized the progress of microrobots in dentistry. Microrobots can magnify differences that are imperceptible to the naked eye, leading to more precise treatments. They offer unparalleled advantages in procedures like root canal resection, dental pulp treatment, and even tumor treatment (see Figure 4C). Sperm has become a focal point of research in the micro/nanorobot field due to its flagellar structure and innate self-movement capabilities. Sperm's ability to evade human immune responses and deliver drugs has led to the development of various microrobot systems (Medina-Sánchez et al., 2018). In the field of assisted reproduction, studies have explored the use of microrobots, prepared using single sperm, for treating conditions such as oligospermia and azoospermia (Magdanz et al., 2017). However, the functions achievable with only a single sperm cell are limited. Subsequently, Rajabasadi et al. (2022) developed a microrobot carrier capable of carrying multiple sperm, constructed from various intelligent materials (see Figure 4D). This microrobot can achieve *in situ* sperm capacitation through localized heparin release and degrade the cumulus complex surrounding the oocyte, thereby enhancing the probability of fertilization.

3 Conclusion and future perspective

This paper serves as a comprehensive summary of the remarkable achievements in the application of micro/nanorobots in the field of medicine, particularly in the domains of biosensors, image diagnosis, targeted drug delivery, and minimally invasive surgery. Micro/nano robots offer advantages that traditional treatment methods cannot match, including their ability to reach deep tissues, minimize trauma, and enhance treatment efficiency. Presently, research in this field is still in its infancy, and there remain significant challenges to overcome on the path toward clinical transformation. One primary challenge is ensuring the biosafety of these micro/nano robots. Given their need to navigate deep tissues or even aggregate, it is imperative that these robots exhibit non-toxic and degradable characteristics. Additionally, concerns arise regarding the generation of chemical waste during robot operations, which may potentially harm the human body. While some biodegradable micro/nano robots have been successfully developed, precise control over their degradation environment and timeline remains essential. Moreover, these biodegradable robots primarily undergo degradation in PBS solutions or animal models, leaving their parameters and functions in a human environment largely uncharted. A second significant challenge revolves around the control of these robots and the aspiration to orchestrate their collective movement. Future advancements driven by fields like artificial intelligence may allow for the autonomous movement of robot clusters, even facilitating coordination between individual robots. Such developments hold tremendous promise, especially in complex treatment domains like large-scale medication and tumor immune environment therapy. The third major challenge involves the reduction of material and production costs to enable mass production of these robots. This endeavor intersects with materials science and 3D printing technologies. Researchers aim to explore a broader range of biological and synthetic materials while seeking more efficient and cost-effective fabrication methods. The ultimate goal is to establish a safe and widely accessible micro/nano robot system, ensuring that more individuals can benefit from precise and efficient medical treatments. In conclusion, the journey toward realizing the full potential of micro/nanorobots in the treatment of human diseases is long and multifaceted. Numerous details await exploration, including ethical considerations. It is anticipated that research into the micro/nano robot platform will experience rapid growth in the coming decade. As long as safety and controllability conditions are met, micro/nano robots hold the potential to revolutionize the field of medical treatment.

Author contributions

TS: Conceptualization, Data curation, Investigation, Writing–original draft, Writing–review and editing. JC: Data curation, Investigation, Project administration, Writing–review and editing. JZ: Data curation, Methodology, Project administration, Writing–review and editing. ZZ: Writing–review and editing. YZ: Data curation, Investigation, Writing–review and editing. JS: Data curation, Investigation, Resources, Supervision, Validation, Writing–review and editing. HC: Conceptualization, Funding acquisition, Project administration, Resources, Supervision, Writing–review and editing.

Funding

The author(s) declare financial support was received for the research, authorship, and/or publication of this article. This work was supported by Research and Innovation Fund of the First Affiliated Hospital of Harbin Medical University (Grant No. 2022M24).

Conflict of interest

The authors declare that the research was conducted in the absence of any commercial or financial relationships that could be construed as a potential conflict of interest.

Publisher's note

References

Attia, A. B. E., Balasundaram, G., Moothanchery, M., Dinish, U. S., Bi, R., Ntziachristos, V., et al. (2019). A review of clinical photoacoustic imaging: current and future trends. *Photoacoustics* 16, 100144. doi:10.1016/j.pacs.2019.100144

Aydin, S. (2015). A short history, principles, and types of ELISA, and our laboratory experience with peptide/protein analyses using ELISA. *Peptides* 72, 4–15. doi:10.1016/j.peptides.2015.04.012

Aziz, A., Pane, S., Iacovacci, V., Koukourakis, N., Czarske, J., Menciassi, A., et al. (2020). Medical imaging of microrobots: toward *in vivo* applications. *ACS Nano* 14 (9), 10865–10893. doi:10.1021/acsnano.0c05530

Bianchi, F., Masaracchia, A., Shojaei Barjuei, E., Menciassi, A., Arezzo, A., Koulaouzidis, A., et al. (2019). Localization strategies for robotic endoscopic capsules: a review. *Expert Rev. Med. Devices* 16 (5), 381–403. doi:10.1080/17434440.2019.1608182

Breger, J. C., Yoon, C., Xiao, R., Kwag, H. R., Wang, M. O., Fisher, J. P., et al. (2015). Self-folding thermo-magnetically responsive soft microgrippers. *ACS Appl. Mater Interfaces* 7 (5), 3398–3405. doi:10.1021/am508621s

Chen, X. Z., Jang, B., Ahmed, D., Hu, C., De Marco, C., Hoop, M., et al. (2018). Small-scale machines driven by external power sources. *Adv. Mater* 30 (15), e1705061. doi:10.1002/adma.201705061

Cheng, C., Yinan, X., Zongxin, X., Lei, S., Yanan, X., and Yanli, Y. (2022). Robotic and microrobotic tools for dental therapy. *J. Healthc. Eng.* 2022, 1–12. doi:10.1155/2022/3265462

Dahroug, B., Tamadazte, B., Weber, S., Tavernier, L., and Andreff, N. (2018). Review on otological robotic systems: toward microrobot-assisted cholesteatoma surgery. *IEEE Rev. Biomed. Eng.* 11, 125–142. doi:10.1109/RBME.2018.2810605

Darmawan, B. A., Gong, D., Park, H., Jeong, S., Go, G., Kim, S., et al. (2022). Magnetically controlled reversible shape-morphing microrobots with real-time X-ray imaging for stomach cancer applications. *J. Mater Chem. B* 10 (23), 4509–4518. doi:10.1039/d2tb00760f

de Ávila, B. E. F., Angsantikul, P., Li, J., Angel Lopez-Ramirez, M., Ramírez-Herrera, D. E., Thamphiwatana, S., et al. (2017). Micromotor-enabled active drug delivery for *in vivo* treatment of stomach infection. *Nat. Commun.* 8 (1), 272. doi:10.1038/s41467-017-00309-w

de Ávila, B. E. F., Lopez-Ramirez, M. A., Báez, D. F., Jodra, A., Singh, V. V., Kaufmann, K., et al. (2016). Aptamer-modified graphene-based catalytic micromotors: off–on fluorescent detection of ricin. *ACS Sens.* 1, 217–221. doi:10.1021/acssensors.5b00300

Deng, J., Zhao, S., Liu, Y., Liu, C., and Sun, J. (2021). Nanosensors for diagnosis of infectious diseases. *ACS Appl. Bio Mater* 4 (5), 3863–3879. doi:10.1021/acsabm.0c01247

Fan, X., Jiang, Y., Li, M., Zhang, Y., Tian, C., Mao, L., et al. (2022). Scale-reconfigurable miniature ferrofluidic robots for negotiating sharply variable spaces. *Sci. Adv.* 8 (37), eabq1677. doi:10.1126/sciadv.abq1677

Gao, W., Dong, R., Thamphiwatana, S., Li, J., Gao, W., Zhang, L., et al. (2015). Artificial micromotors in the mouse's stomach: a step toward *in vivo* use of synthetic motors. *ACS Nano* 9 (1), 117–123. doi:10.1021/nn507097k

Gao, W., Uygun, A., and Wang, J. (2012). Hydrogen-bubble-propelled zinc-based microrockets in strongly acidic media. *J. Am. Chem. Soc.* 134 (2), 897–900. doi:10.1021/ja210874s

Gong, D., Celi, N., Zhang, D., and Cai, J. (2022). Magnetic biohybrid microrobot multimers based on *chlorella* cells for enhanced targeted drug delivery. *ACS Appl. Mater Interfaces* 14 (5), 6320–6330. doi:10.1021/acsami.1c16859

Gröhl, J., Schellenberg, M., Dreher, K., and Maier-Hein, L. (2021). Deep learning for biomedical photoacoustic imaging: a review. *Photoacoustics* 22, 100241. doi:10.1016/j.pacs.2021.100241

Gultepe, E., Randhawa, J. S., Kadam, S., Yamanaka, S., Selaru, F. M., Shin, E. J., et al. (2013). Biopsy with thermally-responsive untethered microtools. *Adv. Mater* 25 (4), 514–519. doi:10.1002/adma.201203348

Han, D., Yan, G., Wang, Z., Jiang, P., Liu, D., Zhao, K., et al. (2020). The modelling, analysis, and experimental validation of a novel micro-robot for diagnosis of intestinal diseases. *Micromachines (Basel)* 11 (10), 896. doi:10.3390/mi11100896

Harder, P., İyisan, N., Wang, C., Kohler, F., Neb, I., Lahm, H., et al. (2023). A laser-driven microrobot for thermal stimulation of single cells. *Adv. Healthc. Mater* 12, e2300904. doi:10.1002/adhm.202300904

Hegde, C., Su, J., Tan, J. M. R., He, K., Chen, X., and Magdassi, S. (2023). Sensing in soft robotics. *ACS Nano* 17 (16), 15277–15307. doi:10.1021/acsnano.3c04089

Ji, F., Li, T., Yu, S., Wu, Z., and Zhang, L. (2021). Propulsion gait analysis and fluidic trapping of swinging flexible nanomotors. *ACS Nano* 15 (3), 5118–5128. doi:10.1021/acsnano.0c10269

Joseph, A., Contini, C., Cecchin, D., Nyberg, S., Ruiz-Perez, L., Gaitzsch, J., et al. (2017). Chemotactic synthetic vesicles: design and applications in blood-brain barrier crossing. *Sci. Adv.* 3 (8), e1700362. doi:10.1126/sciadv.1700362

Kadry, H., Noorani, B., and Cucullo, L. (2020). A blood-brain barrier overview on structure, function, impairment, and biomarkers of integrity. *Fluids Barriers CNS* 17 (1), 69. doi:10.1186/s12987-020-00230-3

Leong, T. G., Randall, C. L., Benson, B. R., Bassik, N., Stern, G. M., and Gracias, D. H. (2009). Tetherless thermobiochemically actuated microgrippers. *Proc. Natl. Acad. Sci. U. S. A.* 106 (3), 703–708. doi:10.1073/pnas.0807698106

Li, H., Wang, Z., Ogunnaike, E. A., Wu, Q., Chen, G., Hu, Q., et al. (2021). Scattered seeding of CAR T cells in solid tumors augments anticancer efficacy. *Natl. Sci. Rev.* 9 (3), nwab172. doi:10.1093/nsr/nwab172

Li, T., Chang, X., Wu, Z., Li, J., Shao, G., Deng, X., et al. (2017b). Autonomous collision-free navigation of microvehicles in complex and dynamically changing environments. *ACS Nano* 11 (9), 9268–9275. doi:10.1021/acsnano.7b04525

Li, T., Li, J., Morozov, K. I., Wu, Z., Xu, T., Rozen, I., et al. (2017a). Highly efficient freestyle magnetic nanoswimmer. *Nano Lett.* 17 (8), 5092–5098. doi:10.1021/acs.nanolett.7b02383

Li, T., Li, J., Zhang, H., Chang, X., Song, W., Hu, Y., et al. (2016). Magnetically propelled fish-like nanoswimmers. *Small* 12 (44), 6098–6105. doi:10.1002/smll.201601846

Li, T., Yu, S., Sun, B., Li, Y., Wang, X., Pan, Y., et al. (2023). Bioinspired claw-engaged and biolubricated swimming microrobots creating active retention in blood vessels. *Sci. Adv.* 9 (18), eadg4501. doi:10.1126/sciadv.adg4501

Lin, R., Yu, W., Chen, X., and Gao, H. (2021). Self-propelled micro/nanomotors for tumor targeting delivery and therapy. *Adv. Healthc. Mater* 10 (1), e2001212. doi:10.1002/adhm.202001212

Liu, D., Liu, X., Chen, Z., Zuo, Z., Tang, X., Huang, Q., et al. (2022). Magnetically driven soft continuum microrobot for intravascular operations in microscale. *Cyborg Bionic Syst.* 2022, 9850832. doi:10.34133/2022/9850832

Ma, L., Dichwalkar, T., Chang, J. Y. H., Cossette, B., Garafola, D., Zhang, A. Q., et al. (2019). Enhanced CAR-T cell activity against solid tumors by vaccine boosting through the chimeric receptor. *Science* 365 (6449), 162–168. doi:10.1126/science.aav8692

Magdanz, V., Medina-Sánchez, M., Schwarz, L., Xu, H., Elgeti, J., and Schmidt, O. G. (2017). Spermatozoa as functional components of robotic microswimmers. *Adv. Mater* 29 (24), 201606301. doi:10.1002/adma.201606301

Manohar, S., and Gambhir, S. S. (2020). Clinical photoacoustic imaging. *Photoacoustics* 19, 100196. doi:10.1016/j.pacs.2020.100196

Mayorga-Martinez, C. C., Vyskočil, J., Novotný, F., Bednar, P., Ruzek, D., Alduhaishe, O., et al. (2022). Collective behavior of magnetic microrobots through immuno-sandwich assay: on-the-fly COVID-19 sensing. *Appl. Mater Today* 26, 101337. doi:10.1016/j.apmt.2021.101337

Medina-Sánchez, M., Xu, H., and Schmidt, O. G. (2018). Micro- and nano-motors: the new generation of drug carriers. *Ther. Deliv.* 9 (4), 303–316. doi:10.4155/tde-2017-0113

Middelhoek, KINA, Magdanz, V., Abelmann, L., and Khalil, I. S. M. (2022). Drug-Loaded IRONSperm clusters: modeling, wireless actuation, and ultrasound imaging. *Biomed. Mater* 17 (6), 8. doi:10.1088/1748-605X/ac8b4b

Mohammadinejad, R., Karimi, S., Iravani, S., and Varma, R. S. (2016). Plant-derived nanostructures: types and applications. *Green Chem.* 18, 20–52. doi:10.1039/c5gc01403d

Mu, H., Liu, C., Zhang, Q., Meng, H., Yu, S., Zeng, K., et al. (2022). Magnetic-driven hydrogel microrobots selectively enhance synthetic lethality in MTAP-deleted osteosarcoma. *Front. Bioeng. Biotechnol.* 10, 911455. doi:10.3389/fbioe.2022.911455

Nelson, B. J., Kaliakatsos, I. K., and Abbott, J. J. (2010). Microrobots for minimally invasive medicine. *Annu. Rev. Biomed. Eng.* 12, 55–85. doi:10.1146/annurev-bioeng-010510-103409

Nguyen, K. T., Go, G., Choi, E., Kang, B., Park, J. O., and Kim, C. S. (2018). A guide-wired helical microrobot for mechanical thrombectomy: a feasibility study. *Annu. Int. Conf. IEEE Eng. Med. Biol. Soc.* 2018, 1494–1497. doi:10.1109/EMBC.2018.8512455

Nguyen, K. T., Kim, S. J., Min, H. K., Hoang, M. C., Go, G., Kang, B., et al. (2021). Guide-wired helical microrobot for percutaneous revascularization in chronic total occlusion in-vivo validation. *IEEE Trans. Biomed. Eng.* 68 (8), 2490–2498. doi:10.1109/TBME.2020.3046513

Peng, F., Tu, Y., Men, Y., van Hest, J. C., and Wilson, D. A. (2017). Supramolecular adaptive nanomotors with magnetotaxis behavior. *Adv. Mater* 29 (6), 201604996. doi:10.1002/adma.201604996

Rajabasadi, F., Moreno, S., Fichna, K., Aziz, A., Appelhans, D., Schmidt, O. G., et al. (2022). Multifunctional 4D-printed sperm-hybrid microcarriers for assisted reproduction. *Adv. Mater* 34 (50), e2204257. doi:10.1002/adma.202204257

Sattayasamitsathit, S., Kou, H., Gao, W., Thavarajah, W., Kaufmann, K., Zhang, L., et al. (2014). Fully loaded micromotors for combinatorial delivery and autonomous release of cargoes. *Small* 10 (14), 2830–2833. doi:10.1002/smll.201303646

Solovev, A. A., Xi, W., Gracias, D. H., Harazim, S. M., Deneke, C., Sanchez, S., et al. (2012). Self-propelled nanotools. *ACS Nano* 6 (2), 1751–1756. doi:10.1021/nn204762w

Soto, F., Martin, A., Ibsen, S., Vaidyanathan, M., Garcia-Gradilla, V., Levin, Y., et al. (2016). Acoustic microcannons: toward advanced microballistics. *ACS Nano* 10 (1), 1522–1528. doi:10.1021/acsnano.5b07080

Soto, F., Wang, J., Ahmed, R., and Demirci, U. (2020). Medical micro/nanorobots in precision medicine. *Adv. Sci. (Weinh)* 7 (21), 2002203. doi:10.1002/advs.202002203

Srivastava, S. K., Medina-Sánchez, M., Koch, B., and Schmidt, O. G. (2016). Medibots: dual-action biogenic microdaggers for single-cell surgery and drug release. *Adv. Mater* 28 (5), 832–837. doi:10.1002/adma.201504327

Tang, X., Yang, Y., Zheng, M., Yin, T., Huang, G., Lai, Z., et al. (2023). Magnetic-acoustic sequentially actuated CAR T cell microrobots for precision navigation and *in situ* antitumor immunoactivation. *Adv. Mater* 35 (18), e2211509. doi:10.1002/adma.202211509

Tapia-Siles, S. C., Coleman, S., and Cuschieri, A. (2016). Current state of micro-robots/devices as substitutes for screening colonoscopy: assessment based on technology readiness levels. *Surg. Endosc.* 30 (2), 404–413. doi:10.1007/s00464-015-4263-1

Tu, Y., Peng, F., and Wilson, D. A. (2017). Motion manipulation of micro- and nanomotors. *Adv. Mater* 29 (39). doi:10.1002/adma.201701970

Tumino, E., Visaggi, P., Bolognesi, V., Ceccarelli, L., Lambiase, C., Coda, S., et al. (2023). Robotic colonoscopy and beyond: insights into modern lower gastrointestinal endoscopy. *Diagn. (Basel)* 13 (14), 2452. doi:10.3390/diagnostics13142452

Ullrich, F., Bergeles, C., Pokki, J., Ergeneman, O., Erni, S., Chatzipirpiridis, G., et al. (2013). Mobility experiments with microrobots for minimally invasive intraocular surgery. *Invest. Ophthalmol. Vis. Sci.* 54 (4), 2853–2863. doi:10.1167/iovs.13-11825

Vilela, D., Cossío, U., Parmar, J., Martínez-Villacorta, A. M., Gómez-Vallejo, V., Llop, J., et al. (2018). Medical imaging for the tracking of micromotors. *ACS Nano* 12 (2), 1220–1227. doi:10.1021/acsnano.7b07220

Wållberg, H., and Ståhl, S. (2013). Design and evaluation of radiolabeled tracers for tumor imaging. *Biotechnol. Appl. Biochem.* 60 (4), 365–383. doi:10.1002/bab.1111

Wang, Y., Liu, X., Chen, C., Chen, Y., Li, Y., Ye, H., et al. (2022). Magnetic nanorobots as maneuverable immunoassay probes for automated and efficient enzyme linked immunosorbent assay. *ACS Nano* 16 (1), 180–191. doi:10.1021/acsnano.1c05267

Wu, Y., Lin, X., Wu, Z., Möhwald, H., and He, Q. (2014). Self-propelled polymer multilayer Janus capsules for effective drug delivery and light-triggered release. *ACS Appl. Mater Interfaces* 6 (13), 10476–10481. doi:10.1021/am502458h

Wu, Z., Si, T., Gao, W., Lin, X., Wang, J., and He, Q. (2016). Superfast near-infrared light-driven polymer multilayer rockets. *Small* 12 (5), 577–582. doi:10.1002/smll.201502605

Wu, Z., Troll, J., Jeong, H. H., Wei, Q., Stang, M., Ziemssen, F., et al. (2018). A swarm of slippery micropropellers penetrates the vitreous body of the eye. *Sci. Adv.* 4 (11), eaat4388. doi:10.1126/sciadv.aat4388

Wu, Z., Wu, Y., He, W., Lin, X., Sun, J., and He, Q. (2013). Self-propelled polymer-based multilayer nanorockets for transportation and drug release. *Angew. Chem. Int. Ed. Engl.* 52 (27), 7000–7003. doi:10.1002/anie.201301643

Xi, W., Solovev, A. A., Ananth, A. N., Gracias, D. H., Sanchez, S., and Schmidt, O. G. (2013). Rolled-up magnetic microdrillers: towards remotely controlled minimally invasive surgery. *Nanoscale* 5 (4), 1294–1297. doi:10.1039/c2nr32798h

Xie, H., Sun, M., Fan, X., Lin, Z., Chen, W., Wang, L., et al. (2019). Reconfigurable magnetic microrobot swarm: multimode transformation, locomotion, and manipulation. *Sci. Robot.* 4 (28), eaav8006. doi:10.1126/scirobotics.aav8006

Yan, X., Zhou, Q., Vincent, M., Deng, Y., Yu, J., Xu, J., et al. (2017). Multifunctional biohybrid magnetite microrobots for imaging-guided therapy. *Sci. Robot.* 2 (12), eaaq1155. doi:10.1126/scirobotics.aaq1155

Yan, Y., Jing, W., and Mehrmohammadi, M. (2020). Photoacoustic imaging to track magnetic-manipulated micro-robots in deep tissue. *Sensors (Basel)* 20 (10), 2816. doi:10.3390/s20102816

Yang, J. (2020). Janus microdimer swimming in an oscillating magnetic field. *R. Soc. Open Sci.* 7 (12), 200378. doi:10.1098/rsos.200378

Yang, R., Wei, T., Goldberg, H., Wang, W., Cullion, K., and Kohane, D. S. (2017). Getting drugs across biological barriers. *Adv. Mater* 29 (37). doi:10.1002/adma.201606596

Yu, H., Tang, W., Mu, G., Wang, H., Chang, X., Dong, H., et al. (2018). Micro-/Nanorobots propelled by oscillating magnetic fields. *Micromachines (Basel)* 9 (11), 540. doi:10.3390/mi9110540

Yu, S., Li, T., Ji, F., Zhao, S., Liu, K., Zhang, Z., et al. (2022). Trimer-like microrobots with multimodal locomotion and reconfigurable capabilities. *Mater. Today Adv.* 14, 100231. doi:10.1016/j.mtadv.2022.100231

Yu, S., Sun, Z., Zhang, Z., Sun, H., Liu, L., Wang, W., et al. (2021). Magnetic microdimer as mobile meter for measuring plasma glucose and lipids. *Front. Bioeng. Biotechnol.* 9, 779632. doi:10.3389/fbioe.2021.779632

Yu, Z., Li, L., Mou, F., Yu, S., Zhang, D., Yang, M., et al. (2023). Swarming magnetic photonic-crystal microrobots with on-the-fly visual pH detection and self-regulated drug delivery. *InfoMat* 5, e12264. doi:10.1002/inf2.12464

Zhang, F., Zhuang, J., Li, Z., Gong, H., de Ávila, B. E., Duan, Y., et al. (2022b). Nanoparticle-modified microrobots for *in vivo* antibiotic delivery to treat acute bacterial pneumonia. *Nat. Mater* 21 (11), 1324–1332. doi:10.1038/s41563-022-01360-9

Zhang, W., Deng, Y., Zhao, J., Zhang, T., Zhang, X., Song, W., et al. (2023). Amoeba-inspired magnetic venom microrobots. *Small* 19 (23), e2207360. doi:10.1002/smll.202207360

Zhang, Y., Zhang, L., Yang, L., Vong, C. I., Chan, K. F., Wu, W. K. K., et al. (2019). Real-time tracking of fluorescent magnetic spore-based microrobots for remote detection of *C. diff* toxins. *Sci. Adv.* 5 (1), eaau9650. doi:10.1126/sciadv.aau9650

Zhang, Z., Wang, H., Yang, H., Song, W., Dai, L., Yu, S., et al. (2022a). Magnetic microswarm for MRI contrast enhancer. *Chem. Asian J.* 17 (17), e202200561. doi:10.1002/asia.202200561

Zhao, S., Sun, D., Zhang, J., Lu, H., Wang, Y., Xiong, R., et al. (2022). Actuation and biomedical development of micro-/nanorobots-A review. *Mater. Today Nano* 18, 100223. doi:10.1016/j.mtnano.2022.100223

frontiers | Frontiers in Bioengineering and Biotechnology

TYPE Original Research
PUBLISHED 21 February 2024
DOI 10.3389/fbioe.2024.1361617

OPEN ACCESS

EDITED BY
Tianlong Li,
Harbin Institute of Technology, China

REVIEWED BY
Haoran Mu,
Shanghai General Hospital, China
Aihui Wang,
University of California, Los Angeles, United States

*CORRESPONDENCE
Conghui Han,
hanchdoctor@st.btbu.edu.cn
Xiaoke Wu,
xiaokewu2002@vip.sina.com

†These authors have contributed equally to this work and share first authorship

RECEIVED 26 December 2023
ACCEPTED 23 January 2024
PUBLISHED 21 February 2024

CITATION
Jiang F, Zheng Q, Zhao Q, Qi Z, Wu D, Li W, Wu X and Han C (2024), Magnetic propelled hydrogel microrobots for actively enhancing the efficiency of lycorine hydrochloride to suppress colorectal cancer.
Front. Bioeng. Biotechnol. 12:1361617.
doi: 10.3389/fbioe.2024.1361617

Magnetic propelled hydrogel microrobots for actively enhancing the efficiency of lycorine hydrochloride to suppress colorectal cancer

Fengqi Jiang[1,2,3†], Qiuyan Zheng[4†], Qingsong Zhao[5], Zijuan Qi[6], Di Wu[2], Wenzhong Li[2], Xiaoke Wu[1,7*] and Conghui Han[1,3*]

[1]Department of Urology, Xuzhou Clinical School of Xuzhou Medical University, Xuzhou Central Hospital, Xuzhou, Jiangsu, China, [2]Department of General Surgery, Heilongjiang Provincial Hospital, Harbin, China, [3]School of Life Sciences, Jiangsu Normal University, Xuzhou, Jiangsu, China, [4]Department of Pharmacy, The Second Affiliated Hospital of Harbin Medical University, Harbin, China, [5]Postdoctoral Programme of Meteria Medica Institute of Harbin University of Commerce, Harbin, China, [6]Department of Pathology, Heilongjiang Provincial Hospital, Harbin, China, [7]Department of Obstetrics and Gynecology, First Affiliated Hospital, Heilongjiang University of Chinese Medicine, Harbin, China

Research and development in the field of micro/nano-robots have made significant progress in the past, especially in the field of clinical medicine, where further research may lead to many revolutionary achievements. Through the research and experiment of microrobots, a controllable drug delivery system will be realized, which will solve many problems in drug treatment. In this work, we design and study the ability of magnetic-driven hydrogel microrobots to carry Lycorine hydrochloride (LH) to inhibit colorectal cancer (CRC) cells. We have successfully designed a magnetic field driven, biocompatible drug carrying hydrogel microsphere robot with Fe_3O_4 particles inside, which can achieve magnetic field response, and confirmed that it can transport drug through fluorescence microscope. We have successfully demonstrated the motion mode of hydrogel microrobots driven by a rotating external magnetic field. This driving method allows the microrobots to move in a precise and controllable manner, providing tremendous potential for their use in various applications. Finally, we selected drug LH and loaded it into the hydrogel microrobot for a series of experiments. LH significantly inhibited CRC cells proliferation in a dose- and time-dependent manner. LH inhibited the proliferation, mobility of CRC cells and induced apoptosis. This delivery system can significantly improve the therapeutic effect of drugs on tumors.

KEYWORDS

colorectal cancer, magnetic-driven, microrobots, lycorine hydrochloride, Fe_3O_4 particle

1 Introduction

Colorectal cancer (CRC) has always been a public health problem due to its high incidence rate and mortality. The data in the GLOBOCAN 2020 global report shows that CRC ranks third in terms of new cases (193,159,0 10%), and second in terms of cancer-related deaths (935,173 cases, 9.4%) (Ionescu et al., 2023). Currently, the treatment of patients with metastatic colorectal cancer (mCRC) mainly focuses on chemotherapy,

supplemented by surgery and radiotherapy. With the development of therapeutic approaches, the survival period and quality of life of patients have been significantly improved (Sunakawa et al., 2016). However, overall, the 5-year survival rate of mCRC patients with mCRC remains low, at approximately 15% (Ohishi et al., 2023). Genetic mutations often lead to increased drug resistance in tumor cells, making existing treatment methods ineffective in controlling tumor growth and spread (Qunaj et al., 2023). Therefore, researchers have been searching for new treatment strategies to overcome this challenge (Cruz-Martins, 2023).

Compounds from plant sources have the advantages of low cost, high stability, high safety, and multi-targeting, which make them highly valuable in clinical applications (Avila-Carrasco et al., 2019). Lycorine hydrochloride (LH), as an active alkaloid, is extracted from the medicinal plant Lycoris radiate (Shi et al., 2021). In recent years, the research on the anti-tumor effect and mechanism of LH has been increasing. It has been found that LH can exert anti-tumor activity through multiple pathways and multiple signaling pathways, which is specifically reflected in the regulation of the occurrence and development of multiple tumors through one pathway, or the regulation of the same tumor through different signaling pathways (Ji et at., 2017; Li et al., 2020; Li et al., 2021). Although there have been many reports on the anti-tumor effects of LH, there have been relatively few studies on its role in CRC.

When normal cells are affected by synthetic lethal drugs and lead to serious side effects, synthetic lethality shows its limitations and shortcomings. As a result, patients may be forced to interrupt treatment due to strong side effects during treatment (Chen et al., 2020). In contrast, the precision drug delivery system may enhance the synthesis of lethal drugs in the tumor site while reducing side effects (Li et al., 2023). Micro/nano-robots have been innovatively adopted to solve problems related to Brownian motion and viscous forces, and to utilize different power sources for movement (Chen et al., 2018; Wang et al., 2021; Zhao et al., 2022). The magnetic-driven microrobots that achieves precise manipulation by changing the strength and direction of the magnetic field has great potential for clinical application in drug treatment of tumors, which has aroused great interest among researchers (Li et al., 2017; Wang et al., 2020; Ji et al., 2021; Zhang et al., 2023; Li et al., 2023). By precisely controlling the magnetic field, microrobots can be guided to the tumor site and release drugs, which not only greatly improves the therapeutic effect of drugs, but also significantly reduces a series of problems such as drug cytotoxicity and serious complications (Chen et al., 2018; Mu et al., 2022; Wang et al., 2022). This technology is expected to provide new solutions for tumor treatment in the future (Wang et al., 2021).

2 Materials and methods

2.1 Preparation of microfluidic chip

The microfluidic chip device is consisted of PDMS construction, capillary tubes, dispensing needles, and rubber tubes. The rubber tubes are used as microchannels for the dispersed phase and continuous phase. One end of the capillary tube is inserted into the PDMS body, and the other end is connected to the rubber tubes. In experiment, the fluid flows into the PDMS construction through the rubber tubes and capillary tube in sequence, where the micro droplets are sheared, and then flows out collectively through the rubber tube at the other end. All openings on the device surface are sealed with leak-proof oil sealant and left to stand for 15 min for the sealant to cure. The device is then stored in a cool and dry place.

2.2 Preparation of continuous phase and dispersed phase

2.2.1 Continuous phase (oil phase):

20 μL of Tween 20 (surfactant) was dropped into 20 mL of vegetable oil and stir to mix thoroughly. Then the mixed liquid was placed in a vacuum drying box, evacuate to 1,000 Pa for 30 min to remove bubbles in the mixed solution to obtain the continuous phase fluid required for the experiment.

2.2.2 Dispersed phase (water phase):

(1) 300 mg of gelatin (glue strength: ~250 g Bloom, Aladdin, China) was added into 7 mL of deionized (DI) water and then was stirred for 30 min at 40°C using magnetic stirrer until the gelatin was dissolved.
(2) 20 mg of photoinitiator (2-hydroxy-4′-(2-hydroxyethoxy)-2-methylpropiophenone) (Macklin, Shanghai, China) was added into 3 mL of DI water. Then mixed liquid was stirred for 10 min at 30°C using magnetic stirrer to obtain photoinitiator aqueous solution.
(3) The gelatin aqueous solution and the photoinitiator aqueous solution were mixed, and 0.1 mL of acid-base buffer was added.
(4) The Fe_3O_4 particles (20 nm) and LH were added into the mixed solution, and adjust the concentrations to 2.5% and 20 μM, respectively.

2.3 External magnetic field device

A three-degree-of-freedom Helmholtz coil, a multi-function data acquisition device, and three single-channel output power amplifiers jointly constitute the external rotating uniform magnetic field. By controlling the current and voltage of the Helmholtz coil, a circular external rotating uniform magnetic field can be generated on any plane in three-dimensional space to drive the microrobots to move in different ways (Wang et al., 2023). In the experiment, the cell-culture dish was placed in the center of the three-dimensional Helmholtz coil, where the magnetic field intensity was evenly distributed. After adding the drug-loaded microrobot, turning on the magnetic field can drive the microrobot to move towards the cells.

2.4 Cells and reagents

CRC cell lines DLD-1 and LoVo, as well as human intestinal epithelial cell line NCM460, are provided by Fuheng Cell Centre (Shanghai, China). LoVo cells were cultured in RPMI 1640 medium (Gibco; Thermo Fisher Scientific, Inc.), while DLD-1 and NCM460 cells were cultured in Dulbecco's modified Eagle's medium (DMEM; Thermo Fisher Scientific, Inc., Waltham, MA, United States). Both media were supplemented with 10% fetal

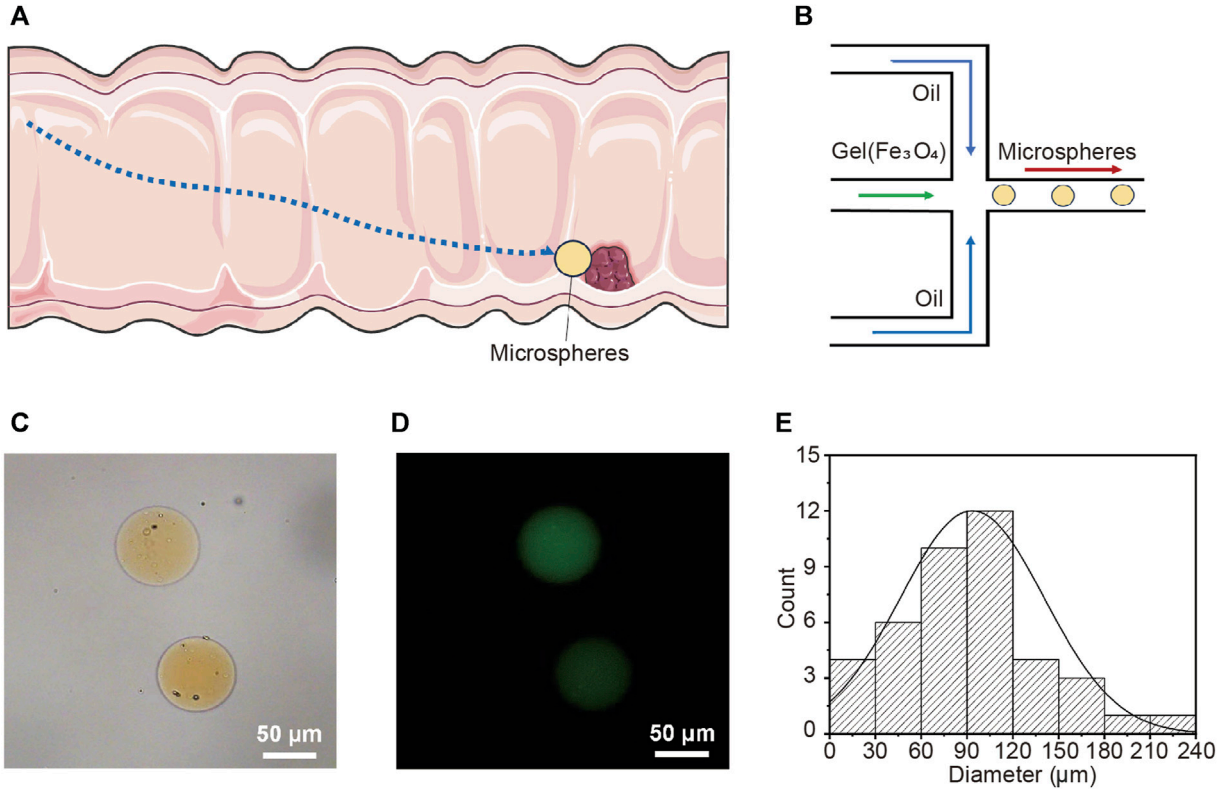

FIGURE 1
Targeted drug release in intestine using magnetic-driven hydrogel microrobots. **(A)** Schematic overview of magnetic-driven hydrogel microrobots for drug release in intestine. **(B)** The fabrication of magnetic-driven hydrogel microrobots using microfluidic chip. **(C)** The optical microscopy image of magnetic-driven hydrogel microrobots. **(D)** Fluorescence microscopic images of magnetic-driven hydrogel microrobots. **(E)** Particle size distribution of magnetic-driven hydrogel microrobots.

bovine serum (FBS; Gibco; Thermo Fisher Scientific, Inc.) and 1% antibiotic (Sigma-Aldrich, United States). All cells were cultured in a standard humidified incubator at 37°C under an atmosphere with 5% CO_2. LH (cat. no. L101559) was purchased from Aladdin Industrial Corporation (Shanghai, China) and was dissolved in dimethyl sulfoxide (DMSO) to prepare a stock solution of 77.16umol/L.

2.5 MTT assay

The cytotoxicity of LH was conducted by MTT assay. Cells were incubated in 96-well plate (5×10^3 per/well) for 24 h, then treated with different concentrations of LH (0–100 μM) for 48 h. After staining with MTT solution (5 mg/mL, 20 μL/well, 4 h) (Sigma-Aldrich, Merck KGaA, Darmstadt, Germany), 150 μL of DMSO was added to each well to solubilize the formazan crystals. A microplate reader (ELx808, BioTek Instruments, Winooski, VT, United States) was employed to detect the plate at the wavelength of 490 nm. Three biological experiments were performed.

2.6 Plate colony-forming assay

CRC cells (0.5×10^3) were cultured in 6-well plates for 24 h. Three groups were set up, including a negative control group (NC), LH-alone (20 μM), and a magnetic microrobot drug-loading group (LH-robot) (20 μM). Treatments were conducted on days 2, 4. After 10 days, the cells were fixed with methanol and stained with a 0.5% crystal violet solution. Three biological experiments were performed.

2.7 Wound healing assay

DLD-1 and LoVo cells (90% confluence) were scratched with a sterile 200-μL pipette tip and then treated with LH and LH-robots (20 μM) separately. After 48 h, the width of the scratch was observed. The scratch was imaged under a microscope (magnification, ×100). The widths of the scratches were analysed with ImageJ V1.8.0 (NIH, Bethesda, MD, United States). Three biological experiments were performed.

2.8 Transwell assay

The invasion experiment was conducted using a Transwell chamber. Before cells seeding, 50 μL of Matrigel was added to the upper chamber to coat the polycarbonate membrane. DLD-1 and LoVo cells were treated with LH alone and LH-robots (20 μM) separately and then cultured for 24 h. After resuspension in FBS-free medium, they were inoculated into the upper chamber (1×10^4 cells/200 μL medium per well). Then, the lower chamber containing 700 μL of medium with 10% FBS was used as a hemoattractant. After 48 h of

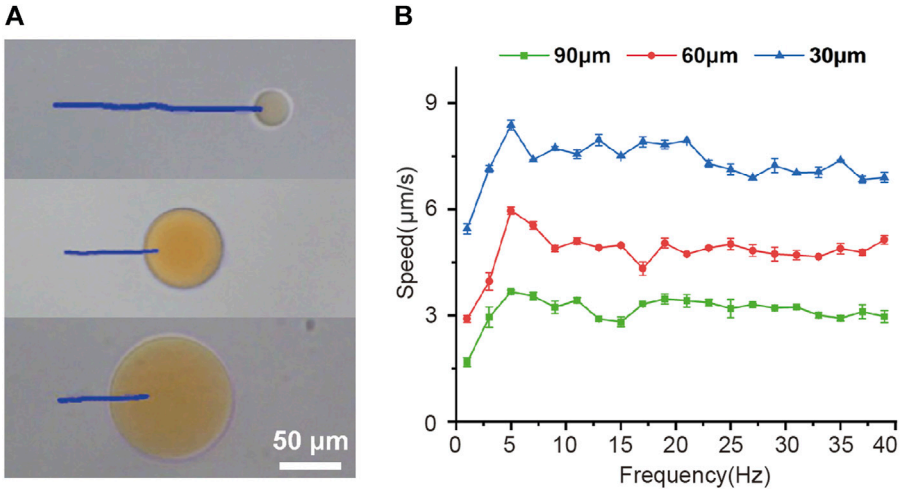

FIGURE 2
Magnetically actuated motility of magnetic-driven hydrogel microrobots. **(A)**Tracking lines illustrating the traveled distances of microrobots of different sizes over a 14 s period in a rotating uniform magnetic field of 15 mT and 5 Hz. **(B)** The velocity of microrobots of different sizes varied with the drive frequency from 2 to 40 Hz.

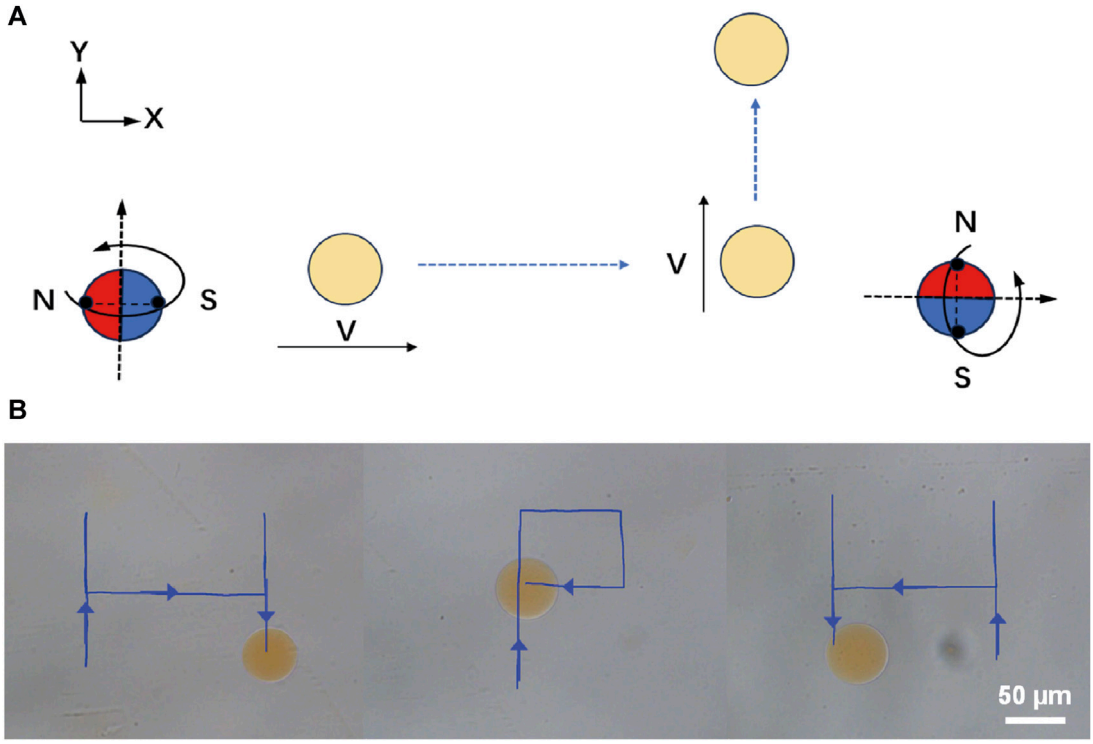

FIGURE 3
Controllable and flexible motility performance of magnetic-driven hydrogel microrobots. **(A)** Change of the direction of movement of the microrobots caused by changing the magnetic field. **(B)** Controllable motion of microdimer swimmer.

incubation, cells on the polycarbonate membrane were wiped off, and then methanol was used to fix the cells penetrating to the dorsal side, followed by staining with a 0.5% crystal violet solution. Under a microscope (magnification, ×100), 5 randomly selected fields were quantitatively analysed. Three biological experiments were performed.

2.9 Apoptosis assay

DLD-1 and LoVo cells were seeded in 6-well plates (2.5×10^5 per/well) and allowed to adhere overnight. Then, LH alone and LH-robots (20 μM) were added separately, and the cells were incubated

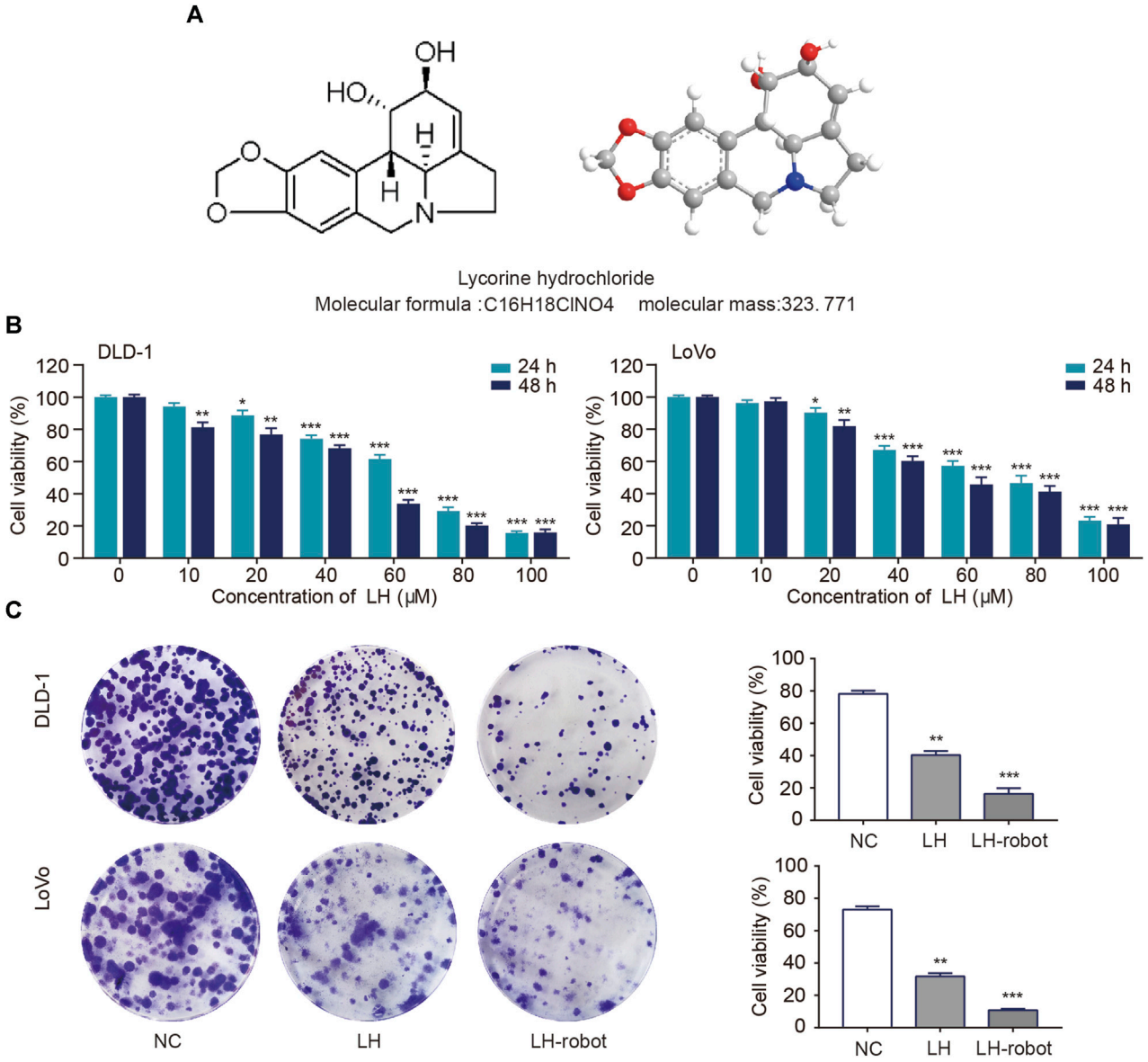

FIGURE 4
Effect of LH and LH-robot on CRC cell proliferation. **(A)** Chemical and three-dimensional structures of LH. **(B)** An MTT assay was performed to measure CRC cell viability following LH (0–100 μM) treatment. **(C)** The influence of LH alone and LH-robot on the colony formation of CRC cells. *$p < 0.05$ and **$p < 0.01$ and ***$p < 0.001$ vs. NC group.

for 48 h before being harvested and stained with an Annexin V-FITC/PI Apoptosis Detection kit (catalog no. FXP018; 4A Biotech). FACS DiVa 6.1.3 (BD Biosciences, Franklin Lakes, NJ, United States) was used to analyze apoptosis. Three biological experiments were performed.

2.10 Statistical analysis

All data were shown as means ± SD via at least triplicate samples. A two-tailed, Student's t test was used for testing the significance between two groups. Statistical analyses were performed using GraphPad PRISM 9 (GraphPad Software, Inc.) A one-way analysis of variance (ANOVA) with Dunnett's test was performed to test the significance for multiple comparisons. A statistical significance was assumed at $p < 0.05$.

3 Results

3.1 Preparation of magnetic drive microrobot delivery system

Autonomous micro/nano-robots can propel and navigate in various liquid media, and are expected to provide revolutionary technological advancements for drug delivery, microsurgery, and micro/nano-engineering (Xiao et al., 2022; Yang et al., 2022; Wang et al., 2021; Gao et al., 2021; Zhang et al., 2023). Magnetic

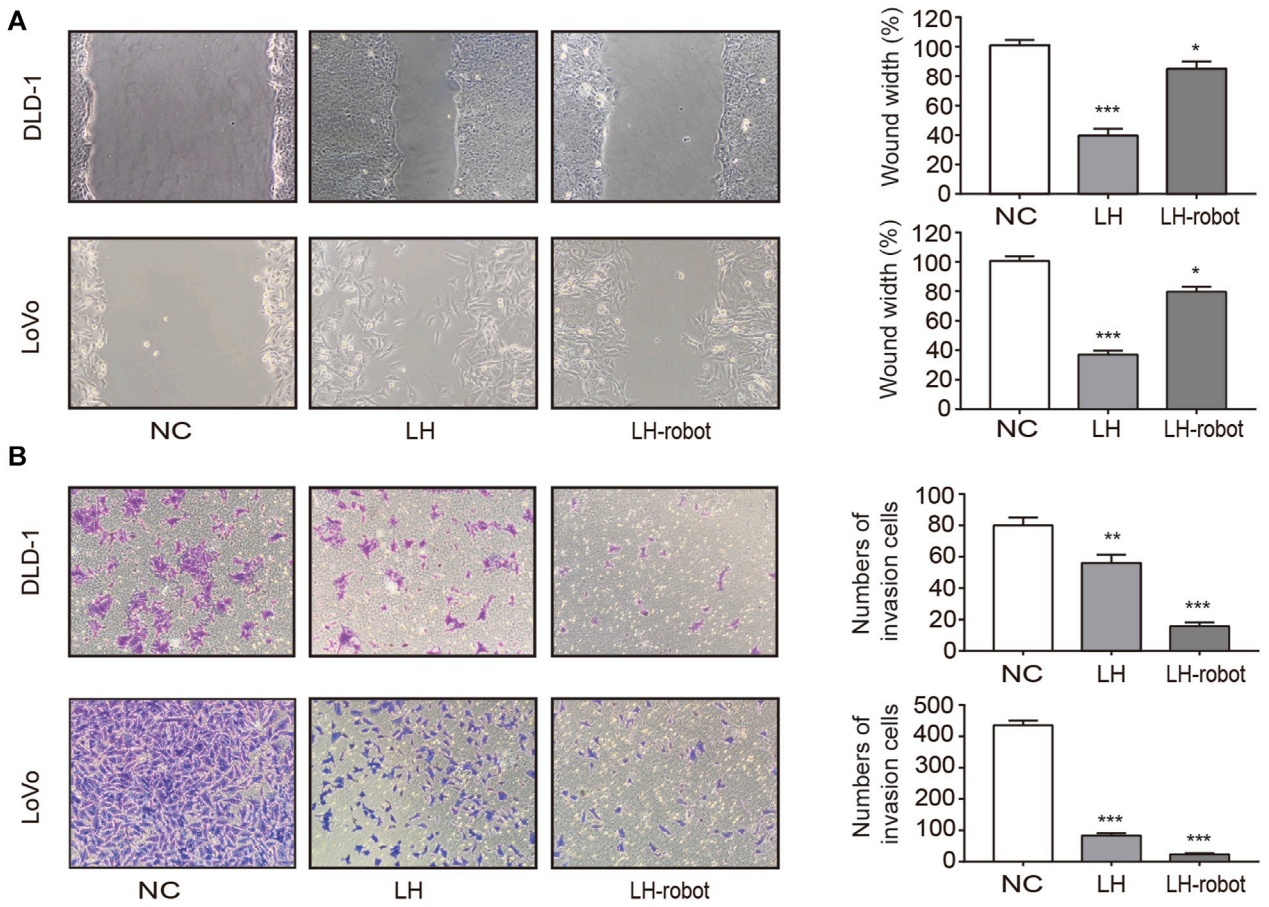

FIGURE 5
Effect of LH and LH-robot on CRC cell mobility. **(A)** Wound healing assay of LH alone and LH-robot on CRC cells at non-toxic concentrations (20μM, 24 h). Magnification, ×100. **(B)** Invasion assays of CRC cells pretreated with LH and LH-robot at non-toxic concentrations (20μM, 24 h). Magnification, ×100. *$p < 0.05$ and **$p < 0.01$ and ***$p < 0.001$ vs. NC group.

nanorobots show great potential in practical biomedical applications due to their wireless fuel-free actuation, strong propulsion, precise motion control, and high biocompatibility (Wang and Zhang, 2021; Xie et al., 2020; Zhou et al., 2021; Yang et al., 2023). This study describes the preparation of magnetic-driven hydrogel microrobots. It has the capability to transport drug LH through the digestive channel and into the intestine. Subsequently, the microrobot, driven by an external magnetic field, precisely maneuvers to the target lesion location for drug release and treatment (Figure 1A). This application demands that the microrobot is capable of loading drugs, exhibiting magnetic responsiveness, and possessing a biocompatible structure. Additionally, the microrobot should have a disintegrable body structure for drug release. Figure 1B illustrates the fabrication process of the magnetic-driven hydrogel microrobot. The hydrogel microrobot is fabricated using a microfluidic chip based on the principle of flow focusing. In the flow convergence device, the dispersed phase fluid and continuous phase fluid pass through a narrow region under pressure. At the micro-droplet generation site, there are three fluid streams, with the continuous phase fluid symmetrically distributed on both sides. The dispersed phase fluid in the middle is focused and sheared by the continuous phase fluids on both sides, forming micro-droplets. The micro-droplets are subsequently cured and solidified on the surface under UV light exposure, thus transforming into magnetic-driven hydrogel microrobots. In this process, the continuous phase is plant oil, and the dispersed phase is a gelatin aqueous solution containing photoinitiator, along with Fe_3O_4 particles and the LH.

The optical microscopy image shown in Figure 1C displays the spherical geometry of the microrobots. The clearly visible yellow microparticles inside the microrobot indicate the successful loading of Fe_3O_4 particles. The fluorescent microscope image (Figure 1D) illustrates that the desired drug loading has been achieved. The loading of drugs and Fe_3O_4 particles decreased in the homogeneity of the gelatin solution as the dispersed phase, leading to a lack of strict uniformity in the size of the generated microrobots. Figure 1E presents the statistical analysis of the size distribution of the prepared microrobots, indicating that the size distribution follows a generally normal distribution. The average diameter is approximately 90 μm, predominantly distributed within the range of 30~120 μm, exhibiting a high degree of monodispersity. In the microfluidic chip, the generation rate and size of microrobots can be modulated by altering the flow rate ratio, viscosity, and channel dimensions of the continuous and dispersed phase fluids.

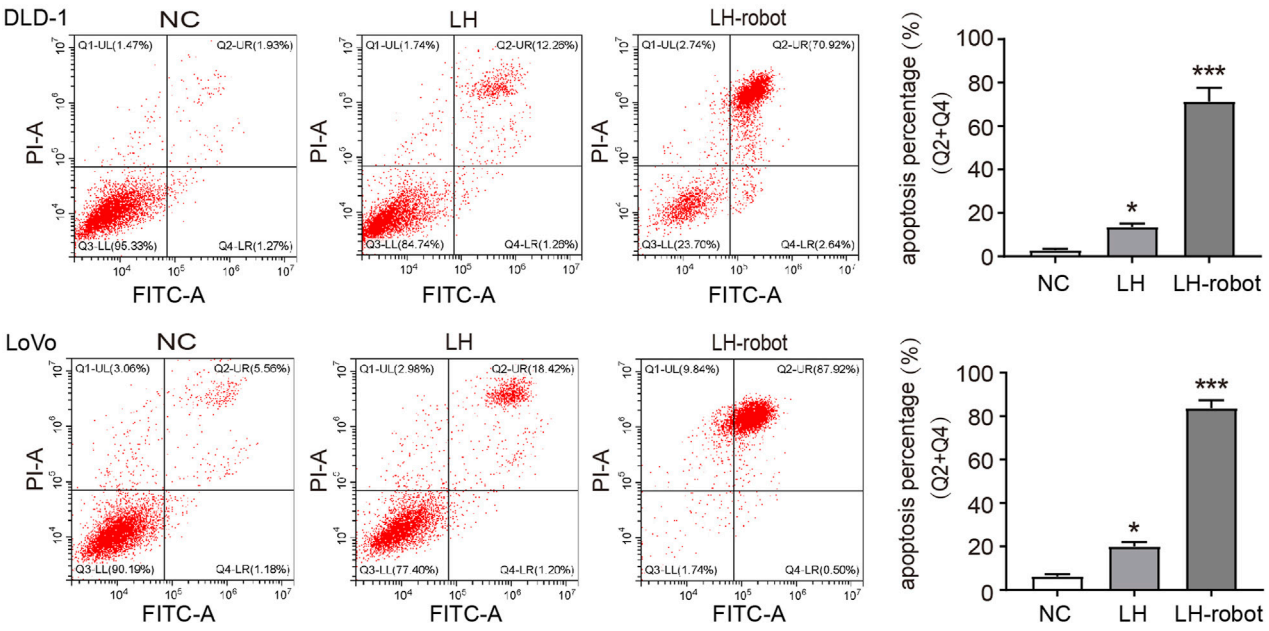

FIGURE 6
The apoptosis of CRC cells after treatment of LH and LH-robot separately. *$p < 0.01$ and ***$p < 0.001$ vs. NC group.

Then the effect of frequency of the rotating magnetic field on the velocity of magnetic-driven hydrogel microrobot was investigated experimentally as well. Figure 2A shows the trajectories of different-sized microrobots over a period of 14 s under the conditions of a magnetic force of 15 mT and a driving frequency of 5 Hz. It can be seen that larger microrobots exhibit smaller movement speeds. To further reveal the magnetic field-driven motion performance of microrobots, we explore the variation of microrobots' velocity with the magnetic frequency increased from 2 to 40 Hz and shown in Figure 2B, for a 30 μm microrobots, the speed increased linearly with the driving frequency and reached a maximum velocity of 8.4 μm/s at 5 Hz, further increasing the frequency reduced the velocity. Such a maximum synchronized frequency is called step-out frequency (Xie et al., 2019; Yu et al., 2019). The occurrence of the out-of-step phenomenon and the increase in drag caused by the increasing speed are the reasons we speculate for this variation. After the step-out phenomenon occurred, the speed of the microrobot fluctuates within a certain range as the frequency of the magnetic frequency increase. Furthermore, the 60 and 90 μm microrobots showed the same movement performance and obtained the highest velocities of 6 μm/s and 3.7 μm/s, respectively. This magnetically actuated motility of magnetic-driven hydrogel microrobots of different sizes can provide guidance for the customization of microrobots for different working conditions.

For the application of micro/nano-scale robots in precision medical procedures, the ability of remote driving has very attractive characteristics (Chirarattananon et al., 2014; Xie et al., 2019; Aram et al., 2022; Zhang et al., 2022). Here, we demonstrate the remote locomotion of Janus magnetic-driven hydrogel microrobots. Figure 3A illustrates the control strategy of three-dimensional rotating magnetic field generated by the three degrees of freedom Helmholtz coil and corresponding movement of microrobots. First, a circularly polarized rotating magnetic field applied in the X-Z plane excited the microrobot rolled along X-axis. When the rotating magnetic field was changed and applied in the Y-Z plane, the locomotion direction of microrobot changed to the Y-axis. The propulsion direction of the microrobot could be altered by changing the direction of rotating magnetic field manually. Based on this rule, we realized the controllable trajectory movement of microrobot by modulating the magnetic field. As shown in Figure 3B, the microrobot walked along letter "H"-, "P"-, and "H"-shaped trajectory. The microrobot realized flexible direction switching under the drive of magnetic field of 15 mT and 5 Hz. This remote controllable movement capability provides support for targeted locomotion of magnetic-driven hydrogel microrobots on the complex surface of the intestine.

3.2 Magnetic-driven microrobots significantly enhances the ability of LH to inhibit CRC cells

- The chemical structure formula and 3D structure of LH are shown in respectively. Cell proliferation was assessed using MTT and colony formation assays (Chan et al., 2023). CRC cells were exposed to multiple concentrations (0–100 μM) of LH for 24 and 48 h. MTT assay results showed that LH significantly inhibited CRC cells proliferation in a dose and time-dependent manner (Figure 4B). Notably, LH showed minimal cytotoxicity towards NCM460 cells (Supplementary Figure S1). We chose a non-lethal concentration of 20 μM of LH and compared the effects of single drug administration with microrobot-based drug delivery on CRC cells. A large

number of previous studies (Zhang et al., 2021; Zhou et al., 2021) have shown that Fe_3O_4 as a component of magnetic drive micro-nano robot will not cause biological tissue and cell damage, so the blank control group in this study containing a small dose of Fe_3O_4 will not cause additional effects. The colony formation experiment showed that the drug under the control system of magnetic microrobots had a more significant ability to inhibit the proliferation of CRC cells (Figure 4C).

Metastasis is the process by which cancer cells grow in organs far away from their primary organ, and is the deadliest manifestation of cancer (Xia et al., 2023). The vast majority of cancer patients die from metastatic disease, rather than primary tumors (Chen et al., 2019). Tumour cell mobility is essential for metastasis and is typically assessed by wound healing and Transwell assays (Jin et al., 2019). As shown in Figure 5A the wound healing speed in the cells treated with LH-robot was significantly slower. The Transwell assay results showed a significant decrease in the invasion ability of the experimental group cells, especially in the magnetic microrobot-based drug delivery group (Figure 5B).

Apoptosis is a programmed cell death that balances the ratio of cell survival and death. Cancer cells have the ability to escape apoptosis, so aimed at inducing cancer apoptosis is a very important direction for treating cancers (Elbanna et al., 2021). Cytotoxic chemotherapy and radiotherapy attempt to trigger apoptosis through endogenous pathways by acting on cell division and/or directly damaging DNA, and are currently the main methods for treating cancer through the induction of apoptosis mechanisms (Wanner et al., 2020; Barroso et al., 2023). In our experiments, we observed that LH has the ability to induce apoptosis in CRC cells, and the magnetic propelled hydrogel microrobots significantly enhance this ability (Figure 6).

4 Conclusion

We have fabricated a magnetic driven, biocompatible hydrogel microrobot loaded with Fe_3O_4 particles. Through the regulation of external magnetic fields, the movement of microrobots can be precisely controlled, enhancing the anticancer ability of LH on CRC cells. This technology can achieve precise delivery and efficient utilization of drugs, thereby reducing the toxic side effects and improving the therapeutic effect. Therefore, microrobot technology has broad prospects in cancer treatment.

Data availability statement

The raw data supporting the conclusion of this article will be made available by the authors, without undue reservation.

Author contributions

FJ: Conceptualization, Data curation, Formal Analysis, Funding acquisition, Investigation, Methodology, Project administration, Resources, Software, Supervision, Validation, Visualization, Writing–original draft, Writing–review and editing. QZh: Conceptualization, Writing–review and editing. QZ: Data curation, Writing–review and editing. ZQ: Data curation, Software, Writing–review and editing. DW: Data curation, Writing–review and editing. WL: Data curation, Writing–review and editing. XW: Conceptualization, Project administration, Supervision, Validation, Writing–review and editing. CH: Conceptualization, Project administration, Supervision, Writing–review and editing.

Funding

The author(s) declare financial support was received for the research, authorship, and/or publication of this article. This work was supported by the National Natural Science Foundation of China, Grant/Award Numbers: 12271467; Xuzhou Clinical Medicine Expert Team Project, Grant/Award Number: 2018TD004; Scientific Research Project of Heilongjiang Provincial Health Commission (No. 20210404080106); Heilongjiang Province Postdoctoral Fund (No. LBH-Z21170); Natural Science Foundation of Heilongjiang Province (No. LH 2020H063).

Conflict of interest

The authors declare that the research was conducted in the absence of any commercial or financial relationships that could be construed as a potential conflict of interest.

Publisher's note

Supplementary material

The Supplementary Material for this article can be found online at: https://www.frontiersin.org/articles/10.3389/fbioe.2024.1361617/full#supplementary-material

References

Aram, E., Moeni, M., Abedizadeh, R., Sabour, D., Sadeghi-Abandansari, H., Gardy, J., et al. (2022). Smart and multi-functional magnetic nanoparticles for cancer treatment applications: clinical challenges and future prospects. *Nanomater. (Basel)* 12 (20), 3567. doi:10.3390/nano12203567

Avila-Carrasco, L., Majano, P., Sánchez-Toméro, J. A., Selgas, R., López-Cabrera, M., Aguilera, A., et al. (2019). Natural plants compounds as modulators of epithelial-to-mesenchymal transition. *Front. Pharmacol.* 10, 715. doi:10.3389/fphar.2019.00715

Barroso, T., Melo-Alvim, C., Ribeiro, L., Casimiro, S., and Costa, L. (2023). Targeting inhibitor of apoptosis proteins to overcome chemotherapy resistance-A marriage between targeted therapy and cytotoxic chemotherapy. *Int. J. Mol. Sci.* 24 (17), 13385. doi:10.3390/ijms241713385

Chan, C., Deng, Y., Peng, B., Chiang, P., Wu, L., Lee, Y., et al. (2023). Anti-colorectal cancer effects of fucoidan complex-based functional beverage through retarding proliferation, cell cycle and epithelial-mesenchymal transition signaling pathways. *Integr. Cancer Ther.* 22, 15347354231213613. doi:10.1177/15347354231213613

Chen, C., Xu, Z., Zong, Y., Ou, B., Shen, X., Feng, H., et al. (2019). CXCL5 induces tumor angiogenesis via enhancing the expression of FOXD1 mediated by the AKT/NF-κB pathway in colorectal cancer. *Cell Death Dis.* 10 (3), 178. doi:10.1038/s41419-019-1431-6

Chen, X., Jang, B., Ahmed, D., Hu, C., De, M., Hoop, M., et al. (2018). Small-scale machines driven by external power sources. *Adv. Mater* 30 (15), e1705061. doi:10.1002/adma.201705061

Chen, Y., Du, M., Yu, J., Rao, L., Chen, X., and Chen, Z. (2020). Nanobiohybrids: a synergistic integration of bacteria and nanomaterials in cancer therapy. *BIO Integr.* 1, 25–36. doi:10.15212/bioi-2020-0008

Chirarattananon, P., Ma, K., and Wood, R. (2014). Adaptive control of a millimeter-scale flapping-wing robot. *Bioinspir Biomim.* 9 (2), 025004. doi:10.1088/1748-3182/9/2/025004

Cruz-Martins, N. (2023). Advances in plants-derived bioactives for cancer treatment. *Cells* 12 (8), 1112. doi:10.3390/cells12081112

Elbanna, M., Chowdhury, N., Rhome, R., and Fishel, M. (2021). Clinical and preclinical outcomes of combining targeted therapy with radio therapy. *Front. Oncol.* 11, 749496. doi:10.3389/fonc.2021.749496

Gao, C., Wang, Y., Ye, Z., Lin, Z., Ma, X., and He, Q. (2021). Biomedical micro-/nanomotors: from overcoming biological barriers to *in vivo* imaging. *Adv. Mater* 33 (6), e2000512. doi:10.1002/adma.202000512

Ionescu, V., Gheorghe, G., Bacalbasa, N., Chiotoroiu, A., and Diaconu, C. (2023). Colorectal cancer: from risk factors to oncogenesis. *Med. Kaunas.* 59 (9), 1646. doi:10.3390/medicina59091646

Ji, F., Li, T., Yu, S., Wu, Z., and Zhang, Li. (2021). Propulsion gait analysis and fluidic trapping of swinging flexible nanomotors. *ACS Nano* 15 (3), 5118–5128. doi:10.1021/acsnano.0c10269

Ji, Y., Yu, M., Qi, Z., Cui, D., Xin, G., Wang, B., et al. (2017). Study on apoptosis effect of human breast cancer cell MCF-7 induced by lycorine hydrochloride via death receptor pathway. *Saudi Pharm. J.* 25 (4), 633–637. doi:10.1016/j.jsps.2017.04.036

Jin, D., Guo, J., Wu, Y., Du, J., Yang, L., Wang, X., et al. (2019). m^6A mRNA methylation initiated by METTL3 directly promotes YAP translation and increases YAP activity by regulating the MALAT1-miR-1914-3p-YAP axis to induce NSCLC drug resistance and metastasis. *J. Hematol. Oncol.* 12 (1), 135. doi:10.1186/s13045-019-0830-6

Li, C., Deng, C., Pan, G., Wang, X., Zhang, K., Dong, Z., et al. (2020). Lycorine hydrochloride inhibits cell proliferation and induces apoptosis through promoting FBXW7-MCL1 axis in gastric cancer. *J. Exp. Clin. Cancer Res.* 39 (1), 230. doi:10.1186/s13046-020-01743-3

Li, J., Ávila, B., Gao, W., Zhang, L., and Wang, J. (2017). Micro/nanorobotsforbiomedicine:delivery, surgery, sensing, and detoxification. *Sci. Robotics* 15 (4), eaam6431. doi:10.1126/scirobotics.aam6431

Li, M., Liao, X., Li, C., Wang, T., Sun, Y., Yang, K., et al. (2021). Lycorine hydrochloride induces reactive oxygen species-mediated apoptosis via the mitochondrial apoptotic pathway and the JNK signaling pathway in the oral squamous cell carcinoma HSC-3 cell line. *Oncol. Lett.* 21 (3), 236. doi:10.3892/ol.2021.12497

Li, T., Yu, S., Sun, B., Li, Y., Wang, X., Pan, Y., et al. (2023a). Bioinspired claw-engaged and biolubricated swimming microrobots creating active retention in blood vessels. *Sci. Adv.* 9 (18), eadg4501. doi:10.1126/sciadv.adg4501

Li, Y., Cong, Z., Xie, L., Tang, S., Ren, C., Peng, X., et al. (2023b). Magnetically powered immunogenic macrophage microrobots for targeted multimodal cancer therapy. *Small* 19 (42), e2301489. doi:10.1002/smll.202301489

Mu, H., Liu, C., Zhang, Q., Meng, H., Yu, S., Zeng, K., et al. (2022). Magnetic-driven hydrogel microrobots selectively enhance synthetic lethality in MTAP-deleted osteosarcoma. *Front. Bioeng. Biotechnol.* 10, 911455. doi:10.3389/fbioe.2022.911455

Ohishi, T., Kaneko, M., Yoshida, Y., Takashima, A., Kato, Y., and Kawada, M. (2023). Current targeted therapy for metastatic colorectal cancer. *Int. J. Mol. Sci.* 24 (2), 1702. doi:10.3390/ijms24021702

Qunaj, L., May, M., Neugut, A., and Herzberg, B. (2023). Prognostic and therapeutic impact of the KRAS G12C mutation in colorectal cancer. *Front. Oncol.* 13, 1252516. doi:10.3389/fonc.2023.1252516

Shi, S., Li, C., Zhang, Y., Deng, C., Tan, M., Pan, G., et al. (2021). Lycorine hydrochloride inhibits melanoma cell proliferation, migration and invasion via down-regulating p21. *Am. J. Cancer Res.* 11 (4), 1391–1409. eCollection 2021.

Sunakawa, Y., Bekaii-Saab, T., and Stintzing, S. (2016). Reconsidering the benefit of intermittent versus continuous treatment in the maintenance treatment setting of metastatic colorectal cancer. *Cancer Treat. Rev. Cancer Treat. Rev.* 45, 97–104. doi:10.1016/j.ctrv.2016.03.007

Wang, B., Kostarelos, K., Nelson, B., and Zhang, L. (2021a). Trends in micro-/nanorobotics: materials development, actuation, localization,and system integration for biomedical applications. *Adv. Mater* 33 (4), e2002047. doi:10.1002/adma.202002047

Wang, H., Liu, C., Yang, X., Ji, F., Song, W., Zhang, G., et al. (2023). Multimode microdimer robot for crossing tissue morphological barrier. *iScience* 26 (11), 108320. doi:10.1016/j.isci.2023.108320

Wang, Q., Chan, K., Schweizer, K., Du, X., Jin, D., Yu, S., et al. (2021b). Ultrasound Doppler-guided real-time navigation of a magnetic microswarm for active endovascular delivery. *Sci. Adv.* 7 (9), eabe5914. doi:10.1126/sciadv.abe5914

Wang, Q., Du, X., Jin, D., and Zhang, Li. (2022). Real-time ultrasound Doppler tracking and autonomous navigation of a miniature helical robot for accelerating thrombolysis in dynamic blood flow. *ACS Nano* 16 (1), 604–616. doi:10.1021/acsnano.1c07830

Wang, Q., Yang, L., Yu, J., Chiu, P., Zheng, Y., and Zhang, Li. (2020). Real-time magnetic navigation of a rotating colloidal microswarm under ultrasound guidance. *IEEE Trans. Biomed. Eng.* 67 (12), 3403–3412. doi:10.1109/TBME.2020.2987045

Wang, Q., and Zhang, L. (2021). External power-driven microrobotic swarm: from fundamental understanding to imaging-guided delivery. *ACS Nano* 15 (1), 149–174. doi:10.1021/acsnano.0c07753

Wanner, E., Thoppil, H., and Riabowol, K. (2020). Senescence and apoptosis: architects of mammalian development. *Front. Cell Dev. Biol.* 8, 620089. doi:10.3389/fcell.2020.620089

Xia, W., Geng, Y., and Hu, W. (2023). Peritoneal metastasis: a dilemma and challenge in the treatment of metastatic colorectal cancer. *Cancers (Basel)* 15 (23), 5641. doi:10.3390/cancers15235641

Xiao, Y., Zhang, J., Fang, B., Zhao, X., and Hao, N. (2022). Acoustics-actuated microrobots. *Micromachines (Basel)* 13 (3), 481. doi:10.3390/mi13030481

Xie, H., Sun, M., Fan, X., Lin, Z., Chen, W., Wang, L., et al. (2019). Reconfigurable magnetic microrobot swarm: multimode transformation. Locomotion, and manipulation. *Sci. Rob.* 4 (28), eaav8006. doi:10.1126/scirobotics.aav8006

Xie, M., Zhang, W., Fan, C., Wu, C., Feng, Q., Wu, J., et al. (2020). Bioinspired soft microrobots with precise magneto-collective control for microvascular thrombolysis. *Adv. Mater* 32 (26), e2000366. doi:10.1002/adma.202000366

Yang, J. (2020). Janus microdimer swimming in an oscillating magnetic field. *R. Soc. Open Sci.* 7 (12), 200378. doi:10.1098/rsos.200378

Yang, M., Guo, X., Mou, F., and Guan, J. (2022). Lighting up micro-/nanorobots with fluorescence. *Chem. Rev.* 123 (7), 3944–3975. doi:10.1021/acs.chemrev.2c00062

Yang, M., Zhang, Y., Mou, F., Cao, C., Yu, L., Li, Z., et al. (2023). Swarming magnetic nanorobots bio-interfaced by heparinoid-polymer brushes for *in vivo* safe synergistic thrombolysis. *Sci. Adv.* 9 (48), eadk7251. doi:10.1126/sciadv.adk7251

Yu, S., Ma, N., Yu, H., Sun, H., Chang, X., Wu, Z., et al. (2019). Self-propelled janus microdimer swimmers under a rotating magnetic field. *Nanomater. (Basel).* 9 (12), 1672. doi:10.3390/nano9121672

Zhang, B., Zhu, L., Pan, H., and Cai, L. (2023b). Biocompatible smart micro/nanorobots for active gastrointestinal tract drug delivery. *Expert Opin. Drug Deliv.* 20 (10), 1427–1441. doi:10.1080/17425247.2023.2270915

Zhang, D., Gorochowski, T., Marucci, L., Lee, H., Gil, B., Li, B., et al. (2022). Advanced medical micro-robotics for early diagnosis and therapeutic interventions. *Front. Robot. AI* 9, 1086043. doi:10.3389/frobt.2022.1086043

Zhang, H., Li, Z., Gao, C., Fan, X., Pang, Y., Li, Ti., et al. (2021). Dual-responsive biohybrid neutrobots for active target delivery. *Sci. Robot.* 6 (52), eaaz9519. doi:10.1126/scirobotics.aaz9519

Zhang, W., Deng, Y., Zhao, J., Zhang, T., Zhang, X., Song, W., et al. (2023a). Amoeba-inspired magnetic venom microrobots. *Small* 19 (23), e2207360. doi:10.1002/smll.202207360

Zhao, S., Sun, D., Zhang, J., Lu, H., Wang, Y., Xiong, R., et al. (2022). Actuation and biomedical development of micro-/nanorobots - a review. *Mat. Today Nano* 18, 100223–108420. doi:10.1016/j.mtnano.2022.100223

Zhou, H., Mayorga-Martinez, C., Pane, S., Zhang, L., and Pumera, M. (2021). Magnetically driven micro and nanorobots. *Chem. Rev.* 121 (8), 4999–5041. doi:10.1021/acs.chemrev.0c01234

Frontiers in
Bioengineering and Biotechnology

Accelerates the development of therapies, devices, and technologies to improve our lives

A multidisciplinary journal that accelerates the development of biological therapies, devices, processes and technologies to improve our lives by bridging the gap between discoveries and their application.

Discover the latest Research Topics

See more →

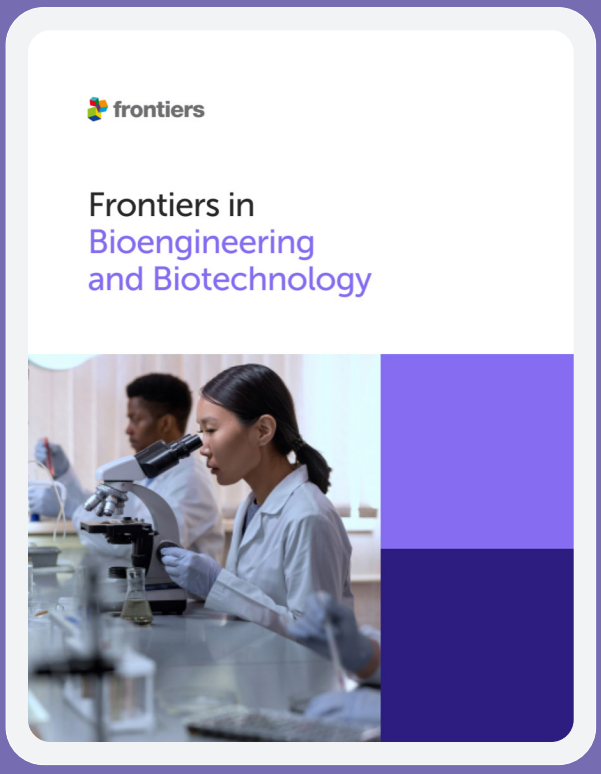

Frontiers

Avenue du Tribunal-Fédéral 34
1005 Lausanne, Switzerland
frontiersin.org

Contact us

+41 (0)21 510 17 00
frontiersin.org/about/contact